UDC 520/524 YU ISSN 0373-3742

PUBLIKACIJE ASTRONOMSKE OPSERVATORIJE U BEOGRADU
PUBLICATIONS DE L'OBSERVATOIRE ASTRONOMIQUE DE BELGRADE

Sv. 49 No. 49

PROCEEDINGS OF THE FIRST HUNGARIAN–YUGOSLAV ASTRONOMICAL CONFERENCE

April 26–27, 1995, Baja, Hungary

Edited by I. Vince, M. S. Dimitrijević and L. Balázs

BEOGRAD
1995

PUBL. OBS. ASTRON. BELGRADE No. 49, 1–214 BELGRADE JUILLET 1995

PUBLICATIONS DE L'OBSERVATOIRE ASTRONOMIQUE DE BELGRADE

FOUNDED IN 1947

Published and copyright © by Astronomical Observatory, Volgina 7,
11050 Beograd, Yugoslavia

Director of the Astronomical Observatory: Dr M. S. Dimitrijević

The publication of this issue is financially supported by the Federal Ministry for Development, Science and Environment and the Ministry of Sciences and Technology of Serbia

Number of copies / tiraž: 500

Production: "Komex" Peć, Vlade Raičevića 1/B

FOREWORD

Could frontiers stop a bird, a river, wind or thought? Could science be divided into small ghettos closed by borders? The science is universal in spirit and without the freedom of scientific activity, the freedom of communication among scientists, the freedom of access to, and dissemination of, scientific information, the science could not bestow its fruits on the whole humanity. This is particularly true of astronomy, since its laws are the same to all and do not depend on politics. To a real astronomer, each observatory all over the world is his home. There, he may immediately find friends, continue his research, discuss his results. His articles are in the observatory's library. So it is natural that astronomers endeavor to improve mutual communications and to create better conditions for friendship and collaboration.

The first Hungarian - Yugoslav Astronomical Conference is a fruitful realization of our desire to create the conditions for development of better collaboration and of traditionally good relations among Yugoslav and Hungarian astronomers, relations started by Milan Nedeljković, the founder of the Astronomical Observatory in Belgrade and Miklos Tege Konkoly, the founder of the Konkoly Observatory in Budapest. The Conference offered an opportunity to exchange ideas, to discuss results and possibilities for closer collaboration on different topics. The present Proceedings of the Conference are not only a collection of presented invited lectures and posters. They are also a kind of "catalogue" of astronomical activities in Yugoslavia and Hungary, and a testimony to our common wish to collaborate and, by uniting our knowledge, to create a "critical mass" for better consideration of results and for faster development of astronomy.

We decided at the Conference to continue such activity and that joint astronomical conferences of our astronomers be organized regularly with a biennial period. The next one, II Yugoslav - Hungarian Astronomical Conference will be organized by the Belgrade Observatory in 1997, the members of the organizing scientific committee being : M. S. Dimitrijević, I. Vince and L. Balasz. I hope that this series of conferences will become an important contribution of astronomers of our two countries to the development of mutual collaboration and friendship.

Milan S. Dimitrijević

Publ. Obs. Astron. Belgrade No. 49 (1995), 7-13

THE MILKY WAY LOCAL DYNAMICS

S. NINKOVIĆ
Astronomical Observatory, Volgina 7, 11050 Belgrade, Yugoslavia
E-mail sninkovic@aob.aob.bg.ac.yu

Abstract. The dynamics of our own Galaxy (the Milky Way) in the solar neighbourhood is analyzed. It is emphasized that in the framework of the classical approach, which involves the steady state and axial symmetry, the main research directions are the determination of the dynamical constants and the explanation of the local kinematics. In spite of this it seems that the classical approach is not sufficient to explain the entire variety of the observed phenomena. Some of them (vertex deviation, velocity-dispersion increasing with age, etc) in the present author's opinion require its generalization towards a triaxial symmetry and a nonsteady state.

1. INTRODUCTION

As usually the notion "local" applied in galactic astronomy means something referred to the solar neighbourhood. Therefore, the Milky-Way local dynamics studies the dynamics of a small Milky-Way region near the Sun. The more abundant observational material existing for the solar-neighbourhood case compared to other parts of our Galaxy offers many questions for stellar dynamics to be answered. It was just the local kinematics which almost seventy years ago initiated the dynamical study of the galactic rotation. The basic ideas of this theory, as well known, are :

1. the steady state and axial symmetry of the Milky Way as a whole;
2. the ellipsoidal distribution of the residual velocities at the Sun for the disc stars.

These ideas have remained much unchanged. Therefore, the local dynamics of the Milky Way can be considered in two approaches - the classical one based on the two assumptions mentioned above and a more general one where the (inevitable) deviations from both steady state and axial symmetry are taken into account.

2. THE POSSIBILITIES OF THE CLASSICAL APPROACH

In the founding of the Milky-Way local dynamics one can choose different ways. In the present author's opinion the best one is, certainly, which introduces the notion of the dynamical constants (Ninković, 1987b). These are the local values of dynamical quantities, i. e. their values taken at the galactocentric position $R = R_\odot$, $Z = 0$. In the framework of the classical approach the constants of interest are : the local value of the potential, the first radial derivative $(\frac{\partial \Pi}{\partial R})$, the second radial derivative $(\frac{\partial^2 \Pi}{\partial R^2})$ and the second vertical derivative $(\frac{\partial^2 \Pi}{\partial Z^2})$ (in all cases their local values). Higher-order

derivatives are not of interest and in the classical theory all other derivatives up to the second order are zero in the galactic plane.

It is clear that these four quantities are not directly determinable from the observational data, however the theory connects them with some other quantities easier to interpretation. The correspondence is the following

potential corresponds to escape velocity;

its first radial derivative to circular velocity;

its second radial derivative to circular-velocity slope;

its second vertical derivative to cyclical frequency of vertical oscillations.

The relations connecting these quantities are well known and there is no need to present them here. It is clear that there are also other quantities which can be used for the same purpose - for example, the local angular velocity of circular motion instead of the local circular velocity, then the pair local circular velocity and its slope can be substituted by the well-known Oort constants A and B (or more precisely by their dynamical counterparts), etc. The cyclical frequency of vertical oscillations is also known as Kuzmin's parameter, or constant, (C) (e. g. Einasto, 1974) forming thus a system of three dynamical constants.

As well known, the situation with all these values is not quite clear. The IAU recommended a value (220 $km\ s^{-1}$) for the local circular velocity but without recommending any particular values for the Oort constants and also for the Kuzmin one (Kerr and Lynden-Bell, 1986); the escape velocity was not even treated in this report probably because it is least reliably known. In addition, the local-escape-velocity problem is not a local problem only, since this question involves the global dark-matter problem.

In spite of all these circumstances the present consideration shall include the local escape velocity. The recent increase of the observational material, above all towards high-velocity stars, has clearly shown that in the solar neighbourhood stars with galactocentric velocities as high as 450 $km\ s^{-1}$ are not rare and therefore this value was advocated as a correct one for the local escape velocity (e. g. Rohlfs and Kreitschmann, 1981). With regard that stars with even higher galactocentric velocities have been also found, it may be considered rather as a lower limit and somewhat higher values have been also proposed (e. g. Ninković, 1987a; Cudworth, 1990). However, in view of the extremely low number density of the stars with exceptionally high galactocentric velocities, the arguments pro et contra coming from studies of the global Milky-Way structure, aimed at answering the dark-matter question, must be also taken into account. Though, at first glance, it seemed that the motion of the Milky-Way satellites was not in favour of a high dark-matter content (e. g. Lynden-Bell et al., 1983), the gradually adventing more recent evidence, especially the case of Leo I(e. g. Lee et al., 1993), seems to suggest a very high Milky-Way total mass so that the prediction of Caldwell and Ostriker (1981) being in favour of a very high local escape velocity (550 - 650 $km\ s^{-1}$) seems justified. In any case the values of 500 - 700 $km\ s^{-1}$ for the local escape velocity clearly suggest that the total mass of the Milky Way significantly exceeds that of its seen matter.

As for the local circular velocity, the situation is certainly more clear than in the case of the local escape one. It could be noticed that the comparatively recent trend has been to correct its value downwards. The value mentioned above, recommended

by the IAU ten years ago, is less than the previous IAU official value of 250 $km\ s^{-1}$ (assumed at the IAU General Assembly in Hamburg in 1964), but there are proposals in favour of even lower values(e. g. Rohlfs and Kreitschmann, 1987). This downwards correcting is frequently followed by a corresponding correcting of the solar galactocentric distance in the same sense so that the resulting changes in the local angular velocity of circular motion are smaller. However, since the first radial derivative of the potential, or the strength of the gravitational field (more precisely radial component, but note that the other one is zero in the plane), depends on both the circular velocity (corresponding angular velocity) and $R_\odot$, their changes will certainly affect its local value. The effect can be illustrated by the following examples : the old IAU official values yield 6250 $km^2\ s^{-2}\ kpc^{-1}$ for the local gravitational-field strength, those actually recommended by it yield about 5700 $km^2\ s^{-2}\ kpc^{-1}$. As extremal examples one may mention that for the same quantity the values proposed by Rohlfs and Kreitschmann (1987) yield about 4300 $km^2\ s^{-2}\ kpc^{-1}$, whereas those of Balázs (1982) yield about 8450 $km^2\ s^{-2}\ kpc^{-1}$!

The local circular-velocity slope can be determined through the ratio of the Oort constants. It can be also related to another dimensionless quantity - the dynamical coefficient γ being the ratio of the second radial derivative of the potential to the square of angular velocity of circular motion - introduced by the present author (Ninković, 1987b). The situation is not quite clear. The examinations of the neutral-hydrogen rotation suggest an approximately flat circular-velocity curve within a sufficiently wide galactocentric-distance range, including the solar region as well (e. g. Haud, 1979; Fich et al., 1989). Such a situation, as easy to see, corresponds to equal moduli of the Oort constants. However, many investigators find a slight decrease in the circular velocity near the Sun - for instance the straight unweighted means presented by Kerr and Lynden-Bell (1986 - Table 10 of their paper). It is interesting to note that such findings do not contradict to the general trend of a flat galactic rotation curve. A good example is, certainly, that of Rohlfs and Kreitschmann (1987) who though on the average find $A = -B$, nevertheless obtain for the solar neighbourhood such a ratio of the Oort-constants moduli which would correspond to a local circular-velocity decrease characteristic for the case of an almost point-mass gravitational field! Of course, one may wonder in what degree such a wavy circular-velocity curve is close to reality, perhaps a smoothing is necessary. Finally, it can be said that most likely the circular velocity in the solar neighbourhood is approximately constant with a tendency of slight decrease. With regard that the second radial derivative depends not on the circular-velocity slope only, i. e. on γ coefficient (Ninković, 1987b), but also on the square of the angular velocity of circular motion, it is useful to present its possible value. If assumed, following the IAU, that the local angular velocity is most likely equal to some 25-26 $km\ s^{-1}\ kpc^{-1}$, then in view of the said above the second radial derivative would lie somewhere between 600 $km^2\ s^{-2}\ kpc^{-2}$ and 800 $km^2\ s^{-2}\ kpc^{-2}$.

In addition, according to the classical theory the ratio of the mean residual-velocity squares along the axes directed to $l = 0°$, $b = 0°$ and $l = 90°$, $b = 0°$, denoted as $\overline{x^2}$ and $\overline{y^2}$, respectively, is determined by the Oort-constants-moduli ratio. For the case of the equal moduli the corresponding value of this ratio is 2. However, the local stellar

kinematics suggests a higher value, usually about 2.56 (e. g. Kulikovskij, 1985, p. 86). Recently the present author (Ninković, 1992) offered a new solution by amending the classical formula with a new term containing the ratio of the asymmetric-drift square to $\overline{\dot{x}^2}$. It seems that with this correction an agreement can be achieved.

The situation with the Kuzmin-constant value seems to be the most unclear. It should be emphasized here that this constant is very important because by its contribution is essentially determined the local value of the potential laplasian, i. e. the local density of the galactic matter. This problem is very well known since long ago - so-called Oort's limit (Oort, 1965) - or the local dark-matter problem since many astronomers have found that this "dynamical" density significantly exceeds that following from stellar statistics. However, the problem seems still far from the solution. In Gliese's (1983) review the whole controversy of the problem was emphasized. Here it can be added that there seems to be something like a systematical tendency of some schools of stellar dynamics for preferring certain values. For example, there are several results of the Tartu astronomers where the values close to those found by means of stellar statistics were communicated (e. g. Einasto, 1974 and the references cited therein; Jõeveer and Einasto, 1976; Haud and Einasto, 1989; Eelsalu, 1990). On the other hand some Western-Europe astronomers have found several times values sufficiently exceeding the value derived from stellar statistics (e. g. Fuchs and Wielen, 1986; Crézé et al., 1989). In the astronomical circles of the Anglo-Saxon countries it seems as practically assumed that the local "dynamcal" density is approximately twice as high as the "statistical" one (e. g. Binney and Tremaine, 1987, p. 17; Freeman, 1987). The present author has also a result on the dynamical local-density determination (Ninković, 1987b) where a value quite close to the statistical one was found.

It is usually thought that this local dark-matter problem has nothing to do with the galactic dark corona because it is not sufficiently flattened (e. g. Binney et al., 1987; Trimble, 1987). For example, it has been demonstrated by the present author that unless the corona is as flattened as the axial ratio not exceeding 0.1, its contribution to the local galactic-matter density cannot be essential (Ninković, 1990).

In general it may be said that the values found dynamically for the local density and exceeding the double statistical value seem unrealistic. Thus, if the local dark-matter problem really exists, most likely the local dark-matter mass does not exceed that of the seen matter. On the other hand, since the local-circular-velocity determination does not indicate an essentially higher disc mass within the Sun, the disc dark matter, if it really exists, should be looked for near the galactic plane. Such a search has been already undertaken, even in the Solar System (e. g. Tremaine, 1990).

3. ELLIPSOIDAL DYNAMICS

The hypothesis of ellipsoidal velocity distribution for the disc stars in the solar neighbourhood is sufficiently well known. It is also well known that it is possible by using the Boltzmann equation to determine the galactic potential on the basis of the known phase-space density represented through the velocity ellipsoid (e. g. Chandrasekhar, 1960). It is interesting to mention that such potential determinations have not yielded a potential function depending on the space coordinates (above all R and Z) in a way

sufficiently close to what, say, the rotation-curve determinations yield (e. g. Sanz, 1987; Sala, 1987; Sala, private communication). Thus one finds another example of discordance between the Milky-Way local dynamics and the global one.

As for this discordance, it is usually borne in mind the ratio of the mean velocity squares $\frac{\overline{\dot{x}^2}}{\overline{\dot{z}^2}}$. As well known, the classical theory of Lindblad yields the value of one for it due to the assumption of only two integrals of motion. Therefore, the discussion goes to another topic now - that of the third integral. As well known, several functions, largely quadratic in the velocity components, have been proposed as approximate integrals of motion (for more details e. g. Ogorodnikov, 1958, p. 296). The question has not been definitely solved yet. Most likely the third independent nonclassical integral of motion exists, but it is not clear in what way it restricts the motion of a test particle. For the case of the galactic disc (nearly circular motion) Lindblad's theory predicts a constant amplitude of the motion along the Z axis so that the part of space occupied by the test-particle orbit is limited vertically by two planes parallel to the main plane of the Milky Way. The calculations of the galactocentric orbits for some disc stars in realistic galactic potentials (e. g. Mullari et al., 1994) shows that the real situation is more complicated which is probably caused by the third-integral nature.

4. BEYOND THE CLASSICAL APPROACH

It is clear that the idea of the steady state and axial symmetry is merely an approximation. There are many phenomena which can be hardly explained in the framework of this hypothesis. The solar neighbourhood, on the other hand, offers for clear reasons many fine details where the deviations from the steady state and axial symmetry can be studied. Some of them should be mentioned : the vertex deviation, the Gould belt, etc. It should be added that the analysis through the Boltzmann equation with the ellipsoidal velocity distribution as working hypothesis is applicable to this case, as well. This can be seen, for instance, from the references cited in the next paragraph.

The vertex deviation is a well known phenomenon. It seems not difficult for explaining if the axial symmetry is generalized towards the triaxial one (e. g. Sanz Catala, 1987). However, it should not be forgotten that the vertex deviation is a characteristic of samples consisting of early-spectral-type stars, i. e. young ones. Therefore, one can ask why the triaxiality effect (if this is really the explanation) is selective against later-spectral-type stars. This circumstance justifies another way, i. e. to look for the explanation in the framework of a nonsteady state including the star formation still active in the disc. Various possibilities have been considered including also the superposition of two stellar systems (e. g. Sanz et al., 1989; Cubarsí, 1990).

In favour of the deviations from the steady state is also the following circumstance. Namely, it has been noticed that the mean squares of the residual-velocity components for the disc samples consisting of younger stars are lower than in the case of the so-called old disc (e. g. Mayor, 1974; Carlberg et al., 1985). This effect seems to be well established in spite of a quantitative disagreement (Freeman's comment - Freeman, 1987). It is possible that the velocity-dispersion increase in the z direction is stronger than in the other two, a phenomenon probably in favour of a nonsteady state. A

possible explanation may be some kind of galactic diffusion (e. g. Wielen, 1977). It is also not impossible that the phenomenon is due to another mechanism important for our Galaxy, such as the spiral density waves (e. g. Balázs, 1982) moving groups (e. g. Eggen, 1986), etc.

5. CONCLUSION

Certainly, the most important conclusion may be that the field of the Milky-Way local dynamics, though sufficiently treated in the past, still offers many tasks for research. During the recent two decades an undoubted progress concerning the local escape velocity was achieved, but on the other hand some old questions, such as the ratio of the Oort constants, the amount of the Kuzmin one, etc, seem to become actual again after a period when they were thought to be known satisfactorily well. As quite clear appears that the interpretation of the phenomena discordant with the steady state and axial symmetry requires most of the efforts.

References

Balázs, B. A. : 1982, "The shape and angular velocity of the galactic spiral pattern", *Hvar Obs. Bull. Suppl. (Proc. V Nat. Conf. Yug. astron.)* **6**, 1-10.

Binney, J., May, A. and Ostriker, J. P. : 1987, "On the flatteening of galactic dark halo", *Mon. Not. R. astr. Soc.* **226**, 149-157.

Binney, J. and Tremaine, S. : 1987, "Galactic dynamics", Princeton University Press, Princeton, New Jersey.

Caldwell, J. A. R. and Ostriker, J. P. : 1981, "The mass distribution within our Galaxy : a three component model", *Astrophys. J.* **251**, 61-87.

Carlberg, R. G., Dawson, P. C., Hsu, T. and VandenBerg, D. A. : 1985, "The age-velocity-dispersion relation in the solar neighborhood", *Astrophys. J.* **294**, 674-681.

Chandrasekhar, S. : 1960, "Principles of stellar dynamics", new edition, Dover Publ., Inc., New York.

Crézé, M., Robin, A. C. and Bienaymé, O. : 1989, "The mass density in our Galaxy II. F dwarfs and K giants as density tracers", *Astron. Astrophys.* **211**, 1-8.

Cubarsí Morera, R. : 1990, "Some kinematics and dynamics from a superposition of two axisymmetric stellar systems", *Astron. J.* **99**, 1558-1568.

Cudworth, K. M. : 1990, "The local galactic escape velocity revisited : improved proper motions for critical stars", *Astron. J.* **99**, 590-594.

Eelsalu, H. : 1990, "The cratering history and the galactovertical oscillation of the Sun", *Publ. Tart. astrof. obs. V. Struve* **53**, 25-32.

Eggen, O. J. : 1986, "Hyades and Sirius supercluster members brighter than magnitude (V) 7.1. II. right ascension six to twelve hours", *PASP* **98**, 423-441.

Einasto, J. : 1974, "Galactic models and stellar orbits", in Stars and the Milky Way System, Proc. First Eur. Astron. Meet., ed. L. N. Mavridis, Springer, Berlin, Heidelberg, New York, pp. 291-325.

Fich, M., Blitz, L. and Stark, A. A. : 1989, "The rotation curve of the Milky Way to $2R_0$", *Astrophys. J.* **342**, 272-284.

Freeman, K. C. : 1987, "The galactic spheroid and old disk", *Ann. Rev. Astron. Astrrophys.* **25**, 603-632.

Fuchs, B. and Wielen, R. : 1986, "Dynamische Massenbestimmung in der Milchstrasse", *Mitt. Astron. Gesell.* **67**, 374-375.

Gliese, W. : 1983, "The solar neighborhood - knowledge and questions", IAU Coll. 76, eds. A. G. Davis Philip and Arthur R. Upgren, L. Davis Press. Inc., Schenectady, New York, USA pp. 5-14.

Haud, U. A. : 1979, "Krivaya vrashcheniya Galaktiki s uchetom rasshireniya gazovoj sostavlyayushchej", *Pis'ma v AZh* **5**, 124–127.
Haud, U. and Einasto, J. : 1989, "Galactic models with massive corona II. Galaxy", *Astron. Astrophys.* **223**, 95–106.
Jõeveer, M. and Einasto, J. : 1976, "Galactic mass density in the vicinity of the Sun", *Tartu Astrof. Obs. Teated*, **54**, 77–92.
Kerr, F. J. and Lynden-Bell, D. : 1986, "Review of galactic constants", *Mon. Not. R. astr. Soc.* **221**, 1023–1038.
Kulikovskij, P. G. : 1985, "Zvezdnaya astronomiya", Nauka Glav. red. fiz.-mat. lit.
Lee, M. G., Freedman, W., Mateo, M. and Thompson, I. : 1993, "Leo I : the youngest Milky-Way dwarf spheroidal galaxy?", *Astron. J.* **106**, 1420–.
Lynden-Bell, D., Cannon, R. D. and Godwin, P. J. : 1983, "Slippery evidence on the Galaxy's invisible heavy halo", *Mon. Not. R. astr. Soc.* **204**, 87p–92p.
Mayor, M. : 1974, "Kinematics and age of stars", *Astron. Astrophys.* **32**, 321–327.
Mullari, A. A., Nechitailov, Yu. V., Ninković, S. and Orlov, V. V. : 1994, "The orbits of moving clusters in the galactic dynamical models", *Astrophys. Sp. Sci.* **218**, 1–11.
Ninković, S. : 1987a, "Orbital eccentricity study for the spherical component of our Galaxy", *Astrophys. Sp. Sci.* **136**, 299–314.
Ninković, S. : 1987b, "Dynamical constants for our Galaxy", *Publ. Astron. Inst. Czechoslovak Acad. Sci.* **69**, 317–318.
Ninković, S. : 1990, "On the flattening of the galactic corona", *Bull. Astron. Inst. Czechosl.* **41**, 236–242.
Ninković, S. : 1992, "On the local value of the asymmetric drift", *Astrophys. Sp. Sci.* **187**, 159–162.
Ogorodnikov, K. F. : 1958, "Dinamika zvezdnykh sistem", Gos. izd. fiz. - mat. lit., Moskva.
Oort, J. H. : 1965, "Stellar dynamics", in *Galactic Structure, Vol. V of Stars and Stellar Systems*, Blaauw, A. and Schmidt, M. eds., Chicago University Press, Chicago and London, pp. 455–511.
Rohlfs, K. and Kreitschmann, J. : 1981, "A realistic model of the Galaxy", *Astrophys. Sp. Sci.* **79**, 289–319.
Rohlfs, K. and Kreitschmann, J. : 1987, "Kinematics and physical parameters of neutral hydrogen in the inner Galaxy", *Astron. Astrophys.* **178**, 95–105.
Sala, F. : 1987, "Galactic kinematics : an axi-symmetric time-depending model with separable potential", *Rev. Mexicana Astron. Astrof.* **14**, 195–205.
Sanz Subirana, J. : 1987, "Potentials separable in addition for Chandrasekhar models with axial symmetry", *Publ. Astron. Inst. Czechoslovak Acad. Sci.* **69**, 327–330.
Sanz Subirana, J. and Catalá Poch, M. : 1987, "Vertex deviation in the galactic plane", *Publ. Astron. Inst. Czechoslovak Acad. Sci.* **69**, 267–270.
Sanz, J., Cubarsí, R. and Juan, J. M. : 1989, *Astrophys. Sp. Sci.* **156**, 19–28.
Tremaine, S. : 1990, "Dark matter in the solar system", *NATO ASI Ser. , Ser. C. Math. Phys. Sci.*, eds D. Lynden-Bell and G. Gilmore **306**, 37–65.
Trimble, V. : 1987, "Existence and nature of dark matter in the universe", *Ann. Rev. Astron. Astrrophys.* **25**, 425–472.
Wielen, R. : 1977, "The diffusion of stellar orbits derived from the observed age-dependence of the velocity dispersion", *Astron. Asstrophys.* **60**, 263–275.

Publ. Obs. Astron. Belgrade No. 49 (1995), 15-18

STAR COUNT STUDY OF THE INTERSTELLAR DUST CLOUDS

L. G. BALÁZS
Konkoly Observatory, Budapest

Abstract. A method is outlined which allows one to estimate the optical absorption and the distance of the interstellar dust clouds. The procedure is based on the maximum likelihood approach of parameter estimation. The accuracy of the parameter estimation is briefly outlined.

1. STAR COUNTS AS INDICATORS OF THE SPATIAL DISTRIBUTION OF STARS

The location of the stars on the celestial sphere does not offer a direct indication on their spatial distribution. Actually, the two dimensional distribution on the celestial sphere is a projection of a three dimensional sample of objects. There are, however, some measurable properties of the stars like apparent brightness and proper motion which depend on some intrinsic property of the object and on the distance as well. Let us denote the measurable quantity with e and its intrinsic counterpart with E. Then there is a functional relationship

$$e = e(E, r).$$

In a number of cases the dependence of e on the distance r is a power law : r^n where $n = 1$ in case of proper motions and $n = 2$ in case of apparent brightness if there is no interstellar absorption.

According to the Bayes theorem of conditional probabilities we obtain

$$\phi(e) = \int \phi(e|r)g(r)dr$$

where $\phi(e)$, $\phi(e|r)$ and $g(r)$ mean the probability density of e, the conditional probability of e, given r, and the probability density of r, respectively. In this way we get an integral equation connecting the spatial distribution of the stars with the observed distribution assuming that the conditional probability of e given r is known somehow. $\phi(e)$ is estimated from the observations counting the stars in a certain Ω region of the sky and in the interval of $(e; e + de)$. The number of stars obtained in this way is often called star counts.

Due to the integral expression given above the star counts yield some information on the spatial distribution of the stars. If the $\phi(e|r)$ conditional probability is given

the integral expression is a Freedholm-type integral equation. The solution of this equation gives the probability density of the stars in the line of sight. The estimation of the spatial distribution from the star counts i.e. inverting the integral expression is called the inverse approach. The opposite way when one makes some prediction for the star counts, assuming that the spatial distribution is known, is called direct approach.

2. SOLUTION OF THE BASIC EQUATION OF STELLAR STATISTICS

In the most common case the measured quantity is the apparent magnitude m in a certain color range :

$$m = M + 5log_{10}r - 5 + a(r).$$

where M denotes the absolute brightness, r the distance in the line of sight and $a(r)$ is the optical absorption. If M and $\rho = 5log_{10}r - 5a(r)$ are stochastically independent i.e the distribution of the absolute magnitudes does not depend on the distance we obtain

$$A(m) = \int_{-\infty}^{\infty} \Delta(\rho)\Phi(M)d\rho = \int_{-\infty}^{\infty} \Delta(\rho)\Phi(m-\rho)d\rho.$$

In this expression A, Δ, Φ are the probability densities of m, ρ, r, respectively. The integral equation obtained is often called the basic equation of the stellar statistics. It is a general equation, called equation of the convolution, giving the probability density of the sum of two independent probability variables.

There are several approaches to the solution of the basic equation. The serious trouble of the solution appears in the structure of the equation. Since the probability density of the observed quantity is estimated from the observations the function is never given exactly but instead by a quantity having a certain level of stochasticity. This stochastic noise is amplified during the inversion and makes the solution very unstable against the high frequency noise. The common solutions of the basic equation used in the astronomical praxis are summarized in the text books (e.g. Kurth 1967, Mihalas and Binney 1981). A more comprehensive discussion of the problem is given by Balázs (1995).

3. MODELLING STAR COUNTS

The opposite way, called direct approach needs the knowledge of the spatial distribution of the stars and, in the case of computing the distribution of apparent magnitudes, the luminosity function and the spatial distribution of the interstellar absorption.

There are several models for predicting star counts. The most frequently used ones are the models of Bahcall and Soneira (1980) and more recently those of Wainscoat et al. (1992). The models differ from each other on the way how they approximate the

spatial distribution of the stars and the interstellar matter and the luminosity function. The BS model approximates the spatial distribution by a series of exponential disks, the scale heights are dependent on the absolute magnitude, and the halo by a de Vacauleurs (1959) spheroid. The luminosity function used by the model has an analytical form obtained by fitting the empirical data.

The Wainscoat model also has a series of exponential disks but uses dependence of the scale heights not on the absolute magnitudes but on the spectral types. The luminosity function is, correspondingly, a sum of gaussian components belonging to the different spectral types. Besides the exponential disk and halo the Wainscoat model adds further structural elements : bulge, spiral arms and molecular ring.

The cloudy structure of the interstellar matter is not taken into account in these models

4. EFFECT OF DUST CLOUDS ON THE STAR COUNTS

The star count models assume a spatially smoothed distribution of the interstellar absorbing material. According to the usual assumption the spatial distribution of the absorbing material is approximated by an exponential disk with a scale height of 80-100 pc

The presence of the individual dust clouds in the line of sight causes lower star counts in the cloud area in comparison with the surrounding field on the sky. This difference in star counts depends on the absorption and the distance of the cloud. The thickness of the cloud can be neglected.

Approximating the cloud with spatially homogeneous absorption then the a_{cl} absorption and r_{cl} distance can be treated as unknown parameters to be estimated. The estimation can be proceed using the maximum likelihood approach.

Let us have an observed sample of magnitudes $m_1, ..., m_2$ and suppose that there is an absorbing cloud in the line of sight at a distance of r_{cl} and an absorption of a_{cl}. By definition the likelihood function is written in the form

$$L(a_{cl}, r_{cl}) = \sum_{i=1}^{n} log A(m_i | a_{cl}, r_{cl}).$$

Here $A(m|a_{cl}, r_{cl})$ is obtained from the basic equation of the stellar statistics when inserted the model stellar distribution using an absorption law where a cloud of absorption a_{cl} and at a distance of r_{cl} was added to the general smoothed absorption. a_{cl} and r_{cl} are two unknown parameters to be estimated by maximizing the likelihood function.

Maximizing proceeds by solving the following system of equations :

$$\frac{\partial L}{\partial a_{cl}} = \frac{\partial L}{\partial r_{cl}} = 0.$$

In a general case the star counts are not homogeneous over the whole cloud area on the sky. We may generalize the procedure applied in the homogeneous case by dividing the cloud area into subregions where the star counts can be taken uniform.

We may perform the ML analysis independently within the subregions. However, the distance is the same for all of these regions and therefore we may reduce the number of parameters to be estimated by maximizing the following likelihood function :

$$L = \sum_{l=1}^{k} L^{(l)}(a_{cl}^{(l)}, r_{cl})$$

where k is the number of subregions and their likelihood functions and parameters to be estimated labelled by l.

Estimating the parameters it is an important question how reliable they are. There is a general theorem in case of ML estimations giving some hint for the accuracy of parameters obtained in this way. Denoting the value of the likelihood function at the maximum with L_{max} and those at the true value of the parameters with L_0 then

$$2(L_{max} - L_0) \approx \chi_m^2$$

is true asymptotically when the sample size goes to infinity. In the above formula the degree of freedom of the chi square probability variable m is the number of the parameters to be estimated.

Acknowledgements

This work was partly supported by the OTKA grant no. T4341.

References

Bahcall, J. N. and Soneira, R. M. : 1980, *Astrophys. Journ. Suppl.*, **44**, 73.
Balázs, L. G. : 1995, Inverse Problems, accepted for publication.
de Vaucouleurs, G. : 1959, in *Handbuch der Physik*, Vol. **53**, ed. S. Flügge, Springer, Berlin, 311.
Kurth, R. : 1967, *Introduction to the Stellar Statistics*, Pergamon Press.
Mihalas, D. and Binney, J. : 1981, *Galactic Astronomy*, W. H. Freeman and Co.
Wainscoat, R. J., Cohen, M., Volk, K., Walker, H. J. and Schwartz, D. E. : 1992, *Astrophys. Journ. Suppl.*, **83**, 111.

Publ. Obs. Astron. Belgrade No. 49 (1995), 19-39

AN ANALYTICAL PERTURBATION THEORY FOR THE LOW LUNAR POLAR ORBITER

Z. KNEŽEVIĆ
Astronomical Observatory, Volgina 7, 11050 Belgrade, Yugoslavia
E-mail zoran@aob.aob.bg.ac.yu

A. MILANI
Department of Mathematics, Pisa, Italy
E-mail milani@adams.dm.unipi.it

Abstract. We present in this paper a fully analytical theory of motion for the low lunar polar orbiter, intended for the mission analysis i.e. for the preliminary study of the satellite orbit. We first explain how in general one develops an analytic perturbation theory, and describe the requirements to be met and choices to be done to build the theory and compute the solutions. Then we give the basic equations for the theory in question and discuss some particularities and technicalities regarding the methods and procedures employed. The results achieved with the current version of the theory (rms's in semimajor axis, eccentricity and inclination are $\approx 13\,m$, < 0.001 and $< 0.001\,rad$, respectively, in the course of 6 months) are more than enough for the present purpose. Finally, we briefly discuss the limitations of the theory, and ways to improve it if and when the need arises.

1. BUILDING AN ANALYTICAL PERTURBATION THEORY

In order to build an analytical perturbation theory of motion of any natural or artificial celestial body, one has to know precise answers to several apparently simple questions. So, for example, it is necessary to know what kind of motion the theory is supposed to describe, which part of the phase space of orbital elements will be covered, what is the minimal/optimal dynamical model needed to meet the requirements on the accuracy and the time stability of the solutions, what kinds of forces are involved, which analytical methods best suite the purpose, etc. The success of any pertubation theory critically depends on the right answers to the above questions (and many other more specific and technical ones), and it is quite a complex task to develop and correctly tune a theory which will perform in the best way, while still keeping the effort and the time needed to complete and apply it within some reasonable limits.

We shall try to show in the following how we have fulfilled such a task in a particular case of building the analytical theory of motion of a low-altitude, nearly-polar lunar orbiter. The purpose of the theory is the mission analysis, i.e. the preliminary study of the satellite orbit which must be at the same time suitable for the experiments to be performed in the framework of the mission and such that the life-time of the satellite

is long enough and manoeuvering as seldom and as little fuel-consuming as possible. In a way, this theory bears some resemblance to the theory of computation of asteroid proper elements (in particular from the viewpoints of basic analytical tools used to construct the theory, and the forms of the solutions and procedures of their analysis), so that one can also refer to it as "the theory of selenocentric proper elements".

Let us first define our problem along the lines described above.

A spacecraft orbiting the Moon is subject to perturbation of its osculating two-body orbital elements, due to the harmonics of the lunar gravity field, to the differential attraction from the Earth and from the Sun, to non gravitational perturbations, and others. The effects of these perturbations belong to three main classes : very short periodic (with periods of the order of the satellite orbital period, i.e. a few hours, or less), medium periodic (with periods longer than one orbital period of the satellite, but shorter than one lunar month), and long periodic. For the sake of simplicity, very short and medium periodic perturbations will be collectively called short periodic. The long term evolution of the orbit, in particular the time series of the periselenium altitude which determines the safety of the mission, depends mostly on the long periodic effects. Thus a numerical computation of the orbit is extremely ineffective as a tool for the study of the qualitative behaviour of the orbit. The computation of a single orbit by brute force numerical integration is not a problem, but a systematic exploration of the phase space to define the safe region and the optimum orbit maintenance strategy is almost impossible.

There are three types of elements involved : osculating, mean and proper. Osculating elements are the instantaneous ones; they can be expressed as a set of orbital elements (e.g. keplerian), and usually they are obtained by a time independent coordinate transformation from the state vector (cartesian position and velocity). Mean elements are obtained from the osculating ones by removing all the perturbations (due to the non spherically symmetric part of the gravity field of the Moon) with short periods. As aforementioned, short periods are by definition shorter than one lunar month, which is also one rotation period of the Moon. Proper elements are obtained by removing from mean elements the long periodic perturbations. Proper elements are therefore solution of an integrable problem, whose time evolution can be computed analytically (and with a comparatively simple formula). However, it has to be remembered that transformation of a non integrable problem into an integrable one cannot be performed in an exact way, but only by neglecting some higher degree and order terms; in practice, this means that the proper elements which should be constant in the trivial dynamics, such as the proper eccentricity, are not exactly constant when computed from a time series of state vectors. Following a procedure well established for asteroid proper elements, we use the standard deviation of these proper elements with respect to their long term mean as a measure of the accuracy of the proper elements theory (see Milani and Knežević, 1990, 1992, 1994).

Intrinsic to any analytic theory is the set of rules governing necessary truncations of the gravity field potential, and of the order of theory in agreement with accuracy requirements. In the particular case, the main choice to be done is the rule to be used to truncate R, the potential of the lunar gravity field. For a low lunar orbiter, the eccentricity can not be large, while the inclination can be large (and indeed we are

here interested mostly in polar orbits). Hence, we are using a rule based upon the eccentricity, such that we truncate all the perturbations to degree 1 in eccentricity; this requires to expand the perturbing function to degree 2 in eccentricity, since some perturbations contain derivatives such as $\partial R/\partial e$. Note that we also perform some truncation which takes into account that the orbit is nearly polar, that is $\cos I$ is small.

A second truncation is with respect to the degree l in the spherical harmonics expansion (see later). This is justified by the fact that the harmonic coefficients C_{lm}, S_{lm} are decreasing with l, roughly proportionally to $1/l^2$, i.e. according to the well known Kaula's (1966) rule. Our theory has no *a priori* upper limit to l, but of course some limitation has to be chosen to control the computational cost, and also to avoid numerical instabilities. Moreover the actual values of the high degree and order harmonic coefficients are highly uncertain, and there is no point in doing very long computations based on unreliable input data.

The third truncation is a truncation to some order in the small parameters appearing in the perturbations. For the computation of the short periodic perturbations, a first order theory is accurate enough. On the contrary, for the long periodic perturbations, if the accuracy required is very high and the time span is very long, some terms belonging to the second order in the small parameters should be added. The current version of our theory does not include these second order terms, also because the uncertainty of the harmonic coefficients results in a larger error in the solution.

Finally, we should define our dynamical model (the current version of our theory does not include the effects of the perturbations due to the Earth and to the Sun, neither the non-gravitational effects), decide on the choice of variables (non-singular, canonical) and perturbation methods (Lagrangian, Hamiltonian), coordinate system (inertial, body-fixed), etc.

2. BASIC EQUATIONS

Let us quickly browse through the basic equations that serve to set up the problem.

2. 1. EQUATIONS OF MOTION

The potential of the lunar gravity field is given in terms of the development into spherical harmonics (Kaula 1966) as a sum of the monopol term (potential of a sphere) and the perturbation (accounting for all the deviations of a real body from a sphere) :

$$U = \frac{GM}{r} + R$$

$$R = \frac{GM}{r} \sum_{l=2}^{+\infty} \left(\frac{R_M}{r} \right)^l \sum_{m=0}^{l} P_{lm}(\phi) \left[C_{lm} \cos m\lambda + S_{lm} \sin m\lambda \right] \qquad (1)$$

Since the $l = 1$ terms are removed by translation of the origin of the reference system to the centre of mass of the Moon, the *perturbing function* R contains only the terms of degree $l \geq 2$. The perturbing function can be expressed as a function

of the usual keplerian orbital elements $(a, e, I, \Omega, \omega, \ell)$ (semimajor axis, eccentricity, inclination to the lunar equator, longitude of node, argument of periselenium, mean anomaly), and expanded as follows :

$$R = \frac{GM}{a} \sum_{l=2}^{+\infty} \left(\frac{R_M}{a}\right)^l \sum_{m=0}^{l} \sum_{p=0}^{l} F_{lmp}(I) \sum_{q=-\infty}^{+\infty} G_{lpq}(e) S_{lmpq}(\omega, \ell, \Omega, \theta) \qquad (2)$$

$$S_{lmpq} = \begin{cases} C_{lm} \cos \Psi_{lmpq} + S_{lm} \sin \Psi_{lmpq} & (l-m \quad \text{even}) \\ -S_{lm} \cos \Psi_{lmpq} + C_{lm} \sin \Psi_{lmpq} & (l-m \quad \text{odd}) \end{cases}$$

$$\Psi_{lmpq} = (l-2p)\omega + (l-2p+q)\ell + m(\Omega - \theta)$$

where θ is the phase of the lunar rotation, namely the angle between some body fixed direction along the equator (Davies et al. 1992) and some inertial direction along the equator; precession of the lunar pole and physical librations can be neglected. The *inclination functions* F_{lmp} and the *eccentricity functions* G_{lpq} can be explicitly computed.

We can now define very short periodic terms in R as those with $l - 2p + q \neq 0$ (i.e., those containing the mean anomaly ℓ); medium period terms are those with $l - 2p + q = 0$ but $m \neq 0$ (i.e. those containing $m\theta$); long periodic terms have both $l - 2p + q = 0$ and $m = 0$. We shall use the following notation :

$$R = \overline{R} + \hat{R} + \tilde{R} \qquad (3)$$

where $\overline{R}$ contains only the long periodic terms, $\hat{R}$ only the medium periodic terms, $\tilde{R}$ only the short periodic ones.

Thus we can formally define the mean elements by saying that they are such that the equations of motion for them contain only the derivatives of $\overline{R}$. The algorithm we want to define contains two stages : first the short periodic perturbations (containing the derivatives of $\hat{R} + \tilde{R}$) are removed, second we truncate $\overline{R}$ in such a way to obtain an integrable system, which we can solve in closed form.

As already explained, the theory is to be used for the mission analysis of low lunar polar orbiters. Low orbits imply low eccentricities, e.g. for an orbit with a mean altitude of $100\,Km$ eccentricities larger than about 0.06 result in crash against the Moon in the periselenium. Low eccentricities, in turn, require using of the variables which are not singular for $e = 0$. Therefore we switched to the nonsingular variables :

$$h = e \sin \omega; \qquad k = e \cos \omega \qquad (4)$$

For other elements such a switch was not necessary, and we eventually started with Lagrangian equations of motion in mixed variables :

$$\frac{da}{dt} = \frac{2}{na}\frac{\partial R}{\partial \lambda}$$

$$\frac{dh}{dt} = \frac{\beta}{na^2}\frac{\partial R}{\partial k} - k\frac{\cot I}{na^2\beta}\frac{\partial R}{\partial I}$$

$$\frac{dk}{dt} = -\frac{\beta}{na^2}\frac{\partial R}{\partial h} + h\frac{\cot I}{na^2\beta}\frac{\partial R}{\partial I}$$

$$\frac{dI}{dt} = \frac{\cot I}{na^2\beta}\frac{\partial R}{\partial \omega} - \frac{1}{na^2\beta \sin I}\frac{\partial R}{\partial \Omega}$$

$$\frac{d\Omega}{dt} = \frac{1}{na^2\beta \sin I}\frac{\partial R}{\partial I} \tag{5}$$

where $\beta = \sqrt{1-e^2}$

2. 2. DYNAMICS OF THE MEAN ELEMENTS

Now let us start by discussing long periodic perturbations, that is the effect of the perturbing potential $\overline{R}$, and by ignoring $\hat{R}+\tilde{R}$; hence, we are considering the dynamics in the phase space of the mean elements.

The perturbing potential $\overline{R}$ contains only the terms of the expansion (2) in which $l-2p+q=0$ and $m=0$, therefore only the so called "zonal" harmonics of the gravity field :

$$\overline{R} = \frac{GM}{a}\sum_{l=2}^{+\infty}\left(\frac{R_M}{a}\right)^l C_{l0}\sum_{p=0}^{l} F_{l0p}(I)G_{lpq}(e)S_q(\omega) \tag{6}$$

$$S_q(\omega) = \begin{cases} \cos(-q\omega) & (l \text{ even}) \\ \sin(-q\omega) & (l \text{ odd}) \end{cases}$$

$$q = 2p - l$$

Let us next expand the eccentricity function in powers of eccentricity $G_{lpq}(e) = g^0_{lpq}e^{|q|} + g^1_{lpq}e^{|q|+2} + \ldots$, where the upper index of g denotes merely that this is the coefficient of the first (g^0), second (g^1), etc. term in the development. The truncation to degree 2 in eccentricity e (that is in h, k) implies that the value of the index q must be between -2 and $+2$; since in the long periodic terms $q = 2p - l$, then for a given value of l there are only few possible values of p. For even $l = 2s$, $p = s, s+1, s-1$ are the only admissible values; for odd $l = 2s+1$, p can only be $s, s+1$. As a result for each value of s there are only 5 terms to be computed. The final result can be expressed by means of only four quantities A, C, D, W, each a function of a and of the inclination I only :

$$\sigma = \frac{GM}{na^3}\beta\left(\frac{R_M}{a}\right)^2 = n\beta\left(\frac{R_M}{a}\right)^2 \approx n\left(\frac{R_M}{a}\right)^2$$

$$A = \sigma\sum_{s=1}\left(\frac{R_M}{a}\right)^{2s-2} C_{2s,0}F_{2s,0,s}(I)g^1_{2s,s,0}\,2$$

$$C = \sigma\sum_{s=1}\left(\frac{R_M}{a}\right)^{2s-2} C_{2s,0}\left[F_{2s,0,s+1}(I)g^0_{2s,s+1,2} + F_{2s,0,s-1}(I)g^0_{2s,s-1,-2}\right]2$$

$$D = \sigma\sum_{s=1}\left(\frac{R_M}{a}\right)^{2s-1} C_{2s+1,0}\left[F_{2s+1,0,s}(I)g^0_{2s+1,s,-1} - F_{2s+1,0,s+1}(I)g^0_{2s+1,s+1,1}\right]$$

β disappearing since $\beta \approx 1 + O(e^2)$. The equations of motion (5) for the nonsingular variables h, k, when truncated to degree 1, then become :

$$\frac{dh}{dt} = (A + C)k - Wk + O(h^2 + k^2)$$

$$\frac{dk}{dt} = -(A - C)h + Wh - D + O(h^2 + k^2) \tag{7}$$

If $R = \overline{R}$, the component of the angular momentum along the lunar polar axis is an integral of motion : $H = \sqrt{GMa(1-e^2)}\cos I = const$, thus a separate equation of motion for I is not needed; the semimajor axis a is also constant, since the mean anomaly ℓ does not appear in the potential. If the orbit is nearly polar, then the changes in inclination are small : this can be deduced by differentiating the integral H, from which we obtain, by using (5) :

$$\frac{dI}{dt} = -\frac{\cos I}{\sin I\,\beta^2}\left(h\frac{dh}{dt} + k\frac{dk}{dt}\right) = \frac{\cos I}{\sin I}\,k\,D + O(h^2 + k^2) \tag{8}$$

While equation (8) is applicable for every inclination, if the orbit is nearly polar, with $\cos I = O(e)$, then all the right hand side is $O(e^2)$ and can be neglected in our truncation. Thus we can assume that the coefficients A, C, D, W in (7) are constant. Equation (7), once $O(e^2)$ and $O(e\cos I)$ have been neglected, is a system of linear differential equations with constant coefficients.

Geometrically, it is clear that (7) has a single equilibrium point for $k = 0, h = h_F$ with :

$$h_F = \frac{D}{C - A + W} \tag{9}$$

Thus there is a particular solution of the long periodic equation which has constant mean h and k; this *frozen orbit* has eccentricity $e_F = |h_F|$. The existence of a frozen orbit with nonzero eccentricity results from $D \neq 0$, that is from the presence of odd

zonals, i.e. from the asymmetry between the northern and southern hemispheres of the Moon. The other solutions describe ellipses in the mean h, k plane (see Figure 1).

We define the proper eccentricity e_P as the length of the semiaxis of these ellipses in the h direction. $e_P = 0$ for the frozen orbit. The proper argument of periselenium ω_P is the phase of the solution of the linear equation (7), thus it is –within our approximation– a linear function of time. The frequency Λ_1 of ω_P is small, corresponding to periods of a few years; for this reason the separation of the long periodic perturbations from the short periodic ones is justified.

The proper inclination I_P is such that

$$\cos I_P = \sqrt{1 - e^2} \cos I \tag{10}$$

I_P can be described as the value of I_P corresponding to the origin in the h, k plane on the $\sqrt{1 - e^2} \cos I = const$ surface, that is $\cos I_P$ is the minimum value compatible with this integral. For the longitude of the node Ω, starting from the usual Lagrange equation :

$$\frac{d\Omega}{dt} = \frac{1}{na^2\beta \sin I} \frac{\partial R}{\partial I} \tag{11}$$

and by the same method we obtain :

$$\frac{d\Omega}{dt} = V + Zh + O(h^2 + k^2) \tag{12}$$

and V and Z can be considered as constants by the same argument as above. In this way we can derive a solution for the long periodic perturbations on Ω, which revolves with average frequency Λ_2, also very small.

2. 3. DYNAMICS OF THE OSCULATING ELEMENTS

To build a theory of short periodic perturbations let us recall the distinction between medium and very short period perturbations, that is the splitting of the perturbing potential R into three parts $R = \overline{R} + \hat{R} + \tilde{R}$.

Since the medium period perturbations on the eccentricity are much larger than the very short periodic ones, let us first handle $\hat{R}$.

2.3.1 *Medium periodic perturbations*

The medium period part of the perturbing function is :

$$\hat{R} = \frac{GM}{a} \sum_{l=2}^{+\infty} \left(\frac{R_M}{a} \right)^l \sum_{m=1}^{l} \sum_{p=0}^{l} F_{lmp}(I) G_{lpq}(e) J_{lm} S_{lmp}(\omega, \Omega, \theta), \tag{13}$$

where $q = l - 2p$ and $m \neq 0$ to isolate the medium periodic terms. The trigonometric part is defined as follows :

$$S_{lmp} = \begin{cases} \cos \\ \sin \end{cases} [(-q)\omega + m(\Omega - \theta) - \delta_{lm}] \quad \begin{cases} l - m & \text{even} \\ l - m & \text{odd} \end{cases} \tag{14}$$

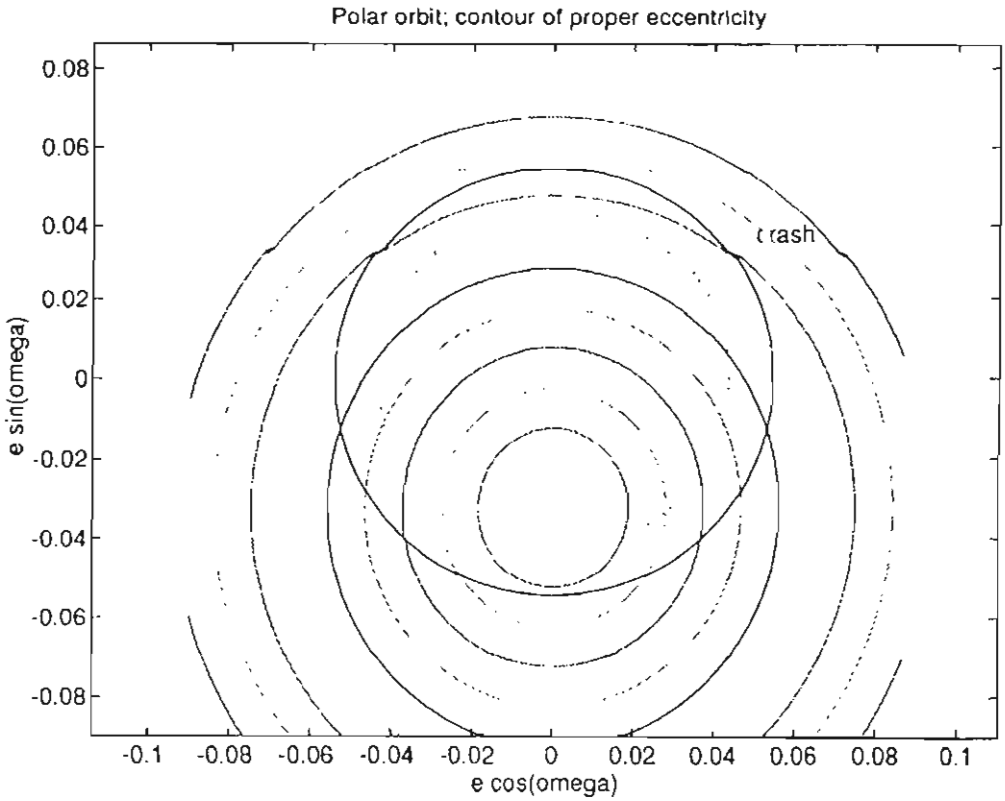

Fig. 1. Contour curves of the proper eccentricity in the mean k, h plane. The solutions of the long periodic perturbations equations move clockwise along these curves. When the distance from the origin in this plane, that is the mean eccentricity, grows too much, hard landing occurs. This plot is for a mean inclination of exactly 90° and for the Konopliv et al. (1993) model of the lunar potential.

In these formulas the harmonic coefficients C_{lm}, S_{lm} have been replaced by the corresponding amplitude and phase J_{lm}, δ_{lm} :

$$J_{lm} = \sqrt{C_{lm}^2 + S_{lm}^2}; \qquad \delta_{lm} = \arctan \frac{-S_{lm}}{C_{lm}} \tag{15}$$

To compute the medium period perturbations we use a canonical transformation method. To do this, we need to adopt a canonical coordinate system which also removes the $e = 0$ singularity (but not the $I = 0$ singularity); this is accomplished by a small modification of the coordinate system introduced by Poincaré :

$$\left\{\begin{array}{l}\omega\\ \ell\\ \Omega\\ G\\ L\\ H\end{array}\right\} \longrightarrow \left\{\begin{array}{l}\xi = \sqrt{2L-2G}\cos\omega\\ \lambda = \ell + \omega\\ \Omega\\ \eta = \sqrt{2L-2G}\sin\omega\\ L\\ H\end{array}\right\} \tag{16}$$

where :

$$L = \sqrt{\mu a}; \qquad G = \sqrt{\mu a(1-e^2)}; \qquad H = \sqrt{\mu a(1-e^2)}\cos I\,. \tag{17}$$

The Hamilton function in these variables is :

$$F(\lambda, \xi, \Omega, L, \eta, H; \theta) = \frac{GM}{2L^2} + R \tag{18}$$

where θ, the phase of the lunar rotation, is a known linear function of time :

$$\frac{d\theta}{dt} = \nu \tag{19}$$

Note again that for the medium period perturbations $\hat{R}$ does not depend on the fast variable λ (ω being incorporated into ξ, η) :

$$\hat{F}(-, \xi, \Omega, L, \eta, H; \theta) = \frac{GM}{2L^2} + \overline{R} + \hat{R}; \quad \text{and} \quad \frac{dL}{dt} = 0 \tag{20}$$

In order to remove terms with $m\theta$ we perform the canonical transformation :

$$\hat{F}(\xi, \Omega, \eta, H; L, \theta) = \hat{F}'(\xi', \Omega', \eta', H'; L) \tag{21}$$

Notice that the variable L does not play any rôle as a dynamical parameter and does not need to be transformed; the purpose of the transformation is to eliminate the dependency on θ, that is all the medium period terms from the Hamiltonian. This transformation is performed by means of the generating function in mixed variables $\mathbf{q} = (\xi, \Omega)$ being the coordinates, and $\mathbf{p} = (\eta, H)$ being the momenta :

$$\begin{aligned} S = S(\mathbf{q}, \mathbf{p}') &= \xi\eta' + \Omega H' + \hat{S}_1 \\ \hat{S}_1 &= \int \hat{R}\, dt \end{aligned} \tag{22}$$

so that :

$$\begin{aligned} p_i &= p_i' + \frac{\partial \hat{S}_1}{\partial q_i} \\ q_i &= q_i' - \frac{\partial \hat{S}_1}{\partial p_i'} \end{aligned} \tag{23}$$

We would like to stress that the need to use this method, rather than the simpler non canonical perturbation theory, arises from the particular properties of the problem. In the low altitude lunar satellite case, the medium period perturbations on h, k are comparatively large with respect to the initial values of the same variables; actually, in many mission analysis simulations, the initial value is $e = 0$, that is $h = k = 0$. Therefore it is not consistent to compute a first order perturbation by setting the values of the variables h, k in the right hand side at their initial values, otherwise most of the right hand side just disappears when initial $e = 0$. Truncation to degree 1 in eccentricity can be performed consistently also with the non canonical formalism, but truncation to order 1 in the perturbations to h, k result in an inconsistent approximation. We have therefore adopted a method which does not truncate the transformation, but fully accounts for the implicit nature of the transformation equations, without replacing old variables for the new ones in the right hand side. In essence, since the equations are linearised, our method is a form of the Newton's method normally used to prove the results of the KAM (Kolmogorov, Arnold, Moser) theory.

Having defined the formalism, the detailed computations are very similar to the ones performed for the long periodic perturbations. The generating function $\hat{S}_1$ is truncated to degree 2 in e, and again the number of terms is reduced to three for each harmonic l, m with l even, and two for each harmonic l, m with l odd. Then the derivatives of $\hat{S}_1$ are computed with respect to the non singular variables h', k and transformed into the derivatives with respect to η', ξ by means of the equations :

$$\begin{aligned} \frac{\partial \hat{S}_1}{\partial \eta} &= \frac{1}{\sqrt{L}} \frac{\partial \hat{S}_1}{\partial h} - h \frac{\cot I}{\sqrt{L}\beta} \frac{\partial \hat{S}_1}{\partial I} \\ \frac{\partial \hat{S}_1}{\partial \xi} &= \frac{1}{\sqrt{L}} \frac{\partial \hat{S}_1}{\partial k} - k \frac{\cot I}{\sqrt{L}\beta} \frac{\partial \hat{S}_1}{\partial I} \end{aligned} \tag{24}$$

Then we can switch back to the usual non singular variables h, k by using :

$$k = \frac{\xi}{\sqrt{L}} + O(e^3); \qquad h = \frac{\eta}{\sqrt{L}} + O(e^3) \tag{25}$$

and the final transformation equations have the form :

$$A \begin{pmatrix} h' \\ k' \end{pmatrix} = B \begin{pmatrix} h \\ k \end{pmatrix} + C \tag{26}$$

which are implicit equations (because of the mixed variables appearing in the generating function $\hat{S}_1$), but linear (because of the truncation to degree 1 in h, k). Therefore they can be solved simply by :

$$\begin{pmatrix} h' \\ k' \end{pmatrix} = A^{-1} \left[B \begin{pmatrix} h \\ k \end{pmatrix} + C \right] \tag{27}$$

The 2x2 matrices A, B have as entries linear combinations of even harmonic coefficients, while the vector C contains linear combinations of odd harmonics :

$$A = \begin{pmatrix} 1 + \sum_{s=1} \sum_{m=1}^{2s} \frac{1}{-m\nu} C^-_{2s,m} \begin{bmatrix} \cos \\ \sin \end{bmatrix} \Psi_{2s,m} & 0 \\ -\sum_{s=1} \sum_{m=1}^{2s} \frac{1}{-m\nu} (A_{2s,m} - C^+_{2s,m} - W_{2s,m}) \begin{bmatrix} \sin \\ -\cos \end{bmatrix} \Psi_{2s,m} & 1 \end{pmatrix}$$

$$B = \begin{pmatrix} 1 & -\sum_{s=1} \sum_{m=1}^{2s} \frac{1}{-m\nu} (A_{2s,m} + C^+_{2s,m} - W_{2s,m}) \begin{bmatrix} \sin \\ -\cos \end{bmatrix} \Psi_{2s,m} \\ 0 & 1 + \sum_{s=1} \sum_{m=1}^{2s} \frac{1}{-m\nu} C^-_{2s,m} \begin{bmatrix} \cos \\ \sin \end{bmatrix} \Psi_{2s,m} \end{pmatrix}$$

$$C = \begin{pmatrix} \sum_{s=1} \sum_{m=1}^{2s+1} \frac{1}{-m\nu} D^+_{2s+1,m} \begin{bmatrix} -\sin \\ \cos \end{bmatrix} \Psi_{2s+1,m} \\ \sum_{s=1} \sum_{m=1}^{2s+1} \frac{1}{-m\nu} D^-_{2s+1,m} \begin{bmatrix} \cos \\ \sin \end{bmatrix} \Psi_{2s+1,m} \end{pmatrix}$$

where (introducing again compact notation) :

$$A_{2s,m} = \sigma \left(\frac{R_M}{a} \right)^{2s-2} J_{2s,m} F_{2s,m,s}(I) g^1_{2s,s,0} 2$$

$$C^+_{2s,m} = \sigma \left(\frac{R_M}{a} \right)^{2s-2} J_{2s,m} \left[F_{2s,m,s-1}(I) g^0_{2s,s-1,-2} + F_{2s,m,s+1}(I) g^0_{2s,s+1,2} \right] 2$$

$$C^-_{2s,m} = \sigma \left(\frac{R_M}{a} \right)^{2s-2} J_{2s,m} \left[F_{2s,m,s-1}(I) g^0_{2s,s-1,-2} - F_{2s,m,s+1}(I) g^0_{2s,s+1,2} \right] 2$$

$$D^+_{2s+1,m} = \sigma \left(\frac{R_M}{a} \right)^{2s-1} J_{2s+1,m} \left[F_{2s+1,m,s}(I) g^0_{2s+1,s,-1} + F_{2s+1,m,s+1}(I) g^0_{2s+1,s+1,1} \right]$$

$$D^-_{2s+1,m} = \sigma \left(\frac{R_M}{a} \right)^{2s-1} J_{2s+1,m} \left[F_{2s+1,m,s}(I) g^0_{2s+1,s,-1} - F_{2s+1,m,s+1}(I) g^0_{2s+1,s+1,1} \right]$$

$$W_{2s,m} = \sigma \left(\frac{R_M}{a} \right)^{2s-2} J_{2s,m} \cot I \, \frac{dF_{2s,m,s}(I)}{dI} \, g^0_{2s,s,0}$$

The medium periodic perturbations on H (hence I) and Ω are computed directly from :

$$H = H' + \frac{\partial \hat{S}_1}{\partial \Omega}; \qquad \Omega = \Omega' - \frac{\partial \hat{S}_1}{\partial H'} \tag{28}$$

In this case we do not need, to the level of approximation we are using, to account for the mixed variables appearing in $\hat{S}_1$, and therefore for the implicit nature of equations (28), because our theory is meant to be used for mission analysis, thus the accuracy in inclination does not need to be as high as in eccentricity (changes in $\sin I$ of a few 0.01 cannot result in hard landing). The theory could be improved by using the same Newton's method formalism -used for k, h'- also for the variables Ω, H', if this is required.

2.3.2 *Very short periodic perturbations*

The most important perturbations with a very short period are the ones on the semimajor axis; on the semimajor axis there are perturbations neither with long nor with medium periods. The very short periodic perturbations on h, k, I, Ω are small and therefore less important, but they can be accounted for by an analogous procedure if the accuracy requirements are strict.

The relevant very short periodic part of the perturbing function can be expanded as follows. Let us first introduce :

$$\Theta_{lmr} = r\lambda + m(\Omega - \theta) - \delta_{lm}; \quad \lambda = l + \omega; \quad r = l - 2p + q; \quad \frac{d\Theta_{lmr}}{dt} = rn - m\nu \tag{29}$$

Then (always truncating at the same level of approximation) :

$$\tilde{R} = \frac{GM}{a} \sum_{l=2} \left(\frac{R_M}{a}\right)^l \sum_{m=0}^{l} \sum_{p=0}^{l} F_{lmp}(I) \sum_{q=-1}^{1} g^0_{lpq} e^{|q|} J_{lm} \begin{Bmatrix} \cos \\ \sin \end{Bmatrix} (\Theta_{lmr} - q\omega) + O(e^2) \tag{30}$$

where the summation should be performed only for the terms with $r = l - 2p + q \neq 0$. Then, by using the usual Lagrange equation for the semimajor axis :

$$\frac{1}{a}\frac{da}{dt} = \frac{2}{na^2}\frac{\partial \tilde{R}}{\partial \lambda} \tag{31}$$

the very short periodic perturbations can be directly computed.

3. RESULTS

In order to illustrate the behaviour of a low lunar polar orbit, we have plotted in Fig. 2 the time evolution (for about one lunar month) of the osculating values of non-singular orbital elements h, k. All the three periodicities involved are clearly visible in the plot : the very short period changes (of the amplitude of $\approx 2 - 3 \times 10^{-4}$) are superimposed onto the medium period variations (amplitude $\approx 5 \times 10^{-3}$), while the long period variation appears as an overall trend roughly in the direction upper left to lower right corner of the plot. The data for this plot come from numerical integration in which use was made of the GEODYNE software system, with Konopliv et al. (1993) 60×60 model of the lunar gravity field (R. Floberghagen, private communication).

In order to assess the accuracy, reliability and efficiency of the algorithm we developed on the basis of the described theory, we have performed a great number of different tests. Here, however, we shall report only on two kinds of tests, those which in the most straightforward and compact way show the quality of our results. The first test consists of the computation of proper elements for each input record, containing osculating elements output from the numerical integrator. The result of the test can be assessed in the simplest way by computing the RMS of the deviations of the proper elements, as computed, from their average value. Since a perfect proper element should be exactly constant, this RMS measures the inaccuracy resulting from the truncations and approximations performed in the computation.

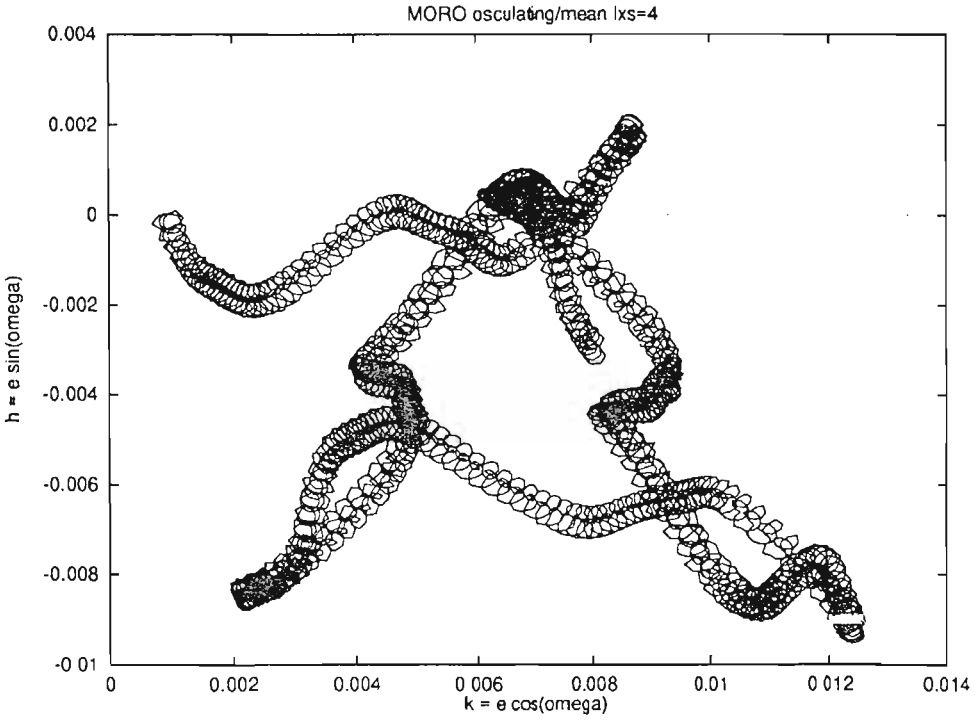

Fig. 2. Osculating h vs. k plane. Variations due to perturbations of three different periodicities are clearly distinguished in the plot. Numerical integration from GEODYNE; time span about one lunar month.

In Figure 3, we thus compare osculating and proper semimajor axis time variations; in Figure 4, the corresponding variations of the inclination are given, while in Figure 5, the same is shown for the eccentricity. Numerical integrations used in these plots are made with the USOC software system (G. Lecohier, private communication), and pertains to a polar orbiter with a mean altitude of 100 Km, initial eccentricity 0.02 and initial $\omega = 270°$. The lunar gravity potential used was the Lemoine et al. (1994) 70x70 model, which includes the Clementine tracking data. Integration included only the effects of the Moon (remember that our theory in the present version does not include the other effects, in particular the Earth). The selenographic longitude of the node corresponds to nearly 0° at date 2000/1/1/ 00 : 00 : 00. This orbit "decays" after 275 days (perilune goes below 20 km).

Although there are still some unremoved oscillations of the proper values left (in particular the trend of increase with time of the amplitude of proper eccentricity; see later), the overall conclusion is that the results are very good. The proper semimajor axis variations are astonishingly small ($\leq$ 13 meters only), while the rms's of both

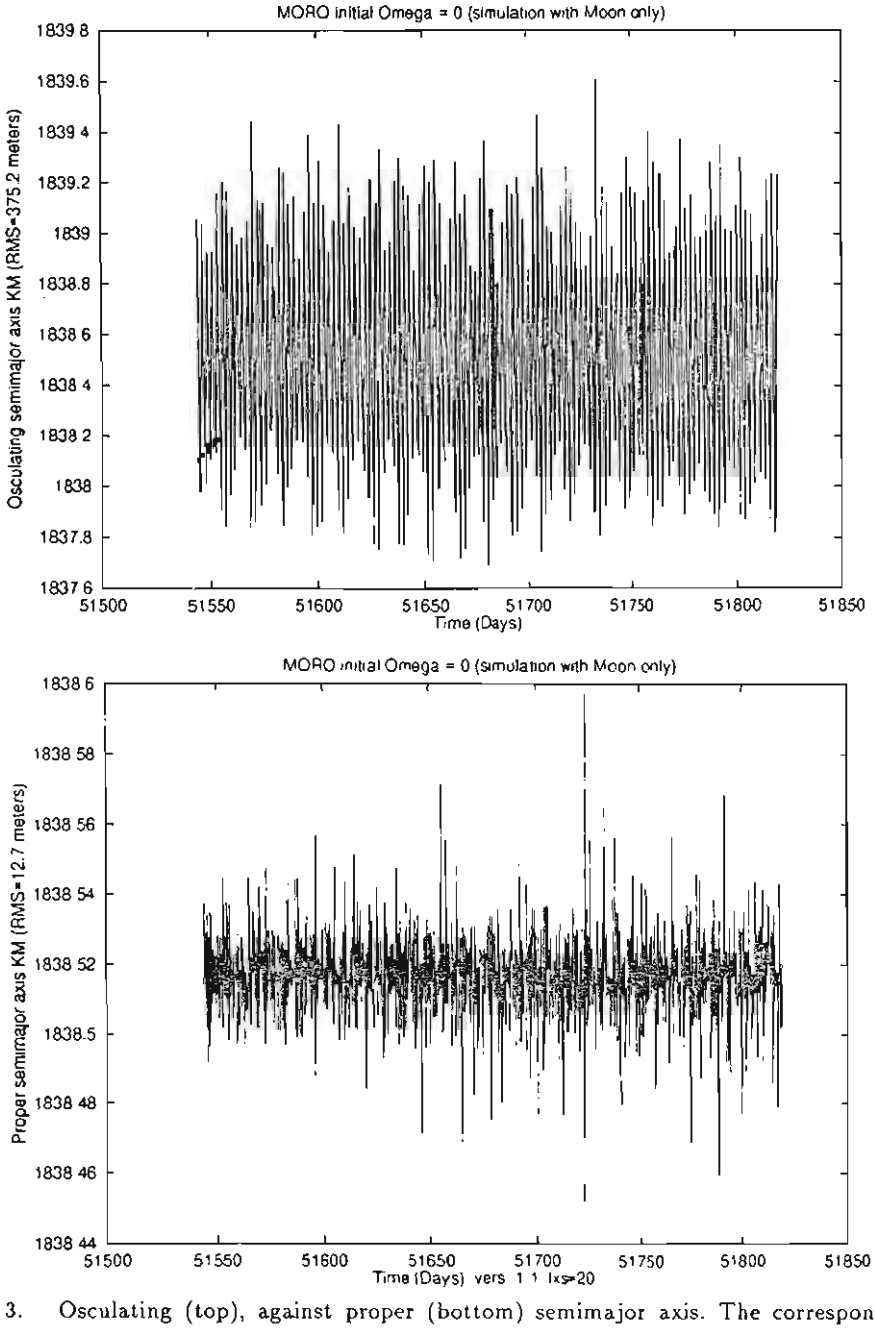

Fig. 3. Osculating (top), against proper (bottom) semimajor axis. The corresponding RMS's are given in the labels of y-axes; note the difference of the y-scales. Numerical integration from USOC, period 275 days.

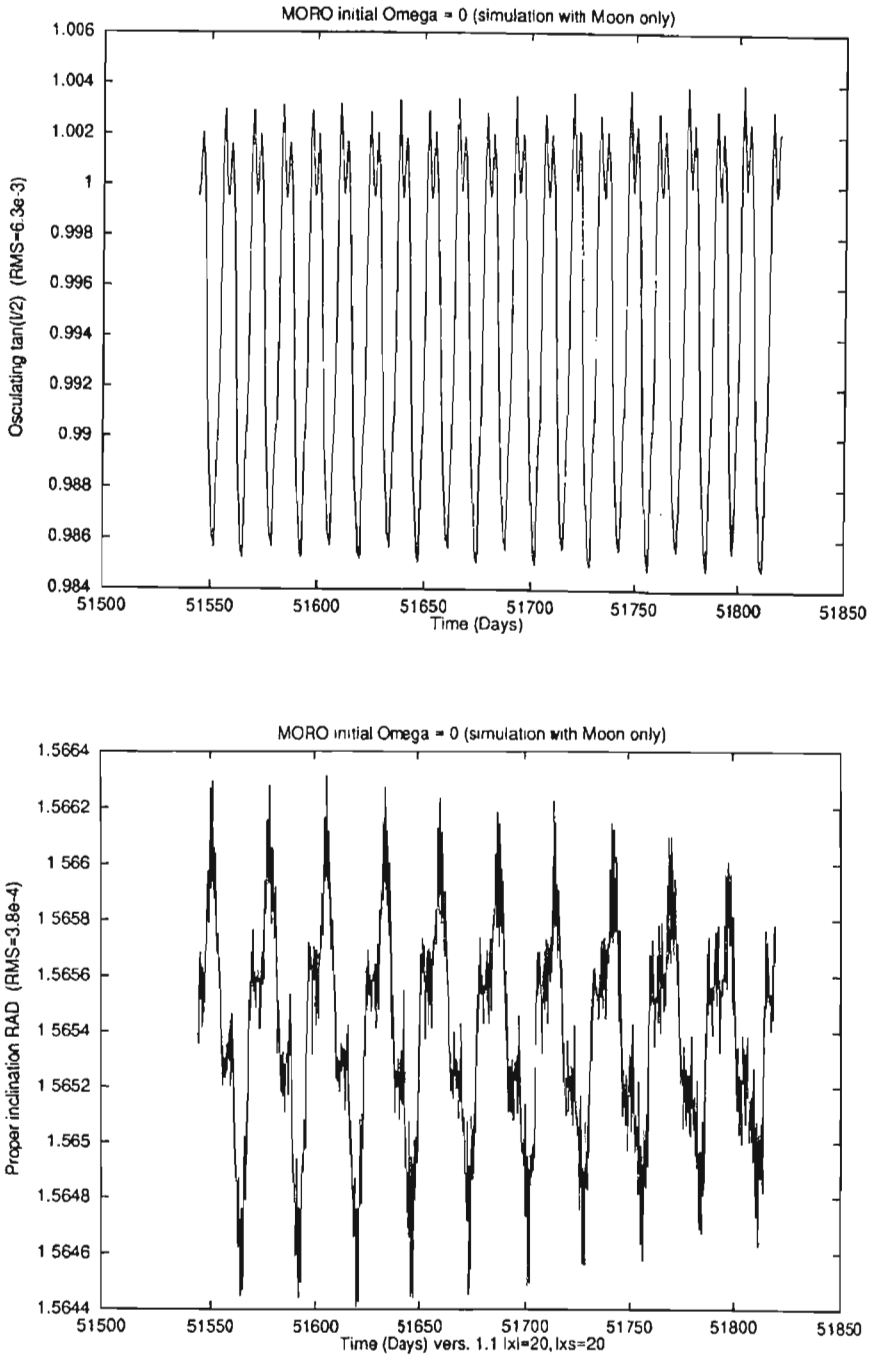

Fig. 4. The same as Figure 3, but for the inclination. Note that osculating values (top) are given in terms of the $\tan I/2$, while proper ones (bottom) are in terms of the inclination itself.

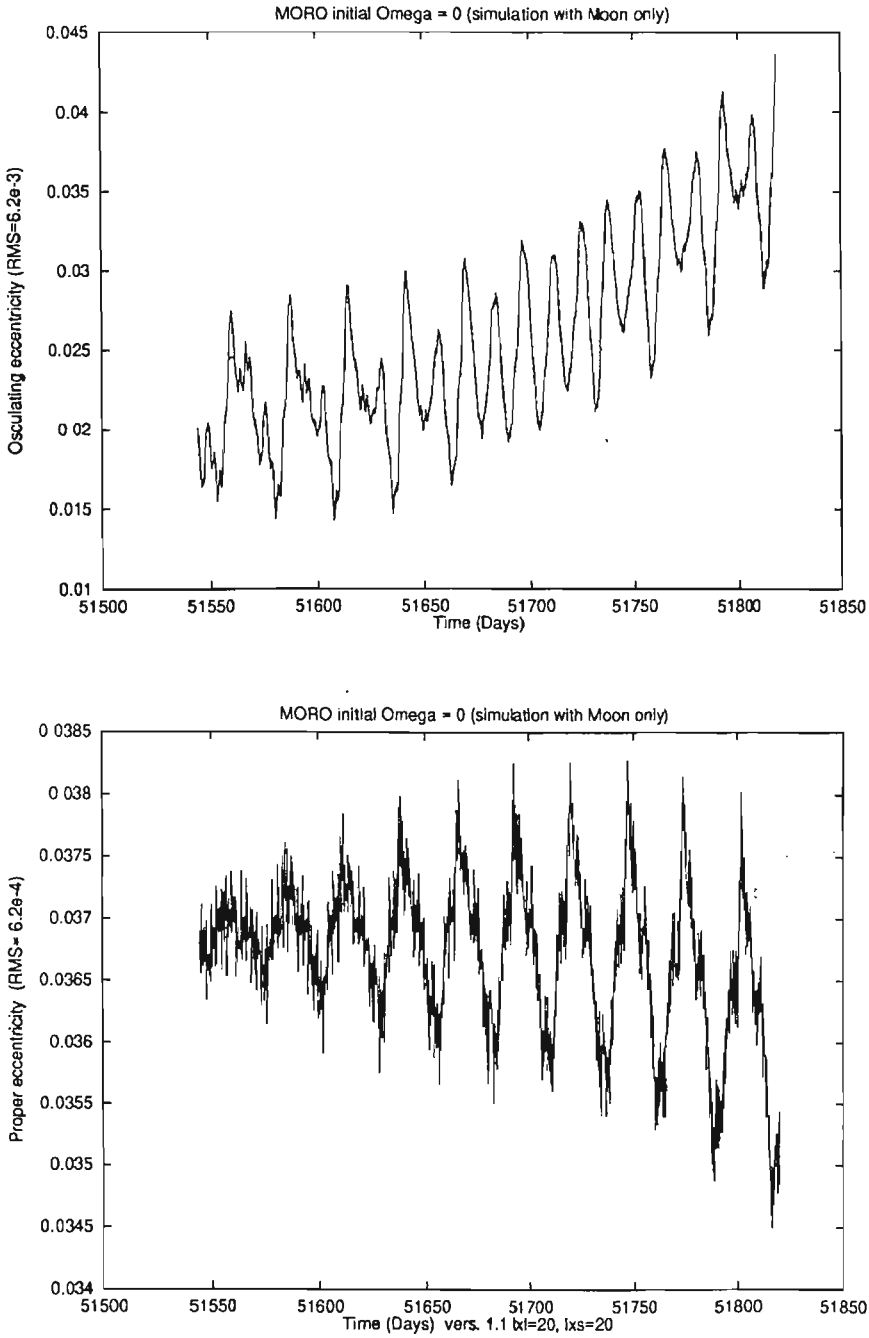

Fig. 5. The same as Figure 3, but for the eccentricity. The trend of increase with time of the amplitude of proper eccentricity is due to second order effects and/or to effects from harmonics of degree higher than 20.

proper inclination (in radians) and (more important) of proper eccentricity are less than 10^{-3}, which is more than enough for the mission analysis purposes.

The second test is even more demanding : we have computed analytically a solution for the same time span of the numerical test. What we do in fact is to compute the proper elements for the initial instant of the numerical integration, propagate them analytically for a span of time covered by integration, and recompute the osculating values for these instants of time for which the values are sampled in the numerical integration. Then we compute the difference between the analytical and the numerical solution.

In Figures 6 and 7 differences of the analytically propagated and the osculating values of h, k and $\tan I/2$ are shown, for the same USOC integration decribed above and lasting 275 days. Harmonics up to 20×20 are used in the computation, with coefficients taken again from the lunar gravity field model by Lemoine et al. (1994). The trend apparent in the differences of h, k is due to second order effects and/or to effects from harmonics of degree higher than 20. However, for about 6 months (more than enough with respect to typical duration of a mission) theory provides solution at the entirely satisfactory 0.001 level of accuracy in eccentricity. Hence, one can conclude that, although the analytical theory is not meant to provide precise ephemerides of the satellite, but only to study the qualitative long term behaviour of the orbit (e.g. for manoeuver planning purposes), this test shows its capability to actually predict the orbit in a qualitatively correct way and even quantitatively with a reasonable accuracy, more than presumably it is needed for the preliminary mission analysis required in the mission definition phase.

4. LIMITATIONS OF THE CURRENT THEORY

Let us in conclusion briefly discuss limitations of the current theory. We have already mentioned afore some open problems, which are responsible for the remaining errors and uncertainties of the presently achievable results, but represent at the same time the possibilities for future developments and improvement.

The theory described in this paper employes some assumptions and performs some truncations and simplifications with respect to a complete problem. The choices we have made correspond to the requirements arising from its use for the purpose of the preliminary mission analysis of a low lunar polar orbiter. However, these assumptions and simplifications ought to be explicitly stated, to be able to remove them if later the need arises for a theory capable of higher accuracy and/or more general applicability. In this section we list all these limitations, together with a few comments on what should be done to remove each one of them.

As for the effects not included in the current version, perturbations by the Earth are not accounted for, but are of a size relevant for a more accurate solution. Given the theory available from Kaula (1962), we anticipate no special difficulty in including these effects both in the long and in the short periodic perturbations. Gravitational perturbations from the Sun are smaller (by a factor $\simeq 200$) than those of the Earth, therefore they will not be needed, unless an extremely accurate theory is required for real time operations. On the contrary the effects of radiation pressure can be relevant,

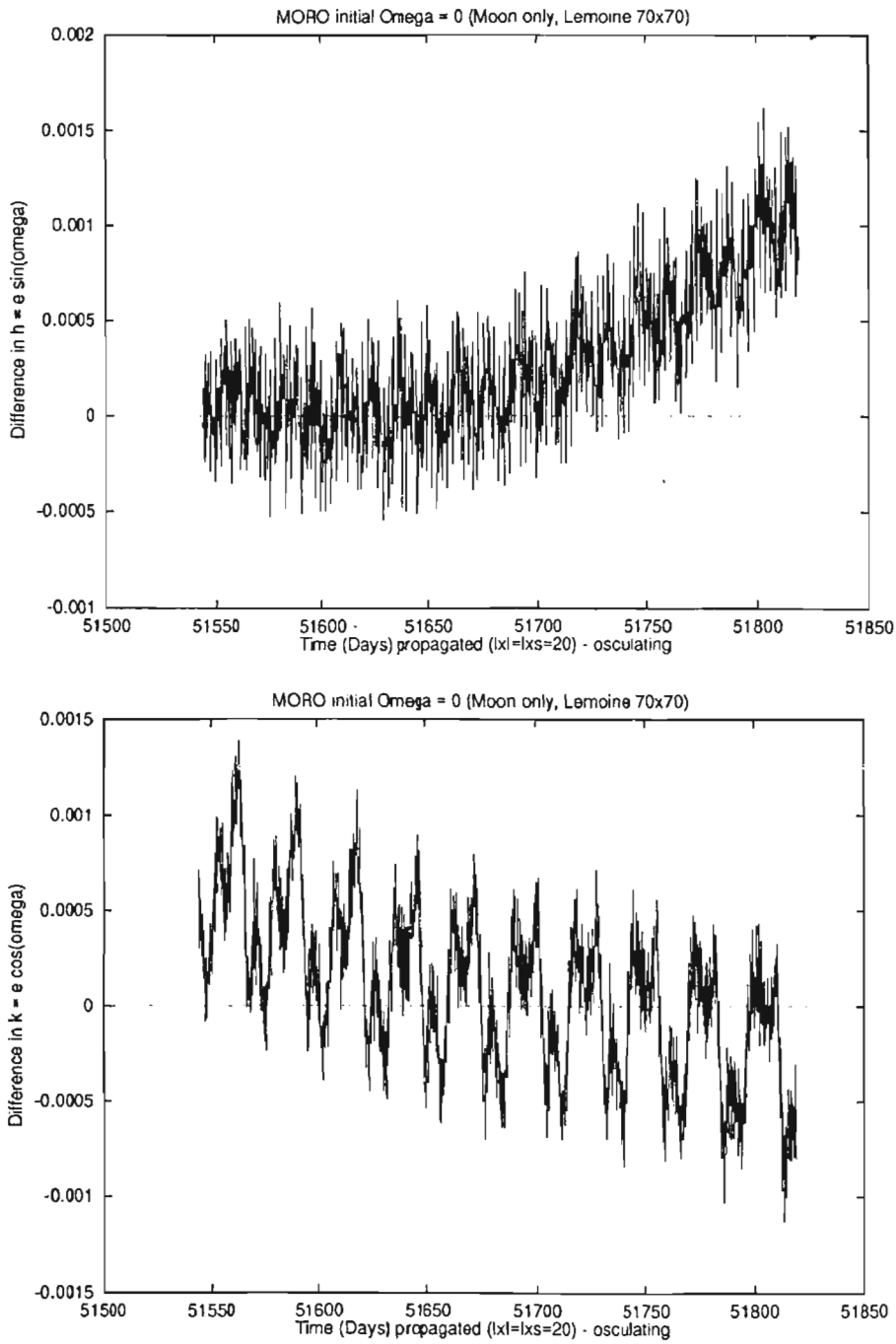

Fig. 6. Differences of the analytically propagated values of h (top) and k (bottom) and their counterparts coming from the numerical integration.

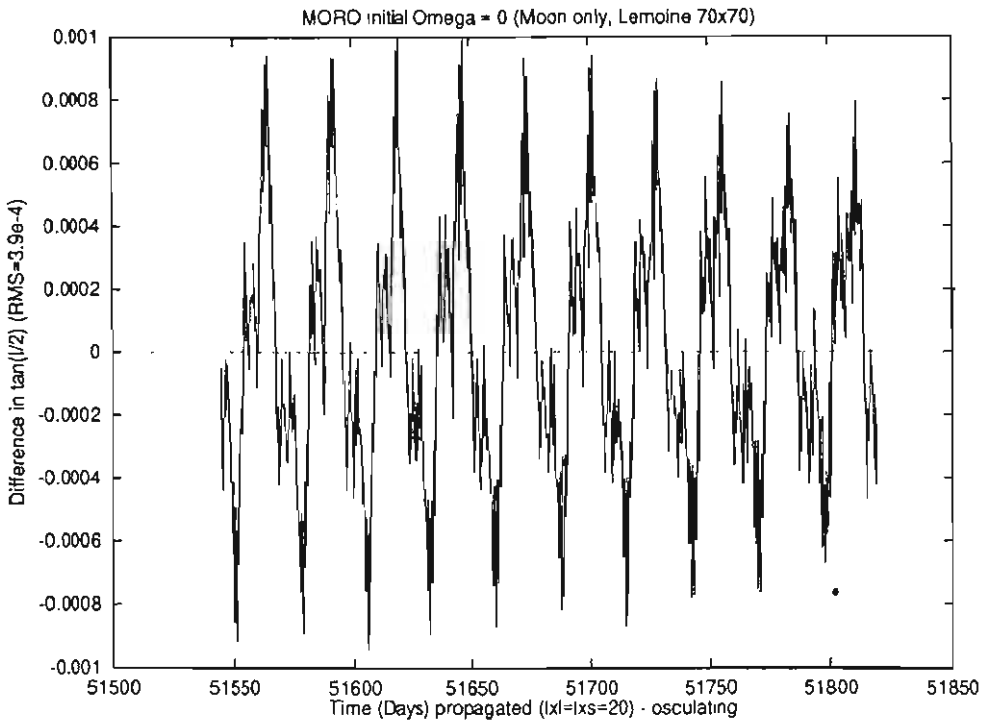

Fig. 7. The same as Figure 6, but for the $\tan I/2$.

at least when the lunar satellite undergoes eclipses (Milani et al., 1987); in one of the test we performed, the change in proper semimajor axis due to the long periodic effects of radiation pressure accumulates to $\simeq 50\,m$. An analytic theory of radiation pressure would be possible, but requires additional effort.

By using the semianalytical integration (that is, numerical integration of the analytical perturbation equations), and comparing it with the results of a purely analytical propagation, we have been able to measure the size of the neglected second order effects. This difference has a medium periodic component (mostly $m = 1, 2, 3$) and a long periodic component, which accumulates to about 0.001 in h, k over 275 days. This source of error was considered unimportant at this stage of development of mission analysis tools, because the uncertainty in the lunar potential results in a much larger uncertainty in the long term behaviour. However, the inclusion of the main second order long periodic effects is certainly a worthwhile upgrade of our theory, which would become necessary when a better model of the lunar gravity field will be available.

As pointed out in Section 2 (see comment with eq. (28)), we have chosen to replace I' with I in the mixed variable generating function, when the perturbations on I and

Ω are computed. This results in lower accuracy with respect to the full solution of the implicit equations, which was adopted for the h, k variables. This choice is justified by the lower accuracy required in the inclination, with respect to the eccentricity, for mission analysis purposes. This limitation could be removed by the use of the same algorithm, namely one step of Newton's method, to the whole set of four variables $h, k, \Delta I, \Delta\Omega$.

The current version of our theory is not suitable to compute the perturbations due to very high harmonics, e.g. $l > 40$. Given the present state of the art for the lunar potential models, in which the harmonics of such a high degree mostly reflect the a priori constraints used in the collocation process, to compute the perturbations up to such a high l would be meaningless. However, when a reliable potential model will be available, it will become necessary to ensure enough performance and numerical stability even for high l. The main source of the loss of efficiency of our program for growing l is the enormous size of the files of coefficients of the inclination functions; the number of records in these files grows like l^4. The performance could be improved by taking full advantage of the truncation in the harmonics of the mean anomaly (that is by limiting the size of $r = l - 2p + q$). The loss of accuracy due to this truncation is not very large, and mostly affects the semimajor axis. On the orher hand, the numerical instability problems arise because the coefficients of the monomials in $\sin I$ in F_{lmp} grow very fast with l; e.g. these coefficients become larger than the inverse of the machine error for $l \simeq 50$. The resulting numerical instability could be avoided by expanding F_{lmp} in a neighbourhood of $I = 90°$.

The precession of the lunar pole results in a drift of the inclination in the true of date system (that is, with respect to the current lunar pole). After a few years, the inclination appearing in the coefficients $F_{lmp}(I)$ becomes noticeably different from the one in the true of epoch system we are using, and this results in a degradation of the solutions, because of a less accurate removal of medium periodic perturbations (mostly $m = 1$). This could be improved, if the need arises for a longer time span to be covered by mission analysis software, by explicitly accounting for this effect.

At the moment we are computing the very short periodic perturbations only for the semimajor axis. The very short periodic perturbations on h, k are less than 0.0005, thus their computation is not needed for the present requirements. However, the theory is available and these terms can be easily added if the need arises. We do not compute the perturbations on the mean anomaly, because we think that this element is not really used at all in mission analysis; again, this computation could be done if needed.

The approximation by which the coefficients of the long periodic equations (7) can be considered constant is not consistent for non polar orbits; the changes are of the order of $e \cos I$, hence they are of the second order if $\cos I$ is of the order of e. The very notion of a frozen orbit must be taken with some reserve for an orbit with low inclination.

As a matter of principle, most of our theory could be applicable to satellites of other bodies, including asteroids and comets. However, the modifications required are far from trivial, and they depend essentially on the ratios between the orbital and the rotation frequencies.

References

Davies, M. E., Abalakin, V. K., Brahic, A., Bursa, M., Chovitz, B. H., Lieske, J. H., Seidelmann, P. K., Sinclair, A. T. and Tjuflin, Y. S. : 1992, Report of the IAU/IAG/COSPAR working group on cartographic coordinates and rotational elements of the planets and satellites, *Celestial Mechanics*, **53**, 377–397.

Kaula, W. M. : 1962, Development of the lunar and solar disturbing functions for a close satellite, *A*stron. J. **67**, 300-303.

Kaula, W. M. : 1966, *Theory of Satellite Geodesy*, Blaisdell Publishing Company, Waltham, Toronto and London.

Konopliv, A. S., Sjogren, W. L., Wimberly, R. N., Cook, R. A. and Vijaraghavan, A. : 1993, A High Resolution Lunar Gravity Field and Predicted Orbit Behaviour *A*AS Paper, 93-622. Presented at the 1993 AAS/AIAA Astrodynamics Specialist Conference, Victoria, B.C..

Lemoine, F. G., Smith, D. E. and Zuber, M.T . : 1994, A 70th degree and order gravity model for the Moon, P11A-9, EOS, *T*rans. American Geophys. Union **75**, No. 44.

Milani, A. and Knežević, Z. : 1990, Secular Perturbation Theory and Computation of Asteroid Proper Elements. *Celestial Mechanics*, **49**, 347–411.

Milani, A. and Knežević, Z. : 1992, Asteroid Proper Elements and Secular Resonances. *I*carus, **98**, 211–232.

Milani, A. and Knežević, Z. : 1994, Asteroid Proper Elements and the Dynamical Structure of the Asteroid Main Belt, *I*carus, **107**, 219–254.

Milani, A., Nobili, A. M., and Farinella, P. : 1987, *Non gravitational perturbations and satellite geodesy*, A. Hilger, Bristol.

Publ. Obs. Astron. Belgrade No. 49 (1995), 41-56

TOMOGRAPHIC IMAGING OF SOLAR-TYPE STARS

PRELIMINARY RESULTS FROM MUSICOS 1992 CAMPAIGN

S. JANKOV

Astronomical Observatory, Volgina 7, 11050 Belgrade, Yugoslavia

E-mail sjankov@aob.aob.bg.ac.yu

Abstract. In the past decade the methods of Tomographic Imaging proved to be a powerful tool to spatially resolve the surface and environment of stars. These techniques of indirect stellar imaging from photometry and spectroscopy allow to obtain, from the light curve and line profile disturbances (observed with high signal-to-noise ratio, spectral resolution and adequate phase coverage), an information about spatial distribution of quasistationnary structures in stellar atmospheres and environments. They have a wide range of application in stellar physics, particularly providing a knowledge of crucial importance to understand the stellar magnetic activity and physical processes related to it. We describe the scientific interest for tomographic interpretation of temporal photometric or spectroscopic variability along the rotational phase of solar-type stars. The basic principle of Tomographic Imaging of stellar surfaces is described, as well as the problem of regularization arising from the ill-posed nature of the inversion. We present the practical application based on data obtained from MUlti SIte COntinuous Spectroscopy (MUSICOS) international network of high resolution spectrometers around the world and we discuss the importance of such a program for systematic observations of long term spectroscopic and photometric variations of solar-type stars for the study of starspot distribution, active region evolution, differential motions and cyclic activity on time scales of several years and decades, in order to provide the stellar equivalent to the study of solar activity.

1. INTRODUCTION

1.1. SOLAR-TYPE ACTIVITY ON STARS

The evidence collected from dedicated observations of several types of active stars in the past is strongly suggestive of a solar-type scenario with activity levels from the solar value to orders of magnitude higher. Activity phenomena are usually observed in red dwarfs, giants, T- Tauri and young stars, close late-type binaries because of deep convection zones and high rotation rates leading to differential rotation and efficient dynamos. They manifest themselves as flux variation in the continuum and emission lines over a wide range of wavelengths on timescales ranging from a few seconds, minutes (flares), hours and days (rotational modulation by active structures), to months and years (active region evolution, cyclic activity and differential motions).

The first evidence for stellar photospheric spots has been obtained from the photometric light curve periodic modulation. These quasi-sinusoidal flux variations are attributed (except an eventual eclipse) to the rotational modulation of a nonuniform distribution of photospheric spots. In the case of RS CVn and BY Dra systems the

slow migration (towards decreasing orbital phases) of these photometric waves has also been discovered (Catalano and Rodonò 1967), suggesting the change in the spot distribution over the surface. Systematic observations have shown almost sinusoidal light curves to become multipeaked or even flat, indicating also the variations in the spot number and size.

Some indirect indicators as the presence of TiO absorption bands in the spectra of fast rotating late-type stars in binary systems as HR 1099 implied that a substantial fraction of the photosphere must be spotted (Ramsey and Nations, 1980). By analogy with the Sun, the appearance of spots could be attributed to intense sub-photospheric magnetic fields which inhibit the convective energy transport until the surface. In particular the presence of dark spots and bright plages has been inferred from modeling the periodic low-amplitude photometric variations due to rotational modulation of spot-plage visibility (e.g. Rodonò et al 1986).

The rotational modulation of chromospheric emission in the Ca II H and K lines was shown for several RS CVn systems in the Mt Wilson H and K variability survey (Vaughan et al., 1981). Results from a joint IUE and ground based observations (Rodonò et al., 1987) have shown, for the RS CVn system II Peg, that the chromospheric and transition region emission reaches a maximum when the visible photometry is at minimum, thus indicating that chromospheric plages cover, in first approximation, an area correlated to the photospheric spots. Spot and plage modeling indicated that their physical characteristics are close to the solar ones, but they can cover up to 50% of the stellar surface (Byrne et al., 1987). Some empirical relations were established (Mangeney and Praderie 1984, Noyes et al. 1984) between the coronal or chromospheric activity and the rotational velocity through the Rossby number, suggesting that the heating is related to the production of magnetic energy through a dynamo mechanism. Also the rapid variations in X-ray, radio and in the optical occurring on dMe, RS CVn, T-Tauri, etc. stars are reminiscent of flares as observed on the Sun.

However, little was known about the actual distribution of those magnetic structures and activity phenomena before the advent of high signal-to-noise observations with CCD and Reticon detectors has stimulated the development of quantitative mathematical methods for studying the spatially resolved stellar surfaces by the means of Doppler Imaging methods. These methods allow, for the first time, to compare the photospheric images with the signatures of chromospheric, transition region or coronal emission, to describe the vertical stratification and energy balance of magnetic structures and to monitor the changes, associated with active region behaviour, over months and years in order to track differential motions, and constrain theories of internal rotation and dynamo.

1. 2. DEVELOPMENT OF DOPPLER IMAGING TECHNIQUE

The intensity rotational modulation gives a one dimensional projection in longitude of the surface structures. It provides an indirect way of *imaging* the star i.e. recovering the information not only in longitude L but also in latitude B. In a method developed by Deutsch (1970) for chemically peculiar stars, the variation of line equivalent widths has been adjusted by parameters describing the development in spherical harmonics

of the stellar surface inhomogeneities. This method did not make full use of the profile, mainly due to the low spectral resolution and low signal-to-noise ratio available then on photographic plate spectra.

Khokhlova and Ryabchikova (1970, 1975) and Falk and Wehlau (1974) proposed to use the full information contained in the line profile. Khokhlova and Ryabchikova modelised the local abundances for two Ap stars using a trial-and-error profile fitting.

Different formulations of the Doppler Imaging method have been proposed or applied to various observations. Goncharskij et al. (1982) formulated the problem of finding local abundances, for Ap stars, in terms of an integral equation assuming that the emission intensity in the continuous spectrum does not depend on the position. Vogt and Penrod (1983) gave the physical principle of Doppler Imaging of late-type stars and used a trial-and-error profile fitting method to reconstruct the stellar map.

A simple variant of the Doppler Imaging method has been applied by Gondoin (1986), to observations of HR1099, by identifying bumps components in the profile and following their velocity changes with rotational phase. Neff (1988), Walter (1987) and collaborators have developed a spectral imaging method adjusting IUE Mg II emission spectra of the system AR Lac with a minimal number of components.

Vogt et al. (1987) described the method of Doppler Imaging for spotted solar-type stars expressing the relation between local surface intensities and the observed spectral profile in matrix form by approximating the projection matrix as the marginal response of data pixel to changes in image pixel. To obtain the image-data transformation they assumed that the spot does not make a significant contribution to the observed flux, and the shape and strength of the line profile is the same in the spot as it is in the photosphere.

Jankov (1987) developed the methods of tomographic indirect stellar imaging from projections, based on the principle of flux rotational modulation, giving a full mathematic formulation in terms of matricial formalism, in the general case in which both spot and photosphere make a significant contribution to the observed line, treating explicitly the problem of nonlinearity of the image data transformation due to variable continuum flux level of spotted solar-type stars. In the Tomographic Imaging approach the problem of image reconstruction from spectroscopy and the problem of image reconstruction from photometry has been treated with the same mathematical formalism.

2. PRINCIPLE AND METHOD OF STELLAR TOMOGRAPHIC IMAGING

Comparing with imaging from photometry the Doppler Imaging approach provides an additional axis spatially resolved and the possibility to map different levels of the stellar 3-Dimensional atmosphere by using selected spectral lines. In addition, the available signal-to-noise from ground based photometry is not sufficient to obtain the required image resolution.

However the constraints from photometry dimension are important since they allow to obtain the better reliability of the reconstructed image (Jankov and Foing 1992). Moreover the high-speed and high signal-to-noise photometry from space can provide

the sufficient resolution in order to constraint the Tomographic Imaging of velocity fields (Jankov, in preparation).

Here we describe the principle and method for flux rotational modulation imaging of solar-type stars, treating the problem of indirect stellar imaging from projections to recover the *specific intensities* on the surface of a star, from its integrals (fluxes) over the parts of the stellar surface observed at different angles of view.

The approach concerns only the determination of the specific intensities on a stellar surface, supposing the local velocity and magnetic fields to be *a priori* known or negligible. In fact, when dealing with imaging of photospheres, in the optical wavelength regions, the variation of contribution due to inhomogeneous velocity fields and moderate magnetic fields (Zeeman splitting) can be assumed to be negligible comparing with the rotational broadening of fast rotators.

Since one cannot observe directly the specific intensities, but only their integrals over the apparent stellar disc, i.e. the fluxes, the projection r is defined as the flux-type integral :

$$P_r = \iint_{\Gamma_r} I_c(M, \lambda_0)[1 - \varepsilon + \varepsilon \cos \Theta_{rk}] \cos \Theta_{rk} \mathrm{d}S \tag{1}$$

where $I_c(M, \lambda_0)$ is the intensity distribution on a star, $\cos \Theta_{rk}$ is the angle between the line of sight and the outward normal of the k-th element of the stellar surface $\mathrm{d}S$, ε is limb darkening coefficient, and Γ_r represents the domain of integration for the flux detected in the corresponding detector pixel of the spectrograph or for the flux detected by the photometer. The domain Γ_r is determined by the projection onto a stellar surface (Fig. 1) of a) the constant velocity strip for the case spectroscopic data b) the visible stellar disc for the case of photometric data.

The principle of Doppler Imaging is shown on Fig. 1. When a signal from the spot is detected at some velocity, the spot position will be undetermined in the domain of the projection of the corresponding constant velocity strip (dark shadowed region). During the stellar rotation the same spot will be detected in some other velocity position, whose projection domain is depicted with the light shadowed region. The spot position can be determined as an intersection of two shadowed regions.

However, the stellar surface is mapped using the complete set of domains for all detector pixels obtained for different angles of view as shown in Fig. 2 for the case of Doppler Imaging and in Fig. 3 for the case of imaging from photometry. Note that for the case of imaging from photometry the details above the subobservers latitude can be localized only by the supplementary flux modulation due to the different surface projection when the detail is turning around the pole.

Given a number of projections at different angles of view, the estimation of the corresponding distribution $I_c(M, \lambda_0)$ on the stellar surface is the basic problem of the image reconstruction from available types of observations.

In practice the strict surface integrals (1) have to be replaced by the strip integrals because of the unavoidable limits set by the resolution of the instrument. So, the image resolution should be finite and one can use $N_L \times N_B$ digitization in which the picture region is divided into $J = N_L \times N_B$ array of pixels that will be referred to as the resolution pixels.

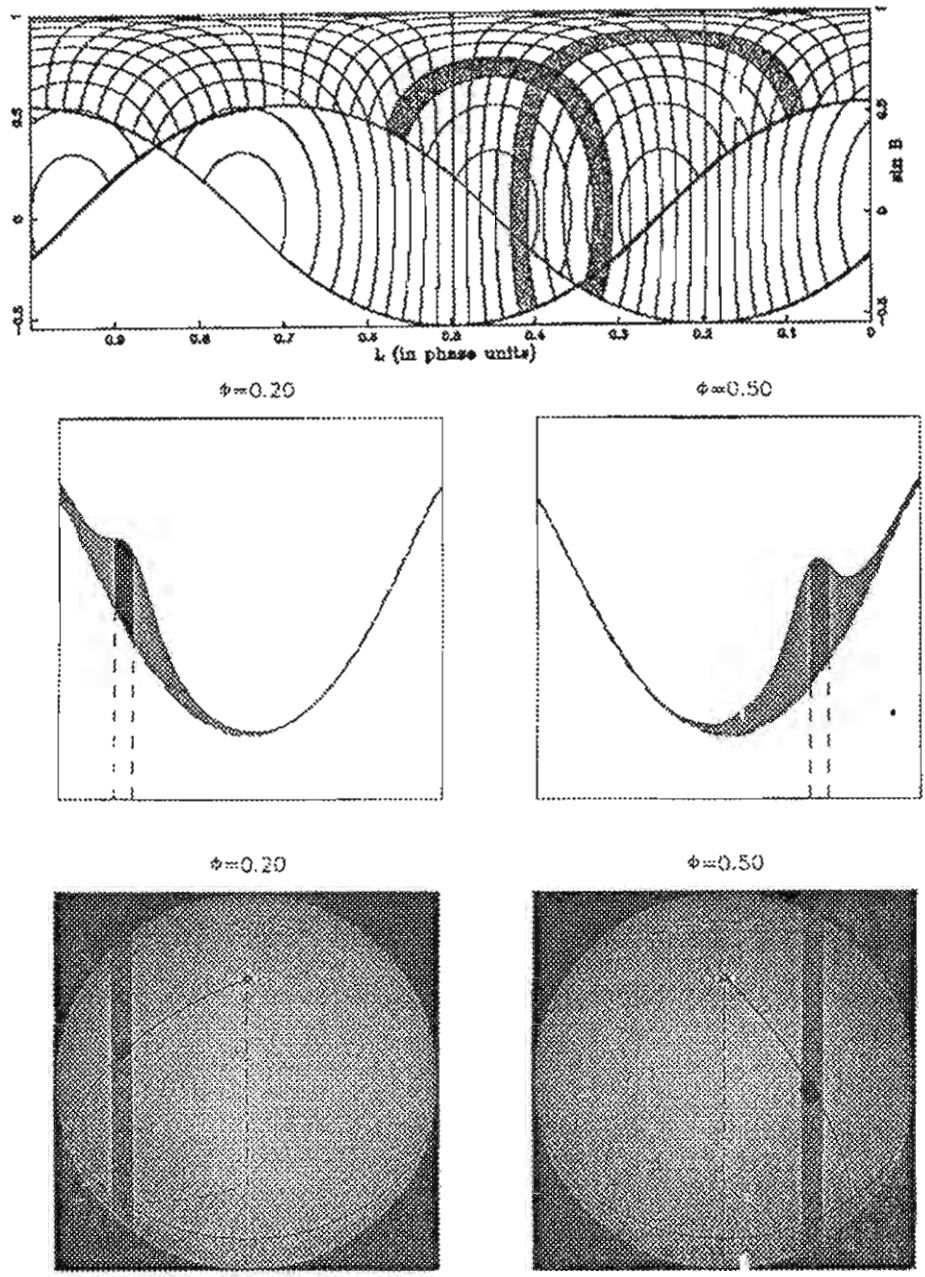

Fig. 1. The principle of localization of stellar surface details by intersection of two domains Γ_r corresponding to the two different angles of view (phases). The shadowed regions depict the projection of the constant velocity strips onto a stellar surface. The parts of the stellar surface visible at the particular phases are limited by the stellar limb here projected as the lower envelopes of equal velocity strips.

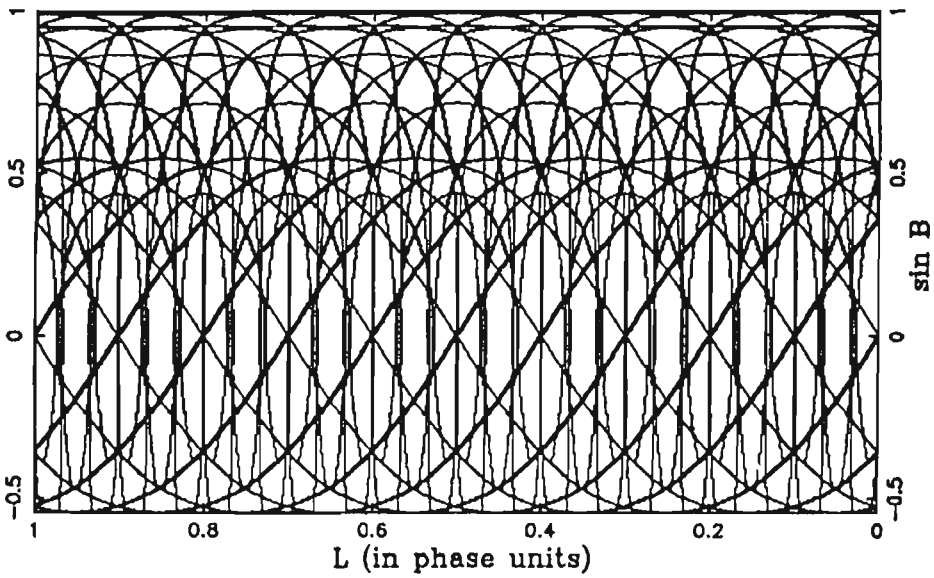

Fig. 2. Doppler Imaging network. The network on a stellar surface as it is formed when the star is observed in 10 equidistant view angles (phases), while the projected rotational velocity is resolved by the detector in 10 resolution elements. Basically this network is used to localize the details on a stellar surface.

Algorithmically that leads to the discretization of the problem and allows to translate the physical problem into the indirect imaging terms considering the general image-data transformation : $Y_{\rm I} = \mathbf{R} * X_{\rm J}$, where J and I are the dimensions of the image space and data space respectively and $\mathbf{R}$ is a mapping which takes a function in the image (X_j) space into a function in the data (Y_i) space. In our case the image $X_{\rm J}$ concerns the distribution of stellar surface brightness $I_{\rm c}(M, \lambda_0)$ and the operator $\mathbf{R}$ is described by some combination of the integrals (1) :

$$\mathbf{R} = f(P_{\rm r}).$$

In the case of Photometry Imaging the image is mapped into a light curve and in the case of Doppler Imaging the effect of the operator $\mathbf{R}$ is described by the dynamic difference spectrum, as illustrated on Fig. 4.

Jankov (1987) showed that the problem of Doppler Imaging can be fully linearized when the *shape* of the local spectrum does not depend on the position on a stellar surface while the problem of imaging from photometry is intrisically linear. In practice, to benefit for the linearized image-data transformation, one should choose the spectral line with low sensitivity to the temperature. Note also, that in solar-type scenario, for the stellar photospheres (where the brigt plages are several hundred Kelvins hotter and dark spots are several thousand Kelvins cooler than surrounding), the effect of the line profile dependence is cancelled since the surface brightness is proportional to

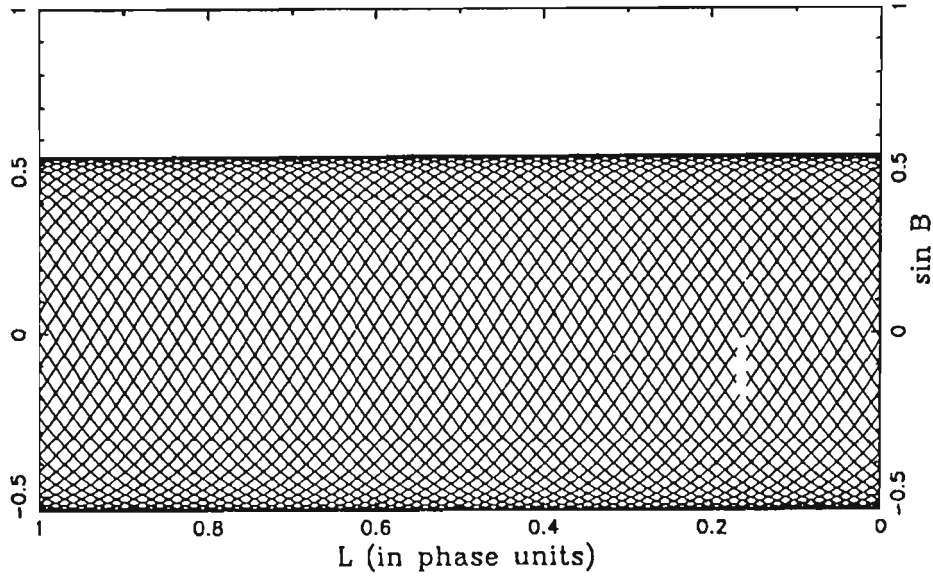

Fig. 3. Photometry Imaging network. The network on a stellar surface as it is formed when the star is observed in 50 equidistant view angles (phases). This network is formed only by the stellar limb and provides the enhanced photometrical rotational modulation. Basically this network is used to localize the details on a stellar surface below the subobservers latitude.

$T_{\rm eff}^4$, and the coolest spot regions do not contribute significantly to the observed line. For this reason the dependence of the local line profile on temperature is important only in the limited range of several 100 Kelvins around the photospheric temperature.

In such a way the operator **R** can be replaced by a matrix $R_{\rm IJ}$ and the problem can be formulated in the linear representation :

$$Y_i = \sum_{j=1}^{\rm J} R_{ij} X_j \qquad i = \overline{1,\rm I}. \tag{2}$$

In the general case, when the shape of the local line profile depends on the position on a stellar surface as a function of limb angle and local physical conditions (temperature, pressure, etc.), the image-data transformation can be still represented by the equation (2), (Jankov, 1992), however it is intrisically non-linear since the entries of the projection matrix $R_{\rm IJ}$ depend on the image vector $X_{\rm J}$. In that case, the entries of the matrix $R_{\rm IJ}$ cannot be evaluated analytically, but using line synthesis programs with an accurate model of stellar atmosphere (including full temperature and limb angle dependence of the line profile).

However, neglecting the limb angle dependence of the *shape* of the local line profile the grid of the spectra of the homogeneous, non-rotating standard stars with surface temperatures in the range from spot to surface temperature of the star under investigation, can be used to obtain the corresponding entries of the matrix $R_{\rm IJ}$ and

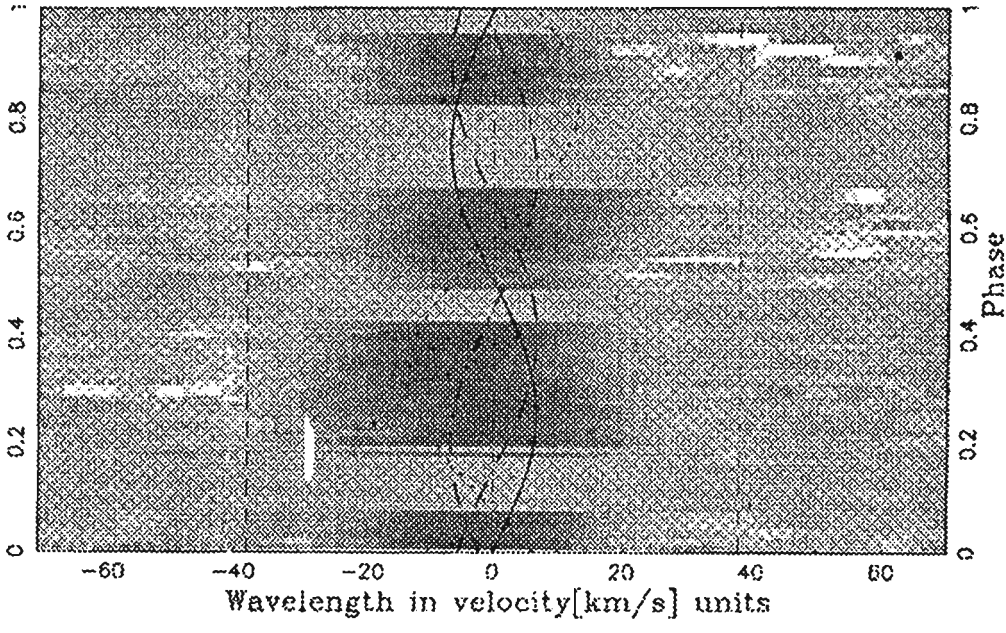

Fig. 4. Dynamic difference spectrum. This spectrum is arranged from sixty difference spectra where immaculate star line profiles are substracted from spotted star line profiles observed during the campaign. The projected velocity curves of the spots which positions are determined posterior to reconstruction are also presented. The stellar surface is extended over the rotational profile limits, depicted as vertical dashed lines, due to the convolution with the intrinsic line profile.

to complete the formulation of the problem. Since the limb-angle dependence of the local line profile has smaller influence on the integrated line profile than possible weak blends, a grid of observed spectra used as model input of the imaging code is likely to yield more accurate results than a table of synthetic profiles because the undetected blends are automatically excluded.

Again, considering only the spot regions that make a significant contribution to the observed line, one can use a grid of spectra of reference stars in the limited range around the photospheric temperature of the star to be imaged in order to handle the Tomographic Imaging reconstruction with the required degree of accuracy.

3. INVERSE PROBLEM

3. 1. SOURCES OF THE ILL-POSED NATURE OF THE INVERSE PROBLEM

The task of the indirect imaging reconstruction problem is to recover the image function X_J from the observed set of data Y_I. Generally, that task is not a trivial one because the matrix R_{IJ} can be singular and the solution X_J does not exist as R_{IJ}^{-1}

does not exist. Even if R_{IJ}^{-1} exists, there can be more than one R_{IJ}^{-1}, the nature of which is used being dependent on X_J and in that case the solution is not unique (Jankov and Foing, 1992). In the presence of noise, the question of existence, uniqueness, stability and image resolution are, generally, closely related, except if one deals with the star with the inclination not close to $\pi/2$ or to 0 where only the problem of stability remains.

In the noiseless and infinitely resolved world, Eq. (2) should be considered, (since there should not be a star, which inclination equals exactly 0 or $\pi/2$), as a solution does exist and is unique if $rank(R_{IJ}) = I = J$.

However, in the real world the question of fundamental practical importance is whether the solution is stable against small perturbations in the data function. In our case the matrix R_{IJ} is badly conditioned and the problem of the image reconstruction is fundamentally ill-posed, thus high performance regularization algorithms are crucially needed.

In addition to the noise in the observed profiles there are three principal sources of the ill-posed nature of the problem of inversion of the equation (2) in the Doppler Imaging approach :

a) Incompleteness of data

b) The projection matrix R_{IJ} is determined by the estimated quantities (the parameters determining the orientation of the star and orbital elements of a binary system) containing systematic and random errors.

c) Some details of the stellar surface are observed in non-optimal conditions (close to limb). Using the complete set of spectra for all observed phases, the image is spanned by the related strips, producing the global instability.

3. 2. MAXIMUM ENTROPY REGULARIZATION

The regularized solution can be obtained by minimizing an appropriate "regularizing functional", of the image function subject to the classical constraint $\chi^2 = \chi_0^2$:

$$\sum_{i=1}^{I} \left((Y_i - \sum_{j=1}^{J} R_{ij} \hat{X}_j)/\sigma_i \right)^2 = \chi_0^2$$

where χ_0^2 is determined by the required confidence level to data statistics χ^2, $\hat{X}_J$ is the solution, and σ_i is the standard error on datum i. The data statistic χ^2 is used to measure the discrepancy between observed and modeled data, while the χ^2 surfaces are convex ellipsoids in J dimensional image space.

To deal with the problem of the ill-posed nature of the inversion, the supplementary information should also be used in the form of well suited additional observations, as for example the temperature constrains from VRI photometry, or *a priori* information imposed on spectra or on the stellar image.

There are various alternatives for the choice of the regularizing functional each of them defining different methods of regularisation (Titterington, 1985). The choice of the regularizing functional depends generally on the prior information about the image function. Choosing the Kullback-Leibler distance one deals with the maximum

entropy approach where the solutions are chosen by maximizing the configurational entropy with respect to the the prior solution ${}^0X_J$:

$$\sum_{j=1}^{J} \hat{X}_j ln(\hat{X}_j / {}^0X_j).$$

Since the χ^2 surfaces are convex ellipsoids in image space and entropy surfaces are also strictly convex there is an unique point on the hypersurface $\chi^2 = \chi_0^2$ possessing the greatest entropy and the maximum entropy reconstruction is unique for the given data sample (Skilling and Bryan 1984).

4. RESULTS FROM MULTI-SITE OBSERVATIONS

4. 1. OPTIMAL STRATEGY OF OBSERVATIONS

In order to obtain the Doppler Image with the required number of resolved elements on the stellar surface, the strategy of observations, consistent with the spectral and temporal resolution, should be defined. Since one can have access only to strip integrals, when it is a question of spectroscopic data, we are in fact limited in the amount of information we can extract about the original distribution. The consequence is that, in practice, a finite number of phases to be observed suffice, and once this sufficient set of phases have been observed, the additional observations will contribute no more information than repetition of existing phases would contribute. If the star is resolved in latitude by N_L equivalent zones, N_L being proportional to the product of rotational velocity of the star and spectral resolving power, the complete set of data is obtained by observing each of the resolved zones in the central meridian i.e. by observing the star in $N_\Phi = N_L$ equidistant phases.

The other important parameter is the finite exposure time of the spectrum and corresponding spectrum signal-to-noise ratio. For the fixed duration of the observations, the image resolution limit is determined by the spectral and temporal resolution. Spectral and temporal resolution are determined by the noise thus, finally, the image resolution, and also the quality of the restoration, for optimally sampled data, are limited by the signal-to-noise ratio. We note that, in principle, the regularization algorithms using the *a priori* information allow some degree of super resolution by providing an the solution even in the case when $J > I$. However, in the case of indirect stellar imaging, one should not pretend to get much more resolution than allowed by the data.

The strategy of observations is also determined by other scientific goals that require :

a) a continuous observation ideally covering at least 2 rotational periods of the system in order to distinguish transient phenomena (as stellar flares) from the rotational modulation. In particular, for the stars with periods close to one day, a convenient phase coverage is impossible to obtain without continuous observations,

b) repeated observations of the same object in order to follow the evolution of the active structures.

On the basis of previous discussion, one can see that the optimal strategy of observations linked to Tomographic Imaging requires continuous spectroscopic monitoring over the rotational period of the star. To achieve the listed requirements a specific observational program was designed. MUSICOS (MUlti-SIte COntinuous Spectroscopy) is an international program (Catala et al. 1993) whose task is to facilitate continuous spectroscopic coverage of stars, using multi-site observations on existing telescopes of the 2m class distributed around the world. The observational campaigns are organized as frequent as possible in order to monitor the long term activity of selected targets.

4. 2. OBSERVATIONS AND IMAGE RECONSTRUCTION OF HR 1099

The second MUSICOS campaign was organized in December 1992 using the spectrographs existing on-site and fiber-fed MUSICOS spectrograph that was transported to Mauna Kea (Hawaii). Sixty high-resolution and high signal-to-noise ratio CCD spectra of the RS CVn binary system HR 1099 (K1 IV+G5 V) were obtained during the campaign at Observatoire de Haute-Provence, France (OHP) Beijing Astronomical Observatory, China (BAO) and University of Hawaii, USA (UH).

At OHP the AURELIE spectrograph, equipped with a Thomson 2048 pxl linear detector, yielding a wide spectral range ($\approx$ 6370–6490 Å) at a spectral resolution of 30 000, was used. The data reduction was carried out with the help of the MIDAS image processing system running on a Vax 4500 computer at Meudon Observatory.

At BAO, the ISIS fibre-spectrograph coupled with a 6-slice Bowen-Walraven image slicer allowed maximal throughput at a spectral resolution of 31 000. With a Tektronix 512×512 pxl detector, the spectra span 36 Å around 6434 Å. The data were reduced using the optimal extraction procedure of Horne (1986).

At UH, the MUSICOS spectrograph (Baudrand & Böhm 1992) was used. With a Tektronix 2048×2048 pxl detector, 64 orders are obtained in a single exposure, covering a spectral domain ranging from 4370 to 8760 Å at a spectral resolution of 30 000. The data were reduced using a dedicated software called MUSBIC. In this preliminary analysis though, we use order #88 only, which contains the classical Ca I and Fe I Doppler Imaging lines spanning about 100 Å around 6420 Å.

The details of the data acquisition and reduction are given in Jankov and Donati (1994).

The technique was applied to the moderately strong photospheric absorption Ca I λ 6439 Å line in order to recover the image of the photospheric surface of the primary star. The image reconstruction was performed using the spectra of the standard star HR 3762 (K0) for the primary component of HR 1099, and HR 4182 (G5) for the companion. The fundamental stellar parameters (listed in Table I) and orbital elements were adopted from Fekel (1983).

The spectra of standard stars were broadened by the rotational profile calculated using the values listed in Table I and shifted to the wavelength corresponding to the orbital motion. Contribution of each spectrum was determined using the values of effective temperature, radius, limb darkening coefficient and the photometric light curve. Fig 5 shows the photometry of HR 1099 obtained during the campaign (around the Julian date 2449000) but also four years before and one year after.

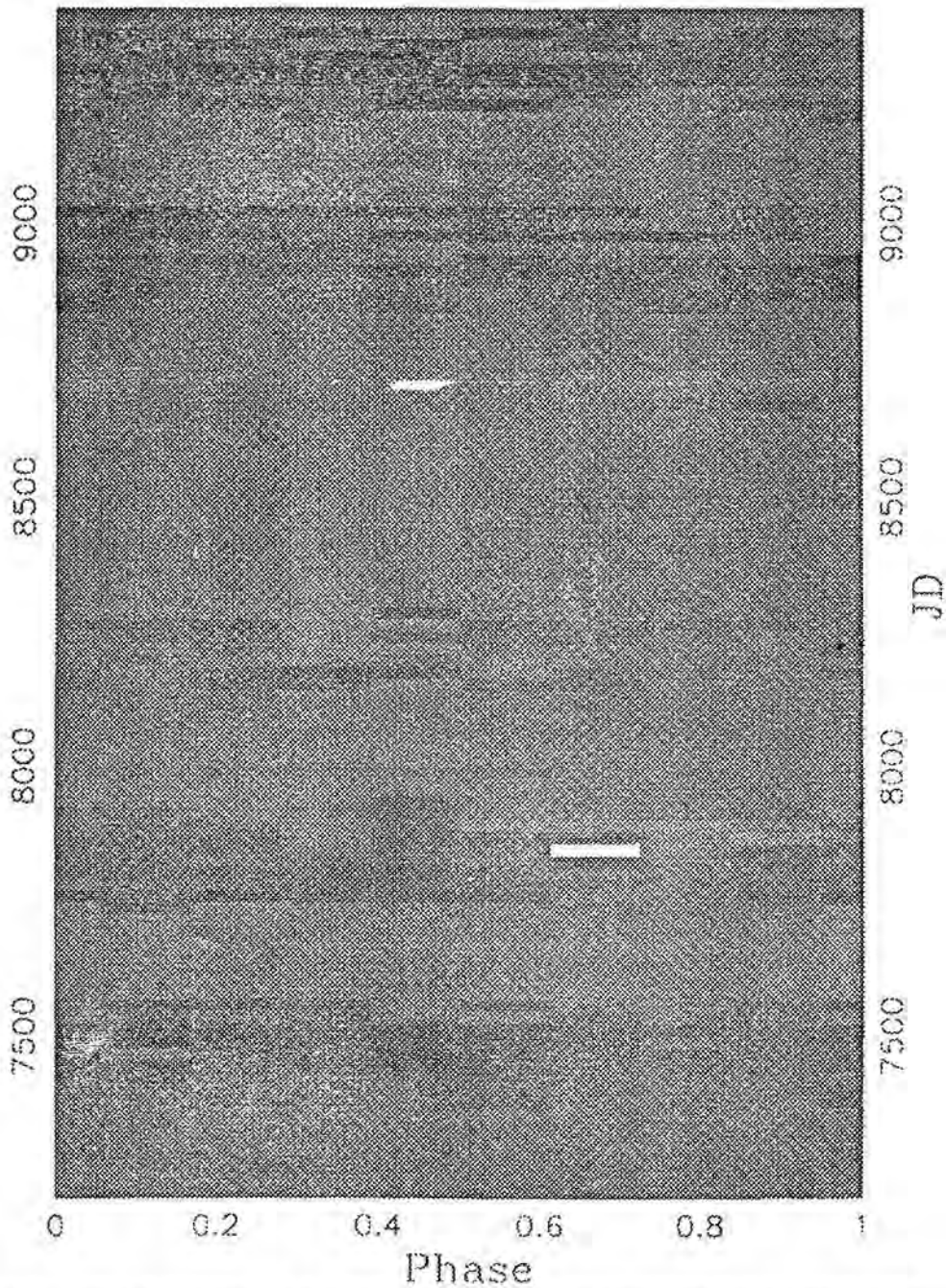

Fig. 5. APT photometry of HR 1099 from 1988 to 1993. The maximum and minimum fluxes detected in that interval are white and black respectively, intermediate values are represented by corresponding levels of gray while the uniform gray areas represent the intervals with available photometry.

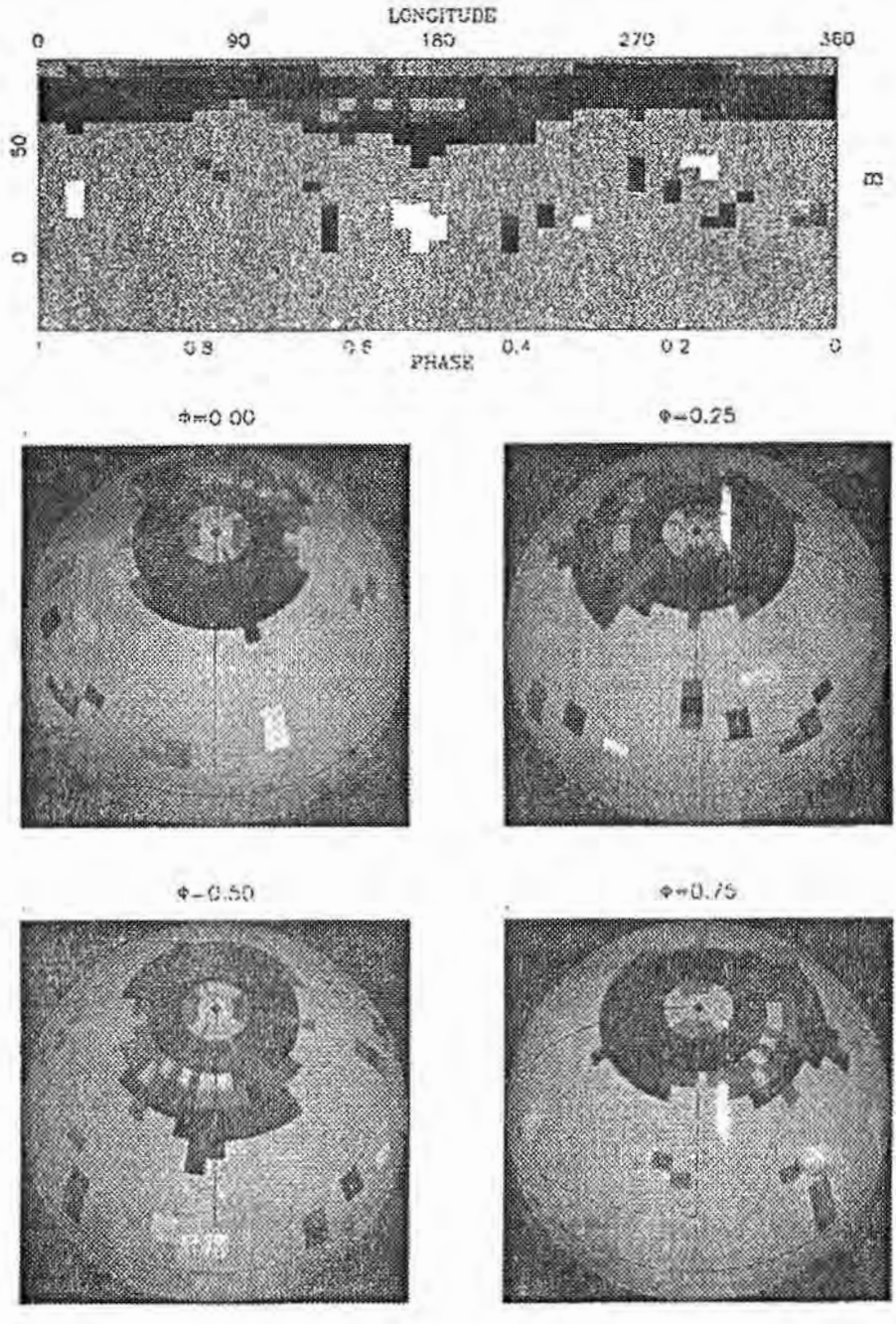

Fig. 6. Unconstrained tomographic image reconstruction of HR 1099 from MUSICOS 1989 (December) data. Darker gray scales depict lower specific intensities.

TABLE I
Stellar parameters used in reconstruction

Parameter	Primary	Secondary
$V_{eq} \sin i (km\,s^{-1})$	38	12
limb darkening ϵ	0.65	0.55
$T_{effective}$ (K)	4500	5730

To calculate the projection matrix, the stellar surface was divided in 45 longitude and 24 latitude bands, defining 980 spatial resolution pixels in the stellar image.

The search strategy employed for the image reconstruction consisted in minimizing χ^2 until reaching the hypersurface χ_0^2 by the constrained gradient method. The entropy was further maximized on the hypersurface $\chi^2 = \chi_0^2$ until reaching the parallelity of the gradients of χ^2 and entropy i.e., practically, until reaching the neighbourhood of the maximum entropy point defined so that cosine of the angle between the gradients is greater or equal to 0.99. The reconstructed image as well as the stellar disc as it would be seen in four successive rotational phases are presented on Fig. 6.

Note that small value of χ_0^2, adopted for this reconstruction, provides the high-frequency details at low latitudes that are likely to be artifacts. While, at this stage, it is not possible to argue if the low-latitude details (bellow 40° are artifacts or not, the high-latitude details are reliable. Particuraly interesting is the dark spot at $\Phi = 0.55$ $B = 50°$ that can be related to the rapid change of the light curve that started to develop at $\Phi \approx 0.55$ during the campaign and evolved, in the next year, towards $\Phi \approx 0.45$ (see Fig. 5). Since, in December 1992, we probably localized the region where the spot was generated, the image reconstruction from the data in 1993 will give the answer concerning its further evolution.

5. DISCUSSION

The photometric and spectroscopic Tomographic Imaging is a powerful tool to spatially resolve the surface and environment of stars providing an access to the information about quasistationnary phenomena. The image resolution and confidence in the reconstructed map are closely related to the global parameters of the star, such as brightness, equatorial velocity, inclination etc. and to the instrumental characteristics as signal-noise ratio, speed or resolution.

These methods have a wide range of application in astrophysics, particularly providing a knowledge of crucial importance to understand the stellar magnetic activity and physical processes related to it.

The objectives of such studies are to obtain the spatial distribution of activity phenomena, to understand the differences with their solar equivalent, to model the active atmospheric regions, to study the correlation between the structures observed at different heights, and monitor the changes associated with active region behaviour, cyclic activity, dynamo phenomena and differential rotation.

The study of solar-type phenomena on spatially resolved stars allows now, for the first time, to intercompare directly activity phenomena on stars and on the sun,

and to understand better solar processes by modelling them on stars with different parameters. On solar-type stars, spots, plages, intense chromospheric/coronal heating, winds, flares and other aspects of stellar activity are fundamentally magnetic in character. The interest for studying chromospheres/coronae of solar-type stars, apart from its own, arise also from the fact that they are excellent laboratories for using, testing and improving radiative transfer and modelling theories under conditions of non-LTE and non radiative equilibrium. It is also possible to diagnose, from the chromospheric/coronal structure and dynamics, the trace of subjacent phenomena associated with the existence of the magnetic fields in stellar surfaces, that are governed by the convective and internal properties of the stars. Some stellar situations allow to isolate better the physical processes at work in the various aspects of stellar activity. The activity relations with stellar parameters give also a tool for studying the global origin and consequences of magnetic field in solar-like stars.

References

Baudrand, J., Böhm, T. : 1992, *Astron. Astrophys.* **259**, 711.

Byrne, P. B. et al. : 1987, *Astron. Astrophys.* **180**, 172.

Catala, C., Foing, B. H., Baudrand, J. et al. : 1993, *Astron. Astrophys.* **275**, 245.

Catalano, S., Rodonò, M. : 1967, *Mem. Soc. Astron. Ital.* **38**, 395.

Deutsch, A. J. : 1970, *Astrophys. J.* **159**, 985.

Falk, A. E., Wehlau, W. H. : 1974, *Astrophys. J.* **192**, 409.

Fekel, F. C., 1983, *Astrophys. J.* **268**, 274.

Goncharskij, A. V., Stepanov, V. V., Khokhlova, V. L., Yagola, A. G. : 1982, *Sov. Astr.* **26**, 690.

Gondoin, P. : 1986, *Astron. Astrophys.* **160**, 73.

Horne, K. D., 1986, *PASP*, **98**, 609.

Jankov, S. : 1987, DEA, Université Paris VII, Meudon Observatory.

Jankov, S., Foing, B. H. : 1987, in *Cool Stars, Stellar Systems, and the Sun*, eds. J. L. Linsky and R. E. Stencel, Springer-Verlag, Berlin Heidelberg, p. 528.

Jankov, S. : 1992, Ph.D. Thesis, Université Paris VII.

Jankov, S., Foing, B. H. : 1992, *Astron. Astrophys.*, **256**, 533.

Jankov, S., Donati, J.-F. : 1994, in Proceedings of the Second MUSICOS workshop, in press.

Khokhlova, V. L., Ryabchikova, T. A. : 1970, *Astrofizika*, **6**, 227.

Khokhlova, V. L., Ryabchikova, T. A. : 1975, *Astr. and Space Science*, **34**, 403.

Mangeney, A., Praderie, F. : 1984, *Astron. Astrophys.* **130**, 143.

Neff, J. : 1988, Ph.D. thesis, University of Colorado, Boulder.

Noyes, R. W., Hartman, C. W., Baliunas, S. L., Duncan, D. K., Vaughan, A. H. : 1984, *Astrophys. J.* **279**, 763.

Ramsey, L. W., Nations, H. L. : 1980, *Astroph. J. Letters*, **348**, L121.

Rodonò, M., Cutispoto, G., Pazzani, V., Catalano, S., Byrne, P. B., Doyle, J. G., Butler, C. J., Andrews, A. D., Blanco, C., Marilli, E., Linsky, J. L., Scaltriti, F., Busso, M., Cellino, A., Hopkins, J. L., Okazaki, A., Hayashi, S. S., Zeilik, M., Helston, R., Henson, G., Smith, P., Simon, T. : 1986, *Astron. Astrophys.* **165**, 135.

Rodonò, M., Byrne, P. B., Neff, J. E., Linsky, J. L., Simon, T., Butler, C. J., Catalano, S., Cutispoto, G., Doyle, J. G., Andrews, A. D., Gibson, D. M. : 1987, *Astron. Astrophys.* **176**, 267.

Semel, M. : 1989, *Astron. Astrophys.* **225**, 456.

Skilling, J., Bryan, R. K. : 1984, *Mon. Not. R. astr. Soc.* **211**, 111.

Titterington, D. M. : 1985, *Astron.Astrophys.* **144**, 381.

Vaughan A. H., Baliunas, S. L., Middelkoop, F., Hartmann, L. W., Mihalas, D., Noyes, R. W., Preston, G. W. : 1981, *Astrophys.J.* **250**, 276.

Vogt, S. S., Penrod, G. D. : 1983, *Publ. Astron. Soc. Pac.* **95**, 565.
Vogt, S. S., Penrod, G. D., Hatzes, A. P. : 1987, *Astrophys. J.* **321**, 496.
Walter, H. M, Neff, J. E., Gibson, D. M., Linsky, J. L., Rodonò, M., Gary, D. E. and Butler C. J : 1987, *Astron. Astrophys.* **186**, 241.

Publ. Obs. Astron. Belgrade No. 49 (1995), 57-62

FLARE STARS IN STAR CLUSTERS AND THE FAINT END OF THE STELLAR LUMINOSITY FUNCTION

G. SZECSENYI-NAGY

Department of Astronomy, Lorand Eotvos University
Budapest VIII. Ludovika ter 2. H-1083 HUNGARY

Abstract. Flare stars belong to the red dwarfs, the faintest stellar objects known. dK and dM stars contribute about half of the total stellar mass in the solar vicinity. Since they are unobservable in the r¿100 pc range they are a kind of dark matter candidates. Probably at least half of these stars are flare stars which can be detected (during high amplitude outbursts) at a significantly larger distance. This fact makes these faint objects and their investigation exceptionally important. The results of a two decades long photometric and astrometric programme are summarized below.

1. INTRODUCTION

The very first observation of a flare phenomenon on a star other than the Sun was made by E. Hertzsprung in 1924. He successfully photographed the sudden brightness increase of a star now called DH Carinae. He noticed and misinterpreted the phenomenon explaining it as the consequence of an impact of an asteroid into the star. During the next decades the frequency and the time-development of similar events observed by others and, as the strongest evidence, the reoccurences of the phenomenon in the case of the same stars, made this naive hypothesis to be rejected. However, the truth is that the real physical causes of this phenomenon, called the flare activity have not been found yet. This may explain why the study of flare stars is still a popular field for the astrophysicists of the last decade of the XXth century.

At rest these variables, called UV Ceti-type after their well known representative, are red dwarfs with extremely low energy output. Their spectra contain emission lines, and in most of the cases they can be classified as (dK)-dMe their decimal classes running from M0 to M6.5. Because their absolute visual magnitudes are between +10 and +18 with a few exception, only the ones in the immediate solar neighbourhood can be observed with photoelectric photometers and spectrographs mounted onto small or medium sized telescopes. But there are hardly more than fifty of that type (Kunkel 1965) and there is only a dozen, which flare up with a high enough frequency that it would be worthwhile to observe them photometrically in uninterrupted mode. Fortunately in the early fifties Haro and Morgan discovered that these peculiar stars seem to cluster in certain parts of the sky (Haro and Morgan 1953). Objects with similar properties to that of UV Ceti were identified in the Orion nebula and its close

neighbourhood, though at first they were considered as a separate class of the variable stars, and therefore they were called flash- not flare stars. Since the so called Orion association - presumably to which the majority of these variables belong - is so far from the solar system that the individual photoelectric observation of its red dwarfs would be wasteful, photographic methods have been used for the observation of the whole field of this association and other stellar aggregates.

2. THE OBSERVATIONS

The photometric observations have been made most frequently in the UV or blue ("photographic") range of the electromagnetic spectrum with large field and fast astro-cameras, mainly of the Schmidt type. These telescopes are extremely effective in the ultraviolet since their optics is composed of a highly reflective mirror and a very thin correcting plate, made of a kind of UV-transparent glass. Since the intrinsic brightness variation of these stars during a flare up is definitely the most prominent in the UV- continuum and seconds or minutes later in some spectral lines, the strategy of taking long series of short photographic exposures of those regions of the sky which contain nearby - and preferably young - star clusters or associations proved to be very successful. Following the study of the Orion association researchers in Hungary and other countries investigated a lot of galactic clusters and groups of stars and discovered that flare stars can be recognized in many of them. There are two limitations of their detection. First, the galactic clusters almost without exception can be found in the Milky Way, where the interstellar absorption is the strongest. Second the flare stars are of extraordinarily low luminosity. Since 1952, the beginning of the photographic patrolling of star clusters and other suspicious stellar groups flare stars have been discovered and identified in the field of at least half a dozen nearby aggregations (Szecsenyi-Nagy 1990 and references therein). The most important discovery for us was the one showing flare stars in the field of Eta Tauri or of the Pleiades. This relatively young open cluster is not too far away from us (its distance being 126 pc or its distance modulus about 5.5 magnitude) and is very nicely placed on the fall-winter sky of the observers of the northern hemisphere. The cluster has known member stars spread over a sky field of at least 30-50 square degrees and is reasonably abundant in low mass red dwarf stars too. The results of our decades-long flare programme combined with those of the Abastumani, Asiago, Byurakan, Padova, Palomar, Rozhen, Sonneberg, Tautenburg and Tonantzintla teams have been published mostly in observatory bulletins as well as annals or conference proceedings. It is worthwhile therefore to summarize those ones, which may be of greater importance in other fields of astronomy and astrophysics.

3. PHOTOMETRIC PROPERTIES OF FLARE STARS DISCOVERED IN FIELDS OF STELLAR AGGREGATES

Based on our own results and data collected from the literature we were able to demonstrate the existence of a more or less definitive correlation between the ultraviolet flare amplitude (expressed in magnitudes) and the apparent ultraviolet brightness of the quiescent star. Since all of these stars were found in the vicinity of the Pleiades cluster,

they were supposed to be cluster members and only some objects could be exceptions (definitely not more than 2-3 in the region) of it. The outcome of the study was that those stars which are fainter in minimum, are able to produce the flares of the greatest known amplitudes (up to 6-8 magnitudes) in the ultraviolet band (Szecsenyi- Nagy 1980). However the significant spread was annoying enough and urged me forward the introduction of a new parameter describing more conveniently the energetic properties of the flare phenomena. The Ultraviolet Flare Overproduction (or briefly UFO, just to give a scientific meaning to this then remarkably popular abbreviation) is given in USO (Ultraviolet Solar Output) units and shows a definite exponential correlation with the duration of the flares expressed in minutes. The greatest problem in that study and its extensions was, that only a limited number of Pleiades flares had been photometrically well calibrated and published in detail. For the photometric data collected by the Hungarian team an other, even more significant relation has been found. In this the ultraviolet output of the flare at the maximum point of its "light curve" has been expressed in USO units and has been compared to the total UFO of the same star during the same event. A linear correlation of the two parameters has been found with a coefficient of correlation exceeding 0.95 and this suggests that the ultraviolet over- production of the stellar flares in Pleiades field are in excellent correlation with the ultraviolet overproduction of the given flare's peak point. In order to characterize the energetic properties of Pleiades field flare stars more exactly an other program has been run. Altogether more than 500 flare ups and their photometric data were ordered into a flare database and reduced systematically. A new variable, the cumulative flare overproduction (both in the ultraviolet and in the photographic range) has been defined and computed and plotted against increasing amplitude limits. The result is a graph, looking like an almost straight echelon the slope of which provides the new parameter characterizing the energetic properties of the object in the ultraviolet or in the photographic bands. This method proved to be incredibly sensitive to the physical constitution of the objects. The echelon graph of one of the stars investigated showed a strange, doubly-sloped structure, which suggested the duplicity of the object being composed of two flare stars of different activity. Later it has been found, that the star is really a binary (Szecsenyi-Nagy 1988).

Having collected enough photometric data about flares of almost 600 flare stars of the field of the Pleiades cluster, it was clear, that some of the stars are much more active than others. From our own observations and from data published by the members of the other teams I was able to list 17 stars with at least 10 observed flare ups although hundreds of stars produced only one or two flares during the same time. Or not? This was not absolutely clear whether every star got the same amount of attention (or observing time). I had to correct the observations of the different groups to this effect which is the result of the differences between the photographic cameras of the observatories (caused mainly by the various photometric fields and speed of the telescopes). To overcome these diffi- culties the Largest Common Field (LCF) of the Eta Tauri fields has been defined and based on it the time-like parameter PMT (Pleiades Mean Time) has been introduced. The latter successfully randomized the data of the photometric observations and proved to be an excellent variable being suitable to substitute total or effective observing time (Szecsenyi-Nagy 1986, 1990b).

As a by-product of the use of the new time parameter PMT significant long-term variations of the flaring activity of the flare stars discovered in the Eta Tauri fields were found. These variations appear as a specific pattern in the time distribution of the observed flare ups (in fact on the flare up versus PMT graph). What we see is that short periods (some years) of enhanced flare activity are embedded in far longer ones (decades), during which the star seems to be very much alike its low-activity neighbours. It may be very important in statistical investigations, that activity variations of this kind which convert them into quiescent red dwarfs temporarily, very probably screen a lot of flare stars from the astronomers' view. Another result of the same study was the discovery of the cyclic activity of the star CPFS91 and the estimation of the length of its activity cycle which is in the 20 years range, not far from the magnetic cycle of our Sun (Szecsenyi-Nagy 1989). It has been found too that the flaring frequency of at least two out of three active flare stars - irrespective of their cluster membership probability, apparent brightness or average flare frequency - can vary by a factor of ten. Since the photometric fields centered upon Eta Tauri contain flare stars of very different ages (the Pleiades cluster members are in the 50-80 million years age bracket whilst the star which has produced the most of the observed flare events in the field belongs to the Hyades group and is about 600-800 million years old, moreover some of the stars can be foreground objects with ages similar to that of the galactic field or of that of the Sun - some billions of years). The most important statements of that study can be summarized as follows (Szecsenyi-Nagy 1990) :

(i) the ratio of randomly flaring objects amongst Pleiades members is the same (1/3) as amongst the whole sample while the changeable activity seems to be more general

(ii) activity cycles are characterized by short high activity and much (4 to 20 times) longer low activity or even inactive periods

(iii) flaring frequency in maxima can exceed the minimum frequency by a factor of 5-25

(iv) activity changes of this character were observed on stars of the same spectral type (dM3) but very different ages (50 million to approximately 5000 million years)

4. CLUSTER FLARE STARS AND THE LUMINOSITY FUNCTION

At the time of its discovery the Hertzsprung-Russell diagram (or the HRD) did not contain red dwarf stars at all. Stars less luminous than the Sun were extremely underrepresented in the sample of that time. This is of course absolutely normal, since faint and red objects could have hardly been recorded by the very low sensitivity photographic materials and slow optical systems used by the observers of those years. With the advent of giant telescopes and even more with the extended use of modern astronomical cameras, which were able to record huge fields of the sky simultaneously, the number of red dwarfs incredibly increased. As our recently published textbooks tell the story, most of the stars are main sequence stars and at least three quarters of these are red dwarfs (dK and dM spectral class objects). Based on these statistical values it becomes clear that the majority of the stars building up the Galaxy

are red dwarfs. Unfortunately these objects are extremely faint and this fact severely limits the probability of their discovery. We were able to spot these objects only in the close vicinity of the Sun. The result is that 70 stars and 85 farther from the Sun the statistics is worsening step by step. In the kpc distance range the faintest dwarfs are practically unobservable and going deeper into the galactic disk or halo even the "brighter red dwarfs" will disappear. At the same time it is well known, that galaxies and amongst them our own too seem to be much slimmer than they would have to be in order to keep their companions. Where and in which forms this mass can exist? This is a very difficult problem, and no definitive answer has been given yet to it.

Why can flare stars help in answering? The idea is that flare stars, because of their strange behaviour and extremely large amplitude brightness variations, can be observed to much farther than the quiescent red dwarfs. Another advantage of these objects is that they are often concentrated into star clusters and associations (Szecsenyi-Nagy 1986a, 1986b) and this fact offers the possibility of locating them using photometric and other data concerning brighter stars of the same cluster or group. The most shocking result of the photographic flare patrols and the statistical investigations based on the data collected by these programs is that the most actively observed young clusters are extremely rich in flare stars. The Pleiades e.g. contains at least 3-5 times more of this species than the total number of its stars discovered before the start of international flare programs. It was shown in the early eighties that the field scrutinized by the photo- graphic cameras hid more than a thousand flare stars around Eta Tauri. In the next decades many of these objects were identified thanks to their flare activity and it was calculated too, that tens of thousands of hours of photographic observations are needed to discover the large majority of these faint stars (Szecsenyi-Nagy 1983). With the introduction of the new semiconductor based detectors (or simply CCD cameras) and other revolutionary observing techniques and methods into the flare star research programs as suggested by the author too (Szecsenyi- Nagy 1990c, 1994, 1995), we will learn much more in much shorter time than has been found during the past half century.

Acknowledgements

The author acknowledges the partial support of this research by the National Scientific Research Foundation (grant OTKA-T 7595).

References

Haro, G. and Morgan, W. W. : 1953, *Ap. J.* vol. **117**, p. 73.
Kunkel, W. : 1965, *An Optical Study of Stellar Flares*, Texas Univ., Austin. p.3.
Szecsenyi-Nagy, G. : 1980, In "Flare Stars, FUOrs and Herbig-Haro Objects", ed. by L. V. Mirzoyan, Yerevan, p. 129.
Szecsenyi-Nagy, G. : 1983, *Publ. of the Astron. Inst. of the Czech. Acad. of Sciences*, Praha, No. 56, p. 218.
Szecsenyi-Nagy, G. : 1986, In "Flare Stars and Related Objects", ed. by L. V. Mirzoyan, Yerevan, p. 101.
Szecsenyi-Nagy, G. : 1986a, *Publ. Astron. Dept. Eotvos Univ.* Budapest, No. 8, p. 59.
Szecsenyi-Nagy, G. : 1986b, *Publ. Astron. Dept. Eotvos Univ.*, Budapest, No. 8, p. 101.

Szecsenyi-Nagy, G. : 1988, In "Activity in Cool Star Envelopes", Astrophysics and Space Science Library, Vol. **143**, eds. O. Havnes et al. p. 69.
Szecsenyi-Nagy, G. : 1989, In "IAU Colloquium No. 104 Solar and Stellar Flares Poster Papers", ed. by B. M. Haisch and M. Rodono, Catania, p. 143.
Szecsenyi-Nagy, G. : 1990, *Publ. Astron. Dept. Eotvos Univ.*, Budapest, No. 9, p. 308.
Szecsenyi-Nagy, G. : 1990a, *Astrophysics and Space Science* Vol. **170**, p. 63.
Szecsenyi-Nagy, G. : 1990b, In "Flare Stars in Star Clusters, Associations and the Solar Vicinity", eds. L. V. Mirzoyan et al. p. 71.
Szecsenyi-Nagy, G. : 1990c, In "Star Clusters and Associations", Publ. Astr. Dept. Eotvos Univ., Budapest, No. 10, p. 55.
Szecsenyi-Nagy, G. : 1994, In "IAU Symposium No. 161 Astronomy from Wide-Field Imaging", eds. H. T. MacGillivray et al. p. 61.
Szecsenyi-Nagy, G. : 1995, In "IAU Colloquium No. 148 Future Utilisation of Schmidt Telescopes" eds. R. Cannon et al., (in press).

Publ. Obs. Astron. Belgrade No. 49 (1995), 63-65

LIGHT CURVE CHANGES IN ECLIPSING BINARIES

L. PATKÓS

Konkoly Observatory of the Hungarian Academy of Sciences, H-1525 Budapest XII, Box 67, Hungary
E-mail patkos@ogyalla.konkoly.hu

Abstract. The eclipsing binary SV Cam has been monitored at Konkoly Observatory since 1973. This binary system showed both period and light curve changes. Main reason of the light curve changes were dark spots on the surface of the primary component, causing migrating distortion waves. A peculiar brightening was also observed. Another kind of light curve variations were optical flares.

1. INTRODUCTION

The close binary system SV Cam ($m_v = 8.40 - 9.11\ mag$, $p\ :\ 0.59^d$, $sp\ :\ G2 - 3V + K4 - 5V$) belongs to the short period group of RS CVn variables (Hall 1976). It was found to be variable by Guthnick (1929). The period and the type of light variation were determined by Detre (Dunst 1933). Asymmetry in the light curve was first established by Wood (1946). Van Woerden (1957) found irregular light-curve changes and small random period fluctuations. First spectroscopic data were published by Hiltner (1953) and by Hill et al. (1975).

2. PERIOD CHANGES

Observed long-term variations in the O-C curve interpreted Sommer (1956) as a 57.5 year light-time effect caused by the presence of a third body in the system. As this period was incompatible with van Woerden's (1957) observations, Frieboes-Conde and Herczeg (1973) tried to fit the O-C data with another sine-wave with a period of 72.8 years. To fit further observations Hilditch et al. (1979) also used a third body revolving around the eclipsing pair with a period of 64.1 years but in an eccentric orbit.

3. SPECTROSCOPY

Spectroscopic data from Rainger et al. (1991) show a systemic radial velocity of $\gamma = -11.2 \pm 5.5 kms^{-1}$ for SV Cam. They also reanalysed former observations from Lucy and Sweeney (1971), from which $\gamma = -16.2 \pm 8.8 kms^{-1}$ was derived. This difference in γ of $5.0 \pm 1.3 kms^{-1}$ gives some hint at the presence of a third body in the system. (The expected orbital motion about a third body with an orbital period

of 65-75 years would have a semiamplitude of about 2 kms^{-1} and hence difficult to measure). They also determined the mass function of the system.

4. PHOTOMETRY

Different photometric studies (e.g. Milano 1981, Patkós 1982a, Milano et al. 1983, Cellino et al. 1985 and others) showed extensive light curve and period changes in the system SV Cam. As generally expected for RS CVn type stars, these light curve changes are interpreted as caused by magnetic activity and large spots on the stellar surface. Detailed study of the dark spots on the surface of the primary component causing the distortion wave has been made by Zeilik et al. (1988). They also determined the system parameters as well as Sarma et al. (1989). These determinations of the system parameters were based mainly on the intensive photometric monitoring of SV Cam which has been carried out at Konkoly Observatory in U, B, and V since 1973. Part of these observations (1973-1980) was published (Patkós 1982a). The monitoring of SV Cam has been continued since then with the same intensity. Further observations will be published later. Main results of the first published part are :

I. There exist a "distortion wave" in the system.

II. The wave migrates towards increasing orbital phase, but its speed seems to be not constant.

III. All the observed light curves with the migrating distortion wave are below an upper envelope curve (except the cases IV and VI). There exist an observed light curve (J.D. 2442404-405) which seems to be nearly identical with this upper envelope curve (Patkós 1982a).

IV. The peculiar brightness increase observed between J.D. 2442460-523 (Patkós 1982b) was interpreted as the appearance of a temporarily existing bright spot near the equator of the primary star (Hempelmann and Patkós 1991).

V. The existence of other (but smaller) bright spots was demonstrated at J.D. 2441978, 981 and 982 (Patkós 1982e). Then within a week three independent primary minima were observed. In each case there was a step at the bottom of primary minimum. This phenomenon can be explained by the eclipse of a white spot on the surface of the primary component. The brightness of this spot was not enough to observe it in full light, but in the case of transit eclipse even small brightness differences on the surface of the eclipsed component could be established. Because of the differential rotation the spot was moving and so on the light curves observed two weeks earlier and one month later (and on other light curves of SV Cam) no step at the bottom of primary minima is present. Note that in this case not only the brightness difference between spot and surroundings but also the size of the spot had to be small in contrast to spot models derived by us and by others.

VI. Another case for the light curve growing over the envelope curve was observed at J.D. 2445582 when flare events at around phase 0.61 and at the bottom of primary minimum occurred (Patkós 1981). They were significant in all three colours (U,B,V).

VII. Optical flare events seem to be very rare in RS CVn systems. (Another very alike event was reported by Zeilik et al. (1983) at XY UMa). A previous (but smaller) optical flare in the system SV Cam was also reported by Patkós (1989) but dislike the

J.D. 2445582 event that flare wasn't significant in the B and V light curves. It could be observed only in U.

As conclusion of the first part of the monitoring of SV Cam we find that the best light curve to determine the system parameters is the one observed at J.D. 2442404-405 because this is the most symmetrical one in the 1973-1980 period and spottedness is assumed to be minimal in the system at that time too (Patkós 1982a, p : 42).

References

Cellino, A., Scaltriti, F. and Busso, M. : 1985, *Astr. Astrophys.* **144**, 315.
Detre, L. (Dunst) : 1933, *Astr. Nachr.*, **249**, 213.
Frieboes-Conde, H. and Herczeg, T. : 1973, *Astr. Astrophys. Suppl.*, **12**, 1.
Guthnick, P. : 1929, *Astr. Nachr.*, **235**, 83.
Hall, D. S. : 1976, in "Multiple periodic Variable Stars", ed. W. S. Fitch (Dordrecht : Reidel), p. 287. (IAU Coll. No. 29).
Hempelmann, A. and Patkós, L. : 1991, *Astron. Nachr.* **312**, 19.
Hilditch, R. W., Harland, D. M., McLean, B. J. : 1979, *Mon. Not. R. astr. Soc.*, **187**, 797.
Hill, G., Hilditch, R. W., Younger, F., Fisher, W. A. : 1975, *Mem. R. astr. Soc.* **79**, 131.
Hiltner, W. A. : 1953, *Astrophys J.* **118**, 262.
Lucy, L. B. and Sweeney, M. A. : 1971, *Astron J.*, **76**, 544.
Milano, L. : 1981, in "Photometric and Spectroscopic Binary Systems" ed. E. B. Carling and Z. Kopal (Dordrecht : Reidel), p. 331.
Milano, L., Russo, G. and Mancuso, S. : 1983, in "Activity in Red Dwarf Stars", ed. P. B. Birne and M. Rodono (Dordrecht : Reidel), p. 393.
Patkós, L. : 1981, *Astrophys. Letters*, **22**, 1.
Patkós, L. : 1982a, *Comm. Konkoly Obs.*, No 80. p.1-99.
Patkós, L. : 1982b, in "Ejection and Accretion of Matter in Binary Systems", ed. J. Tremko (Bratislava : VEDA), p.61.
Patkós, L : 1982e, in "Magnetic and Variable Stars", eds : M. Marik, L. Szabados, Comm. Konkoly Obs. No. 83. p.218.
Patkós, L. : 1989, in "Variable Phenomena in Close Binary Stars", ed. L. Patkós, Comm. Konkoly Obs. 10, (No 93.), p. 271.
Rainger, P. P., Hilditch, R. W. and Edwin, R. P. : 1991, *Mon. Not. R. astr. Soc.*, **248**, 168.
Sarma, C. V. S. R., Sarma, M. B. K., Sanwal, N. B. : 1989, *J. Astrophys. Astr.* **10**, 307-346.
Sommer, R. : 1956, *Astr. Nachr.*, **283**, 155.
van Woerden, H. : 1957, *Leiden Ann.*, **21**, 3.
Wood, F. B. : 1946, *Contr. Princeton Obs.* No. 21, p. 40.
Zeilik, M., DeBlasi, C., Rhodes, M. and Budding, E. : 1988, *Astrophys. J.*, **332**, 293.
Zeilik, M., Elston, R. and Henson, G. : 1983, *Astron. J.* **88**, 532.

Publ. Obs. Astron. Belgrade No. 49 (1995), 67-68

SOME RECENT RESULTS IN THE THEORY OF NONLINEAR STELLAR PULSATIONS

G. KOVÁCS
Konkoly Observatory, Budapest

Abstract. We focus the discussion on the utilization of the very nonlinear nature of the light curves of classical pulsating stars (Cepheids and RR Lyrae stars).

1. BUMP CEPHEIDS

Following the suggestion of Simon & Schmidt (1976) it has been shown (Buchler, Moskalik & Kovács 1990; Kovács & Buchler 1989) that the characteristic variation of the bump on the light and velocity curves of the Galactic Cepheids is caused by the $2\omega_0 \approx \omega_2$ resonance between the fundamental and first overtone modes. This connection between the frequencies of the normal modes and the nonlinear feature on the light curve enables us to estimate the masses of the Bump Cepheids. This is very similar to the method applied in the case of the double-mode stars. In a follow-up paper Moskalik, Buchler & Marom (1991) proved that due to the recently found enhancement of the metal opacities (Rogers & Iglesias 1992), the bump masses become concordant with those given by the evolution theories.

2. METAL ABUNDANCES OF CEPHEIDS AND RR LYRAE STARS

Considering the general idea of the dependence of the shape of the light curve on the star's physical parameters, Kovács & Zsoldos (1995) showed that there exist simple relations between the observed iron abundances and the Fourier parameters of the light curves of RR Lyrae stars. The method enables one to estimate [Fe/H] from the light curves alone. Jurcsik & Kovács (1995) successfully applied the method on an independent sample of globular cluster variables. In a subsequent paper Zsoldos (1995) extended the method to the Galactic Cepheids.

References

Buchler, J. R., Moskalik, P. and Kovács, G. : 1990, *Ap. J.*, **351**, 617.
Jurcsik, J. and Kovács, G. : 1995, in *Astrophysical Applications of Stellar Pulsation*, IAU Coll. 155, ASP Conf. Ser., Eds. : R. S. Stobie and P. A. Whitelock.
Kovács, G. and Buchler, J. R. : 1989, *Ap. J.*, **346**, 898.
Kovács, G. and Zsoldos, E. : 1995, *Astron. Astrophys.*, **293**, L57.
Moskalik, P., Buchler, J. R. and Marom, A. : 1991, *Ap. J.*,
Rogers, F. J. and Iglesias, C. A. : 1992, *Ap. J. Suppl.*, **79**, 507.
Simon, N. R. and Schmidt, E. : 1976, *Ap. J.*, **205**, 162.
Zsoldos, E. : 1995 in *Astrophysical Applications of Stellar Pulsation*, IAU Coll. 155, ASP Conf. Ser., Eds. : R. S. Stobie and P. A. Whitelock.

Publ. Obs. Astron. Belgrade No. 49 (1995), 69-70

THE INFLUENCE OF COLLISIONS WITH CHARGED PARTICLES ON STELLAR LINE SPECTRA

M. S. DIMITRIJEVIĆ
Astronomical Observatory, Volgina 7, 11050 Belgrade, Yugoslavia
E-mail mdimitrijevic@aob.aob.bg.ac.yu

Abstract. The astrophysical importance of the line broadening due to the interaction between emitter(absorber) and charged particles (Stark broadening) is discussed. A review of semiclassical calculations of Stark broadening parameters and comparison of different semiclassical procedures is presented too, as well as the comparison with critically selected experimental data and more sophisticated, close coupling calculations. Approximate methods for the calculation of Stark broadening parameters, useful especially in such astrophysical problems where large scale calculations and analyses must be performed and where a good average accuracy is expected, have also been discussed.

Among the various pressure broadening mechanisms, broadening due to interaction between emitter and charged particles (Stark broadening) is dominant in several cases. For $T_{eff} > 10^4$K, hydrogen, the main constituent of a stellar atmosphere is mainly ionized, and the main collisional broadening mechanism for spectral lines is the Stark effect. This is the case for white dwarfs and hot stars of O, B and A0 type. Even in cooler star atmospheres as e.g. Solar one, Stark broadening may be important. For example, the influence of Stark broadening within a spectral series increases with the increase of the principal quantum number of the upper level and consequently,Stark broadening contribution may become significant even in the Solar spectrum.

An important problem where we need reliable Stark broadening data is also the determination of chemical abundances of elements from equivalent widths of absorption lines. Stark broadening data are also required for the estimation of the radiative transfer through the stellar plasmas, especially in subphotospheric layers and for opacity calculations. In such a case data for especially large numbers of lines are needed. An illustrative example might be the article on the calculation of opacities for classical cepheid models (Iglesias *et al.* 1990), where 11,996,532 spectral lines have been taken into account, and where Stark broadening is important.

Stellar spectroscopy depends on very extensive list of elements and line transitions with their atomic and line broadening parameters. It is difficult to state in general terms which are the relevant transitions since the atmospheric composition of a star is not known a priori, and many interesting groups of stars exist with very peculiar abundances as compared to the Sun.

The interest for a very extensive list of line broadening data is additionally stimulated by spectroscopy from space. In such a manner an extensive amount of spectro-

scopic information over large spectral regions of all kind of celestial objects has been and will be collected, stimulating the spectral–line–shape research.

The most sophisticated theoretical method for the calculation of a Stark broadened line profile is of course the quantum mechanical strong coupling approach. However, due to its complexity and numerical difficulties, only a small number of such calculations exist. In a lot of cases such as e.g. complex spectra, heavy elements or transitions between more excited energy levels, the more sophisticated quantum mechanical approach is very difficult or even practically impossible to use and, in such cases, the semiclassical approach remains the most efficient method for Stark broadening calculations.

Here is presented a review of semiclassical calculations of Stark broadening parameters and comparison of different semiclassical procedures is discussed, as well as the agreement with critically selected experimental data and more sophisticated, close coupling calculations. Approximate methods for the calculation of Stark broadening parameters, useful especially in such astrophysical problems where large scale calculations and analyses must be performed and where a good average accuracy is expected, have also been discussed.

References

Iglesias, C. A., Rogers, F. J. and Wilson, B. G. : 1990, *Astrophys. J.* **360**, 221.

Publ. Obs. Astron. Belgrade No. 49 (1995), 71-72

ASTRONOMY IN SERBIA

M. S. DIMITRIJEVIĆ
Astronomical Observatory, Volgina 7, 11050 Belgrade, Yugoslavia
E-mail eaop021@yubgss21.bg.ac.yu

Abstract. A short history of the development of astronomy in Serbia is presented as well as the present situation and scientific results.

The Belgrade Observatory has been founded in 1887, by Milan Nedeljković. He was sent by the government of young independent Serbia to Paris, to study astronomy and meteorology in 1879. It is interesting to see his study programme, as written by the Ministry of Education and Religion, which envisaged two years of astronomy, mathematics, meteorology, mechanics and geodesy. In the third year he was to have practice at astronomical and meteorological institutions in Paris and to continue the study of astronomy and meteorology with the emphasis on the use of astronomical and meteorological instruments. One half of the forth year he was to be in London and the second half to be devoted to a visit of principal astronomical and meteorological institutions in Europe. He spent 5 years in France, endeavouring to prepare himself well for the important task of founding the first astronomical institution, as well as university-level teaching of astronomy and meteorology in Serbia.

Belgrade Observatory was not only the first astronomical institution in Serbia but likewise a nucleus for the development of meteorology, seismology and geomagnetic research. For more than a century, a pleiad of scientists with an important contribution to the world science and to the scientific life in Serbia, is connected with the activities of Belgrade Observatory.

The second director of this institution was Djordje Stanojević, the first Serbian astrophysicists, who in 19th century published scientific papers in the journal of French Academy of Sciences (Comptes rendus). The famous French astronomer Janssen, entrusted him with the direction of the French expedition for the observation of total solar eclipse of 19th August 1887 in Petrovsk (Russia). He constructed a station for the solar research in Sahara and worked there with an international group of astronomers in 1891-1892. He was in addition a professor of physics at the Belgrade University, one of its first rectors and he made an important contribution concerning the electrification of Belgrade and Serbia.

The most famous Serbian astronomer, Milutin Milanković was one of directors of this institution too. He explained why and how glacial periods originated and gave an astronomical basis to the climatological history of our planet. On account of his contribution to the science, a crater on the Moon, another one on Mars and one asteroid, were named after him.

Thanks to the results of the work on the minor planets of the researchers M. Protić (discovered of 33 minor planets) and P. Djurković (6 minor planets) there are minor planets with permanent names 1554 Yugoslavia, 1564 Serbia, 157 Beograd, 1605 Milankovitch, 2244 Tesla...

Good relations and collaboration between Hungarian and Serbian astronomers were initiated by the founders of Astronomical Observatories in Budapest and Belgrade, Miklos Tege Konkoly and Milan Nedeljković, and the report on the Konkoly's visit of Belgrade Observatory in October 1902. is a nice testimony to it.

Currently, Astronomical Observatory in Belgrade has 25 astronomers. Together with 7 astronomers at the Belgrade University, their researches are under the project Physics and Motion of Celestial Bodies. On the large meridian circle are carried out observations of stars for the Hipparchos programme as well as the stars near radio sources. On the large vertical circle planets and fundamental stars have been observed during 1994. During this year have also been observed minor planets, the comet Macholz (1994o), the comet Nakamura - Nishimura - Macholz (1994m) and the comet Borrelly. The work on the analytical and semianalytical theory of the minor planet proper element determination and on the analytical theory of the secular perturbations of the minor planet motion has been continued. The work on the investigation of chaotic nature of the minor planet motion (stable chaos) was started. At large refractor (65cm), 353 measurements of 133 double and multiple systems discovered in Belgrade and 124 measurements of 53 other systems were performed. On the same instrument optical polarization of stellar radiation, in accordance with the existing longterm programme, was investigated. The observation reduction and the preliminary result analysis are in progress. Spectral observations of Solar radiation flux for 31 chosen spectral lines was continued within a program of their examination during a Solar cycle. Their equivalent widths have been measured as well. On the basis of the examination of double star spectral line profiles modulation, by using the method of indirect imaging, the stellar surface structure has been studied. Stark broadening parameters for a number of spectral lines have been investigated and determined. Infrared Mg I spectral lines, important for the Solar plasma diagnostics, have been investigated. The influence of ion-atom radiative collisions on the continuous optical spectrum in Solar plasma and in helium rich DB white dwarf atmospheres as well as on the opacity was considered.

This is only a part of the scientific activities on Belgrade Observatory during 1994. During this year, Serbian astronomers working on the project Physics and Motion of Celestial Bodies, published 109 bibliographical units. Out of them, 23 are published in the international journals such as Astron. Astrophys. (4), Astron. Astrophys. Suppl. Series (8), Astrophys. Space Sci. (2), Solar Physics (1), Planet.Space Sci. (2), Physica Scripta (2), Astrophys. Lett. Commun. (2), J.Quant.Spectrosc. Radiative transfer (1), J. Phys. D (1).

We hope that the closer collaboration with the Hungarian astronomers will enlarge additionally the "critical mass", and will exert its influence on the faster development of astronomy in both countries.

Publ. Obs. Astron. Belgrade No. 49 (1995), 73-76

SOME CHARACTERISTICS OF INTRINSIC POLARIZATION OF Be STAR κ Dra

J. ARSENIJEVIĆ, S. MARKOVIĆ-KRŠLJANIN, I. VINCE and S. JANKOV
Astronomical Observatory, Volgina 7, 11050 Belgrade, Yugoslavia

Abstract. The intrinsic polarization parameters of κ Dra in V-color measured at Belgrade Observatory during the 14 years period (1979-1992) are presented. The changes of polarization percentage are discussed with the data of V-color photometry and Hα emission line equivalent widths.

1. INTRODUCTION

Rapidly rotating B stars with temporary hydrogen emission are known as Be stars since 1931 (Struve, 1931). These stars may throw off matter at their equatorial edges forming disk-like envelopes. Although a great number of well organized investigations in wide range of the electromagnetic spectrum exists, we are still far from understanding the phase change B to Be. Good example is the star κ Dra (HD 109387) of the spectral type B6 IIIpe and projected rotational velocity $V \sin i$ =200 km/s (Hirata, 1994). Balmer emission of this star was already discovered in 1890 by Pickering. During almost two last decades various systematic polarimetric, photometric and spectroscopic investigations have been done. In spite of that, many questions stay still open . In this paper, on the basis of some existing observations of the star κ Dra we will try to formulate the most interesting questions.

2. OBSERVATIONS

2. 1. POLARIZATION

Polarimetric observations at Belgrade Observatory from 1974 till 1992 were carried out with the 65-cm Zeiss refractor and the stellar polarimeter (Kubičela *et al.*, 1976), which was modified in 1979 to enable one to obtain digital magnetic records suitable for further computer processing. The measurements were done in the V spectral region. Integration of the raw polarimetric signal was done in 4-second intervals. The angular velocity of the analyzer was one turn per minute. In most cases under "one measurement" we understand up to 8 one-minute polarimetric sine-wave signals phase-averaged. The typical standard deviation of one 8 minute individual measurement is 0.07% for Stokes parameters Q and U.

The complete revision of the system constants was carried out for the observations till 1990 with all standard stars. The consequences of this revision are the small changes of the system constants and calculated polarization parameters published before 1990.

In determination of the intrinsic polarization the interstellar components were estimated or used from the literature. For the star κ Dra the procedure of evaluating of the interstellar component is thoroughly described in Arsenijević *et al.* (1986).

Polarimetric data presented in Figure 1 cover the period of 14 years (1979 - 1992) when the annual mean values of the intrinsic polarization percentage change from 0.15% in 1980 to 0.54% in 1985. After 1985 polarization percentage decreases till 1991. It seems that during 1992 started the new period of increasing polarization percentage. But the minimum value is higher than the values during 1980 - 1981.

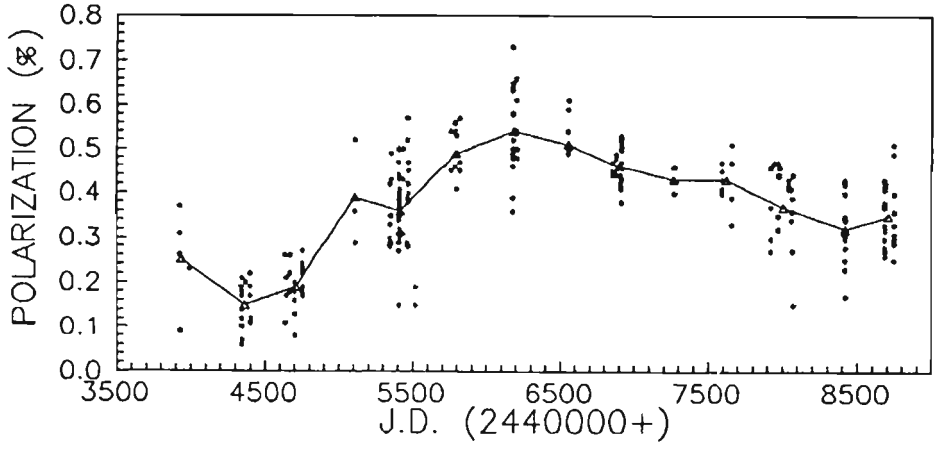

Fig. 1. Intrinsic polarization percentage of the star κ Dra in V-spectral region.

The existence of the intrinsic polarization means the existence of the sufficient electron density in the region of the envelope below the H_α emitting layer. According to the polarization variation in Q,U plane Arsenijević *et al.* (1994) have found that the region of the envelope responsible for the polarization has an axial symmetry. The individual polarization percentage increased during 1979 - 1986 by a factor of about 5 - 6. In annual mean values this factor is about 3.6. For the moment, the main thing is to point out that the intrinsic polarization reflects directly the state of the lower part of the envelope. So, the changes of the intrinsic polarization reflect the changes of the envelope shape and electron density.

2. 2. EQUIVALENT WIDTH OF H_α EMISSION

Figure 2. taken from the article of Yuza *et al.* (1993) shows H_α emission line equivalent width and its change practically simultaneously observed as the polarization. This emission comes from a large emitting volume, extended cool outer atmosphere. Over the interval of time 1979 - 1986, the equivalent width of H_α emission line increased by the factor of about 3 (Arsenijević *et al.*, 1994). This long-term variable and extended emitting part of the envelope gives the information on the formation and the distruction of the envelope. Using Dasch *et al.* (1992) statistical relation, the effective emitting envelope is found to have increased from 4 to 6.5 stellar radii.

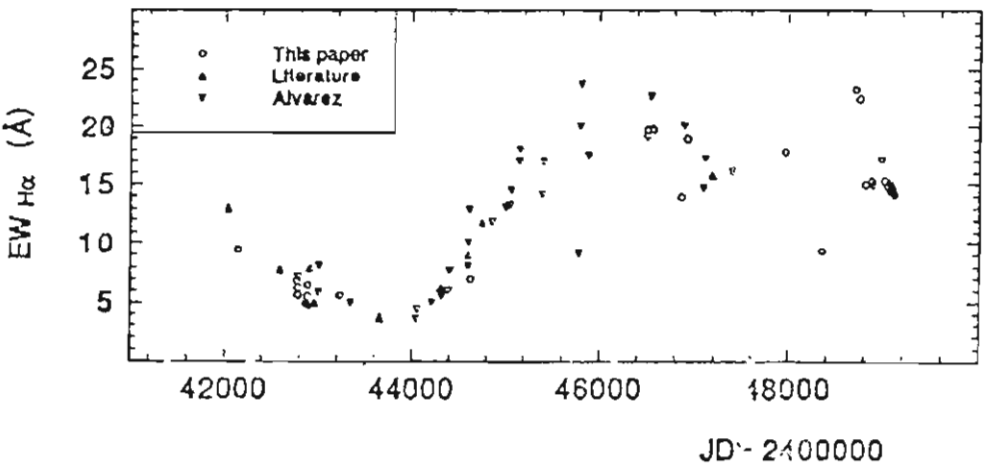

Fig. 2. The change of the equivalent width of H_α emission of the star κ Dra (from Yuza *et al.*, 1993).

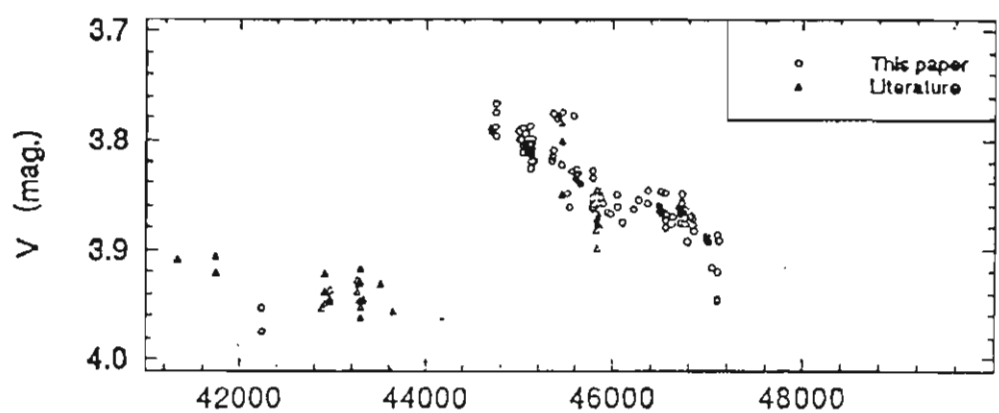

Fig. 3. Light changes of the star κ Dra (from Yuza *et al.*, 1993).

2. 3. V-COLOR PHOTOMETRY

The light curve in Figure 3, taken from Yuza *et al.* (1993), shows, according to Hirata (1994) a steep brightening and subsequent gradual decline. Traditionally, the photometric variations are attributed to the variation in the envelope of the star, but Hirata (1994) concluded that the steep brightening of κ Dra has originated not in the envelope but in the stellar photosphere. There are no observations in the interval of time that can allow us to determine the beginning of the brightening. Thus, nobody can say now which part of the star is responsible for the brightness variation.

3. ANALYSIS

The estimated moment of the minimum of the equivalent width of H_α emission is about JD 2443500. The polarization percentage has the minimum on about JD 2444350. The time lag of polarization is about 850 days. But, the emission activity started, roughly speaking, about 400 days before the polarimetric one. Both, the emission and the polarization come from the different layers of the same envelope. The question is why we observe such a large phase shift.

Very important interval of time about minima of H_α emission and polarization is not covered by brightness observations. We do not exactly know what has happened with V magnitude during the time interval of the small envelope activity in H_α emission. But, it seems that during small values of H_α emission and polarization percentage the V magnitude was high. During the period of increasing polarization, V magnitude exhibits a decreasing tendency. This is usual for Be stars. The unusual fact is that V magnitude continues to decrease after the maximum of polarization.

The estimated moments of the maxima of H_α emission and polarization percentage happened respectively on JD 2446400 and JD 2446500 approximatelly. The delay of the polarization maxima is about three months. We can say that the emission maximum at H_α coincides with the maximum of the intrinsic polarization. If these quantities are the tracers of the envelope formation and the destruction after maxima of polarization and emission, starts the envelope destruction. Why V magnitude continues to decrease? For the moment, we have in mind a very high electron density as an explanation. It could attenuate the brightness by scattering and diminish also the polarization by multiple scattering independently of the envelope geometry and in spite of the envelope staying large. This presumption is supported by the very gradual H_α emission decrease.

The long-term variation periodicity of about 23 years for V magnitude and H_α emission is confirmed by Yuza *et al.* (1993). It would be very interesting to point out here that the period of polarization percentage change is approximately two times smaller, about 11 years. Of course, this is valid if the observed second maximum of polarization on JD 2447960 will be confirmed by more observations.

References

Arsenijević, J., Jankov, S., Djurašević, G., Vince, I. : 1986, *Bull. Obs. Astron. Belgrade*, **136**, 6.

Arsenijević, J., Jankov, S., Marković-Kršljanin, S., Hubert, A. M., Hubert, H., Chambon, M. Th., Floquet, M., Mekkas, A. : 1994, *Proceedings of IAU Symp.* 162, (L. A. Balona, H. F. Henrichs and J. M. Le Contel, Eds.), Kluwer Acad. Publ., Dordrecht/Boston/London, 234.

Dasch, J., Hummel, W., Hanuschik, R. W. : 1992, *Astron. Astrophys. Suppl. Ser.* **95**, 437.

Hirata, R. : 1994, private communication.

Kubičela, A., Arsenijević, J., Vince, I. : 1976, *Publ. Dept. Astron. Univ. Belgrade*, **6**, 25.

Struve, O. : 1931, *Aph. J.* **73**, 94.

Yuza, J., Harmanec, P., Božić, H., Pavlovski, K., Žižňovský, J., Tarasov, A. E., Horn, J., Koubský, P. : 1993, (preprint).

Publ. Obs. Astron. Belgrade No. 49 (1995), 77-80

ON SOME ITERATION FACTORS FAMILIES IN SOLUTION OF LINE TRANSFER PROBLEM WITH DEPTH–DEPENDENT PROFILE FUNCTION

O. ATANACKOVIĆ-VUKMANOVIĆ
Astronomical Observatory, Volgina 7, 11050 Belgrade, Yugoslavia
E–mail oatanackovic@aob.aob.bg.ac.yu

E. SIMONNEAU
Institut d'Astrophysique, 98 bis Boulevard Arago, 75014 Paris, France

Abstract. Several iteration factors families are defined for solving the line transfer problem with depth–dependent profile function.

1. INTRODUCTION

The line radiation transport by the two–level atoms in a constant property medium is the problem whose well–known solutions serve to check the computational properties of the new numerical methods.

In previous papers (Simonneau and Atanacković -Vukmanović , 1991; Atanacković -Vukmanović and Simonneau, 1994) this instance is used to examine the convergence properties of a new iterative procedure that efficiently revise and accelerate Λ iteration scheme by the use of quasi–invariants of the problem (so–called iteration factors). The idea of the monochromatic variable (depth–dependent) Eddington factors is generalized to the relevant frequency dependent variables of the line formation problem. The formal solution of the radiative transfer (RT) equation used for the computation of the iteration factors and the solution of the integrated moment equations closed by these factors are performed in turn. In order to provide the closure of the system, on one hand, and to be good quasi–invariants, on the other, iteration factors are to be defined as the ratios of the corresponding intensity moments. In distinction from the case of depth–independent profile function φ_x considered in the above– cited papers, where the RT moment equations as well as the iteration factors are obtained by successive integrations over profile φ_x , spatial variation in φ_x does not allow such integrations on the left hand side of RT equation, and hence, requires a different procedure.

2. ITERATION FACTORS

For the sake of simplicity in presentation and using the standard notation, we consider the time independent RT equation for a static, plane-parallel, one- -dimensional and semi-infinite atmosphere with no background continuum and for completely redistributed line radiation :

$$\mu \frac{d}{d\tau} I_x(\mu, \tau) = \varphi_x(\tau)[I_x(\mu, \tau) - S(\tau)] \quad , \tag{1}$$

with the line source function given by :

$$S(\tau) = \varepsilon B(\tau) + (1 - \varepsilon) \int_{-\infty}^{\infty} \varphi_x(\tau) J_x(\tau) dx \quad . \tag{2}$$

Here the absorption profile coefficient is τ dependent. In order to get the moments of Eq. (1), generally we can proceed in two ways. The first is to complete integration over $d\mu$ and $\mu d\mu$, respectively, whereupon the frequency integration is to be performed within the range $[-x_N, x_N]$, where the last frequency point x_N is chosen so that the monochromatic optical depth at this frequency and for a geometrical depth one or two orders of magnitude greater than the thermalization length is much lesser than 1.

Then the system of moment equations has the following form :

$$\begin{aligned} \frac{d}{d\tau} H(\tau) &= J_\varphi(\tau) - S(\tau) \\ \frac{d}{d\tau} K(\tau) &= H_\varphi(\tau) \quad . \end{aligned} \tag{3}$$

Apart from the most straightforward closure relations :

$$F = \frac{K}{J_\varphi} \tag{4a}$$

and

$$f_H = \frac{H}{H_\varphi} \tag{4b}$$

considered in Atanacković -Vukmanović and Simonneau (1993), denoted here as family A, we can introduce a new one (family B) that will explicitly take into account only the non-local coupling of the radiation field. Keeping the generalized Eddington factor $F(\tau)$, we define new factor $\tilde{f}_H$ given by the ratio of the "non-local" parts ("active-transfer" terms) of the radiation field intensity moments :

$$\tilde{f}_H = \frac{\tilde{H}}{\tilde{H}_\varphi} = \frac{H - \dfrac{S}{2} \displaystyle\int E_3(\tau_x) dx}{H_\varphi - \dfrac{S}{2} \displaystyle\int E_3(\tau_x) \varphi_x dx} \quad . \tag{5}$$

Due to the fact that the "passive in transfer" terms are isolated and that we iterate only on the non-local terms of the intensity moments, with this type of iteration factors better convergence properties are expected.

The other possibility to define the system of moment equations is to consider the outgoing and incoming intensities separately in the frame of the two-stream model for the radiation field. By performing the μ-integration of the RT equations over the interval [0,1] :

$$\pm\frac{d}{d\tau}I_x^{\pm}(\mu,\tau) = \varphi_x(\tau)[I_x^{\pm}(\mu,\tau) - S(\tau)]$$

and the frequency integration by applying $\int_{-x_N}^{x_N} dx$ like for getting (3), we obtain the system :

$$+\frac{d}{d\tau}H^{+} = J_{\varphi}^{+} - S$$
$$-\frac{d}{d\tau}H^{-} = J_{\varphi}^{-} - S \quad ,$$

coupled by the source term :

$$S = \varepsilon B + (1-\varepsilon)(\frac{J_{\varphi}^{+} + J_{\varphi}^{-}}{2}) \quad .$$

The above system can be closed by the third (C) family of the iteration factors :

$$\theta^{\pm} = \frac{H^{\pm}}{J_{\varphi}^{\pm}} \quad . \tag{6}$$

With these factors some improvements can also be expected since the two-point boundary nature of the transfer phenomenon is now explicitly taken into account.

3. RESULTS

For the sake of simplicity, the comparison of the convergence properties among the three types of the iteration factors is performed for the well-known instance of constant property medium. The behaviour of the line source function vs. $log\tau$ in the course of iterations is shown in Fig 1. for the case $\varepsilon = 10^{-4}$ and for the three iteration factors families. The convergence is achieved in 28, 18 and 13 iterations for the A-, B- and C-type factors, respectively, with an error of about 1%. It can be seen that the stability and the speed of convergence are better when the iteration factors are progressively better defined from the physical point of view.

4. CONCLUSION

In this paper two new iteration factors families are defined for the case when the profile function is depth dependent. Apart from the most straightforward one (type A), new factors are defined to include explicitly the non-local coupling of the radiation field by means of the non-local parts of the corresponding intensity moments (type B) as well as to take into account the two-point boundary nature of the radiative transfer via a separate treatment of the outward and inward directed variables (type C). This purely academic consideration however, like the one involving factors defined for the constant property case, confirms again that the more the factors are related to the physics of the problem the more rapidly convergence is achieved.

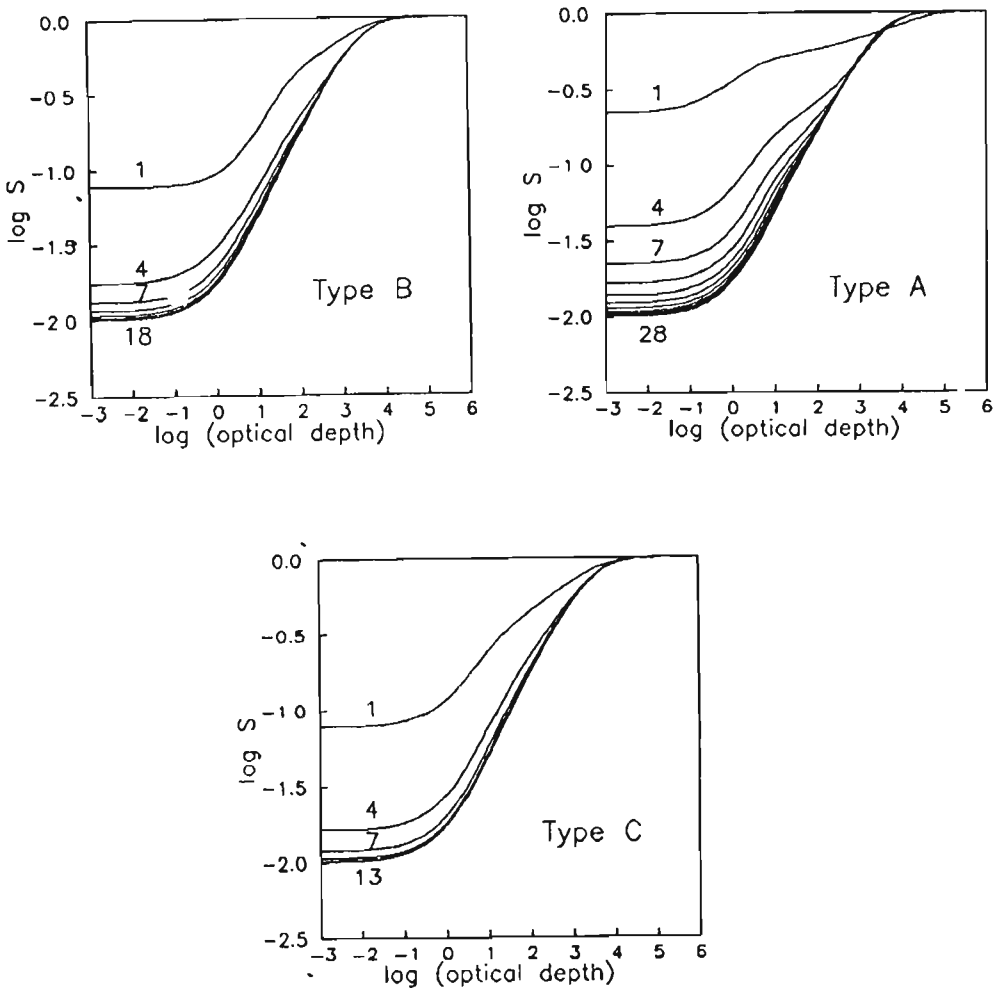

Fig. 1. The line source function obtained by the use of A-,B- and C-type factors in the labelled number of iterations

References

Atanacković-Vukmanović, O., Simonneau, E. : 1993, *Publ. Obs. Astron. Belgrade*, **44**, 41–44.

Atanacković-Vukmanović, O., Simonneau, E. : 1994, *J. Quant. Spectrosc. Radiat. Transfer*, **51**, No. 3, 525–543.

Simonneau, E., Atanacković-Vukmanović, O. : 1991, in *Stellar atmospheres : Beyond Classical Models*, (Eds. L. Crivellari et al.), Kluwer Acad. Publ., 105–110.

Publ. Obs. Astron. Belgrade No. 49 (1995), 81-88

GIANT CONVECTIVE ROLLS AND SUNSPOT GROUP TILTS

T. BARANYI and A. LUDMÁNY
Heliophysical Observatory of the Hungarian Academy of Sciences, H-4010 Debrecen, P.O.Box 30., Hungary
E-mail baranyi@tigris.klte.hu

Abstract. The theoretically predicted non-axisymmetric giant convection pattern has been studied by using its probable twisting influence on the emerging magnetic fields. The studies resulted in an evidence for a giant cell pattern with longitudinal wave number l=11 which has a rotation rate differing by $\Delta\omega = -0.35$ degrees/day from that of the Carrington system.

1. INTRODUCTION

Hale's law describes the most important features of the orientations of the sunspot groups adequately, apart from the few apparent exceptions certainly caused by the confusion of nearby groups. So, it is plausible to suppose that the internal magnetic fields producing the active regions are basically azimuthal toroidal fields. However, the sunspot groups emerge with a tilt, i.e. the straight line connecting the leading and following parts declines from the E-W direction, and later, primarily under the influence of the dynamics of the solar surface, the angle of this tilt changes, it diminishes in many cases, mainly at higher latitudes (Gilman and Howard, 1986). We may suppose, however that at the moment of the birth this tilt may yield information about the subsurface influences on the rising flux tubes. If so, two mechanisms seem to be possible : (1) the local distortion of unknown origin of the azimuthal flux rope causes an instability of the flux at the bottom of the convection zone, and the rising material can drag the flux, in this case the distortion itself would be the cause of the appearance of the active region, (2) the (no matter why) rising flux tube can be rotated throughout the bulk of the convective layer by unspecified velocity fields. The two mechanisms perhaps do not exclude each other, but the latter type is more probable as we shall see later.

The data of the Debrecen Photoheliograph Results 1977 (Dezső et al.,1987) were used, this is the only material containing the positions of the preceding and following parts of the active regions. Only those sunspot groups were considered in a previous work (Baranyi and Ludmány, 1992, referred to as Paper I henceforth), for which the catalog recorded both the appearance and the forming of the bipolar character within three days (except the groups belonging to the previous cycle), this means 76 sunspot groups in 1977. Later on (Baranyi and Ludmány, 1993, Paper II) the material has been completed to 88 sunspot groups considering only the firs days of the bipolar character.

2. DISTRIBUTION OF TILTS OF EMERGING SUNSPOT GROUPS

The first important property of the orientations is that the angles of the tilts have different signs on either hemispheres. Therefore positive sign was attributed to the angle of the active region's axis, if the preceding part was nearer to the equator than the following one, that means $\mid B_f \mid - \mid B_p \mid > 0$, and the angle is negative if $\mid B_f \mid - \mid B_p \mid < 0$ on both hemispheres, B_f and B_p denote the heliographic latitudes of the following and preceding parts respectively. 58 cases were positive and 30 negative in the given material, this is a rate similar to that found by Howard (1991, 1993). So, if indeed an internal flux-twisting mechanism exists (which will be supposed henceforth) then it cannot be a globally homogeneous feature, but it must be structured.

Two types of geometries can be hypothesized for the supposed internal structure : axially symmetric and non symmetric cases. In the former case we should have latitudinal bands on either hemispheres having alternative twisting influences on the flux ropes. This would be a similar geometry to that of the giant rolls described by Ribes et al. (1985). However, no latitudinal distribution can be pointed out on the basis of the present material and approach.

The study of the non-axisymmetric cases is much more complicated. Many attempts have been made to recognize any longitudinal pattern in the distribution of the angles. There is no sensible structure in the Carrington coordinate system, therefore we supposed that the angular distribution is related to a certain subsurface formation of unknown angular velocity. At first we varied the angular velocity of this hypothetical internal formation by small steps, and searched for any distinguishable longitudinal domains containing sunspot groups of identical sings of tilt. Nothing could have been recognized for domains of size between 90° and 30°.

The only published internal longitudinal structural pattern sc far is the so-called "banana-roll" system. These hypothetical cells would be the manifestations of a global convection and, although observationally not yet confirmed, they have been resulted in independent theoretical calculations (Glatzmaier, 1984; Gilman and Miller, 1986). They are long meridional features and take the shape of a bunch of bananas, so that the material ascends in the border of two given "bananas" and it descends in the consecutive border. The longitudinal wave number of this pattern can be as high as 36, but according to the calculations, the most probable wave numbers are 10-12 (Glatzmaier, 1984, Gilman and Miller, 1986).

After several trials it became obvious, that purely the signs of the angles do not show any simple distribution. We also realized that the emerging sunspot groups cannot have equal importances and appropriate weights had to be attributed to them depending on their sizes and tilt angles. The following procedure has been performed : a hypothetical internal sector structure was considered with a given l wave number, say l=11 (this means 22 banana rolls with alternating directions of velocity field, their longitudinal size equals to 16.36°) and alternating positive and negative signs were attributed to them. If the position of a sunspot group of positive (negative) weight coincided with a positive (negative) sector respectively, than the absolute value of its weight was added to a sum of weights (ΣW), if not, then it was not added, so this

sum of weights characterizes the coincidence of the given sunspot group tilts with the supposed sector structure. Considering the finite distance of the preceding and following parts (2.5 degrees on average in the present material) we allowed for a strip of tolerance of either 2.5 degrees or 1/6 sector widths on both sides of a sector beyond the sector border. Thus the following three definitions were used :

Definition 1 (Paper I) : if the sunspot group has an angle α_i (in degrees) and area A_i (in millionths of the solar hemisphere) on the i-th day of its existence (i=1,2,3), then let its weight :

$$W = \Sigma \alpha_i \sqrt{A_i}$$

Definition 2 (Paper II) : the same as in definition 1 but using only the first day's angle and area allowing more (88) sunspot groups :

$$W = \alpha \sqrt{A}$$

Definition 3 (Paper II) corresponds to definition 2 but the strip of tolerance is equal to one sixth of the sector width.

Four further parameters were varied :

(a) The longitudinal wave number l from 2 until 15.

(b) If the angular velocity of this hypothetical sector structure differs from that of the surface, then it should be taken into account in calculating the coincidence of the position of an emerging flux with a sector. The $\Delta\omega$ differences (internal ω minus Carrington- ω) were computed in the range of $-3.2 \leq \Delta\omega \leq 4.1$ (degrees/day) by steps of 0.01 (degrees/day). These limits were taken from the Figure 1 of Hill's (1987) review.

(c) The position (phase) of the sector structure in the Carrington system has to be shifted through the range of two sectors (one wave) by 2° steps in order to find the best coincidence.

(d) The sectors may have a curvature (Glatzmaier (1984); Gilman and Miller (1986)), it was computed by the formula : $4Z \sin B$, Z has been varied from 0 to 36 by steps of 2.

The above (a)-(d) parameter-variations yield a huge amount of ΣW -values (almost 1.3 million configurations) and the question is, whether or not a given parameter configuration results in a convincingly high ΣW -value. The highest values of ΣW have been chosen for all l and $\Delta\omega$ values ((a) and (b) parameters) from the possible phases and curvatures ((c) and (d) parameters). If we plot the $(\Sigma W - \Delta\omega)$ histograms for all wave numbers then the peaks characterize the coincidence of the observed tilts with the considered sector structure. There is a remarkable peak at l=11 and about $\Delta\omega = -0.37$ degrees/day for all the three definitions but its predominance is much more convincing if the ΣW - values are normalized to the highest achievable ΣW (complete coincidence) and averaged for the three definitions at all l and $\Delta\omega$ -values ($\overline{\Sigma W}$). Figure 1 shows the result. Only $\overline{\Sigma W}$ -values higher than 3s level are indicated.

The most remarkable feature of Figure 1 is the band of high maxima exceeding the 5s level at l=11 and about $\Delta\omega = -0.37$ deg/day. The curvature of the sectors, the Z-parameter mentioned under (d) is very small (Z=0-4) for all the peaks constituting

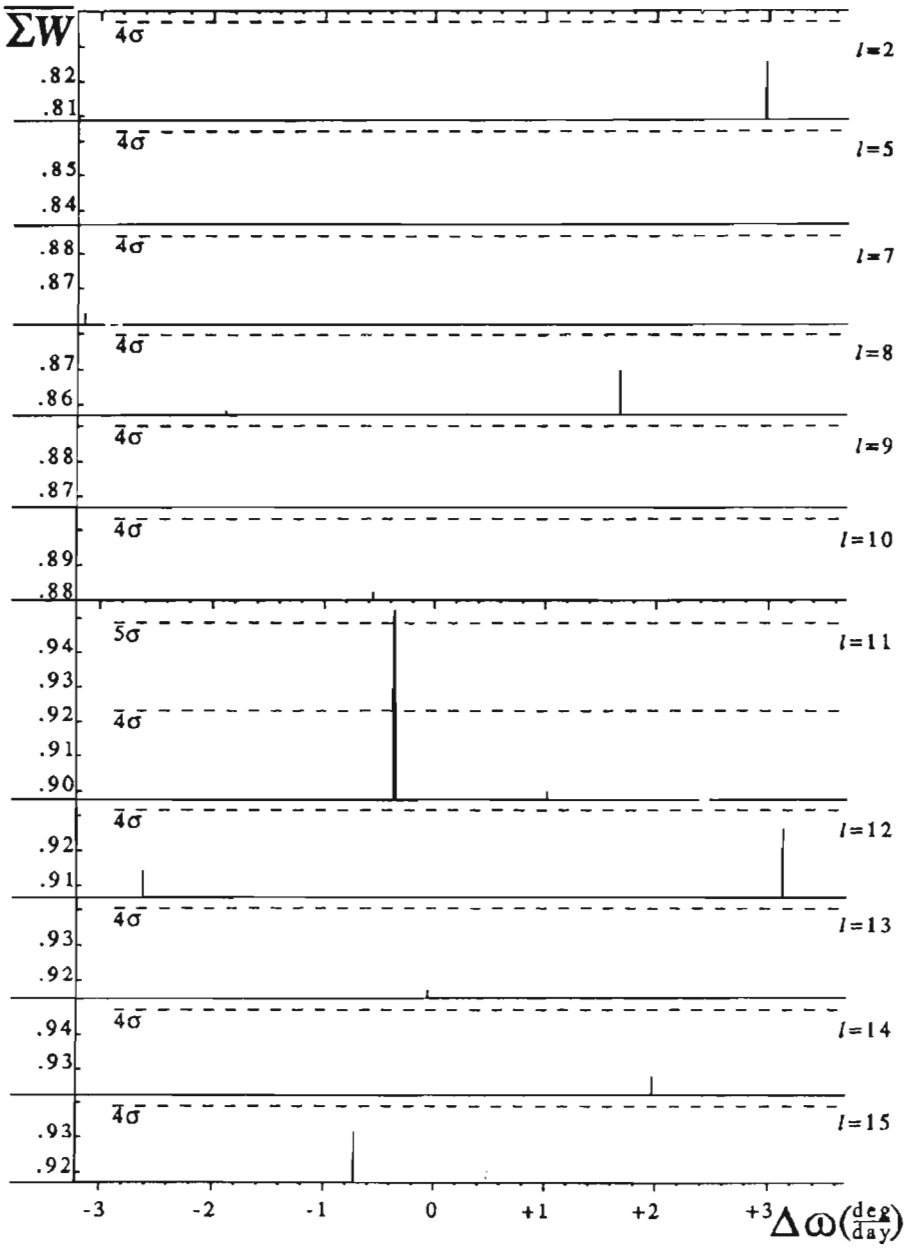

Fig. 1. Normalized sums of orientation weights ($\overline{\Sigma W}$) characterizing the coincidence of the tilts of emerging sunspot groups with various supposed internal sector structures as functions of longitudinal wave number (l) and difference of the internal-outer rotation rates ($\Delta\omega$). Only values above 3s level are displayed. The band of high values at l=11 and $\Delta\omega = 0.37$ deg/day indicate a probable internal structure.

the band, the distribution of the peaks is nearly gaussian. All possible concurrent peaks prove to be spurious and disappear in the averaging.

3. SUMMARY OF RESULTS

The tilts of axes of new active regions are not unidirectional; in two thirds of the examined cases the preceding part declines to the equator (positive tilt), in the rest of the cases the tilts are opposite.

If we suppose that there is a non-axisymmetric global convection system predicted by theory ("banana rolls"), then it is possible that the magnetic features are turned clockwise at the places of rising and expanding material, and anti-clockwise in the sinking, contracting material in the northern hemisphere and in the opposite direction in the south on account of the Coriolis forces, see Figure 2. This interpretation is not impossible because the rise of a magnetic flux is more favourable and probable in the domain of rising (and consequently positively turning) material than in the region of sinking, in accordance with the point (1).

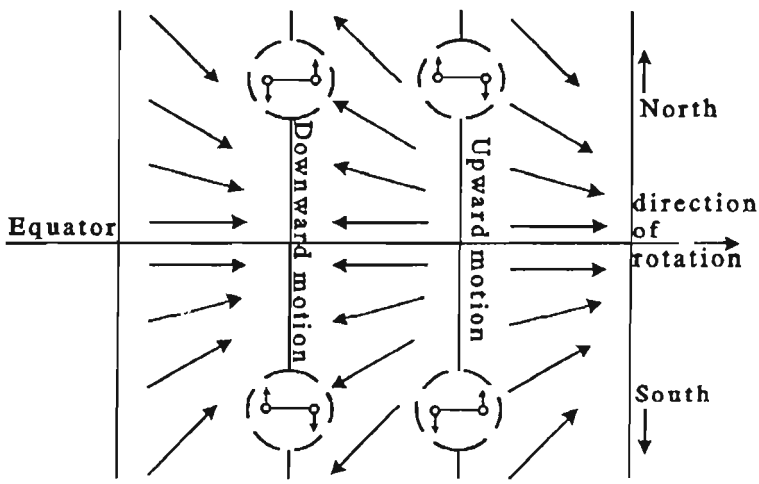

Fig. 2. Schematic view of three adjacent sectors close to the equator expected by theory. The rising-spreading as well as the contracting-sinking areas cause the plotted distortions of the azimuthal velocities on account of the Coriolis-force. The turning influence acting on the emerging fluxes are inserted in the dashed circles, the turn is positive in the rising regions in both hemispheres.

We defined a sum of weights (ΣW) to describe the coincidence of the given tilts with the corresponding sectors and this ΣW has been computed for several internal rotation rates and curvatures and for fourteen longitudinal wave numbers : l=2,..,15. If we assume that the "banana rolls" structure really exists and acts on the tilts of the emerging flux ropes, than the best fit (largest ΣW) can be achieved with the following

parameters : wave number : l=11, difference of its angular velocity from that of the Carrington system : $\Delta\omega = -0.35$ degrees/day (in other units $\nu = 444.6nHz$ or $\Omega = 2.79\mu rad/sec$), and the curvature of the rolls is negligible.

4. SOME ADDITIONAL REMARKS

It is worth comparing the above results with some observational and theoretical findings.

The inwards increasing angular velocity reported by many authors and based mainly on tracer measurements is certainly localized to the vicinity of the surface (see the review article of Hill, 1987) and it is possible that the layer of the mentioned global convection as a whole rotates somewhat slower than the surface, as is indicated e.g. by oscillation measurements (Duvall and Harvey, 1984; Brown 1985 and 1986; Libbrecht 1986; Rhodes et al., 1987 and 1991) and by theoretical considerations (Glatzmaier, 1985; Gilman and Foukal, 1979). It is noteworthy that Gilman and Howard (1984) measured the variations in the solar rotation rate; they subtracted the average rotation rate of the period 1967-1982 from the annual rates and the residual of the year 1977 is -0.32 degrees/day (see their Figure 1), almost the value found above, indicating perhaps that there was no substantial difference between the internal and surface rotation rates in this year as was also the case eleven years later in the regions above $0.75R\odot$ according to Goode and Dziembowski (1991), but this problem cannot be discussed without further data. In any case the same procedure can result in different rotation rates on different periods. Furthermore this angular velocity is smaller than those reported by Stenflo (1989) or Bai and Sturrock (1991) indicating that these data do not refer to the regions studied by these authors.

As for the wave number, the theoretical arguments are based on computations indicating maxima around l=10-12 in both of the thermal and kinetic energy spectra and also in the rates of maintenance of differential rotation by angular momentum transport (Glatzmaier, 1984; Gilman and Miller, 1986). So it can be assumed that the most probable number of waves is about 11 (22 sectors or "bananas") and their most probable characteristic size is $\pi/11$ at any given moment, and although many other sizes can appear temporarily, they cannot be distinguished with the present method as yet. This sector width is perhaps related to the size of the convective layer. These large N-S rolls stir up the whole convective region, they extend over almost the whole convective layer, so the thickness of this layer probably determines the possible number of the rolls being capable to optimal mixing. The wave number l=11 (22 sectors) means an angular extension of 16.36 degrees and an equatorial spatial extension of $0.286R\odot$ on the surface. This is not necessarily the size of the rolls but with such dimensions they could extend to the whole convective layer which has been measured to be as deep as $0.287R\odot$ (Christensen-Dalsgaard et al. 1991).

Parameters other than the angular velocity can also be variable in time such as the wave number and the curvature of rolls. Computations indicate (Glatzmaier, 1984; Gilman and Miller, 1986) that these formations, if they exist, are not very stable. Therefore an investigation of the present type cannot be performed on a much longer period because of the evolution of the given formation. Temporally separate

structures could be confused (which can take place in our case as well in spite of the clear predominance of the l=11 main band). Furthermore, the sizes of the sectors obviously cannot be precisely equal, which results probably in further false peaks.

We cannot study the N-S symmetry of the rolls as suggested by Brown and Gilman (1984) because the division of the limited material leads to restricted reliability, so at the moment we have simply to exploit the theoretical assumption of the symmetry and the whole unified material should be considered by using appropriate conventions of signs in both hemispheres.

As far as the axisymmetric or "doughnuts" rolls (Ribes et al., 1985) are concerned, we suggested that the two types of rolls could be reconciliated in time because 1977 is a minimum year with poloidal magnetic field and perhaps the toroidal field would enhance the axisymmetric geometry, but Gilman (1993) argued that this alternation should also cause variations in the differential rotation profile which is not yet observed. Glatzmaier (1987) notes that the "doughnut" rolls are observed but they cannot be theoretically explained as yet, and at the same time the banana rolls seem to be well established by theory, but they are not yet detected directly. He refers to a Spacelab experiment imitating similar geometry (Toomre et al., 1987). He attempts to resolve the apparent controversy by supposing the coexistence of the two types of motions : the meridional rolls are restricted to a shallow layer below the surface (so they do not have appreciable twisting effect) and the more extended banana-roll structure acts in the deeper regions, this idea was later discussed and supported also by Roberts (1991). If this is the case than these latter columnar giant convection cells constitute the deepest suspected structural pattern in the Sun. Therefore they are hardly detectable by spectroscopy, but perhaps the above method offers a chance.

It should be admitted that the present material does not allow to get a final proof of the existence of the columnar giant cells, it yields just a remarkable signal which might be the signature of them in the given year. Further studies should cover a longer period but this will be more complicated on account of the probable variability of the pattern. A further parameter : the length of the studied interval should also be varied and these variable intervals should be shifted along the whole interval in order to find the most persistent patterns. This needs a much longer material than used here so we should concentrate our efforts to the compilation of the Debrecen Photoheliographic Results which is a very long-term project.

Acknowledgements

We express our gratitude to dr. P. Gilman for a helpful discussion and for his advices and kind encouragements. The work was supported by grants OTKA F4142/1993 and T014036/1994.

References

Bai, T. and Sturrock, P. A. : 1991, *Nature*, **350**, 141.
Baranyi, T. and Ludmány, A. : 1992, *Solar Phys.* **139**, 247. (Paper I).
Baranyi, T. and Ludmány, A. : 1993, in *Inside the Stars*, IAU Colloquium 137., Weiss W. W. and Baglin A. eds., ASP Conf. Ser. **40**, pp. 81. (Paper II).

Brown, T. M. : 1985, *Nature*, **317**, 591.
Brown, T. M. : 1986, in *Seismology of the Sun and the Distant Stars, NATO ASI Series C169.*, Gough D. O. ed. D. Reidel, Dordrecht, p.199.
Christensen-Dalsgaard, J., Gough, D. O. and Thompson, M. J. : 1991, *Astrophys. J.* **378**, 413.
Dezső, L., Kovács and Gerlei, O. : 1987, *Debrecen Photoheliographic Results 1977, Publ. Debrecen Obs., Heliographic Series* No. 1.
Duvall, T. L. Jr. and Harvey, J. W. : 1984, *Nature*, **310**, 19.
Gilman, P. A. and Foukal, P. V. : 1979, *Astrophys. J.* **229**, 1179.
Gilman, P. A. and Howard, R. : 1984, *Astrophys. J.* **283**, 385.
Gilman, P. A. and Howard, R. : 1986, *Astrophys. J.* **303**, 480.
Gilman, P. A. and Miller, J. : 1986, *Astrophys. J. Suppl.* **61**, 585.
Gilman P. A. 1993, *personal communication.*
Glatzmaier, G. : 1984, *J. Comp. Phys.* **55**, 461.
Glatzmaier, G. : 1985, *Astrophys. J.* **291**, 300.
Glatzmaier, G. : 1987, in *The Internal Solar Angular Velocity* , Durney B. R. and Sofia S. eds., ASSL Vol. 137., D. Reidel, Dordrecht, p. 263.
Goode, P.R. and Dziembowski, W.A. : 1991, *Nature*, **349**, 223.
Hill, F. : 1987, in *The Internal Solar Angular Velocity*, Durney B. R. and Sofia S. eds., ASSL Vol. **137**, D. Reidel, Dordrecht, p. 45.
Howard, R. : 1991, *Solar Phys.* **136**, p.251.
Howard, R. : 1993, *Solar Phys.* **145**, p.95.
Libbrecht, K. G. : 1986, *Nature*, **319**, 753.
Rhodes, E. J. Jr., Cacciani, A., Korzennik, S., Tomczyk, S., Ulrich, R. K. and Woodard, M. : 1990, *Astrophys. J.* **351**, 687.
Rhodes, E. J., Cacciani, A. and Korzennik, S. : 1991, *Advances in Space Research*, **11** No. 4. 17.
Ribes, E., Mein, P. and Mangeney, A. : 1985, *Nature*, **318**, 170.
Roberts, P. H., 1991, in *The Cool Stars : activity, magnetism and dynamos*, Proc. of IAU Coll. 130. Tuominen I. et al. eds., Springer-Verlag, p.37.
Stenflo, J. O. : 1989, *Astron. Astrophys.* **210**, 403.
Toomre, J., Hart, J. E. and Glatzmaier G. A. : 1987, in *The Internal Solar Angular Velocity*, Durney B. R. and Sofia S. eds., ASSL Vol. **137**, D. Reidel, Dordrecht, p. 27.

Publ. Obs. Astron. Belgrade No. 49 (1995), 89-92

STARK BROADENING OF THE F V $3s^2S$-$3p^2P^O$ AND $3p^2P$-$3d^2D^O$ TRANSITIONS

B. BLAGOJEVIĆ, M. V. POPOVIĆ, N. KONJEVIĆ
Institute of Physics, 11080 Belgrade, P.O.Box 68, Yugoslavia

M. S. DIMITRIJEVIĆ
Astronomical Observatory, Volgina 7, 11050 Belgrade, Yugoslavia

Abstract. The Stark widths of several fourthly ionized fluorine lines have been calculated and measured in the plasma of a pulsed arc. Electron density $2.54 \times 10^{17} cm^{-3}$ was determined from the width of the HeII P_α line while electron temperature of 71200 K is measured from the relative intensities of F IV lines. Our experimental FV widths agree well with our semiclassical theoretical results. The results of another experiment for 3p-3d transition is in a good agreement with our theoretical and experimental data while the discrepancy for 3s-3p transition is rather large. The results of two simple theoretical methods for evaluation of Stark widths are in reasonable agreement with experiment.

1. INTRODUCTION

Broadening and shift of spectral lines in plasmas were the subject of numerous experimental studies (see e.g. Konjević and Wiese 1990. and references therein). Unfortunately, most of the reported data are for the lower ionization stages. The lack of the experimental data makes a detailed test of the Stark broadening theoretical calculations incomplete. The aim of this paper is to supply the theoretical and experimental data for the widths of prominent fourthly ionized fluorine lines for a large electron temperature range. The reported experimental results together with other experimental data will be used for the testing of semiclassical and other theoretical calculations.

2. THEORY

By using the semiclassical-perturbation formalism (Sahal-Bréchot 1969) we have calculated electron- and ion-impact line widths for FV $3s^2S$-$3p^2P^o$ and $3p^2P^o$-$3d^2D$ multiplets. A summary of the formalism is given in Dimitrijević et al 1991. For the comparison with experiment theoretical widths are also evaluated from simplified semiclassical formula (Eq.526, Griem 1974) and modified semiempirical formula (Dimitrijević and Konjević 1980). All necessary data for these calculations are taken from Bashkin and Stonner 1975.

3. EXPERIMENT

Experimental apparatus and procedure are described elsewhere (Blagojević et al 1994) so only minimum details will be given here. The light source was a low pressure pulsed arc with a quartz discharge tube 10 mm internal diameter. The distance between aluminum electrodes was 16.1 cm, and 3 mm diameter holes were located at the center of both electrodes to allow end- on plasma observations. All plasma observations are performed with 1-m monochromator with inverse linear dispersion 8.33 $\AA$/mm in the first order of the diffraction grating, equipped with the photomultiplier tube and a stepping motor. The discharge was driven by a 15.2 μF low inductance capacitor charged to 4.8 kV (peak current 15.8 kA, critically dumped current pulse duration 8.3 μs, pressure of the gas mixture 0.8 torr, continuous flow of the gas mixture 1.4% of SF_6 in He) and fired by ignitron. The stepping motor and oscilloscope are controlled by a personal computer, which was also used for data acquisition. Recordings of spectral line shapes were performed shot-by-shot. At each wavelength position of the monochromator time evolution and decay of the plasma radiation were recorded by the oscilloscope. Four such signals are averaged at each wavelength. To construct the line profiles these averaged signals at different wavelengths and at various times of the plasma existence were used. Spectral line profiles were recorded with instrumental half widths of 0.192 $\AA$. To determine the Stark half widths from the measured profile, a standard deconvolution procedure for the Lorentzian (Stark) and Gaussian (instrumental+Doppler) profiles (Davies and Vaughan 1963) was used. For the electron density measurements we used the width of the HeII P_α 4686 $\AA$ line (Pittman and Fleurier 1986). The axial electron temperatures were determined from intensities of the 2635.37-, 2820.74-, 2823.84- and 2826.13-$\AA$ F IV lines. The spectral response of the photomultiplier-monochromator system is calibrated against standard coiled-coil quartz iodine lamp.

4. RESULTS

Comparison of the experimental and theoretical results for the lines belonging to 3s-3p and 3p-3d transitions are given in Figures 1 and 2 respectively. In these Figures theoretical widths are denoted in the following way : electrons only; •, electrons+ions for our experimental conditions : Δ, electrons +ions for the conditions of the experiment by Glenzer et al 1994; — simplified semiclassical approach after Griem 1974; — — —, modified semiempirical formula, after Dimitrijević and Konjević 1980 : o, this experiment, and D, experimental results by Glenzer et al 1994. Our experimental results compare very well with our theoretical results (electrons+ions) see Figs.1 and 2. Same conclusion one may draw for 3p-3d line of Glenzer et al 1994. However, one may not draw same conclusion for the high temperature result the 3s-3p line, see Fig.1. Although the results of simple formulas, (see Figs.1 and 2) are systematically lower than the experimental results, both simplified approaches agree with experiment within the estimated uncertainties of about 50%.

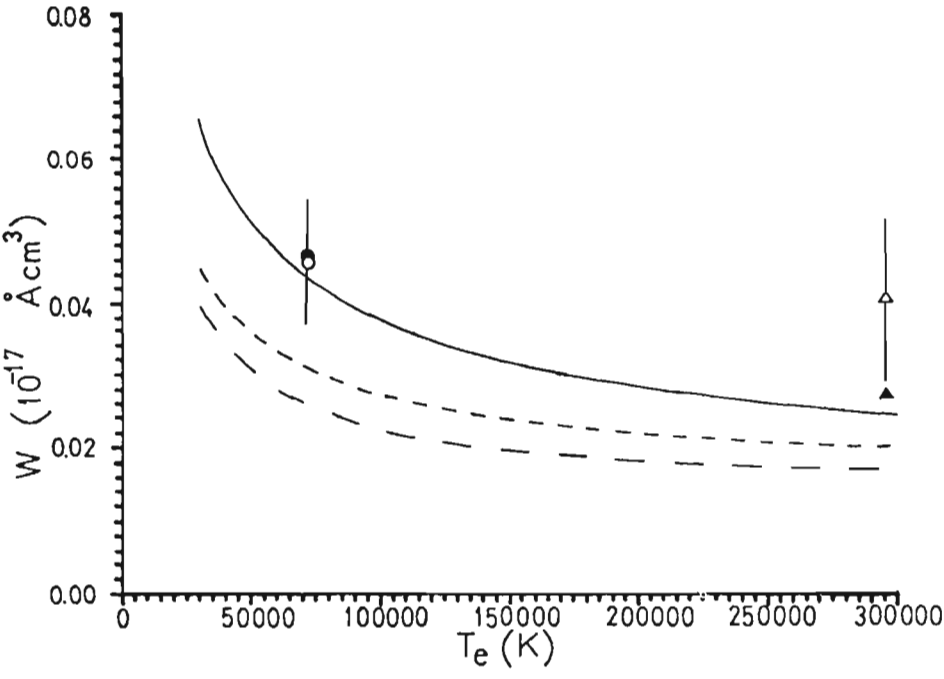

Fig. 1. 3s-3p transition

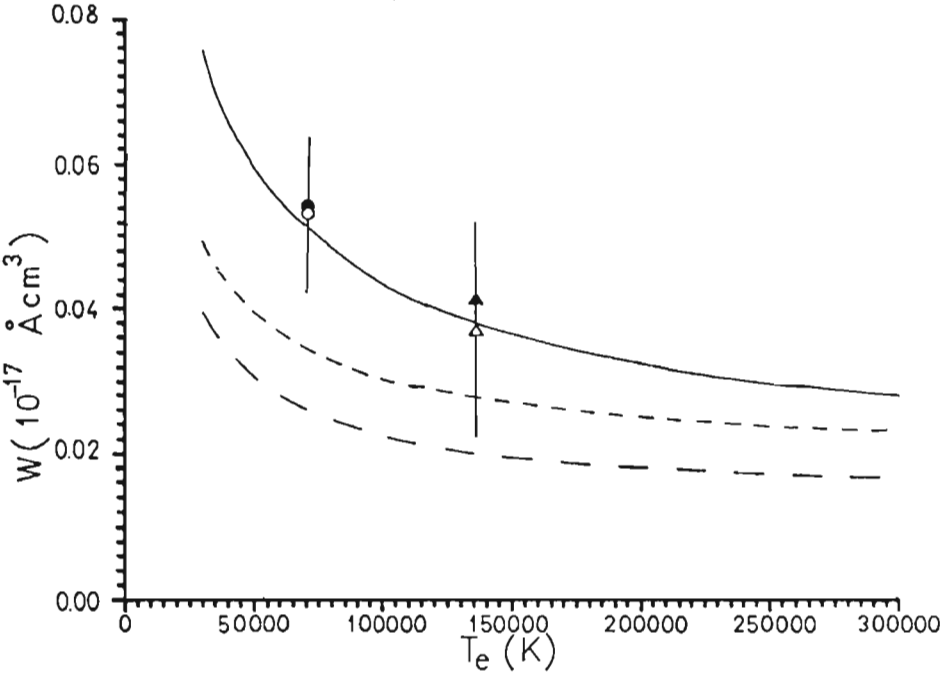

Fig. 2. 3p-3d transition

References

Bashkin, S. and Stonner, J. O. : 1975, *Atomic Energy Levels and Grotrian Diagrams*, Vol.I, North Holland, Amsterdam, p.266.
Blagojević, B., Popović, M. V., Konjević, N. and Dimitrijević, M. S. : 1994, *Phys. Rev. E* **50**, 2986.
Davies, J. T. and Vaughan, J. M. : 1963, *Ap. J.* **137**, 1302.
Dimitrijević, M. S. and Konjević, N. : 1980, *JQSRT*, **24**, 451.
Dimitrijević, M. S., Sahal-Bréchot, S. and Bommier, V. : 1991, *Astron. Astrophys. Suppl. Ser.* **89**, 581.
Griem, H. R. : 1974, *Spectral Line Broadening by Plasmas*, Academic, New York, p. 279.
Konjević, N. and Wiese, W. L. : 1990, *J. Phys. Chem. Ref. Data* **19**, 1307.
Pittman, T. L. and Fleurier, C. : 1986 *Phys Rev. A*, **33**, 1291.
Sahal-Bréchot, S. : 1969, *Astron. Astrophys.* 191; 2, 322 (1969).

Publ. Obs. Astron. Belgrade No. 49 (1995), 93-96

STARK SHIFTS OF N III AND O IV LINES

B. BLAGOJEVIĆ, M. V. POPOVIĆ, N. KONJEVIĆ
Institute of Physics, 11080 Belgrade, P.O. Box. 68, Yugoslavia

M. S. DIMITRIJEVIĆ
Astronomical Observatory, Volgina 7, 11050 Belgrade, Yugoslavia

Abstract. The Stark shifts of several lines belonging to analogous multiplets, $3s^2S$-$3p^2P^o$ and $3p^2P^o$-$3d^2D^2$, of doubly ionized nitrogen and triply ionized oxygen (boron isoelectronic sequence) have been calculated and measured in a plasma of a low pressure pulsed arc. Plasma electron densities are determined from the width of the HeII P_α line. Electron temperatures are measured from relative intensities of NIII lines while temperatures in oxygen mixture are determined from relative intensities of IV lines. Experimental NIII Stark shifts are in reasonable agreement with our semiclassical calculations. In the case of OIV lines theory predicts shifts of the opposite sign. Possible causes of this discrepancy are discussed.

1. INTRODUCTION

While broadening of NIII and OIV spectral lines in plasmas was a subject of several experimental and theoretical studies (see e.g. Konjević and Wiese 1990 and Blagojević et al 1994 and references in both papers) only two experimental results for the shifts of 3s-3p lines are reported (Purić et al 1987). Therefore, here we present the results of experimental and theoretical plasma shift study of the analogous transitions of NIII and OIV (the isoelectronic sequence of boron). These types of studies are very convenient for the testing of theory (similar energy level structure of the emitter with gradual increase of the ionic charge), allowing also determination of the Stark shift and/or width dependence upon ionic charge Z of the emitter which is of importance for the estimation of the broadening parameters for the ions with no available data. Recent experimental study of the Stark shifts along P isoelectronic sequence (4s-4p transition of SII, ClIII and ArIV) shows, as in the case of Stark widths, gradual shift decrease with increasing ionic charge (Kobilarov and Konjević 1990 and Wiese and Konjević 1992). Furthermore, the change of the sign of the shift along the S sequence (4s'-4p' transition of ClII and ArIII) is detected. This shift behavior can be explained by the irregular change of the perturbing energy levels disposition around upper and/or lower level of the transition along the sequence. In this case simple theory (Dimitrijević and Kršljanin 1986) predicted well the sign of the shift. The aim of this paper is to supply the theoretical and experimental data for the Stark shifts for several lines of the analogous transitions of NIII and OIV.

2. THEORY

By using the semiclassical formalism (Sahal-Bréchot 1969, see also Dimitrijević et al 1992) we have calculated electron- and ion-impact Stark line shifts for NIII and OIV 3s S-3p P and 3p P -3d D multiplets, All necessary data for these calculations are taken from Bashkin and Stonner 1975.

3. EXPERIMENT

Experimental apparatus and procedure are described in details elsewhere (Blagojević et al 1994 and Blagojević et al this conference). The light source was a low pressure pulsed arc operated with gas mixtures : 2% nitrogen in helium and 1.4% oxygen in helium. During the spectral line recordings continuous flow of gas mixture was maintained at a pressure of 3 torr. For the line-shift measurements we used line profiles at the different times of the plasma existence (Purić and Konjević 1972). For this technique of shift measurement it is necessary to know plasma parameters (electron density and temperature) at the times when both profiles are recorded. For the electron density measurements we use the width of the HeII P_α 4686 $\AA$ line Pittman and Fleurier 1986). Electron temperatures are determined in nitrogen-helium plasma from the relative intensities of four lines, 4103.43-, 4097.33-, 4634.16- and 4640.64-$\AA$, which belong to NIII. Electron temperatures in oxygen- helium plasma are determined from the Boltzmann plot of the relative intensities of several OIV lines.

4. RESULTS

The experimental results for the Stark shifts Δd_m of NIII and OIV lines are given in Table I together with plasma parameters and estimated errors for the various measured quantities. Table I also contains spectroscopic data for the investigated lines and comparison with our theoretical results Δd_{DSB} (electrons + ions). The shifts of another Comparison of experimental and theoretical data for NIII lines shows a reasonable agreement which is well within estimated uncertainties of both, experiment and theory, see Table I. For OIV lines theory predicts opposite sign of the shift. Possible causes for this discrepancy are eventual configuration mixing.

Table 1.

Ion	Transition	λ_{tab} (A)	N_{e1} ($10^{17}cm^{-3}$)	T_1 (K)	N_{e2} ($10^{17}cm^{-3}$)	T_2 (K)	$\Delta d_m/\Delta N_e$	$\Delta d_m/\Delta d_{DSB}$ (10^{-17} A cm^3)	Ref.
N III	$3s^2S_{1/2}$-$3p^2P^o_{3/2}$	4097.33	1.38	33000	2.52	44300	-3.5[-2]±54%	117	a
	$3s^2S_{1/2}$-$3p^2P^o_{3/2}$	4097.33	~ 0		1.78	50000	-2.3[-2]±36%	3.56	b
	$3s^2S_{1/2}$-$3p^2P^o_{1/2}$	4103.43	1.38	33000	2.52	44300	-3.5[-2]±54%	117	a
	$3s^2S_{1/2}$-$3p^2P^o_{1/2}$	4103.43	~ 0		1.78	50000	-2.3[-2]±36%	3.56	b
	$3p^2P^o_{1/2}$-$3d^2D_{3/2}$	4634.16	1.38	33000	2.52	44300	-3.5[-2]±54%	129	a
	$3p^2P^o_{3/2}$-$3d^2D_{5/2}$	4640.64	1.38	33000	2.52	44300	-2.6[-2]±62%	96	a
O IV	$3s^2S_{1/2}$-$3p^2P^o_{3/2}$	3063.43	2.06	62600	5.07	93600	1.0[-2]±62%	*	a
	$3s^2S_{1/2}$-$3p^2P^o_{1/2}$	3071.60	2.06	62600	5.07	93600	1.0[-2]±62%	*	a
	$3p^2P^o_{1/2}$-$3d^2D_{3/2}$	3403.60	2.06	62600	5.07	93600	1.0[-2]±62%	*	a
	$3p^2P^o_{3/2}$-$3d^2D_{5/2}$	3411.76	2.06	62600	5.07	93600	1.0[-2]±62%	*	a

*, Theory predicts opposite sign of the shift
a, Our work,
b, Purić et al 1988

References

Bashkin, S. and Stonner, J. O. : 1975, "Atomic Energy Levels and Grotrian Diagrams", Vol.I, North Holland, Amsterdam, pp. 132, 186.

Blagojević, B., Popović, M. V., Konjević, N. and Dimitrijević, M. S. : 1994, *Phys. Rev. E*, **50**, 2986.

Dimitrijević, M. S. and Kršljanin, V. : 1986, *Astron. Astrophys.* **165**, 269.

Dimitrijević, M.S., Sahal-Bréchot, S., and Bommier, V. : 1991, Astron. Astrophys. Suppl. Ser. 89, 581.

Kobilarov, R. and Konjević, N. : 1990, *Phys. Rev. A*, **41**, 6023.

Konjević, N. and Wiese, W. L. : 1990, *J. Phys. Chem. Ref. Data*, **19**, 1307.

Purić, J. and Konjević, N. : 1972, *Z. Phys.* **249**, 440.

Purić, J., Djenıže, S., Sre'ković, A., Milosavljević, M., Platiša, M. and Labat, J. : 1988, 14 Summer School and Symp. Phys. Ionized Gases, Contrib. Papers (Eds. Konjević N., Tanović L. and Tanović N.) Sarajevo, Yugoslavia, p.345

Pittman, T. L. and Fleurier, C. : 1986, *Phys. Rev. A*, **33**, 1291.

Sahal-Bréchot, S. : 1969, *Astron. Astrophys.* **1**, 91; **2**, 322.

Wiese, W. L. and Konjević N. : 1992, *JQSRT*, **47**, 185.

Publ. Obs. Astron. Belgrade No. 49 (1995), 97-107

A SEARCH FOR POSSIBLE UNRESOLVED COMPONENTS IN EIGHTEEN ECLIPSING BINARIES

T. BORKOVITS
Department of Astronomy, Eötvös Loránd University, Ludovika tér 2, H-1083, Budapest, Hungary

T. HEGEDÜS
Baja Observatory, Szegedi út, PF.766., H-6500, Baja, Hungary

Abstract. A total of 8507 minima times (6890 visual and 1617 photographic or photoelectric ones) of 18 eclipsing binary stars (*Table 1.*) have been separated and collected from the remarkable collection of late Dieter Lichtenknecker and from the recent literature. Using the Kopal (1978) method for the analysis of the obtained O-C diagrams of these systems (belonging to different types of eclipsing variables) one can classify them into three categories :

1. **'good cases' :** systems with light-time effect resulting third component with reasonable orbital and astrophysical parameters. They are AB And, TV Cas, XX Cep, AK Her. (Figs. 1.-4.)
2. **'probable cases' :** good candidates of multiplicity but the observational data available up to now are insufficient for obtaining satisfactory description. Light-time analysis of these systems has resulted weaker solutions as for the previous group, but they can be held as noticeable targets for the future studies. These systems are W Del, U Peg, AT Peg, ST Per. (Figs. 5.-8.)
3. **'problematical cases' :** For these systems either we do not have enough data for making unambiguos identification of the sinusoidal O-C (due to light-time effect) and thus, we could not find a corresponding good third-body orbit, or the mathematical analysis led to results which are inconsistent with other observational or astrophysical facts. They are RT And, XZ And, OO Aql, Y Cam, RS CVn, TW Cas, CQ Cep, U CrB, MR Cyg and SW Lac. (In the case of TW Cas and SW Lac we couldn't be able to find any LITE solution.) (Figs. 9.-16.)

1. ANALYSIS

All data sequences were handled in the same manner. After making a first plot of the raw O-C diagram, we decided whether it is necessary to remove the effect of another type of major period variation or not. It was necessary to subtract a parabola from the O-C diagram of eight of the 18 studied systems using a least-squares method. The obtained clear, periodic pattern was analyzed by a DFT program written by one of us (T.B.) in view of the data points having equal weights. The software was checked by the MUFRAN code (Kolláth, 1990). With the frequencies coming from the Fourier-analysis an optionally weighted least-squares fitting was performed which

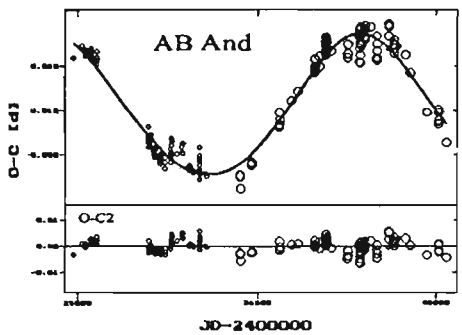

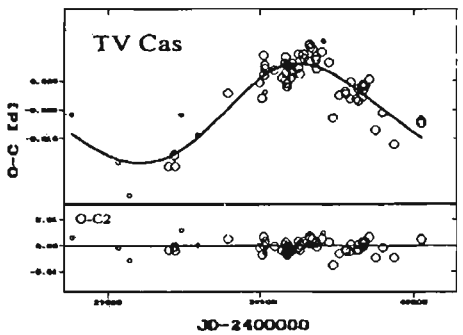

Fig. 1 & 2. Light time (LITE) solutions and residuals for Group 1. stars

The key for all figures: · - visual ◇ - "plate" minima
○ - photographic ○ - photoelectric observations

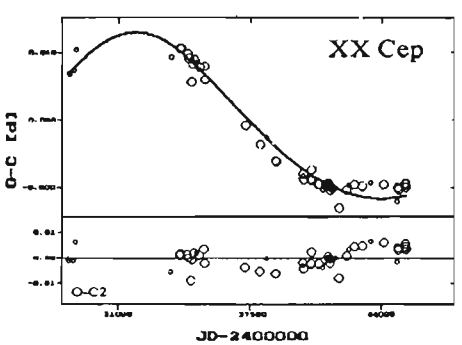

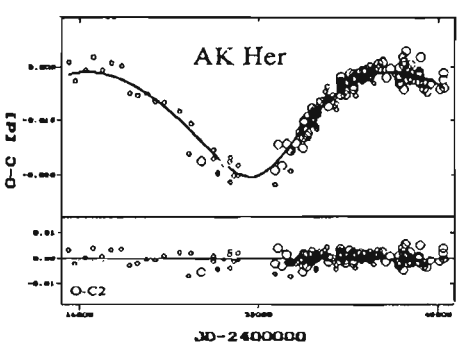

Fig. 3 & 4. Light time solutions and residuals for Group 1. stars

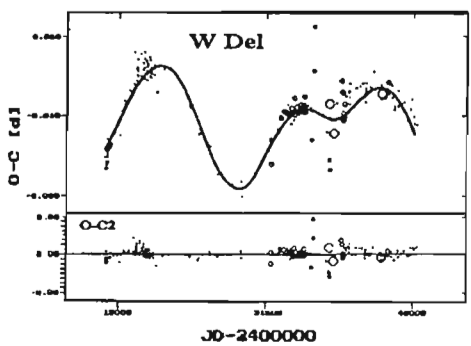

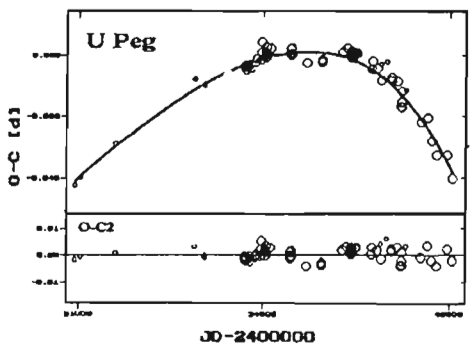

Fig. 5 & 6. Light time solutions and residuals for Group 2. stars

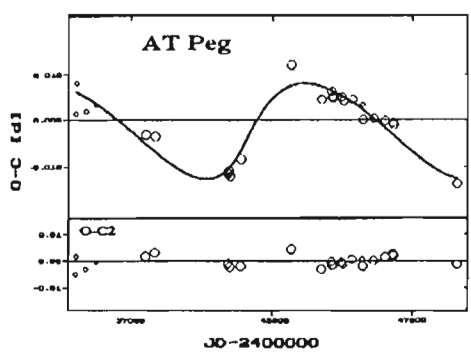

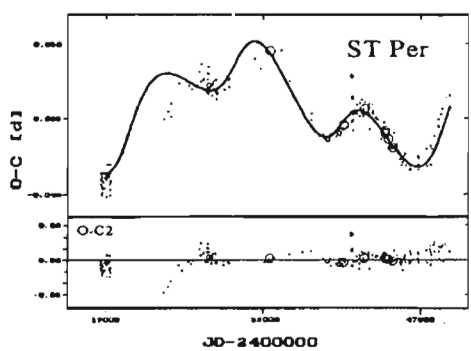

Fig. 7 & 8. Light time solutions and residuals for Group 2. stars

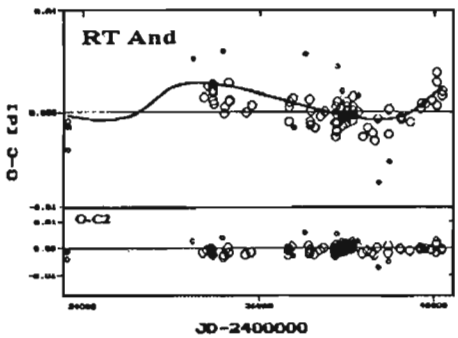

Fig. 9. PgPe points of RT And and the fourth body representation (after whitening with the third body effect)

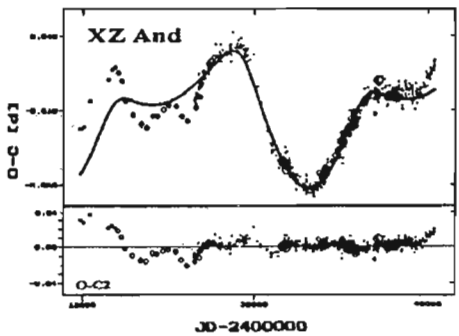

Fig. 10. TOT points of XZ And with our "best" solution

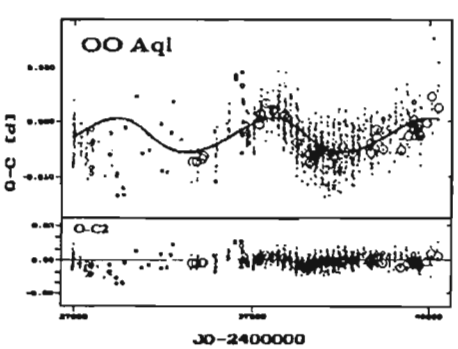

Fig. 11. TOT points of OO Aql with LITE solution made after the removal of a parabola

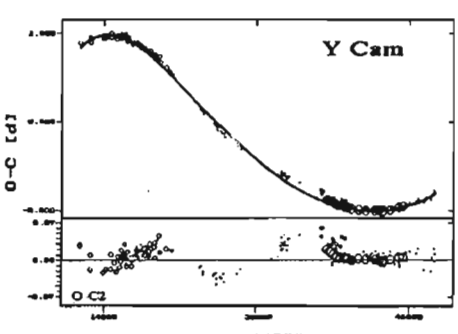

Fig. 12. TOT points of Y Cam with our formal LITE solution

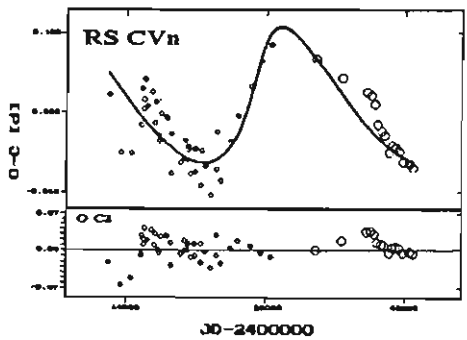

Fig. 13. PgPe points of RS CVn with LITE solution made after the removal of a parabola

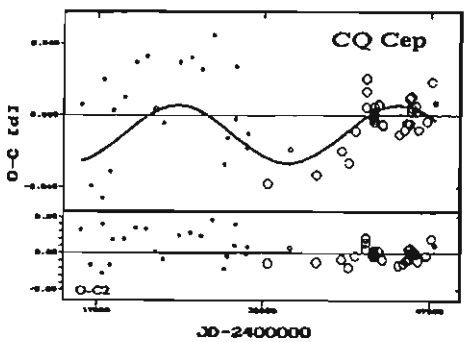

Fig. 14. TOT points of CQ Cep with LITE solution made after the removal of a parabola

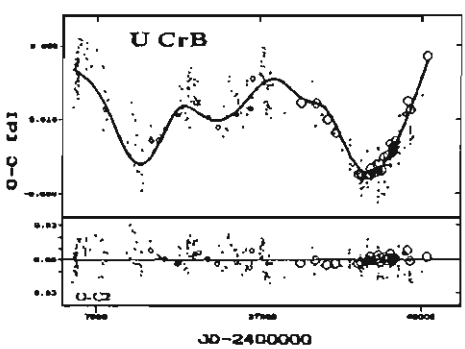

Fig. 15. A four body representation for the TOT points of U CrB

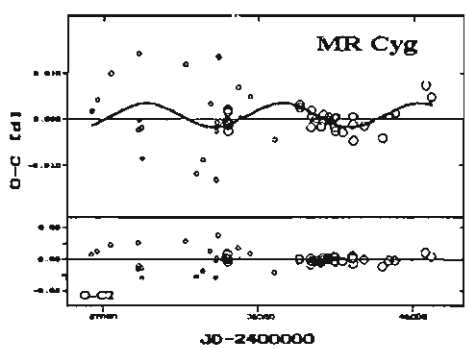

Fig. 16. PgPe points of MR Cyg with LITE solution made after the removal of a parabola

gave the necessary coefficients for the calculation of orbital elements. In general, we have repeated all procedures twice : using all available minima times (TOT), and using only the photographic (without observational results marked as 'plate minima') and photoelectric data (PGPE). There was one case (MR Cyg), when it was necessary to use only the photoelectric observations for achieving some result. The elements of the orbit of the third body were computed by the well-known formulas (Kopal, 1978) :

$$A_1' \sin i' = c\sqrt{a_1^2 + b_1^2} \tag{1}$$

$$e' = 2\sqrt{\frac{a_2^2 + b_2^2}{a_1^2 + b_1^2}} \tag{2}$$

$$\omega' = \arctan\left(\frac{(b_1^2 - a_1^2)b_2 + 2a_1a_2b_1}{(a_1^2 - b_1^2)a_2 + 2a_1b_1b_2}\right) \tag{3}$$

$$\tau' = t_0 - \frac{P'}{2\pi}\arctan\left(\frac{a_1b_2 - b_1a_2}{a_1a_2 - b_1b_2}\right) \tag{4}$$

where $a_{1,2}$,$b_{1,2}$ are the Fourier coefficients coming from the analysis as it was described above (i:e. the method needs first harmonics of the fundamental frequency), A' denotes the semi-major axis of the absolute orbit of the centre of mass of the eclipsing pair around that of the triple system, i', e', ω', t' and P' are the usual elements of the third body orbit. P is the sidereal period of the close pair, while c is the velocity of light.

These equations can be considered to be a good approximation for the smaller excentricities. During the test of our procedure we could obtain reliable results for $e' < 0.6$. Thus, for several cases we used only the first-order approximation shown above.

When the quality of the observational material and the behaviour of the observed variation allowed it, we used the second-order approximation for determination of the orbital data. By this approximation one can determine the orbital elements as follows :

$$e' = \frac{4}{3}\sqrt{\frac{a_3^2 + b_3^2}{a_2^2 + b_2^2}} \tag{5}$$

$$\omega' = \arctan\sqrt{-\frac{(1 - e_2'^2)[16C_1e'^2 - (e'^2 - 8)^2]}{16C_1e'^2 - (3e'^2 - 8)^2}} \tag{6}$$

where $C_1 = \frac{a_1^2+b_1^2}{a_2^2+b_2^2}$;

$$\tau' = t_0 - \frac{P'}{2\pi}\arctan\frac{1 - \frac{a_1}{b_1}\frac{h_1}{g_1}\tan\omega'}{\frac{a_1}{b_1} + \frac{h_1}{g_1}\tan\omega'} \tag{7}$$

$$A_1' \sin i' = c\frac{a_1^2 + b_1^2}{h_1^2 + (g_1^2 - h_1^2)\cos\omega'^2} \tag{8}$$

where

$$g_1 = (1 - \frac{e'^2}{8})\sqrt{1 - e'^2}$$

and

$$h_1 = \frac{1 - 3e'^2}{8}$$

See e.g. at Vinkó (1989). Other designations are the same as above. Because of the features of the Fourier-analysis, sometimes it was necessary to add $P'/2$ to the resulted value of t'. Of course, this approximation needs two harmonics of the fundamental frequency. Relevant coefficients are $a_{1,2,3}$ and $b_{1,2,3}$.

From the orbital parameters determined by the above presented expressions, one can define the mass function as the following :

$$f(m_3) = \frac{m_3^3 \sin^3 i'}{(m_{12} + m_3)^2} = \frac{4\pi^2 A_1'^3 \sin^3 i'}{GP'^2} \tag{9}$$

where m_{12} is the sum of masses of the two component stars of the eclipsing binary system, while m_3 is the mass of the third body. G is the gravitational constant. At this point, the right-hand side of this equation can be computed. In the sense of expression (9) we have a third order equation for the unknown m_3 mass of the third body :

$$m_3 \sin^3 i' - m_2^3 f(m_3) - 2m_3 m_{12} f(m_3) - m_{12}^2 f(m_3) = 0 \tag{10}$$

Of course, the result will contain a free parameter ($\sin i'$) which remains undeterminable from these kind of observations. We shall present (as it was done usually by other authors) the masses of the hypothetical satellites for a few different inclinations of its orbit.

2. RESULTS

Table 2. contains the 18 ephemeris used in our analysis, while the resultant orbital parameters can be found in *table 3.-5.* for the groups I.-III.

Table 1. Main parameters of the investigated systems

Name	T	TOT	PGPE	mag		$sp_1 + sp_2$	M_1	M_2	P	Sources
				max	min					
RT And	A	729	97	8 55	9 47V	F8V	1 52	1 00	0 63	1,2
XZ And	A	753	75	10 02	12 99p	A0+G8 · III	3 23	1 65	1 36	1,3
AB And	W	1148	187	9 50	10 32V	G5+G5V	1 06	1 71	0 33	1,4
OO Aql	W	1085	77	9.2	9 9V	G5V	sum=2 5		0 51	1,8
Y Cam	A	248	57	10 50	12 24V	A8V	2 33	0 50	3 31	1,2
RS CVn	A	93	58	7 93	9 14V	F4IV+K0IVe	1.42	1 35	4 80	1,2
TV Cas	A	657	77	7 22	8 22V	B9V+F7IV	4 04	1 62	1 81	1,5
TW Cas	A	168	72	8 32	8 98V	B9V+A0	2 90	1 18	1 43	1,2
XX Cep	A	191	59	9 13	10 28p	A8V	1 87	0 32	2 34	1,5
CQ Cep	β	58	38	8 63	9 12V	WN5 5+O7	17 5	21 1	1 64	1,6
U CrB	A	269	40	7 66	8.79V	B6V+F8III	4.7	4 4	3 45	1,11
MR Cyg	A	120	53	8 75	9 68V	B3V+B9	7 6	5 7	1 68	1,9
W Del	A	184	32	9 69	12 33V	B9 5Ve+G5	2 01	0 42	4 81	1,5
AK Her	W	330	177	8 29	8 77V	F2+F6	sum=1 5		0 42	1,7
SW Lac	A	1669	402	8 51	9 39V	G8Vp+G8Vp	0 96	1 14	0 32	1,4
U Peg	A	423	79	9 23	10 07V	F3+F3	1 29	0 86	0 37	1,2
AT Peg	A	176	26	8 97	9 75V	A7V	2 2	0 93	1 15	1,10
ST Per	A	206	11	9 52	11 40V	A3V+G-K	2 03	0 39	2 65	1,2

Remarks :

T : type of the light changes (A : Algol, W : W Uma, β : β Lyr.)
TOT : total number of all accepted times of minima of the stars.
$PGPE$: number of photographic and photoelectric times of minima.
mag : brightness of the system in maximum and minimum light (p : photographic, v : V-filter photoelectric stellar magnitudes).
$sp_1 + sp_2$: spectral types of the components according to the GCVS.
M_1, M_2 : masses of the components in Solar Masses.
P : Approximate period of leght changes (in days).

Sources

1 : GCVS 4th ed., Kholopov et al., 1985;
2 : Giannone & Gianuzzi, 1974;
3 : Budding, 1984;
4 : Rovithis-Livaniou et al., 1990;
5 : Van Hamme & Wilson, 1990;
6 : Kartasheva & Svechnikov, 1986;
7 : Nagy, 1985;
8 : Hrivnak, 1989;
9 : Linnell & Kallrath, 1987;
10 : Hill & Barnes, 1972;
11 : Heintze, 1990.

Table 2. Ephemerides used for O-C diagrams

AB And	Min I pgpe	2436109 58041	+0 33188985 E	+5 335 $10^{-11}E^2$	recent paper
TV Cas	Min I pgpe	2444662 27198	+1 81260 E	-8 697 $10^{-10}E^2$	recent paper
XX Cep	Min I pgpe	2444839 8022	+2 33732665 E		GCVS 1985
AK Her	Min I pgpe	2442186 460	+0 42152227 E		Barker&Herczeg (1979)
U CrB	Min I tot .	2437844 37911	+3 45220552 E		Mayer et al (1991)
W Del	Min I tot	2443328 52755	+4 80610015 E	+7 253 $10^{-9}E^2$	recent paper
U Peg	Min I pgpe	2436511 66821	+0 374781439E		GCVS 1985
AT Peg	Min I pgpe	2445219 85614	+1 1460796E	-1 05 $10^{-9}E^2$	recent paper
ST Per	Min I tot .	2442436 577919	+2 6483418 E		recent paper
RT And	Min I pgpe :	2441141 88901	+0 628929513 E		GCVS 1985
XZ And	Min I tot	2423977.1915	+1 357278 E		GCVS 1985
OO Aql	Min I tot :	2438613.21434	+0 5067914 E	-1 618 $10^{-10}E^2$	recent paper
Y Cam	Min I tot	2442961 9276	+3 3056244 E		GCVS 1985
RS CVn	Min I pgpe	2422811 69133	+4 7978765 E	-6 593 $10^{-9}E^2$	recent paper
TW Cas	Min I tot	2442008 3873	+1 4283240 E		GCVS 1985
CQ Cep	Min I tot ·	2432456 706	+1 641247 E	-1 05 $10^{-9}E^2$	recent paper
MR Cyg	Min I pgpe	2433396 4096	+1 67703362 E		GCVS 1985

Table 3. Solutions for group I. systems

	AB And	TV Cas	XX Cep	AK Her
Remarks	1,3,5	1,3,5	3,5	3,5
P'_{orb}	19764.71	21412 46	21888 38	27243 24
e'	0 14	0 16	0 26	0 33
ω'	1 30	0 53	1 32	5 10
τ'	22570 12	37774 42	31054 65	32442 26
$a' \sin i'$	413 19	219 95	968 44	381 88
$f(m_3)$	0 0072	0 0009	0 0751	0 0030
m_3 90°	0 42	0 32	0 89	0 21
60°	0 49	0 37	1 07	0 24
30°	0 92	0 61	2 30	0 45
dev Fr	0 0022	0 0023	0 0026	0 0021
dev O-C	0 0022	0 0023	0 0029	0 0021

Table 4. Solutions for group II. systems

	W Del		U Peg	AT Peg	ST Per	
Remarks	1,2		4	1,4,5	2	
	3 *	4 *			3 *	4 *
P'_{orb}	21444 26	13432 78	49721 00	9168 64	27000 00	9411 77
e'	0 36	0 18	0 43	0 39	0 19	0 24
ω'	4 44	4 30	3 55	6 05	5 80	6 36
τ'	29105 99	38835 92	50631 38	41011 26	48543 06	39904 00
$a' \sin i'$	1094 55	567 70	1188 50	290 70	678 64	426 87
$f(m_3)$	0 1130	0 0402	0 0269	0 0116	0 0170	0 0348
m_3 90°	1 12	0 74	0 59	0 54	0 53	0 70
60°	1 36	0 88	0 69	0 63	0 62	0 80
30°	2 98	1 79	1 39	1 20	1 22	1 67
dev Fr	0 0114		0 0021	0 0013	0 0062	
dev O-C	0.0125		0 0022	0 0021	0 0062	

Table 5. Solutions for group III. systems

	RT And		XZ And		OO Aql	Y Cam	RS CVn	CQ Cep	U CrB		MR Cyg
Remarks	3		2		1,2	2	1,3	1,2	2		1,4
	3 *	4 *	3 *	4 *							
P'_{orb}	40373 22	18680 15	25500 00	13000 00	9214 39	50407 61	21808 53	19974 44	31954 55	18680 15	8343 24
e'	0 56	0 51	0 15	0 33	0 22	0 35	0 54	0	0 24	0 30	0
ω'	4 38	0 03	3.77	1 47	2 57	1 04	0 42	0	2 69	1 67	0
τ'	20201 70	28717 62	7347 38	15204 81	39897 27	62637 82	5519 42	19358 91	30958 56	35900 12	27544 13
$a' \sin i'$	768 70	60 53	874.28	496 24	125 97	13750 00	2036 02	422 17	1008 97	787 82	71.24
$f(m_3)$	0 0110	0 00003	0 0391	0 0266	0 0009	40 0128	0 7034	0 0076	0 0845	0 0567	0 0002
m_3 90°	0 46	0 05	1 09	0 94	0 19	45 18	2 79	2 34	1 73	1 48	0 34
60°	0 54	0 06	1 29	1 11	0 22	66 92	3 49	2 71	2 05	1 75	0 39
30°	1 04	0 11	2.53	2 15	0 40	325 69	9 42	4 86	4 14	3 46	0 69
dev Fr					0 0045		0 0157		0 0070		
dev O-C	0 0019		0 0063		0 0048	0 0147	0 0201	0 0123	0 0072		0 052

Remarks :

1 : results were obtained by subtracting quadratic ephemeris
2 : TOT type results (they were obtained using all kind of minima times)
3 : PGPE type results (they were obtained using only photoelectric and photographic minima)
4 : PE type result (they were obtained using only photoelectric minima)
5 : final results contain the exclusion of the data out of the 3σ

- P' (in days), e', ω' (in rad), τ' (in JD-2400000), $a' \sin i'$ are the orbital elements of the orbit of the eclipsing binary in the triple (multiple) system.
- $f(m_3)$: mass function of the third (fourth) body
- m_3 : mass of the third (fourth) body at different inclinations (in Solar Mass)
- dev Fr are the standard deviation of the data from the Fourier-fitting
- dev O-C are the standard deviation of the data from the LITE orbit of above elements

3. CONCLUSION

We studied a group of stars for achieving modified or new interpretation of their O-C diagram. We could verify and/or improve the orbital elements of third or further satellites of the eclipsing systems studied by earlier authors. For several cases our results are in contradiction with those of the previous investigators.

LITE is a very attractive explanation for rather curious O-C behaviour. However, one must be very careful at the decision whether the results can be acceptable (physically reasonable) or not. We can say for every star that the crucial point will be the new observational data in the future. We shall continue this investigation, by taking into account further eclipsing binaries, and also by monitoring the systems studied here for checking whether the newer times of minima will follow our theoretical approximation or not.

Acknowledgements

The work was partly supported by the OTKA T4330 and OTKA F7318 National Grants, 'For the Hungarian Science' Foundation, and the Local Government of Bács-Kiskun County. We would like to express our great gratitude to late Dieter Lichtenknecker for sending his excellent data collection which has made our work much easier and faster. One of us (T.H.) would like to thank for the additional financial support

delivered to the Baja Observatory by the Foundation 'For the Development of Bács-Kiskun County', the OTP National Savings and Credit Bank, and the plants BÉFA, VARIANT and BLÉVISZ. T.B. would like to acknowledge the technical support (computer accounts, telescope times and library work) for the Konkoly Observatory, Zs. Paragi and I. B. Bíró. Both of us are very appreciate to Drs. Szatmáry and Vinkó (JATE) for their advices.

References

Barker, L. A. and Herczeg, T. J. : 1979, *PASP*, **91**, 247.
Budding, E. : 1984, *Bull. Inf. CDS*, **27**, 91.
Giannone, P. and Giannuzzi, M. A. : 1974, *Ap & SpSci*, **26**, 289.
Heintze, J. R. W. : 1990, *NATO Adv. Stud. Inst. on Active Close Binaries*, Ed. Ibanoglu, Kluwer Acad. Publ., 219.
Hill, G. and Barnes, J. V. : 1972, *PASP*, **84**, 430.
Hrivnak, B. J. : 1989, *ApJ.* **340**, 458.
Kartasheva, T. A. and Svechnikov, M. A. : 1988, *Zvezdi Typa Wolf-Rayet i Rodstv. im. Obj.*, Mater. Vsesoj. Sovesc., Yelva, 14-17 Oct. 1986, Tallin, 126.
Kholopov, P. N., Samus', N. N., Frolov, M. S., Goranskij, V. P., Gorynya, N. A., Kireeva, N. N., Kukarkina, N. P., Kurochkin, N. E., Medvedeva, G. I., Perova, N. B., Shugarov, S. Yu. : 1985, *General Catalog of Variable Stars*, Vol. I, "Nauka", Moscow.
Kolláth, Z. : 1990, *Technical Reports of Konkoly Obs., Hungary*, **No. 1.**
Kopal, Z. : 1978, *Dynamics of Close Binary Systems*, D. Reidel. Co.
Linnell, A. P. and Kallrath, J. : 1987, *ApJ.* **316**, 754.
Mayer, P., Wolf, M., Tremko, J. and Niarchos, P. G. : 1991, *Bull. Astr. Inst. Czech.*, **42**, 225.
Nagy, T. A. : 1985, *PASP*, **97**, 1005.
Rovithis-Livaniou, H., Niarchos, P. G. and Rovithis, P. : 1990, *NATO Adv. Stud. Inst. on Active Close Binaries*, Ed. Ibanoglu, Kluwer Acad. Publ. 253.
van Hamme, W. and Wilson, R. E. : 1990, *Astron. J.* **100**, 1981.
Vinkó, J. : 1989, *Diploma Work*, JATE University TTK, Szeged, Hungary.

Publ. Obs. Astron. Belgrade No. 49 (1995), 109-114

MHD WAVES IN CORONAL ARCADES

V. M. ČADEŽ, J. L. BALLESTER and R. OLIVER
UIB, Dep. de Fisica, E-07071 Palma de Mallorca, Espanya.
E-mail dfsvka9@ps.uib.es

Abstract. The MHD wave behavior in the solar corona with magnetic field having the shape of arcades is investigated. It is shown that a particular analytical solution to the linearized MHD equations can be obtained for perturbations with short wavelengths in the direction of the arcade tunnel.

Two possibilities are considered regarding the related wave frequency : the high frequency domain yields MHD waves propagating along the tunnel of the arcade as a fast MHD mode while the low frequencies produce two decoupled wave modes representing the Alfven and the slow magnetoacoustic wave, both modified by the gravity and the profile of the magnetic field. All these waves are stable, contrary to the case when the magnetic field is purely horizontal and when the magnetic buoyancy instabilities can set in.

1. STATIONARY MAGNETIC ARCADE

Magnetic fields having the shape of arcades are commonly found in the solar corona. They are usually considered as low plasma–β fields meaning that the magnetic pressure significantly exceeds the thermal pressure of the ambient plasma. As the field lines of a coronal arcade emerge from the much denser photosphere, it is obvious that various photospheric processes will cause disturbances that can propagate further into the corona and be responsible for coronal heating and other phenomena (Čadež et.al 1995a, 1995b). It is, therefore, of particular interest to investigate the behavior of such perturbations which is being done either by numerical methods (Oliver et.al. 1993) or analytically (Čadež et.al.1994).

In this paper, we shall restrict our attention to the behavior of the so called *narrow perturbations* whose definition and properties are going to be given below.

Consider a magnetohydrostatic equilibrium of an ideal isothermal plasma with a magnetic arcade in a uniform gravity field along the vertical z–axis :

$$-v_s^2 \nabla \rho_0 + \frac{1}{\mu_0}(\nabla \times \vec{B}_0) \times \vec{B}_0 + \rho_0 \vec{g} = 0 \qquad (1)$$

where $v_s \equiv \sqrt{RT_0}$ is the isothermal ($\gamma = 1$) speed of sound.

The magnetic field of the arcade has two components, both lying in the vertical x, z-plane $\vec{B}_0 = (B_{0x}, 0, B_{0z})$, they are independent of the remaining horizontal y–coordinate and are given by the standard expressions :

$$B_{0x}(x,z) = B_{00}(\psi)\cos\left(\frac{x}{\lambda_B}\right)e^{-z/\lambda_B}, \quad B_{0z}(x,z) = -B_{00}(\psi)\sin\left(\frac{x}{\lambda_B}\right)e^{-z/\lambda_B}$$

The quantity $\psi(x,z)$ does not change along the field line and is known as flux function. If B_{00} is independent of ψ, the considered magnetic field becomes force-free and potential.

The field intensity $B_0 = B_{00}(\psi)\exp(-z/\lambda_B)$, shows an exponential decrease with the height z while the corresponding scale length λ_B remains unspecified at the moment.

For further calculations, it is convenient to replace the pair of Cartesian coordinates (x,z) by a new set θ and ψ in such a way that the new curvilinear coordinate lines $\psi = const.$ coincide with magnetic field lines while $\theta = const.$ lines are orthogonal to them. The y–coordinate remains unchanged and oriented horizontally, along the tunnel of the arcade. Thus :

$$\frac{\psi}{\lambda_B} = \cos\left(\frac{L}{\lambda_B}\right) - \cos\left(\frac{x}{\lambda_B}\right)e^{-z/\lambda_B}, \qquad \frac{\theta}{\lambda_B} = \sin\left(\frac{x}{\lambda_B}\right)e^{-z/\lambda_B}, \qquad y = y$$

The quantity L is used only to define the referent $\psi = 0$ coordinate line and its value can be chosen arbitrarily.

The standard vector field operators take now the following form :

$$\nabla\rho = \frac{1}{h}\frac{\partial\rho}{\partial\psi}\hat{e}_\psi + \frac{1}{h}\frac{\partial\rho}{\partial\theta}\hat{e}_\theta + \frac{\partial\rho}{\partial y}\hat{e}_y \quad \text{and} \nabla\cdot\vec{v} = \frac{1}{h^2}\left[\frac{\partial}{\partial\psi}(hv_\psi) + \frac{\partial}{\partial\theta}(hv_\theta)\right] + \frac{\partial v_y}{\partial y}$$

for the gradient of a scalar ρ and for the divergence of a vector $\vec{v}$ respectively, and :

$$\nabla\times\vec{v} = \frac{1}{h^2}\begin{vmatrix} h\hat{e}_\psi & h\hat{e}_\theta & \hat{e}_y \\ \dfrac{\partial}{\partial\psi} & \dfrac{\partial}{\partial\theta} & \dfrac{\partial}{\partial y} \\ hv_\psi & hv_\theta & v_y \end{vmatrix} \tag{2}$$

for the curl of a vector $\vec{v}$. Here $h \equiv e^{z/\lambda_B} = \left[\left(\frac{\theta}{\lambda_B}\right)^2 + \left(\cos\frac{L}{\lambda_B} - \frac{\psi}{\lambda_B}\right)^2\right]^{-1/2}$

The hydrostatic balance equation (1) can now be expressed in components which gives :

$$v_s^2\frac{\partial}{\partial\theta}\ln(\rho_0 h^\delta) = 0 \quad \text{and} \quad v_s^2\frac{\partial}{\partial\psi}\ln(\rho_0 h^\delta) + \frac{B_{00}^2}{\mu_0\rho_0 h^2}\frac{d}{d\psi}\ln B_{00} = 0 \tag{3}$$

where $\delta \equiv g\lambda_B/v_s^2$.

According to the first equation in Eqs.(3), the expression $\rho_0 h^\delta$ depends only on the variable ψ while the second equation indicates the same property for $\rho_0 h^2$. Therefore $\delta = 2$, meaning that $\lambda_B = 2\lambda$ with $\lambda \equiv v_s^2/g$ being the standard scale height of an

isothermal and non magnetized atmosphere. However, in cases when $B_{00} = const.$ (a potential magnetic field) and/or $B_{00}^2/(\mu_0\rho_0 h^2) \gg v_s^2$ (the low plasma β medium), the value of the parameter δ remains arbitrary. In both cases, namely, the spatial distribution of the plasma density does not affect the magnetic field distribution, they are mutually independent and $\delta = \lambda_B/\lambda$ may have any value.

2. LINEARIZED EQUATIONS

To investigate the behavior of small amplitude isothermal perturbations of the described equilibrium state, we start from the standard set of linearized MHD equations :

$$\frac{\partial\rho_1}{\partial t} + \nabla\cdot(\rho_0\vec{v}) = 0, \qquad \frac{\partial\vec{B}_1}{\partial t} = \nabla\times(\vec{v}\times\vec{B}_0), \qquad p_1 = v_s^2\rho_1,$$

$$\rho_0\frac{\partial\vec{v}}{\partial t} = -\nabla p_1 + \frac{1}{\mu_0}(\nabla\times\vec{B}_0)\times\vec{B}_1 + \frac{1}{\mu_0}(\nabla\times\vec{B}_1)\times\vec{B}_0 + \rho_1\vec{g} \tag{4}$$

Since the basic state is stationary and does not depend on the variable y, any of the perturbed quantities can be taken as a product of a harmonic function of both the time variable t and the spatial coordinate y, i.e. $exp(-i\omega t + ik_y y)$, and a $(\psi,\theta)-$dependent amplitude. In this case the Eqs.(4) reduce to the following system of equations for the perturbation amplitudes :

$$h^2\omega^2 V_\psi + v_A^2\frac{\partial^2 V_\psi}{\partial\theta^2} + i\omega v_s^2\left(\frac{\partial\Pi}{\partial\psi} - \frac{v_A^2}{2v_s^2+v_A^2}\frac{d}{d\psi}\ln v_A^2\,\Pi\right) = 0 \tag{5}$$

$$h^2\omega^2 V_\theta + v_T^2\frac{\partial^2 V_\theta}{\partial\theta^2} + i\omega\frac{c^4}{v_s^2+v_A^2}\frac{\partial\Pi}{\partial\theta} = 0 \tag{6}$$

$$h^2\omega^2 V_y + v_A^2\frac{\partial}{\partial\theta}\left[\frac{1}{h}\frac{\partial}{\partial\theta}(hV_y)\right] - \omega h v_s^2 k_y\Pi = 0 \tag{7}$$

$$i\omega\Pi = \frac{v_s^2+v_A^2}{v_s^2}\left(\frac{\partial V_\psi}{\partial\psi} + ik_y h V_y\right) + \frac{\partial V_\theta}{\partial\theta}. \tag{8}$$

Here $v_T^2 \equiv v_s^2 v_A^2/(v_s^2+v_A^2)$, $\vec{V} \equiv \vec{v}/h$ and Π is the total pressure perturbation normalized to the local gas pressure of the unperturbed medium, i.e. $\Pi \equiv p_{tot}/(v_s^2\rho_0)$ and $p_{tot} \equiv v_s^2\rho_1 + B_{1\theta}B_{00}/(h\mu_0)$.

The obtained set of Eqs.(5)-(8) reduces to the result obtained by (Goedbloed, 1971) for the 2D perturbations with $k_y = 0$ when the Alfven mode, propagating along the tunnel of the arcade, was decoupled from the two remaining modes propagating in the cross sectional plane of the arcade.

In our case, now, all three modes are coupled and an overall analysis of their behavior, based upon the solution of Eqs.(5)-(8), is rather complicated. However, it is possible to examine a particular domain of these perturbations when they have very short wavelengths along the $y-$direction, i.e. the case when k_y takes comparatively large values, contrary to the $k_y = 0$ considered earlier (Goedbloed, 1971).

3. NARROW PERTURBATIONS

The perturbations with large k_y are of a narrow shape in the lateral y–direction and will be referred to as *narrow perturbations*. In other words, we shall consider narrow perturbations as those disturbances whose y–derivatives are much larger than either their ψ– and θ–derivatives or the corresponding derivatives of the basic state quantities. Symbolically :

$$\left|\frac{\partial}{\partial y}\right| = k_y \gg \left|\frac{\partial}{\partial \psi}\right|, \left|\frac{\partial}{\partial \theta}\right| \tag{9}$$

As to the time derivatives, i.e. the perturbation frequency ω, there are two possibilities : the low frequency and the high frequency domains when the y–derivatives are much larger and of the same order respectively as compared to the related time derivatives. Symbolically this would be :

$$\left|\frac{\partial}{\partial y}\right| = k_y \gg \frac{1}{v_s + v_A}\left|\frac{\partial}{\partial t}\right| = \frac{\omega}{v_s + v_A} \text{ the low frequency case} \tag{10}$$

$$\left|\frac{\partial}{\partial y}\right| = k_y \sim \frac{1}{v_s + v_A}\left|\frac{\partial}{\partial t}\right| = \frac{\omega}{v_s + v_A} \text{ the high frequency case} \tag{11}$$

To see what this means, one can consider the typical coronal conditions when $v_A \geq v_s$ and $v_A \sim 10^4 km/s$. In this case the low frequency condition (10) becomes

$$k_y \equiv \frac{2\pi}{\lambda_y} \gg \frac{\omega}{v_s + v_A} > \frac{\omega}{v_A} \equiv \frac{2\pi}{\tau v_A}$$

Consequently, the conditions (10) and (11) now relate the perturbation lateral extend λ_y to the oscillation time period τ as follows :

$$\frac{\lambda_y}{\tau} \ll v_A \sim 10^4 km/s \quad \text{and} \quad \frac{\lambda_y}{\tau} \sim v_A \sim 10^4 km/s$$

for the low frequency and the high frequency cases, respectively.

The low frequency solutions. Consider the low frequency case first with orderings given by (9) and (10). As the large wave number k_y enters only the equations (7) and (8), they can be expressed as follows :

$$\omega \Pi = \frac{1}{h v_s^2 k_y}\left\{h^2\omega^2 V_y + v_A^2 \frac{\partial}{\partial \theta}\left[\frac{1}{h}\frac{\partial}{\partial \theta}(hV_y)\right]\right\} \to 0$$

$$V_y = \frac{1}{ik_y h}\left[\frac{v_s^2}{v_s^2 + v_A^2}\left(i\omega\Pi - \frac{\partial V_\theta}{\partial \theta}\right) - \frac{\partial V_\psi}{\partial \psi}\right] \to 0$$

The Eqs.(5)-(8) finally take a simple form :

$$\frac{\partial^2 V_\psi}{\partial \theta^2} + h^2(\psi,\theta)\frac{\omega^2}{v_A^2(\psi)}V_\psi = 0, \qquad \frac{\partial^2 V_\theta}{\partial \theta^2} + h^2(\psi,\theta)\frac{\omega^2}{v_T^2(\psi)}V_\theta = 0, \tag{12}$$

$$\Pi = 0 \qquad \text{and} \qquad V_y = 0 \tag{13}$$

where $h(\psi, \theta)$ is given in (2).

According to (13), the considered low frequency narrow perturbations are in a total pressure equilibrium and cause no fluid motions in the y–direction. In addition, it can be easily shown from the condition $\nabla \cdot \vec{B}_1 = 0$, that the perturbed magnetic field has no y–component either, i.e. that $B_{1y} = 0$ in this case.

The equations (12) are now decoupled and contain no ψ–derivatives. The initial system of four coupled partial differential equations is thus reduced to only two mutually independent ordinary differential equations. The variable ψ can be treated as a parameter and, consequently, the solutions can be obtained for arbitrary Alfven speed distributions $v_A^2(\psi)$ by integrating Eqs.(12) over the variable θ only.

Both Eqs.(12) are of the same form and can be expressed as :

$$\frac{d^2 V_i}{du^2} + \frac{a_i^2}{1+u^2} V_i = 0, \qquad \text{here} \qquad i = \psi, \theta$$

where :

$$u = \frac{\theta}{\lambda_B \left| \cos\left(\frac{L}{\lambda_B}\right) - \frac{\psi}{\lambda_B} \right|} = \tan\left(\frac{x}{\lambda_B}\right),$$

$$a_\psi^2 = \frac{\omega^2 \lambda_B^2}{v_A^2(\psi)} \quad \text{and} \quad a_\theta^2 = \frac{\omega^2 \lambda_B^2}{v_T^2(\psi)} = \frac{v_s^2 + v_A^2(\psi)}{v_s^2 v_A^2(\psi)} \omega^2 \lambda_B^2 \tag{14}$$

The approximate solution of the above equation can be obtained by means of the WKB method in the following form :

$$V_i = C^{(+)} V_i^{(+)} + C^{(-)} V_i^{(-)}, \qquad C^{(+)}, C^{(-)} = const.$$

where the two linearly independent solutions, $V_i^{(+)}$ and $V_i^{(-)}$, are given by :

$$V_i^{(+)} = a_i^{-1/2} (1+u^2)^{1/4} \cos\left\{ a_i \ln\left[(1+u^2)^{1/2} + u \right] + a_i \ln 2 \right\},$$

$$V_i^{(-)} = a_i^{-1/2} (1+u^2)^{1/4} \sin\left\{ a_i \ln\left[(1+u^2)^{1/2} + u \right] + a_i \ln 2 \right\}.$$

The above solution is valid provided the condition for the WKB approximation is satisfied which, in this case, means that the following inequality holds :

$$\frac{|2-u^2|}{4a_i^2(1+u^2)} \ll 1 \tag{15}$$

It can be easily shown that (15) is satisfied for any value of u if the coefficient a_i is large enough : $a_i \gg 1/\sqrt{2}$. Since $a_\theta \geq a_\psi$ according to definitions (14), this condition becomes :

$$a_\psi \equiv \frac{2\pi \lambda_B}{\tau v_A} \gg \frac{1}{\sqrt{2}} \tag{16}$$

where $\tau \equiv 2\pi/\omega$ is the oscillation time period.

To estimate the condition (16) let us introduce some real values for the solar corona by taking $\lambda_B = 120,000\,km$ and $v_A = 10^4 km/s$. In this case (16) requires $\tau \ll 24\pi\sqrt{2} \approx 110s$. or that oscillations with time period up to 1.5 min. can be treated by the considered WKB method.

The high frequency solutions. In the case when the frequency ω is taken sufficiently large to make the terms with ω^2 of the same order of magnitude as those with k_y^2, the Eqs.(5)-(8) reduce to a simple set of algebraic equations again :

$$h^2\omega^2 V_y - hv_s^2 k_y \omega \Pi = 0, \quad \frac{v_s^2 + v_A^2}{v_s^2} hk_y V_y - \omega\Pi = 0 \quad \text{and} \quad V_\psi = V_\theta = 0 \qquad (17)$$

As can be seen, the high frequency narrow perturbations induce fluid motions in the $y-$direction only and also a varying total pressure. The resulting wave propagates in the $y-$direction, according to the dispersion equation

$$\frac{\omega^2}{v_s^2 + v_A^2(\psi)} - k_y^2 \doteq 0$$

that follows from Eq.(17). This is the fast MHD mode with its phase velocity depending on the variable ψ.

4. CONCLUSION

As can be seen from both solutions obtained in the low and in the high frequency domain, the considered magnetic field configuration is stable with respect to the narrow perturbations which is not the case when the field is purely horizontal (Gilman, 1970). The stability of a magnetic arcade is due to the additional magnetic field curvature stress that opposes the destabilizing action of the magnetic buoyancy.

Acknowledgements

The financial support received from DGICYT is acknowledged by V.M.Čadež while on leave from Institute of Physics, P.O.Box 57, YU-11001 Beograd, Yugoslavia.

References

Čadež, V. M. and Ballester, J. L. : 1994, *Astron. Astrophys.* **292**, 669.

Čadež, V. M. and Ballester, J. L. : 1995a, "Time evolution of MHD disturbances impulsively excited by a localized perturber in a potential coronal arcade" *Astron. Astrophys.*, in press.

Čadež, V. M. and Ballester, J. L. : 1995b, "MHD disturbances in a coronal potential arcade generated by localized perturbers", *Astron. Astrophys.*, in press.

Gilman, P.A. : 1970, *Astrophys. J.* **162**, 1019.

Goedbloed J. P. : 1971, *Physica*, **53**, 412.

Oliver, R., Ballester, J. L., Hood, A. W. and Priest, E. R. : 1993, *Astron. Astrophys.* **273**, 647.

Publ. Obs. Astron. Belgrade No. 49 (1995), 115-119

CONNECTION BETWEEN SUNSPOT PROPER MOTION AND FLARE FREQUENCY

G. CSEPURA and L. GYŐRI
Heliophysical Observatory of the Hungarian Acad. Sci. H-4010 Debrecen P.O.Box 30. Hungary
E-mail csepura@tigris.klte.hu

Abstract. Three adjacent sunspot groups were studied, using white-light heliograms and SGD. Flare activity showed close connection between proper motions and area development of the sunspots.

1. INTRODUCTION

Flare activity of solar active regions is generally believed to depend on sheared configuration of magnetic fields (Hagyard et al., 1984). There are cases when the shear necessary for flare can be attributed to the emergence of a new flux in the spot group (Wang, 1992). But, perhaps, a newly born active region can also influence the magnetic field configuration in a nearby active region (Poleto et al., 1993; Gesztelyi et al., 1993, Csepura 1994). In this paper we are interested primarily in the influence of a newly emerging spot group on a nearby one.

2. DATA

Proper motions of the spots and area development in three nearby active regions NOAA AR 6412(B,C), 6413(A) and 6415(D) have been studied between 13-22 December 1990. White-light full-disk photoheliograms for studying sunspot proper motion and area evolution have been taken at Gyula Observing Station (Hungary), Debrecen Heliophysical Observatory (Hungary) and Helwan Observatory (Egypt). Making use of SGD (No.558, part 1, February 1991), the daily flare frequency and positions have been also determined. Two days, December 16 and 18, have been found to include interesting events.

3. BRIEF HISTORY OF THE ACTIVE REGIONS

NOAA AR 6412 appeared at the east limb of the Sun on December 11, 1990 and disappeared over the west limb on December 24, 1990. It was a large bipolar spot group (Fig.1). NOAA AR 6415 emerged as a new active region on December 16, 1990. It had a fast development phase until December 18 and after this time a fast

declining phase (Fig.1). NOAA AR 6413 rotated on the sun disc on December 11 and disappeared on December 18, 1990. It was a roundish spot in its declining phase without any proper motion (Fig.1,2).

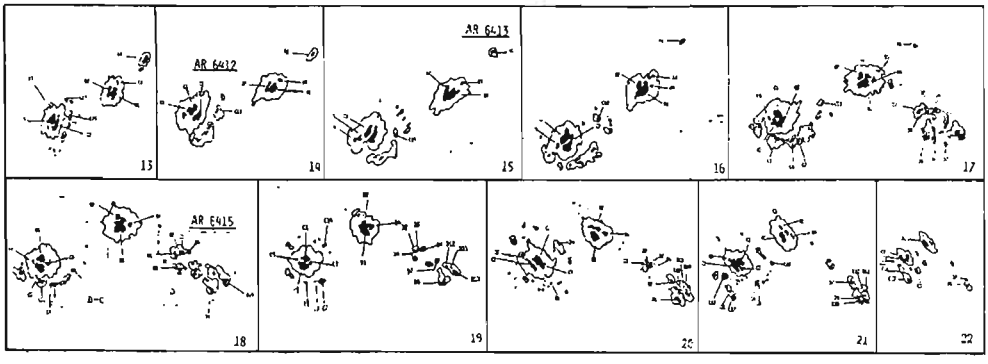

Fig. 1. Development of the sunspots groups in AR 6412(B,C), Ar 6413(A) and AR 6415(D) between 13-21 December 1990.

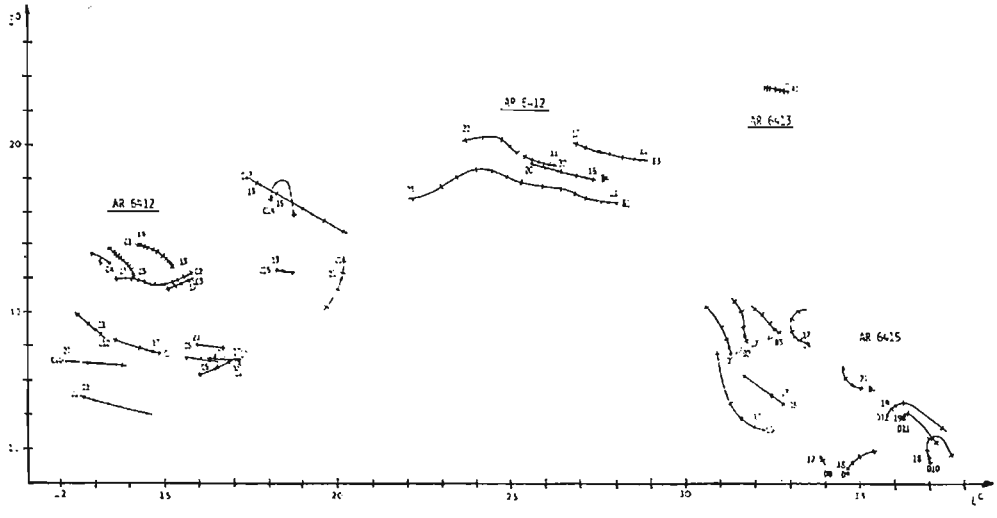

Fig. 2. Proper motions of umbrae in Group A, Group B, Group C and Group D between 11-23 December 1990.

4. EVENTS

a.) Events of December 16

This was the day when the emergence of the newly born region D began (Fig.1). Up to this day area of the active region B,C, continuously raised but from this day it began to decrease (Fig.1,3). From this day on, the spots B1 and B2 in active region

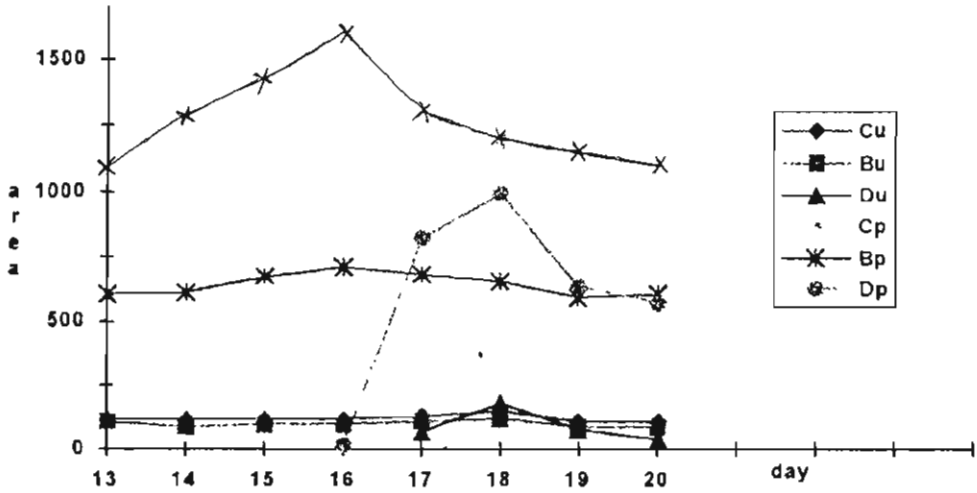

Fig. 3. Development of the total umbral (Cu,Bu,Du,) and whole spots area (Cp,Bp,Dp) of Group B, Group C and Group D between December 13-21, 1990. E xpressed in millionths of the Sun's visible hemisphere.

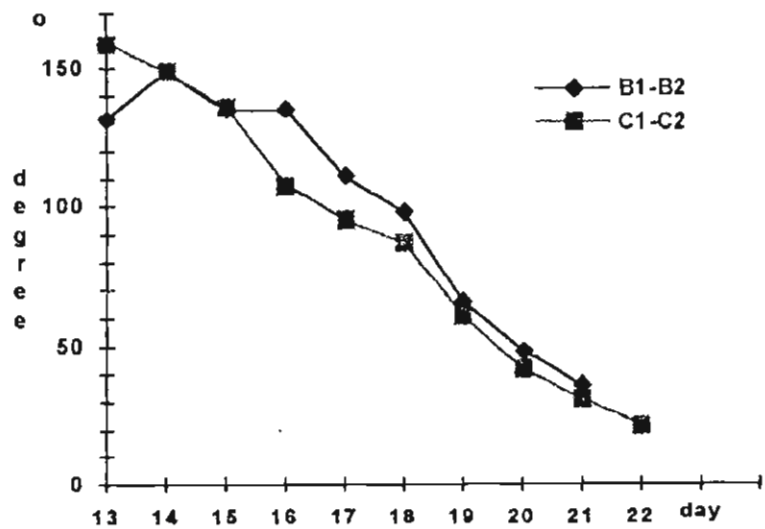

Fig. 4. The rate of daily relative revolution of spots B1-B2 and spots C1-C2.

B,C, began to a relative revolution around each other and in the same active region, there was a sudden increase in the relative revolution of spots C1 and C2. (Fig.1,4). Up to December 16, the occurrences of the flares in active region B,C were scattered over the whole region but on this day they were concentrated between B and C and increased, while, on the contrary, the daily flare frequency in these active regions was found to have a local minimum (Fig.1,5).

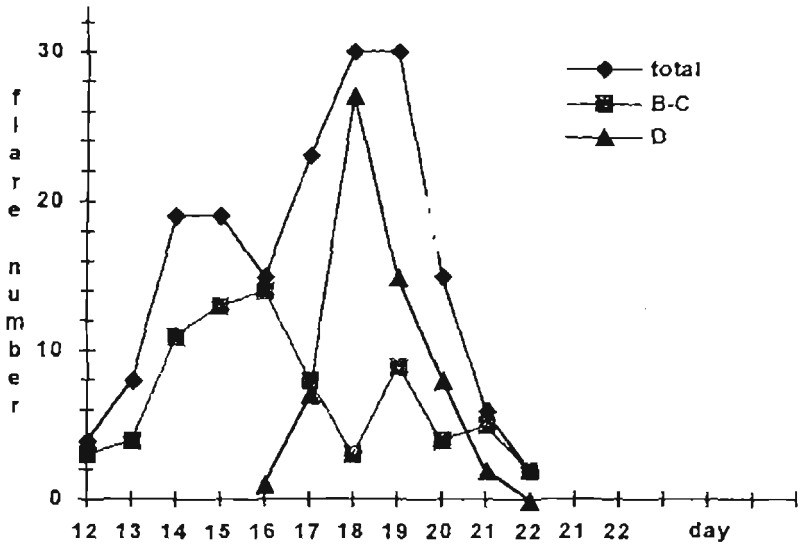

Fig. 5. "total" represent the total daily numbers flares. The ather two curves shows the daily number of flares in the two flares centrums (B-C and D) showns in Fig.1.

It is well known that the emergence of new spots inside in a spot group increase the flare frequency and causes changes in the proper motions of the spots (Schmieder, 1994). From the above facts, it seems that a spot group emerged close to an another one can have an influence on the proper motion and the flare frequency in the other spot group.

b.) Events of December 18

On this day, group D has reached its maximal area and at the same time, the total umbral area had its maximal value also (Fig.3). It is interesting that up to this time the umbral areas of the spots have practically not changed (except group D) but on this day there were a slight increase in their values and after this day the previous values were restored (Fig.3). The positions of the flares after this day is shifted to the group D (Fig.1,5). As it was found on December 16 the rate of the relative revolution of the spots C1 and C2 increased on this day also (Fig.1,4). The above events can probably be explained by the fact that this was the day when group D started declining.

5. DISCUSSION AND CONCLUSIONS

The emergence of new spots inside a pre-existing spot group usually increases the flare frequency and may alter the proper motion pattern of the spots in the AR. In general, young spots show fast proper motions : the faster the emergence, the higher their velocity. An approaching motion between opposite polarity spots of different flux system induces magnetic reconnection : the new emerging magnetic flux is bound to interact (reconnect) with the pre-exiting overlying field leading to flare activity (Heyvaerts, 1977). In case of flux emergence occurring not inside an exiting active

region, but relatively close-by, the mechanism of a possible interaction seems less clear, although observations of the solar corona by the Yohkoh X-ray satellite showed that solar Active Regions are inter-connected by huge coronal loops (see e.g. Porter et al.,1994). Fast appearance and disappearance of a region may lead to re-organization of those interconnecting loops, therefore enhanced flare activity of the pre-exiting region(s). Among adjacent Active Regions the possibility of an under-photospheric connection can not be entirely excluded either (see e.g.van Driel-Gesztelyi et al., 1993), since those regions are members of an active nest (Gaizauskas et. al, 1983). From the coincidences found above the hint can be drawn that quickly evolving sunspot groups might have an influence on the flare activity or even on the pattern of proper motions of other, adjacent groups, although we can not exclude the possibility that the relationship among events of those nearby sunspot groups was not causal, but only pure coincidence.

Acknowledgements

This work was supported by the Hungarian Foundation for Scientific Research under grant No. : OTKA 007422.

References

Csepura, G., Győri, L. and Gerlei, O., : 1994, in *Solar Magnetic Fields*, Schussler M. – and Schmidt W. eds., Cambridge Univirsity Press.

Gaizauskas, V., Harvey, J. W. and Zwaan, C. : 1983, *Asrophys. Journal*, **265**, 1056.

Hagyard, M. J., Smith, J. Jr., Teuber, D. and West, E. A. : 1984, *Solar Phys.* **91**, 115.

Heyvaerts, J., Priest, E. R. and Rust, D. M. : 1977, *Astrophys. Journal*, **216**, 123.

Poletto, G., Gry, G. A. and Machado, M. E. : 1993, *Solar Phys.* **144**, 113.

Porter, J., Moore, R. T., Roumeliotis, G., Shimizu, T., Tsuneta, S., Sturrock, A. and Acton, L. W. : 1994, in *Proc. of Kofu Symposium,*, Enome S.–Hirayama T. eds., NRO Report No.360

Schmieder, B., Hagyard, M. J., Guoxiang, AI., Zhang Hongqi, Kálmán, B., Győri, L., Rompolt, B., Demoulin, P., and Machado, M. E. : 1994, *Solar phys.* **150**, 199.

van Driel-Gesztelyi, L., Csepura, L., Nagy, I., Gerlei, O., Schmieder, B., Rayrole, J. and Demoulin. P., : 1993, *Solar Phys.* **145**, 77.

Wang, H. : 1992, *Solar Phys.* **140**, 85.

Publ. Obs. Astron. Belgrade No. 49 (1995), 121-125

SUNSPOT'S PROPER MOTIONS IN TWO NEARBY ACTIVE REGIONS

G. CSEPURA, L. GYŐRI and O. GERLEI
Heliophysical Observatory of the Hungarian Acad. Sci. H-4010 Debrecen Po. Box. 30. Hungary
E-mail csepura@tigris.klte.hu

Abstract. Using white-light heliograms, the proper motions of two adjacent sunspot groups were studied. A conspicuous similarity between the proper motions of the leader spots of the two active regions has been found. At first, they showed vigorous westward motion after that they stopped on the same day when a new activity in the sunspot groups has set in. This result is in good agreement with the finding of an investigation made earlier in another two active regions (Csepura 1990).

1. INTRODUCTION

The connection between sunspot groups developed nearby has been studied by a numbers of people. It has been pointed out that nearby sunspot groups can show signature of interaction in their proper motion and area development (Matres 1970, Sheeley 1981). In former studies (Csepura et al 1990, L. van Driel-Gesztelyi 1992), it has been experienced that, in two adjacent activity regions, the sunspots moved almost parallel and changed the direction of their motion on the same day at almost the same heliographic longitude. Observation of the simultaneous appearance of new activity in both groups was also reported in these studies. G. Poletto, G. A. Gray and M. E. Machado (1993) claim : "What we image in X-rays is not a long loop (the "bridge") along which some disturbance propagates, but an arcade of shorter loops connecting AR 2522 and AR 2530 -which participates in the general re-arrangement of the field and thus act as a "channel" along which the destabilization progresses and eventually leads, in places where the stored energy is highest - as also revealed by magnetic shear observed in MSFC magnetograms - to the occurrence of a flare".

2. OBSERVATIONS

At the Heliophysical Observatory of the Hungarian Academy of Science in Debrecen and its Gyula Observing Station 226 white-light, full-disk photoheliograms were taken between 21-28 June 1980, which we used for a study of the proper motion and the evolution of Hale regions 16923 and 16931. The method of observation and the computation of the heliographic coordinates is described in the Introduction to the Debrecen Photoheliographic results by Dezso et al. (1988).

3. DEVELOPMENT OF THE ACTIVE REGIONS

In this investigation Hale region 16923 (AR 2522) and Hale region 16931 (AR 2530) were studied. HR 16923 rotated onto the disk on 16 June 1980 as a return of HR 16824. In HR 16931, a sunspot group began to develop on 21 June 1980. These two adjacent region were target of observation for coordinated Flare Buildup Study from 24-30 June 1980 (Fig.1). The overall structure of both sunspot groups were bipolar. The two sunspot groups were within DL=7 and DB=5 degree (Fig.2). The main motions in both regions were those characterizing the bipolar regions : spots in the preceding part of the group moved westward and spots in the following part moved eastward (Fig.2). The dipole axis of HR 16931 was inclined slightly relative to parallels of latitude, with the leading polarity nearer to the equator, that is normal, but the one of HR 16931 was inclined slightly in the opposite direction i.e. with the leading polarity further from the equator. The development of both regions were very fast so that changes in magnetic complexity had time scales¡ 24h (Schmahl 1983). A parasitic polarity (N10), causing increased flare activity in its vicinity, emerged in the preceding polarity region (S3) of HR 16923 near its midpoint on the 23rd (Fig.1).

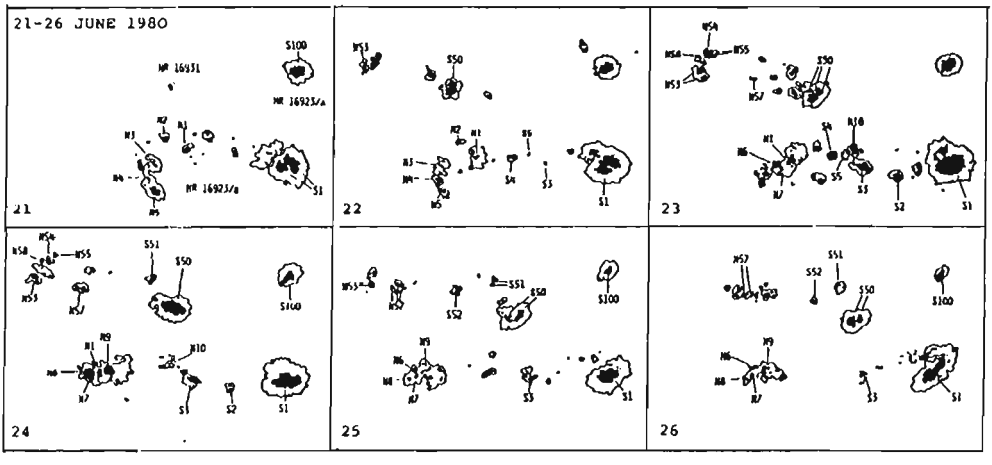

Fig. 1. Development of the sunspot groups in Hale regions 16923/A, 16923/B and 16931 between 21-26 June 1980. The denotations of umbrae show their magnetic polarity : N and S means north and south polarity.

4. PROPER MOTIONS

The most striking common characteristic of the proper motions of the two sunspot groups is the suddenly stop of the vigorous westward motions of their leader spots at 26th and, after it, the change of the direction of this motion at 27th as it can be fairly seen in (Fig.2). This is in full agreement with the result (Csepura 1990) found at the study of another two adjacent active regions (Mt. W. 21517, Mt. W. 21526) that the leader spots of these groups turned simultaneously as its depicted in Fig. 4.

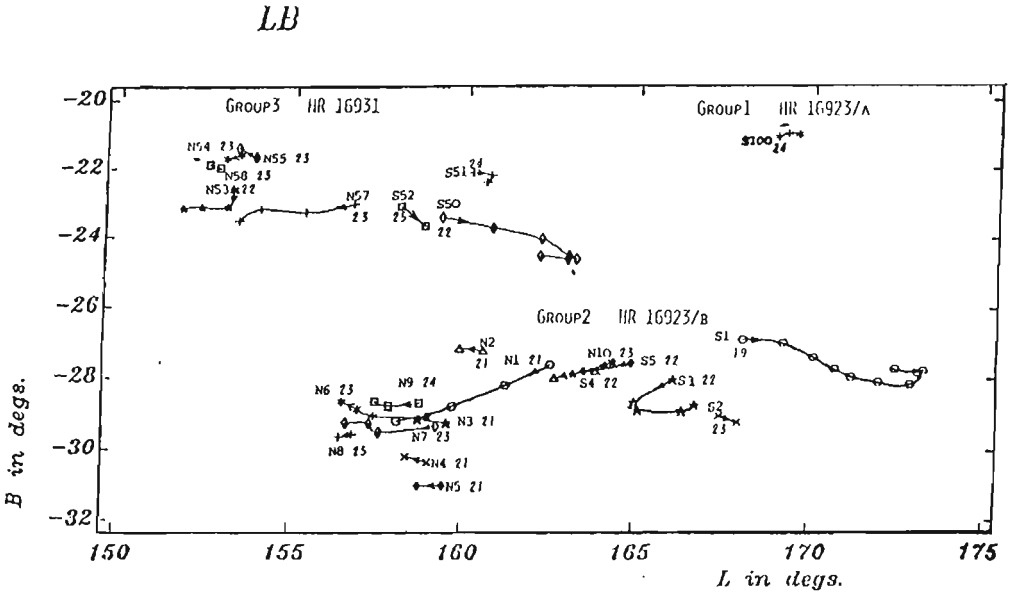

Fig. 2. Proper motions of umbrae in Group1, Group2 and Group3 between 19-28 June 1980. The preceding umbrae are marked with the letter S and the following umbrae with the letter N, referring their magnetic polarity. Italics numbers indicate beginning days.

This sudden change of the motion of the leader spots can be connected to the new activity of HR 16923 which begin to developed in and around its leader spot from 27 June onwards. It was shown by Simnett et al. (1984) and confirmed by Kundu et al. (1984) and by Kundu, Cheng and Schmahl (1990) that, at the time of major flares, extensive magnetic structures linked the two regions in HXIS and in VLA at 6 cm, respectively. Now, on the basis of our investigations, a supposition on a connection below the photosphere, of the two regions, causing the similar proper motion of the leader spots, could emerge. Or, as an another possibility, it could be attributed to the existence of large-scale flows in the vicinity of the close- by developing active regions influencing the motions of these spots. We determined the areal development of these sunspot groups, (Fig. 3). At the time of the beginning of the development of HR 16931, the umbral area of HR 16923 began to decrease and after this the two area increased together. After a few days of increasing in area, their area begin to decrease nearly at the same time (within a day shift). It is worth nothing the shared motions, associated with increased flare activity, of the different polarity spots N10 and S6 in the middle of HR 16923.

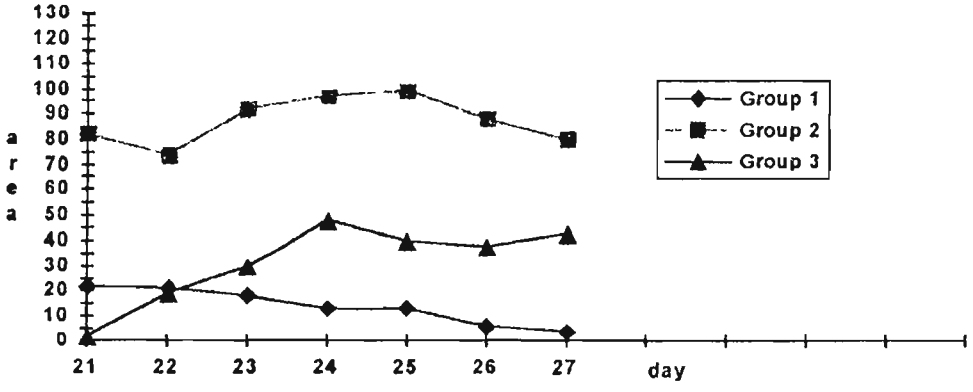

Fig. 3. Development of the total umbral area of Group1, Group2 and Group3 between 21-26 June 1980. Ac represents umbral area in units 0.000001 solar hemisphere.

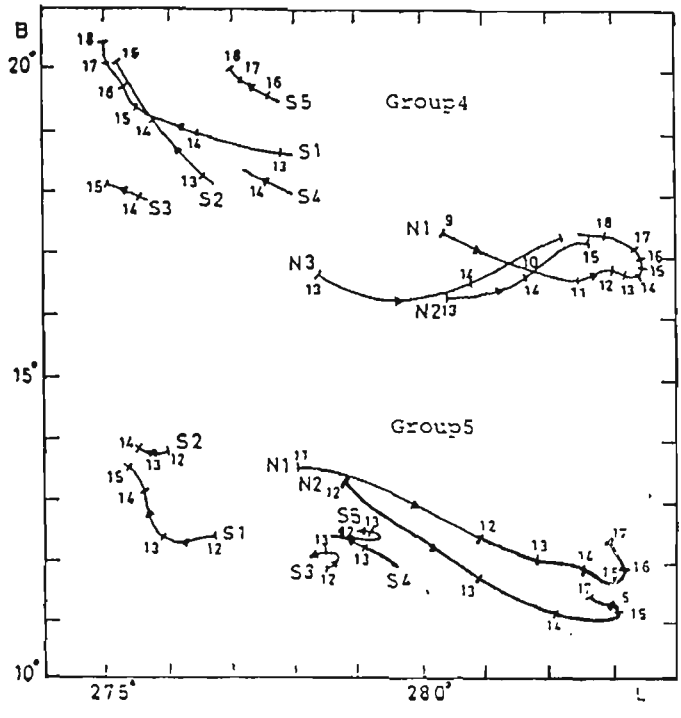

Fig. 4. Proper motions of umbrae in Group4 and Group5 between 9-20 June 1980. The preceding umbrae are marked with the letter N and the following umbrae with the letter S, showing their magnetic polarity, and also with different numbers indicate days.(EPS SOLAR MEETING 1990 Publ. Debrecen Obs. Vol. 7

Acknowledgements

This work was supported by the Hungarian Foundation for Scientific Research under grant No. : OTKA 007422.

References

Csepura, G., van Driel-Gesztelyi, L., Nagy, I., Gerlei, O., Schmieder, B., and Rayrole, L. : 1990, in *The Dynamic Sun* (Proceedings of the EPS 6th European Solar Meeting), Dezső L. ed., pp. 88.

Dezső, L. Gerlei, O. and Kovács, A. : 1988, in *Debrecen Photoheliographic Result*, Pub. Debrecen Obs. Heliographic Series No. 1. 11.

Kundu, M. R., Cheng, C. C., Schmahl, E. J. : 1990, *Solar Phys.* **129**, 343.

Kundu, M. R., Machado, M. E., Erskine, F. T., Rovira, M. G. and Schmahl, E. J. : 1984, *Astron. Astrophys.* **132**, 241.

Martres, M. J. : 1990, *Solar Phys.* **11**, 258.

Poletto, G., Gary, G. A. and Machado, M. E. : 1993, *Solar Phys.* **144**, 113.

Schmahl, E. J. : 1983, *Adv. Space Res. 2*, No. 11. 73.

Sheeley, N. R. : 1981, in *Solar Active Regions* Orral F. Q. ed., Colorado Assoc. Univ. Press, pp. 17.

Simnett, G. M., Harrison, R. A., Hoyong, P. and van Beck, H. F. : 1984, in *SCOSTEP STIP Symp. on Solar/Interplanetary Intervals* , Shea M. A. Smart D. F. and McKenna-Lawlor S. M. P. eds., Maynooth, Eire, Aug. 1982.

Publ. Obs. Astron. Belgrade No. 49 (1995), 127-130

THE HIPPARCOS MISSION AND THE BELGRADE ZENITH-TELESCOPE OBSERVATIONS

G. DAMLJANOVIĆ
Astronomical Observatory, Volgina 7, 11050 Belgrade, Yugoslavia
E-mail gdamljanovic@aob.aob.bg.ac.yu

N. PEJOVIĆ
Astronomical Institute, Faculty of Mathematics,
Studentski trg 16, 11000 Belgrade, Yugoslavia

Abstract. At the beginning of 1990 we started collecting our past observations made with Belgrade ZT and making a new reduction in the FK5 reference frame. After the XXI IAU General Assembly, Buenos Aires 1991, our investigation was made in accordance with the task of Commission 19 of the International Astronomical Union, "Rotation of the Earth", which formed the Working Group on Earth Rotation in the HIPPARCOS reference frame - WG ERHRF to collect the data and create a central data bank of past optical astrometric observations. We cooperate and some results are presented here.

1. INTRODUCTION

The first value of the precise Belgrade latitude, determined in 1947 from visual zenith-telescope - ZT (Askania-Bamberg No 77241, 110/1287 mm) observations by applying Talcott method, was $\varphi = 44°48'13.''167 \pm 0.''008$ (Djurković, Ševarlić, Brkić, 1951). At the beginning of 1949 started regular ZT observations and are still carried out.

From 1990 we started the preparation of the Belgrade ZT observations in a computer readable form and their re-reduction in the FK5 reference frame (in accordance with Msc Thesis "The analysis of the variation of Belgrade latitude in the period 1949-1985" of Goran Damljanović). The HIPPARCOS catalogue had not been finished yet, and we used the PPM catalogue for our re-reduction.

At the XXI IAU General Assembly, Commission 19 formed the WG ERHRF to collect the data and analyse them in the HIPPARCOS reference frame. The Hipparcos Program (ESA 1989) will give the star coordinates, proper motions and parallaxes at the $0.''002$ level of accuracy (at the epoch of observation) for the reference stars used by most of the astronomical stations. The Belgrade ZT observations are at the WG ERHRF list of the best observations performed in the past (Vondrák, Feissel and Essaifi, 1992).

2. PROCEDURE AND RESULTS

The PPM Star Catalogue (Röser and Bastian, 1991), Vol. I and Vol. II, contains 181731 stars north of $-2^{\circ}.5$ of declination, equinox and epoch J2000.0. It is a representation of the FK5 system at higher star densities and fainter magnitudes. It replaces two older catalogues : AGK3 and the SAO Catalogues. For the stars contained in FK5 Part I (the Basic Fundamental Stars) and in FK5 Part II (the Bright Extension Stars), PPM gives the original FK5 data.

The Old Belgrade Latitude Programme - OP (Djurković, Ševarlić, Brkić, 1951) was observed in the period 1949-1960. The New Belgrade Latitude Programme - NP (Ševarlić and Teleki, 1960) was started in 1960 and the observations are still carried out.

The procedure for the re-reduction of NP has been described and the basic results published (Damljanović, 1994). The re-reduction of OP is finished (it will be published) the basic results being :

- the angular value of the micrometer screw revolution (R) is $40.''1073$ for the period 1949-1960 (it is in good accordance with its NP's value, $40.''1080$ for the period 1960-1963),
- the angular division values of the Talcott's levels (L) were : $1.''2581$ for the upper level and $1.''1547$ for the lower one in the period 1949-1960 (they are also in good accordance with their NP's values, $1.''2684$ for the upper level and $1.''1798$ for the lower one in the period 1960-1968),
- the temperature coefficients : $0.''00606$ for the upper level and $0.''00400$ for the lower one in the period 1949-1960.

The re-reduction is in accordance with MERIT standards (Melbourne et al., 1983). The new IAU(1976) coordinate system of astronomical constants, the IAU(1980) nutation model, and the new dynamical reference system (JPL DE200/LE200 Ephemeris, 1984) are used. The FORTRAN programme for refraction is like that used in forming the "Refraction Tables of Pulkovo Observatory" (Abalakin, 1985). The General Catalogue of Trigonometric Stellar Parallaxes (Jenkins, 1952) and The General Catalogue of Stellar Radial Velocities (Wilson, 1953) are used for the calculation of the apparent places of OP and NP stars.

The numerous systematic errors are taken into account. Under both Belgrade latitude programmes : the effect of the statistical parallaxes for the stars without trigonometric ones, the deviation of the vertical, the wind effect, the E-W effect-the error due to the clamp position of the telescope, the effect of the level bubble length variation, the correction for the curvature of the parallel, the temperature terms of the levels, the systematic errors in declinations and proper motions of Talcott's pairs and (sub)groups of OP and NP. The personal equation was taken into account for the NP only. The temperature term, the progressive and the periodic errors of the micrometer screw revolution are not applied (Milovanović et al., 1981).

We used the Student-Fisher criterion for eliminating the excessive instantaneous latitudes resulting from some Talcott's pairs.

The polar motion was eliminated from the material and the observations were brought in accordance with the mean pole BIH1979. After that we made determina-

tions of the systematic errors in declinations and proper motions of Talcott's pairs and (sub)groups of OP and NP.

3. CONCLUSIONS

We investigated numerous systematic errors and the whole material (OP and NP) is corrected for them. Our basic results are a contribution to Hipparcos program - the mean error (of the instantaneous latitude from one Talcott's pair) being less than before.

From the preliminary ZT observations made in 1947 the mean error was $\pm 0.''255$ (Djurković, Ševarlić, Brkić, 1951). The mean error of the OP (1949-1960) was $\pm 0.''220$ (Ševarlić and Teleki, 1960). After our re-reduction the mean error is $\pm 0.''199$ (1949-1960); $\pm 0.''211$ (1949-1951.5) , $\pm 0.''195$ (1951.5-1953.5) , $\pm 0.''192$ (1953.5-1957) , $\pm 0.''205$ (1958-1960).

The mean error of the NP (from 1960 till now) was $\pm 0.''272$ (1960-1965.5) and $\pm 0.''146$ (1969-1974) (Grujić et al. 1989); after our re-reduction the mean error is $\pm 0.''148$ (1960-1985); $\pm 0.''164$ (1960-1963), $\pm 0.''171$ (1964-1967), $\pm 0.''151$ (1968-1970), $\pm 0.''137$ (1971-1972), $\pm 0.''115$ (1973-1976) (Damljanović, 1994).

With a better catalogue in the future (the Hipparcos Catalogue) we can expect to find systematic errors and obtain results with a better accuracy. The observations made with the classical instruments may attain better accordance with those made with new techniques. They may contribute to more through precession and nutation investigations. We take part in that work with our original ZT observations.

References

*** : 1977, "IAU Transaction", *Reidel Publ., Dordrecht*, **XVIB.**

*** : 1984, "JPL DE200/LE200 Ephemeris", *USNO Tapes NA0109 & NA0110.*

*** : 1989, "Hipparcos mission", *ESA, SP-1111* Vol.II, 252.

Abalakin, V. K. : 1985, "Refraction Tables of Pulkovo Observatory (V edition)", NAUKA, Leningrad, GAO AN SSSR.

Djurković, P., Ševarlić, B. and Brkić, Z. : 1951, "Determination de latitude de l' Observatoire Astronomique de Belgrade, 1947", *Publ. Obs. Astron. Belgrade* **4.**

Damljanović, G. : 1994, "On the systematic errors of declinations and proper motions from the Belgrade zenith-telescope observations in the period 1960-1985", *Bull. Astron. Belgrade* **150**, 29-35.

Fricke, W., Schwan, H., Lederle, T. : 1988, "Fifth Fundamental Catalogue (FK5), Part I, The Basic Fundamental Stars", *Veröff. Astron. Rechen-Institut, Heidelberg* **Nr.32.**

Fricke, W., Schwan, H., Corbin, T. et al. : 1991, "Fifth Fundamental Catalogue (FK5), Part II, The FK5 Extension - New Fundamental Stars", *Veröff. Astron. Rechen-Institut, Heidelberg*, **Nr.33.**

Grujić, R., Djokić, M. and Jovanović, B. : 1989, "Analysis of changes in Belgrade geographic latitude over the period 1969.0–1975.0", *Bull. Astron. Belgrade*, **141**, 7-14.

Jenkins, L. F. : 1952, "Gen. Cat. of Trigonometric Stel. Parallaxes", *Yale University Obs.*

Milovanović, V., Teleki, G., Grujić, R. : 1981, *Publ. Astron. Obs. Sarajevo*, **1**, 131.

Melbourne, W. et al. : 1983, "Project Merit Standards", *USNO Circular*, **No. 167.**

Roeser, S., Bastian, U. : 1991, "Positions and Proper Motions (PPM) Star Catalogue", *Astron. Rechen-Institut, Heidelberg.*

Ševarlić, B. and Teleki, G. : 1960, "Le projet d'un Nouveau programme pour le Service de latitude de l'Observatoire", *Bull. Astron. Belgrade*, **XXIV**, Nos 3-4, 19-27.

Vondrák, J., Feissel, M., Essaifi, N. : 1992, "Expected accuracy of the 1900-1990 Earth orientation parameters in the Hipparcos reference frame", *Astron. Astrophys.* **262**, 329–340.

Wilson,R. E. : 1953, "Gen. Cat. of Stel. Radial Velocities", *Mount Wilson Obs., Carnegie Institution of Washington Publ.* **601.**

Publ. Obs. Astron. Belgrade No. 49 (1995), 131-134

ON THE IONIZED IRON LINES STARK BROADENING IN STELLAR SPECTRA

M. S. DIMITRIJEVIĆ
Astronomical Observatory, Volgina 7, 11050 Belgrade, Yugoslavia
E-mail mdimitrijevic@aob.aob.bg.ac.yu

Abstract. Stark broadening parameters for singly-ionized iron a^6D - z^6P^o, a^6D - z^6D^o and a^6D - z^6F^o multiplets, have been calculated by using the semiclassical-perturbation approach. The obtained results have been compared with experimental data and simpler estimates.

1. INTRODUCTION

The research of neutral and ionized iron spectra is of great astrophysical importance due to high abundance of this element and its role in various processes in stellar plasma. Fe II lines are present in solar and stellar spectra and for their analysis or the calculations of synthetic spectra corresponding Stark broadening data are of importance. In spite of the astrophysical meaning of iron, we found only two published experimental investigations of Stark broadening parameters of Fe II lines. Manning *et al.* (1990) have investigated shifts of Fe II a^4D - z^4F^o 2755.73 Å line and Purić *et al.* (1993) widths of 14 lines from a^6D - z^6D^o and a^6D - z^6F^o multiplets. Electron-impact widths for 3 solar multiplets (a^4H - z^4F^o, a^6D - z^6D^o and a^4F - z^4F^o) and 3 multiplets observed in the spectrum of 15 Vulpeculae (Yo-ichi Takeda, 1984) b^4P - z^4F^o, b^4F - z^4D^o and b^4P - z^4D^o), have been calculated by Dimitrijević (1988) within the modified semiempirical approach (Dimitrijević and Konjević, 1980). Simple estimates based on the regularities and systematic trends, by Lakićević (1983) and Purić *et al.* (1993) exist as well.

The strongest Fe II lines correspond to 4s-4p and 3d-4p transitions in $3d^6nl$ and $3d^54snl$ configurations, covering some 1500 observed lines and accounting for the main part of the intensity of the Fe II spectrum (Johanson, 1984). However, if one wishes to perform a more sophisticated calculations it is not easy to collect the sufficiently complete energy level set and to avoid the additional difficulties due to configuration interaction and violation of the LS selection rules. The best situation is just with 4s-4p sextets, measured by Purić *et al.* (1993), where the sufficiently complete energy level set exists and there is not pronounced configuration interactions or critical violations of the LS selection rules (Fawcet, 1987), so that the semiclassical calculations may provide more reliable Stark broadening parameters.

By using the semiclassical-perturbation formalism (Sahal-Bréchot 1969ab), we have calculated Stark broadening parameters for singly-ionized iron $a^6D - z^6P^o$, $a^6D - z^6D^o$ and $a^6D - z^6F^o$ multiplets. Perturbers are electrons, protons and a singly charged perturber with the mass equal to 35 a.u. corresponding to the averaged mass of perturbing ions in Solar atmosphere. A summary of the formalism is given in Dimitrijević *et al.* (1991). The obtained results have been compared with experimental data and simpler evaluations.

2. RESULTS AND DISCUSSION

All details of calculations and results for $a^6D - z^6P^o$, $a^6D - z^6D^o$ and $a^6D - z^6F^o$ multiplets, covering 34 lines within 2328.11-2632.108 *Å* range, will be published in Dimitrijević (1995), for a perturber density of $10^{17}cm^{-3}$ and temperatures T = 5,000 - 150,000 K.

In Table 1 the present theoretical full half-widths have been compared with experimental results (Purić *et al.* 1993a) as well as with the calculations of Dimitrijević (1988) performed by using the modified semiempirical approach (1980) and with simple theoretical estimates of Purić *et al.* (1993b) based on regularities and systematic trends. For the experiment of Purić *et al.* (1993a) SF_6 has been used as a working gas. At T = 30,000 K and electron density of $10^{17}cm^{-3}$ full half width for F II-impact broadening of Fe II 2392.9 *Å* line is 0.00606*Å* and for S II-impact broadening 0.00618*Å*. Since the difference is negligible in comparison with electron-impact broadening, and since the ionized sulphur has the lower ionization potential and the corresponding linewidth is larger, full half width due to S II- impacts has been presented in Table 1 as an upper limit of ion broadening contribution. We can see that semiclassical calculations with the ion broadening contribution included, give larger widths than experiment but within the error bars of theory and experiment. Taking into account the complexity of the Fe II spectrum, the results (Dimitrijević, 1988) obtained by using the modified semiempirical method (Dimitrijević and Konjević, 1980) are in satisfactory agreement with the experimental values. The agreement of simple estimates of Purić *et al.* (1993b) with experimental and semiclassical values is encouraging as well. Simple estimate of Lakićević (1983) gives for $a^6D - z^6D^o$ Fe II multiplet for a perturber density of $10^{17}cm^{-3}$ and the temperature of 20,000 K, full width = 0.068 *Å* which is in encouraging agreement with experimental and semiclassical results. On the other hand the shift of 0.032 *Å* has the different sign. New experimental data for Fe II Stark broadening parameters will be of interest for astrophysics as well as for theoretical investigations of Stark broadening for complex spectra.

TABLE I

Comparison of experimental and theoretical Stark widths (FWHM) at corresponding electron densities N, and temperatures T. WM - experimental widths(FWHM) of Purić *et al.* 1993a; We - present semiclassical widths(FWHM) for electron-impact broadening; WSII - present semiclassical widths (FWHM) for SII- impact broadening; WDK - Dimitrijević (1988); WP - Purić *et al.* 1993b.

Transition	Wavelength [A]	T [10^4K]	N [10^{17}cm^{-3}]	W_M[A]	W_e[A]	W_{SII} A]	W_{DK}[A]	W_P[A]
a^6D-z^6D^o	2598.37	3.00	1.95	0.070	0.117	0.0130	0.068	0.126
		2.90	1.64	0.058	0.100	0.0109	0.059	0.108
		2.80	1.06	0.044	0.066	0.0070	0.038	0.072
	2607.52	3.00	1.95	0.100	0.117	0.0130	0.068	0.126
		2.90	1.64	0.076	0.100	0.0109	0.059	0.108
		2.90	1.27	0.058	0.077	0.0084	0.045	0.084
	2611.87	3.00	1.95	0.096	0.117	0.0130	0.068	0.126
		2.90	1.64	0.090	0.100	0.0109	0.059	0.108
		2.80	1.06	0.072	0.066	0.0070	0.038	0.070
	2613.82	3.00	1.95	0.088	0.117	0.0130	0.068	0.126
		2.90	1.64	0.072	0.100	0.0109	0.059	0.108
		2.80	1.06	0.044	0.066	0.0070	0.038	0.070
	2617.62	3.00	1.95	0.084	0.117	0.0130	0.068	0.126
		2.90	1.64	0.072	0.100	0.0109	0.059	0.108
		2.80	1.06	0.050	0.066	0.0070	0.038	0.070
a^6D-z^6F^o	2373.74	2.80	1.06	0.062	0.057	0.0065	0.034	0.064
	2382.04	3.00	1.95	0.090	0.101	0.0121	0.060	0.114
		2.90	1.64	0.080	0.086	0.0101	0.051	0.098
		2.80	1.06	0.048	0.057	0.0065	0.034	0.064
	2388.63	3.00	1.95	0.076	0.101	0.0121	0.060	0.114
		2.80	1.06	0.044	0.057	0.0065	0.034	0.064
	2404.43	2.70	0.63	0.030	0.034	0.0038	0.020	0.038
	2404.89	3.00	1.95	0.086	0.101	0.0121	0.060	0.112
		2.90	1.64	0.066	0.086	0.0101	0.051	0.096
		2.80	1.06	0.042	0.057	0.0065	0.034	0.064

References

Dimitrijević, M. S. : 1988, in *Physics of Formation of Fe II Lines Outside LTE*, eds. R. Viotti, A. Vittone, M. Friedjung, Astrophysics and Space Science Library, Vol. 138, D.Reidel P.C., p. 211.
Dimitrijević, M. S. : 1995, *Astron. Astrophys. Suppl. Series*, submitted.
Dimitrijević, M. S. and Konjević, N. : 1980, *JQSRT*, **24**, 451.
Dimitrijević, M. S., Sahal-Bréchot, S. and Bommier, V. : 1991, *Astron. Astrophys. Suppl. Series*, **89**, 581.
Johansson, S. : 1984, *Physica Scripta*, **T8**, 63.
Lakićević, I. S. : 1983, *Astron. Astrophys.* **127**, 37.
Manning, J. T., Winefordner, J. D., Palmer, B. A. and Hof, D. E. : 1990, *Spectrochim. Acta*, **45B**, 1031.
Purić, J., Djeniže, S., Srećković, A., Bukvić, S., Pivalica, S. and Labat, J. : 1993a, *Astron. Astrophys. Suppl. Series*, **102**, 607.
Purić, J., Miller, M. H., and Lesage, A. : 1993b, *Astrophys. J.* **416**, 825.
Sahal-Bréchot, S. : 1969a, *Astron. Astrophys.* **1**, 91.
Sahal-Bréchot, S. : 1969b, *Astron. Astrophys.* **2**, 322.
Yo-ichi Takeda : 1984, *Publ. Astron. Soc. Japan* **36**, 149.

Publ. Obs. Astron. Belgrade No. 49 (1995), 135-138

STARK BROADENING OF O V LINES

M. S. DIMITRIJEVIĆ
Astronomical Observatory, Volgina 7, 11050 Belgrade, Yugoslavia
E-mail mdimitrijevic@aob.aob.bg.ac.yu

S. SAHAL-BRÉCHOT
Observatoire de Paris, 92190 Meudon, France
E-mail sahal@obspm.fr

Abstract. Using a semiclassical approach, we have calculated electron-, proton-, and He III-impact line widths and shifts for 19 O V multiplets.

1. INTRODUCTION

The astrophysical interest of oxygen is obvious due to its high cosmical abundance and presence of its different ionization stages in stellar atmospheres. By using the semiclassical-perturbation formalism (Sahal-Bréchot 1969ab), we have calculated electron-, proton-, and ionized helium-impact line widths and shifts for 19 O V multiplets, in order to continue our research of multiply charged ion line Stark broadening parameters. A summary of the formalism is given in Dimitrijević *et al.* (1991).

2. RESULTS AND DISCUSSION

Energy levels for O V lines have been taken from Moore (1980). Oscillator strengths have been calculated by using the method of Bates and Damgaard (1949) and the tables of Oertel and Shomo (1968). For higher levels, the method described by Van Regemorter *et al.* (1979) has been used. In addition to electron-impact full halfwidths and shifts, Stark-broadening parameters due to proton-, and He III- impacts have been calculated. Our results for 19 O V multiplets will be published elsewhere (Dimitrijević and Sahal - Bréchot, 1994, 1995), for perturber densities 10^{17} - 10^{22}cm^{-3} and temperatures T = 40,000 - 2,000,000K. Here will be given in Table 1 only an example of obtained results.

In addition to the present data for 19 O V multiplets, Stark broadening data for 50 O V multiplets for which the set of atomic data needed for semiclassical calculation presently does not exist, have been calculated within the modified semiempirical approach (Dimitrijević and Konjević 1980) and published recently (Dimitrijević 1993a). For 29 of these 50 O V multiplets not included here, exist as well in Dimitrijević (1993b) data calculated within the approximate semiclassical approach (Eq. 526 in Griem 1974).

TABLE I

This Table shows electron- and proton-impact broadening parameters for O V, for perturber density of 10^{17}cm^{-3} and temperatures from 40,000 to 2,000,000 K. Transitions and averaged wavelengths for the multiplet (in Å) are also given. By using c (see Eq. (5) in Dimitrijević *et al.*, 1991), we obtain an estimate for the maximum perturber density for which the line may be treated as isolated and tabulated data may be used.

		Perturbers			
		Electrons		Protons	
Transition	T(K)	Width (Å)	Shift (Å)	Width (Å)	Shift (Å)
		Perturber density = 1 x 10^{+17} cm^{-3}			
O V 2S-2P 629.7 Å C= 0.63E+20	40000.	0.810E-03	0.189E-04	0.123E-05	-0.199E-05
	100000.	0.516E-03	-0.999E-05	0.477E-05	-0.506E-05
	200000.	0.369E-03	-0.987E-05	0.113E-04	-0.947E-05
	500000.	0.245E-03	-0.129E-04	0.230E-04	-0.168E-04
O V 2P 3S 248.5 Å C= 0.12E+19	40000.	0.375E-03	0.152E-04	0.327E-05	0.138E-04
	100000.	0.250E-03	0.260E-04	0.153E-04	0.258E-04
	200000.	0.191E-03	0.263E-04	0.275E-04	0.356E-04
	500000.	0.138E-03	0.250E-04	0.447E-04	0.455E-04
O V 2P 4S 174.6 Å C= 0.19E+18	40000.	0.631E-03	0.645E-04	0.349E-04	0.557E-04
	100000.	0.445E-03	0.723E-04	0.738E-04	0.832E-04
	200000.	0.352E-03	0.699E-04	0.986E-04	0.100E-03
	500000.	0.264E-03	0.614E-04	0.135E-03	0.124E-03
O V 2P 3D 220.4 Å C= 0.15E+19	40000.	0.257E-03	-0.932E-05	0.224E-05	-0.147E-05
	100000.	0.166E-03	-0.775E-06	0.637E-05	-0.347E-05
	200000.	0.122E-03	-0.170E-05	0.103E-04	-0.555E-05
	500000.	0.864E-04	-0.198E-07	0.152E-04	-0.834E-05
O V 2P 4D 170.2 Å C= 0.10E+18	40000.	0.657E-03	0.105E-04	0.224E-04	0.234E-04
	100000.	0.463E-03	0.120E-04	0.431E-04	0.379E-04
	200000.	0.366E-03	0.127E-04	0.581E-04	0.464E-04
	500000.	0.276E-03	0.989E-05	0.814E-04	0.586E-04
O V 3D 4F 728.7 Å C= 0.19E+19	40000.	0.810E-02	-0.165E-03	0.271E-03	-0.446E-03
	100000.	0.555E-02	-0.152E-03	0.623E-03	-0.717E-03
	200000.	0.433E-02	-0.974E-04	0.929E-03	-0.875E-03
	500000.	0.327E-02	-0.535E-04	0.134E-02	-0.110E-02

TABLE I (Cont.)

Transition	T(K)	Electrons Width (Å)	Electrons Shift (Å)	Protons Width (Å)	Protons Shift (Å)
O V 3D 5F 509.4 Å C= 0.14E+18	40000.	0.160E-01	-0.119E-02	0.363E-02	-0.358E-02
	100000.	0.119E-01	-0.114E-02	0.528E-02	-0.489E-02
	200000.	0.959E-02	-0.889E-03	0.701E-02	-0.566E-02
	500000.	0.722E-02	-0.656E-03	0.939E-02	-0.670E-02
O V 2P 3S 215.2 Å C= 0.17E+19	40000.	0.222E-03	0.690E-05	0.935E-06	0.564E-05
	100000.	0.144E-03	0.130E-04	0.552E-05	0.116E-04
	200000.	0.108E-03	0.163E-04	0.112E-04	0.162E-04
	500000.	0.779E-04	0.151E-04	0.205E-04	0.216E-04
O V 2P 4S 156.2 Å C= 0.33E+18	40000.	0.370E-03	0.346E-04	0.110E-04	0.231E-04
	100000.	0.253E-03	0.445E-04	0.275E-04	0.367E-04
	200000.	0.199E-03	0.416E-04	0.417E-04	0.443E-04
	500000.	0.149E-03	0.387E-04	0.585E-04	0.557E-04
O V 3P 4S 716.3 Å C= 0.69E+19	40000.	0.107E-01	0.679E-03	0.237E-03	0.456E-03
	100000.	0.736E-02	0.849E-03	0.574E-03	0.728E-03
	200000.	0.577E-02	0.803E-03	0.855E-03	0.885E-03
	500000.	0.433E-02	0.742E-03	0.119E-02	0.113E-02
O V 3S 3P 2784.8 Å C= 0.14E+21	40000.	0.852E-01	-0.101E-02	0.812E-03	-0.259E-03
	100000.	0.567E-01	-0.100E-02	0.198E-02	-0.609E-03
	200000.	0.431E-01	-0.170E-02	0.291E-02	-0.963E-03
	500000.	0.315E-01	-0.148E-02	0.388E-02	-0.143E-02
O V 2P 3D 192.9 Å C= 0.67E+18	40000.	0.187E-03	-0.824E-05	0.158E-05	-0.230E-05
	100000.	0.121E-03	-0.214E-05	0.493E-05	-0.507E-05
	200000.	0.897E-04	-0.191E-05	0.847E-05	-0.747E-05
	500000.	0.634E-04	-0.933E-06	0.137E-04	-0.106E-04
O V 2P 4D 151.5 Å C= 0.12E+18	40000.	0.497E-03	0.150E-05	0.126E-04	0.451E-05
	100000.	0.348E-03	0.498E-05	0.227E-04	0.865E-05
	200000.	0.273E-03	0.521E-05	0.292E-04	0.119E-04
	500000.	0.206E-03	0.506E-05	0.378E-04	0.153E-04
O V 3P 3D 5591.4 Å C= 0.56E+21	40000.	0.282	-0.697E-02	0.278E-02	-0.464E-02
	100000.	0.189	-0.644E-02	0.829E-02	-0.930E-02
	200000.	0.143	-0.566E-02	0.135E-01	-0.129E-01
	500000.	0.105	-0.499E-02	0.204E-01	-0.169E-01

References

Bates, D. R., and Damgaard, A. : 1949, *Trans. Roy. Soc. London, Ser. A*, **242**, 101.
Dimitrijević, M. S. : 1993a, *Astron. Astrophys. Suppl. Series*, **100**, 237.
Dimitrijević, M. S. : 1993b, *Astro.Lett. and Communications*, **28**, 385.
Dimitrijević, M. S. and Konjević, N. : 1980, *JQSRT*, **24**, 451.
Dimitrijević, M. S., Sahal-Bréchot, S., and Bommier, V. : 1991, *Astron. Astrophys. Suppl. Series*, **89**, 581.
Dimitrijević, M.S., and Sahal-Brchot,S. : 1994, *Bull. Astron. Belgrade* **150**, 95.
Dimitrijević, M. S. and Sahal-Brchot, S. : 1995, *Astron. Astrophys. Suppl. Series*, in press.
Griem, H. R. : 1974, *Spectral Line Broadening by Plasmas*, Academic Press, New York and London.
Moore, C. E. : 1980, *Selected Tables of Atomic Spectra, Atomic Energy Levels and Multiplet Tables, O V*, NSRDS-NBS 3, Section 9, U.S.Dept. of Commerce, Washington.
Oertel, G. K., and Shomo, L. P. : 1968, *Astrophys. J. Suppl. Series*, **16**, 175.
Sahal-Bréchot, S. : 1969a, *Astron.Astrophys.* **1**, 91.
Sahal-Bréchot, S. : 1969b, *Astron.Astrophys.* **2**, 322.
Van Regemorter, H., Hoang Binh Dy, and Prud'homme, M. : 1979, *J. Phys. B*, **12**, 1073.

Publ. Obs. Astron. Belgrade No. 49 (1995), 139-142

STARK BROADENING OF LITHIUM ION LINES IN ASTROPHYSICAL AND LABORATORY PLASMAS

M. S. DIMITRIJEVIĆ
Astronomical Observatory, Volgina 7, 11050 Belgrade, Yugoslavia
E-mail mdimitrijevic@aob.aob.bg.ac.yu

S. SAHAL-BRECHOT
Observatoire de Paris, 92195 Meudon Cedex, France
E-mail sahal@obspm.fr

Abstract. Using a semiclassical approach, we have calculated electron-, proton-, and ionized helium-impact line widths and shifts for 37 Li II multiplets. The resulting data have been compared with existing theoretical values.

1. INTRODUCTION

Profiles of neutral and ionized lithium lines are of interest to astrophysicists since the surface content (abundance) of lithium involves problems correlated with nucleogenesis and with mixing between the atmosphere and the interior (Boesgaard 1988).They should also be of interest for the study of deep Li depletions in the mid-F stars, which were first observed in the Hyades (Boesgaard, Trippico 1986).Even for the study of stars in the late stage of evolution, Stark broadening is of interest since its influence increases with an increase in the principal quantum number (n) of the initial energy level (Vince *et al.* 1985), because the bond between the optical electron and the core becomes weaker and the influence of external electric microfields increases.

Stark-broadening parameters for singly charged lithium lines are of interest for Stark broadening theory investigations as well, since the He-like Li II spectrum is suitable for theoretical research. They are of interest for the examination of regularities and systematic trends within He isoelectronic sequence as well.

By using the semiclassical-perturbation formalism (Sahal-Bréchot 1969ab), we have calculated electron-, proton-, and ionized helium-impact line widths and shifts for 37 Li II multiplets. A summary of the formalism is given in Dimitrijević *et al.* (1991). Here, we discuss the obtained results for Li II, along with a comparison with other theoretical results (Jones *et al.* 1971, see also Griem 1974).

2. RESULTS AND DISCUSSION

All details of calculations as well as the tables of Stark-broadening parameters due to electron-, proton- and ionized-helium impacts for perturber densities of $10^{15} - 10^{17}$cm^{-3} and temperatures T = 5,000 - 40,000 K, will be published elsewhere (Dimitrijević and Sahal-Bréchot 1995ab).

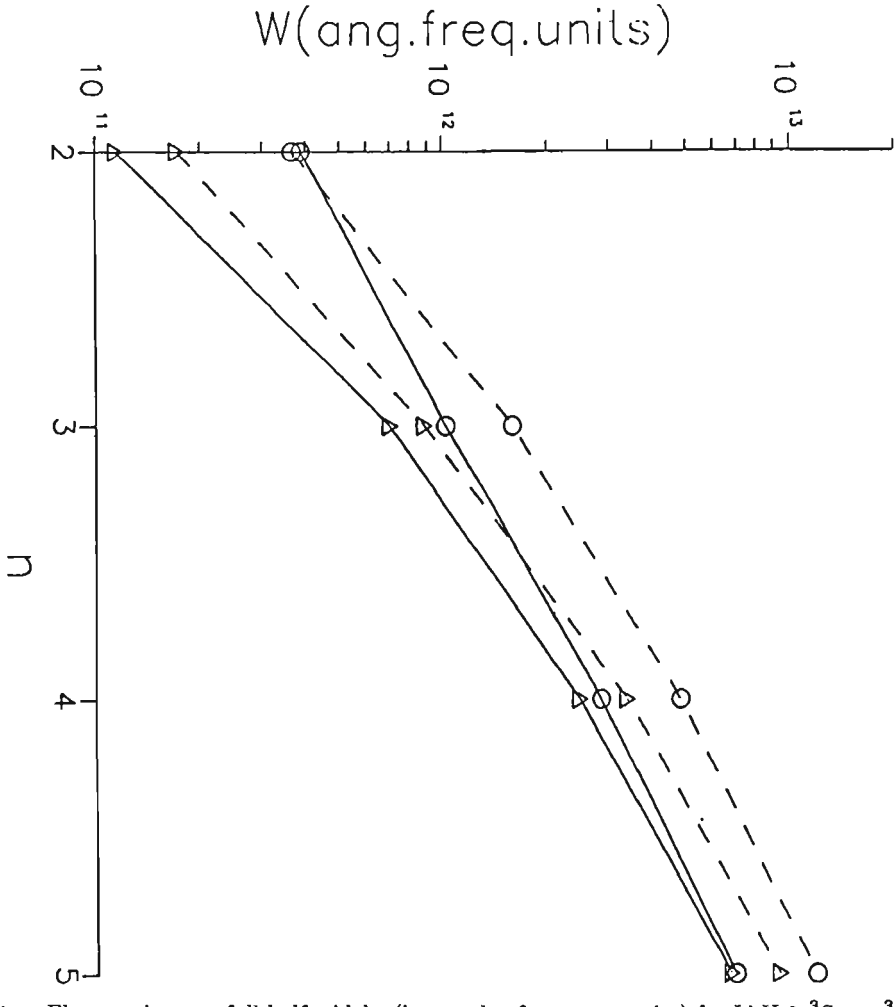

Fig. 1. Electron-impact full half-widths (in angular frequency units) for Li II $2s^3S$ - np^3P^o lines as a function of n for T = 5,000 K (o) and 40,000 K (Δ) at Ne = 10^{17} cm^{-3}. With (___) are denoted present calculations and with (– – –) semiclassical calculations of Jones *et al.* (1971, see also Griem 1974).

In Figs. 1 and 2 the electron-impact full half widths and shifts within the $2s^3S$ - np^3P^o series have been compared with semiclassical results of Jones *et al.* (1971, see also Grem 1974). We can see gradual change of Stark broadening parameters permitting the interpolation of new data or critical evaluation of mutual consistency of existing data, as in our previous analyses (Dimitrijević *et al.* 1991).

We see in Figs. 1-2 that the agreement between present calculation and calculations of Jones *et al.* (1971, see also Griem 1974) is better at higher temperatures, when the inelastic contribution to the width dominates, than at lower ones, when differences in cut-off procedure and the symmetrization influence are more significant. Due to the difference of calculated values, especially for shifts, it is of interest to determine Li II Stark broadening parameters experimentally at different temperatures in order to test the differences in applied theoretical models.

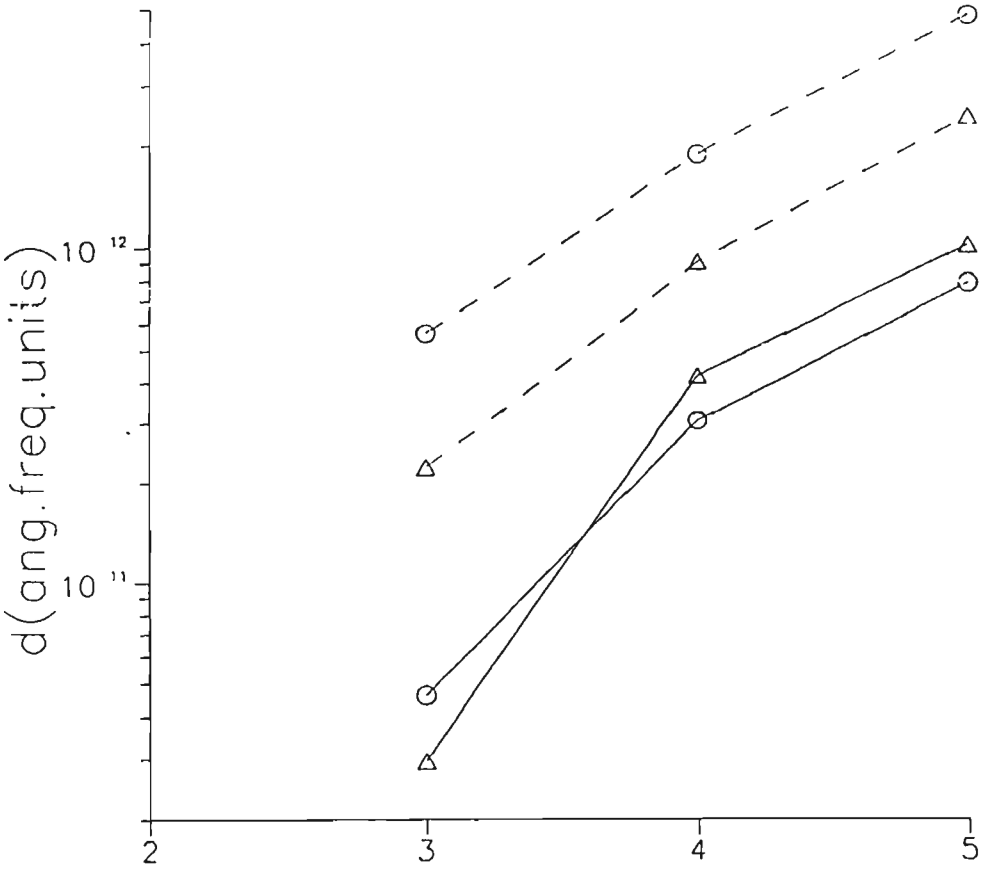

Fig. 2. As in Fig. 1 but for the electron-impact shift.

References

Boesgaard, A. M. : 1988, *Vistas in Astronomy*, **31**, 167.
Boesgaard, A. M., and Trippico, M. J. : 1986, *Astrophys. J.* **302**, L49.
Dimitrijević, M. S. and Sahal-Bréchot, S. : 1995a, *Physica Scripta*, submitted.
Dimitrijević, M. S. and Sahal-Bréchot, S. : 1995b, *Bull. Astron. Belgrade*, **151**, in press.

Dimitrijević, M. S., Sahal-Bréchot, S. and Bommier, V. : 1991, *Astron. Astrophys. Suppl. Series*, **89**, 581.
Griem, H. R. : 1974, "Spectral Line Broadening by Plasmas", Academic Press, New York.
Jones, W. W., Benett, S. M., and Griem, H. R. : 1971, "Calculated Electron Impact Broadening Parameters for Isolated Spectral Lines from Singly Charged Ions Lithium through Calcium", Techn. Rep. No 71-128, Univ. Maryland.
Sahal-Bréchot, S. : 1969a, *Astron.Astrophys.* **1**, 91.
Sahal-Bréchot, S. : 1969b, *Astron.Astrophys.* **2**, 322.
Vince, I., Dimitrijević, M. S. and Kršljanin, V. : 1985, in *Spectral Line Shapes III*, Rostas, F., ed., de Gruyter, Berlin, p.650.

Publ. Obs. Astron. Belgrade No. 49 (1995), 143-144

ADELIC GENERALIZATION OF WAVE FUNCTION OF THE UNIVERSE

B. DRAGOVICH
Institute of physics, P.O.Box 57, 11001 Belgrade, Yugoslavia

Abstract. Recently adelic quantum mechanics has been formulated as p-adic and adelic generalization of ordinary quantum mechanics. Here, we propose adelic quantum mechanics to investigate quantum dynamics of the universe. We show that the Hartle-Hawking approach to quantum cosmology may be generalized in an adelic way. Adelic wave function of the universe is a product of the standard Hartle-Hawking wave function and the corresponding p-adic ones.

1. ADELIC QUANTUM MECHANICS

It is well known that experimental and observational data always belong to the field of rational numbers Q, and theoretical models traditionally use real R and complex numbers C. However, as completion of Q with respect to the usual absolute value gives R, in the same way completion of Q with respect to p-adic norms (p = a prime number) creates the fields of p-adic numbers Q_p (p = 2,3,5,...).

Since 1987, p-adic numbers have been applied in various branches of theoretical and mathematical physics (for a review, see Brekke and Freund 1993, and Vladimirov, Volovich and Zelenov 1994). One of the significant achievements is a formulation of p-adic quantum mechanics, whose complex-valued wave functions depend on p-adic variables. Ordinary and p-adic quantum mechanics may be naturally unified in a form of adelic quantum mechanics (Dragovich 1995).

A mathematical concept to unify real and p-adic numbers is an adele, which is an infinite sequence, $a = (a_\infty, a_2, ..., a_p, ...)$, where $a_\infty \in R$, $a_p \in Q_p$ with the restriction that $a_p \in Z_p = \{x \in Q_p \mid\mid x \mid_p \leq 1\}$ for all but a finite number of p. The set of all adeles A is a ring under componentwise addition and multiplication. An additive character on A is $\chi(xy) = \chi_\infty(x_\infty y_\infty) \prod_p \chi_p(x_p y_p) = exp(-2\pi i x_\infty y_\infty) \prod_p exp 2\pi i \{x_p y_p\}_p$, where $x, y \in A$ and $\{a_p\}_p$ denotes the fractional part of the p-adic expansion of a_p.

On an adelic space A one can define a Hilbert space $L_2(A)$, which is a space of complex-valued and square integrable functions with respect to the Haar measure on A. An orthonormal basis of the adelic Hilbert space consists of infinite products of the orthonormal states $\Psi_\infty \in L_2(R)$ and $\Psi_p \in L_2(Q_p)$, where $\Psi_p(x_p) = \Omega(\mid x_p \mid_p)$ for all but a finite number of p. Here, $\Omega(a) = 1$ if $0 \leq a \leq 1$ and $\Omega(a) = 0$ if $a > 1$.

2. ADELIC QUANTUM COSMOLOGY

The main motivation for application of adeles in quantum cosmology comes from the fact that an adelic spacetime contains archimedean (usual) and nonarchimedean (ultrametric) geometries, which may be present at the very beginning of the universe evolution. Adelic quantum cosmology is the application of adelic quantum theory to the universe as a whole, and it is adelic generalization of the usual quantum cosmology.

The Wheeler-DeWitt equation, as well as the Schrödinger equation, is not appropriate to generalize to p-adic and adelic cases. However, the path integral approach for the fundamental quantum-mechanical amplitudes can be generalized to p-adic and adelic dynamics.

To obtain the Hartle-Hawking (Hartle and Hawking 1983) wave function for the ground state of the universe in adelic quantum cosmology one has to enlarge functional integration over all compact 4-geometries of the real case by adding the corresponding ones of p-adic cases. It means that adelic ground- state of the universe can be presented as

$$\Psi[h_{ij}] = \int \chi_\infty(-S_\infty) D(g_{\mu\nu})_\infty \prod_p \int \chi_p(-S_p) D(g_{\mu\nu})_p ,$$

where h_{ij} is an adelic 3-metric, and $\chi(-S_\upsilon)$, $(\upsilon = \infty, 2, ...)$, are additive characters of the Einstein-Hilbert gravitational actions (without matter fields). Note that $S_\upsilon \in Q_\upsilon$ and must have number field invariant form. In a simple minisuperspace model (with scale factors a_υ) the ground-state wave function should be of the form $\Omega(\mid a_p \mid_p)$ for all but a finite number of p. This is a rather strong restriction which may be helpful in further investigation of quantum cosmology.

According to this approach the universe at very small distances (about the Planck length) consists of real and p-adic spaces in the form of an adelic space.

The adelic de Sitter minisuperspace model is under consideration and will be presented elsewhere.

To better understand many notions contained in this article, see Aref'eva et al. 1991.

References

Aref'eva, I. Ya., Dragovich, B., Frampton, P. H. and Volovich, I. V. : 1991, *Int. J. Mod. Phys. A*, **6**, 4341.

Brekke, L. and Freund, P. G. O. : 1993, *Phys. Reports*, **233**,1.

Dragovich, B. : 1995, *Int. J. Mod. Phys. A*, to be published.

Hartle, J. B. and Hawking, S. W. : 1983, *Phys. Rev. D*, **28**, 2960.

Vladimirov, V. S., Volovich, I. V. and Zelenov, E. I. : 1994, P-adic Analysis and Mathematical Physics, World Scientific, Singapore.

Publ. Obs. Astron. Belgrade No. 49 (1995), 145-150

AN INTERPRETATION OF CB LIGHT CURVE OF ACTIVE CATACLYSMIC VARIABLE OY Car BY USING THE INVERSE-PROBLEM METHOD

G. DJURAŠEVIĆ
Astronomical Observatory, Volgina 7, 11050 Belgrade, Yugoslavia
E-mail gdjurasevic@aob.aob.bg.ac.yu

Abstract. In the paper considered is a model synthesizing the light curves of novae and novae-like stars, as well as of active close binaries (CB) in the phase of an intensive matter exchange between the components with accretion onto a white dwarf. The model considers the radial and azimuthal temperature distributions in the disc allowing a successful interpretation of asymmetric deformed light curves characteristic of these systems. The analysis of the observed light curves is performed by using the inverse-problem method (Djurašević, 1992b) adapted to this model. In the particular case the parameters of the dwarf-nova *OY Car* are estimated on the basis of observations (Wood et al., 1989).

1. INTRODUCTION

In the modern theory of accretion in CB it is important to determine from observations the physical characteristics of the system and accretion disc for the cataclysmic variables such as the novae and novae-like stars. The luminosity of majority of these stars in the quiescent phase (between outbursts) is due to the accretion disc located around the white dwarf and the hot spot on the disc edge. The disc is formed due to a gas stream flowing from the secondary. In the region where the stream touches the disc the temperature is increased and this is known as the hot spot. On account of a relatively low accretion-disc luminosity in the quiescent phase the hot spot in these systems contributes significantly, sometimes dominantly, to the total system luminosity. For this reason the light curves are significantly deformed and they have a characteristic form caused by the ellipse geometry, as well as by the radial and azimuthal temperature distributions in the disc. The CB model (Djurašević, 1992a) developed earlier for the W Ser type systems and the inverse-problem method (Djurašević, 1992b) are adapted for analyzing the light curves of these systems. This particular case comprises the analysis of the observational material (Wood et al., 1989) referred to the dwarf nova *OY Car*. The system's orbital period is about 91 minutes. In the quiescent phase (between outbursts) the light curve has a relatively stable form so that it becomes possible to estimate the basic system's parameters by means of an adequate analysis.

2. THE MODEL

The canonical model of a cataclysmic variable is a Roche lobe-filling cool main sequence star which looses matter into the Roche lobe of the white dwarf. The transferred material has too much angular momentum to fall onto the surface of the white dwarf. Because of the tiny dimensions of the primary, this material flies along its trajectory inside the white dwarf's Roche volume forming a ring around the central object. As viscous forces are at work, the matter gradually looses angular momentum, and this ring spreads out to form a disc which lies in the orbital plane of the system, extending down to the white dwarf. On the disc lateral side, in the zone where the gas stream falls on the disc, there is an intensive hot-spot radiation. The position, size, and temperature of a hot-spot are dependent on the gas-stream parameters, on the forces in the system and on the disc size. A hot-spot causes deformations on a CB light curve, which becomes asymmetric with a characteristic hump, which is due to the intensive hot-spot radiation.

When the matter is approaching the white dwarf it has to get rid of excess gravitational energy, half of which, according to the Virial Theorem, is converted into kinetic energy of the disc material, while the other half is transformed into radiative energy, causing the disc to shine as a luminous object. At the interface between the innermost disc area and the white dwarf (in the nonsynchronous rotation) the motion of disc material will have to be broken down to the velocity of the white dwarf, in the process of which additional radiative energy will be liberated and the boundary layer will be formed.

For the purpose of analyzing light curves of this active CB with an accretion disc around white dwarf, being at the evolutionary phase of an intensive matter exchange between the components, a model for light-curve synthesis has been realized by modifying the model (Djurašević, 1992a), developed for the systems like W Ser. The system components are considered in the framework of nonsynchronous Roche model and the accretion disc of a constant thickness lies in the orbital plane around white dwarf capturing the matter of the neighbouring component.

The primary surrounded by the disc is situated relatively well within the Roche oval, and its rotation can be significantly nonsynchronous. Near the Lagrange equilibrium point L_1 flows from the secondary (which fills the Roche limit) the gas stream 'nourishing' the disc. In the zone where the stream touches the lateral side of the disc a hot spot is formed (Fig.1.). In all details, the model is explained in Djurašević, 1992a. Here only the changes in the details concerning the temperature distribution along the disc radius, which is characteristic for the accretion onto a white dwarf, will be presented.

Without a model of the light distribution in the disc, it is not possible to perform a correct analysis of the eclipse curves for deriving the geometric properties of the system.

The viscosity of the disc material determines how much energy is liberated at any point in the disc, i. e. the temperature distribution along disc radius. With the assumption that the whole disc is stationary, i.e. mass transfer rate $\dot{M}$ is constant throughout the disc, the effective temperature distribution $T_{eff}(r)$ can be described

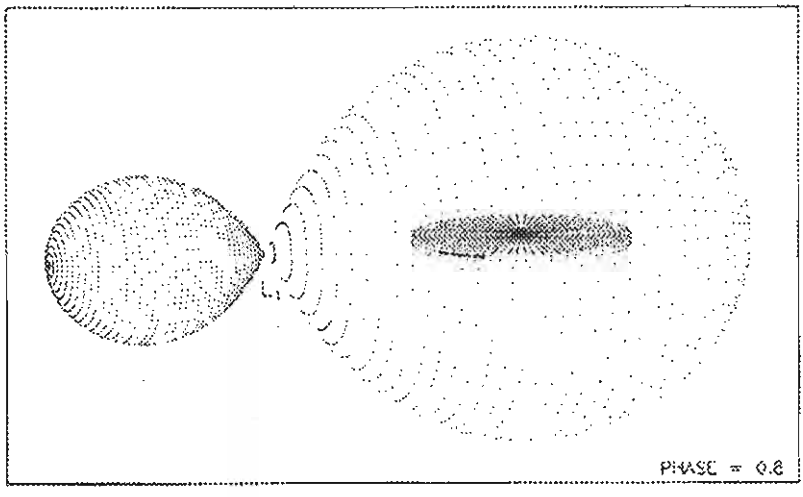

Fig. 1. The Roche model for cataclysmic variables.

by simple analytical formula (Verbunt, 1982) :

$$T_{eff}^4(r) = \frac{3GM_{wd}\dot{M}}{8\pi\sigma r^3}\left(1 - \sqrt{\frac{R_{wd}}{r}}\right), \tag{1}$$

where G and σ are Newton's and Stefan's constants, and R_{wd} is the inner radius of the disc. The assumption is that the disc with its internal side has a contact with the surface of the white dwarf. In the case of magnetic white dwarf, the exact value of disc inner radius is at some distance from the surface, depending on the mass of the star, the field strength, and the mass accretion rate.

The term in brackets accounts for the transfer of angular momentum between the disc and the white dwarf and imposes a certain, though in practice probably unimportant, uncertainty on the value of the effective temperature.

In our model the temperature on the edge of the disc $T_d(r = R_d)$ appears as a parameter. Expressed through this quantity, the temperature distribution in steady state models for optically thick blackbody discs, based on (1), has the form :

$$T_{eff}(r) = \frac{T_d}{C_{fr}}\left(\frac{R_d}{r}\right)^{3/4}\left(1 - \sqrt{\frac{R_{wd}}{r}}\right)^{1/4}, \tag{2}$$

where

$$C_{fr} = \left(1 - \sqrt{\frac{R_{wd}}{R_d}}\right)^{1/4}.$$

In order to include this temperature distribution in the CB-light-curve-synthesis model the disc is divided uniformly into concentric isothermal annuli whose temperature is determined by relation (2) and the radius is determined as the middle of the corresponding annulus. In such a procedure the area of an elementary cell on the disc depends on the radius and it is calculated for each annulus separately, as well as the

corresponding radiation fluxes. As for the other details, the earlier paper (Djurašević, 1992a) should be seen.

In order to enable a successful application of realized CB model in the analysis of the observed light curves to be made, an efficient method unifying the best properties of the gradient method and of the differential-corrections one into a single algorithm is proposed. The inverse problem is solved in an iterative cycle of corrections to the model elements based on nonlinear least-square method. In all details, the method is explained in Djurašević, 1992b.

3. THE ANALYSIS

The interpretation of photometric observations is based on the choice of optimal model parameters yielding the best agreement between an observed light curve and the corresponding synthetic one. Some of these parameters can be determined a priory in an independent way, while the others are found by solving the inverse problem.

The above procedure is applied to analyzing light curves of dwarf nova OY Car. For this system, the eclipse light curves clearly show the presence of two eclipsed objects which are identified with the white dwarf and the hot spot on the edge of the accretion disc.

For the analysis the mean light curves in the U and B filters obtained on March 9, i. e. March 10, 1984 (Wood et al., 1989) are used, when the system was in a quiescent state following a superoutburst that began on 1983 July 28 and preceding a normal outburst that began on 1984 April 1. The physical parameters of OY Car's two stars and the structure of the quiescent disc and hot spot can all be found from detailed analysis of the light curve. Since the difference between the two solutions (U and B curves) is small and the text is limited, here will be presented only the results of the analysis concerning the U-observations.

The mean light curve is shown in Fig. 2, where the measurements are denoted by the symbol (o), and the final synthetic light curve obtained by solving the inverse problem by symbol (*).

In the inverse-problem solving one assumes for the temperature of the secondary T=3000 K based on the spectral type (dM7-dM8). The mass ratio, the dimensions and the temperature of the primary are assumed to be free parameters. The same is valid for the orbit inclination and for the parameters of the disc and of the hot spot.

The obtained results are presented in Table I and in Fig 2. The view of the system at some orbital phases is shown in Fig 3. with parameters obtained by solving the inverse problem.

The results of the present analysis show that for the mass ratio of the components a value of $q = 0.102$ can be assumed, whereas for the orbit inclination $i = 83°.7$ is obtained.

The white dwarf in the center of accretion disc is possibly surrounded by a spherical boundary layer, and in addition by a luminous ring of material around its equator.

The effective temperature of the central object surrounded by the disc in the quiescent phase is about 15 000 K. As can be seen from the analysis, the possible radius of the central sphere is about 0.018 [R=1], whereas for the disc radius one obtains a value of 0.334 [R=1], i. e. 0.01 [R=1] for its thickness. For the temperature on the

TABLE I

Light curve analysis for CB OY Car
1984. Mar 9, 10.

RES (U filter) :
0.3642E − 01 - final sum of square deviations $\sum(O-C)^2$

FREE PARAMETERS AND ERRORS :
0.336E − 01 ± 0.107E − 02 - filling coefficient for the primary's critical oval
0.837E + 02 ± 0.981E − 01 - orbit inclination
0.514E + 04 ± 0.966E + 02 - disc temperature
0.100E − 01 ± 0.324E − 03 - disc thickness [R=1]
0.148E + 05 ± 0.501E + 03 - primary's temperature
0.561E + 00 ± 0.176E − 02 - disc dimension coefficient ($S_d = R_d/R_{yk}$)
0.323E + 03 ± 0.363E + 00 - hot-spot longitude
0.929E + 01 ± 0.468E + 00 - hot-spot angular dimensions
0.257E + 01 ± 0.335E − 01 - hot-spot temperature coefficient ($A_d = T_s/T^d$)
0.102E + 00 ± 0.212E − 03 - mass ratio of the components ($q = m_2/m_1$)

FIXED (*) AND CALCULATED PARAMETERS :
* 0.300E+04 1.0 1.0 - temperature of the secondary T_2 and nonsynchronous rotation coefficients f_1, f_2
* 0.25 0.08 - gravitational-darkening coefficient for the components (1,2)
0.3884 1.0000 - limb darkening coefficient for the components (1,2)
0.9966 0.4050 - limb darkening coefficient (disc, hot spot)
0.0179 0.1910 - polar radii of the components (1,2) [R=1]
0.0179 0.3335 - inner and outer radii of the disc [R=1]

[R=1], the data are expressed in the units of the distance between the centres of the components.

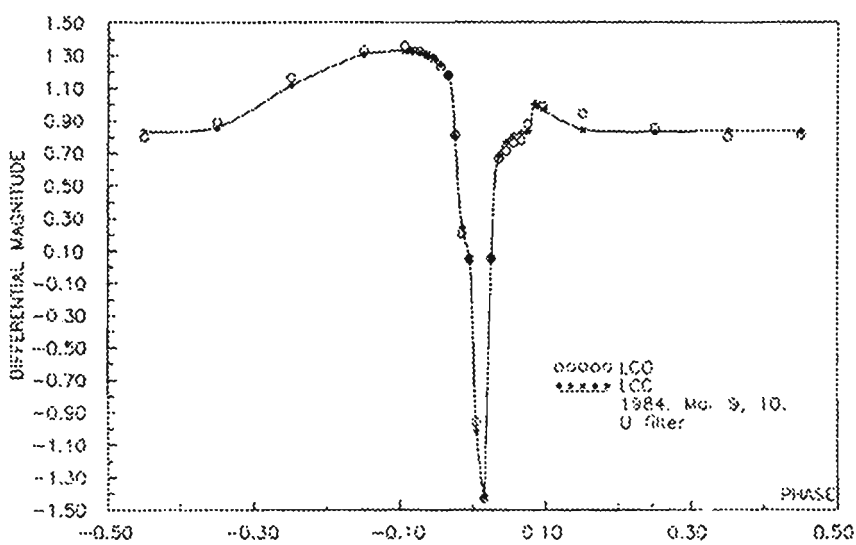

Fig. 2. Mean observed (LCO) and final synthetic (LCC) light curves in solving the inverse problem of active CB OY Car.

disc edge one obtains about 5100 K and the temperature coefficient of the hot spot with respect to the surrounding disc edge temperature is about 2 6, i. e. the temperature in the hot spot can attain 13 000 K. For the hot-spot longitude one obtains 323° and about 9° for its angular dimensions. The analysis shows that more than 50% of the corresponding Roche oval is filled by the disc.

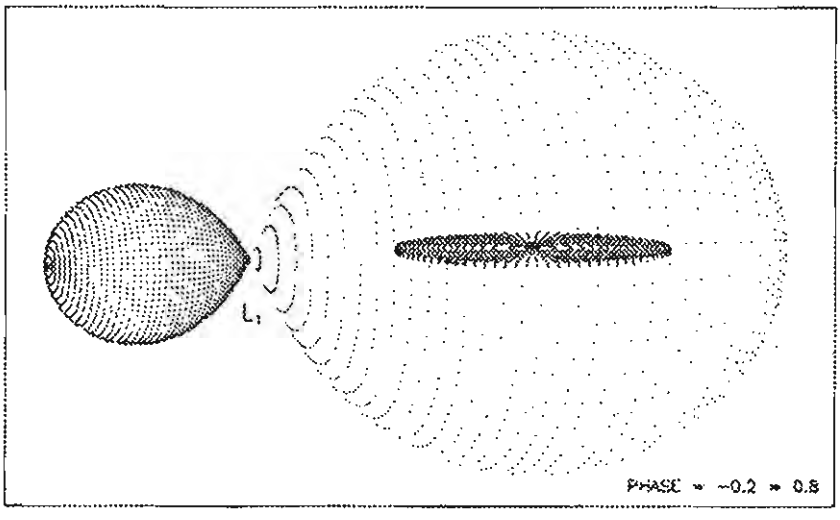

Fig. 3. The view of the CB OY Car at the orbital phase 0.80 with parameters obtained by solving the inverse problem.

The obtained results are in a relatively good agreement with the system parameters estimated earlier (Wood et al., 1989) and found in an independent way. This indicates that the proposed model of the system and the corresponding inverse-problem method presented here briefly are fully applicable to the analysis of active CB light curves in this evolutionary phase.

The radial temperature profile of the disc is consistent with steady mass transfer rate, and is described by relation (2). On the basis of the obtained system parameters and this relation the temperature increase from the disc edge towards its center can be simply estimated and presented graphically.

Acknowledgements

This work has been supported by Ministry for Sciences and Technology of Serbia through the project "Physics and Motions of Celestial Bodies".

References

Djurašević, G. : 1992a, *Astroph. Space Science*, **196**, 267.
Djurašević, G. : 1992b, *Astroph. Space Science*, **197**, 17.
Verbunt, F. : 1982, *Space Sci. Rev.* **32**, 379.
Wood, J. H., Horne, K., Berriman, G. and Wade, R. A. : 1989, *Astrophys. J.* **341**, 974.

Publ. Obs. Astron. Belgrade No. 49 (1995), 151-157

ON THE GLOBAL REGULARIZING TRANSFORMATIONS OF THE RESTRICTED THREE-BODY PROBLEM

B. ÉRDI
Department of Astronomy, Eötvös University
Budapest, Hungary

Abstract. The uniqueness of the general form $q = f(w) = [h(w) + h(w)^{-1}]/4$ of the global regularizing transformations of the restricted three-body problem is shown.

1. INTRODUCTION

In the restricted problem of three bodies two bodies revolve around their center of mass in circular orbits under the influence of their mutual gravitational attraction and a third body, influenced by only the gravitational attraction of the other two bodies, moves in the plane defined by the revolving bodies. It is assumed that the third body has so small mass that it does not influence the motion of the others. All the three bodies are considered as point masses. The problem is to find the motion of the third body.

The equations of motion of the third body, in properly chosen units, in a barycentric coordinate system which rotates uniformly together with the revolving bodies, are (Szebehely, 1967) :

$$\begin{aligned} \ddot{x} - 2\dot{y} &= \Omega_x, \\ \ddot{y} + 2\dot{x} &= \Omega_y, \end{aligned} \tag{1}$$

where

$$\Omega = \frac{1}{2}\left[(1-\mu)r_1^2 + \mu r_2^2\right] + \frac{1-\mu}{r_1} + \frac{\mu}{r_2}, \tag{2}$$

$$r_1 = \sqrt{(x-\mu)^2 + y^2}, \quad r_2 = \sqrt{(x+1-\mu)^2 + y^2}.$$

In Equations (1) x, y are the rectangular coordinates of the third body P_3 (see Figure 1), the dots mean differentiation with respect to the time variable t (which is actually the mean anomaly of the revolving bodies, the primaries), x and y in the index mean partial differentiation, μ is the mass parameter (the mass of the smaller primary divided by the total mass of the primaries), the body P_1 has mass $1-\mu$ and coordinates $(\mu, 0)$, the body P_2 has mass μ and coordinates $(\mu - 1, 0)$, r_1 and r_2 are the distances of P_3 from P_1 and P_2.

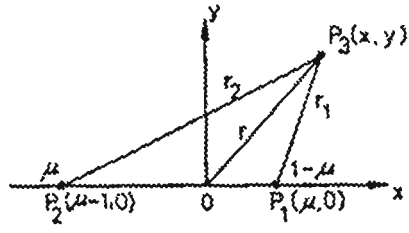

Fig. 1. Notations of the problem.

Equations (1) possess the well known Jacobian integral

$$\dot{x}^2 + \dot{y}^2 = 2\Omega - C, \tag{3}$$

where C is the Jacobian constant.

Equations (1) become singular at collisions of the third body with the primaries when $r_1 = 0$ or $r_2 = 0$. However, these singularities are not of essential character and can be removed by regularizing transformations. An extended summary on the problems and methods of regularization can be found in Hagihara (1975) and in Szebehely (1967).

The regularizing transformations are conveniently written in complex variables. Introducing $z = x + iy$ $(i = \sqrt{-1})$, Equations (1) can be written as

$$\ddot{z} + 2i\dot{z} = \mathrm{grad}_z \Omega, \tag{4}$$

where

$$\mathrm{grad}_z \Omega = \frac{\partial \Omega}{\partial x} + i\frac{\partial \Omega}{\partial y}.$$

By making use of the transformations

$$z = f(w), \tag{5}$$

$$\frac{dt}{d\tau} = \left|\frac{df}{dw}\right|^2, \tag{6}$$

where $w = u + iv$, Equation (4) can be transformed into (Szebehely, 1967)

$$w'' + 2i\left|\frac{df}{dw}\right|^2 w' = \mathrm{grad}_w \Omega^*. \tag{7}$$

Here the prime means differentiation with respect to the new time variable τ and

$$\Omega^* = \left|\frac{df}{dw}\right|^2 \left(\Omega - \frac{C}{2}\right), \tag{8}$$

where in Ω

$$r_1 = |z - \mu|, \quad r_2 = |z + 1 - \mu|.$$

Properly selecting the function $f(w)$, the critical terms $1/r_1$, $1/r_2$ of the potential Ω can be made regular and thus Equation (7) also will be regular.

The Jacobian integral for Equation (7) is

$$|w'|^2 = 2\Omega^*. \tag{9}$$

2. REGULARIZING TRANSFORMATIONS

Several regularizing transformations are known in the literature. The parabolic transformation

$$z = w^2, \tag{10}$$

introduced by Levi-Civita (1904), can regularize a singularity at the origin of the coordinate system. Thus, with a translation of the origin of the coordinate system to either one of the primaries, the collision singularities can be regularized. Accordingly,

$$z = \mu + w^2 \tag{11}$$

will regularize the singularity at P_1 and

$$z = \mu - 1 + w^2 \tag{12}$$

will do that for the singularity at P_2. These transformations are called local regularizations, since they can eliminate only one of the singularities.

There exist transformations which can remove the two singularities together. These are called global regularizing transformations (although in a mathematical sense they are local operations). It is convenient to write these transformations in a coordinate system in which the two primaries are located symmetrically with respect to the origin. The translation

$$q = z + \frac{1}{2} - \mu \tag{13}$$

shifts the origin into the midpoint of the primaries and they will be located at $q = \pm\frac{1}{2}$. Instead of Equation (4) we have

$$\ddot{q} + 2i\dot{q} = \mathrm{grad}_q \Omega \tag{14}$$

with Ω given by Equation (2), but

$$r_1 = \left|q - \frac{1}{2}\right|, \quad r_2 = \left|q + \frac{1}{2}\right|. \tag{15}$$

The transformations

$$q = f(w), \tag{16}$$

$$\frac{dt}{d\tau} = \left|\frac{df}{dw}\right|^2 \tag{6}$$

transform Equation (14) into Equation (7).

The Thiele-Burrau transformation, introduced by Thiele (1895) for $\mu = 0.5$ and generalized by Burrau (1906) for arbitrary μ, can be given as

$$q = \frac{1}{2}\cos w. \tag{17}$$

It is easy to see that in this case $|df/dw|^2 = r_1 r_2$, and thus in Equation (8) the two critical terms are regularized together.

Birkhoff's (1915) transformation can be expressed as

$$q = \frac{1}{4}\left(2w + \frac{1}{2w}\right). \tag{18}$$

In this case $|df/dw|^2 = r_1 r_2/|w|^2$. This expression eliminates the singularities at P_1 and P_2, but introduces a new singularity, $w = 0$, in the transformed plane. However, $w = 0$ corresponds to $q = \infty$ and thus all points of the finite physical plane are regularized by this transformation.

Birkhoff's transformation can be generalized to (Deprit and Broucke, 1963; Arenstorf, 1963)

$$q = \frac{1}{4}\left(w^2 + \frac{1}{w^2}\right). \tag{19}$$

This transformation is called Lemaître's transformation due to its relation to the regularization of the general problem of three bodies by Lemaître (1955). In this case $|df/dw|^2 = 4r_1 r_2/|w|^2$.

There exist other generalizations as well. Wintner (1930) generalized Birkhoff's transformation and in the 'midpoint' coordinate system this can be expressed as

$$q = \frac{1}{2}\frac{(w+\frac{1}{2})^{2n} + (w-\frac{1}{2})^{2n}}{(w+\frac{1}{2})^{2n} - (w-\frac{1}{2})^{2n}}, \tag{20}$$

where n is any positive integer.

Broucke (1965) generalized the Thiele-Burrau transformation to

$$q = \frac{1}{2}\cos nw, \tag{21}$$

and Birkhoff's regularization to

$$q = \frac{1}{4}\left(w^n + \frac{1}{w^n}\right), \tag{22}$$

where n is any nonzero real number.

The global regularizing transformations (17)-(22) can be expressed in the general form

$$q = f(w) = \frac{1}{4}\left[h(w) + \frac{1}{h(w)}\right], \tag{23}$$

where $h(w) = e^{iw}$, $2w$, w^2, and e^{inw}, w^n for the Thiele-Burrau, the Birkhoff, the Lemaître and the two Broucke transformations, respectively, while in the case of Wintner's transformation

$$h = \frac{(w+\frac{1}{2})^n + (w-\frac{1}{2})^n}{(w+\frac{1}{2})^n - (w-\frac{1}{2})^n}.$$

One may ask, why Equation (23) is the general form for the global regularization. Is not there any other form which together with the time transformation (6) results in regularization?

3. UNIQUENESS OF THE GENERAL FORM OF GLOBAL REGULARIZATION

To answer the above question we note that in order to eliminate the singularities at $r_1 = 0$ and $r_2 = 0$ we must have

$$\left|\frac{df}{dw}\right|^2 = \gamma(w)(r_1 r_2)^n. \tag{24}$$

Then forming the product $|df/dw|^2\Omega$, the terms $1/r_1$ and $1/r_2$ become regular. In Equation (24) the function $\gamma(w)$ must be regular at the singularities. As to the exponent n, it is necessary that $n = 1$, since $n > 1$ results in $\Omega^* = 0$ at the singularities, and from Equations (9) and (7) it follows that $w' = 0$, $w'' = 0$ at the singularities. That is, a steady-state solution is obtained in this case.

Thus the determining equation for the function $f(w)$ from Equations (24), (15), (16) is

$$\left|\frac{df}{dw}\right|^2 = \gamma(w)\left|f - \frac{1}{2}\right|\left|f + \frac{1}{2}\right|. \tag{25}$$

With $\gamma = |\alpha|^2$, this equation leads to

$$\frac{df}{dw} = \alpha\sqrt{f^2 - \frac{1}{4}}.$$

By integration we obtain

$$\ln(2f + \sqrt{4f^2 - 1}) = \beta,$$

where $\beta = \int \alpha\, dw$ and the arbitrary constant may be set zero. Solving for f, we obtain

$$f = \frac{1}{4}\left(e^{\beta} + \frac{1}{e^{\beta}}\right) \tag{26}$$

and with $\beta = \ln h(w)$,

$$f = \frac{1}{4}\left[h(w) + \frac{1}{h(w)}\right]. \tag{23}$$

Thus, Equation (23) represents the unique form for the global regularizing transformations when the time transformation is given by Equation (6).

It also follows that

$$\gamma = \left|\frac{d\beta}{dw}\right|^2 = \left|\frac{\frac{dh}{dw}}{h}\right|^2. \tag{27}$$

The simplest form of Equation (26) is obtained for $\beta = w$ or $\beta = iw$, in both cases $\gamma = 1$. Actually, $\beta = iw$ gives the Thiele-Burrau transformation, $f = \frac{1}{2}\cos w$, while $\beta = w$ results in $f = \frac{1}{2}\cosh w$. Both transformations, written explicitly in the coordinates, offer similar formalism using elliptic coordinates. A similar kind of transformation can be obtained with $h = e^{iw}/i$, which results in $f = \frac{1}{2}\sin w$, $\gamma = 1$. All these transformations can be generalized to $f = \frac{1}{2}\cos nw$ (Broucke, 1965), $f = \frac{1}{2}\cosh nw$, $f = \frac{1}{2}\sin nw$, $\gamma = n^2$, where n is any nonzero real number.

Considering Equation (23), it is natural to look for the simplest form of the function $h(w)$ and thus one may take a linear function $h(w) = aw + b$, with a, b arbitrary constants. Among these transformations the only one which leaves the primaries at their places is obtained for $a = 2$, $b = 0$, and this is Birkhoff's transformations.

Simple as it is but it seems so that Equation (25) is not written in the literature. The use of the type of Equation (25) appears in more general problems. For example, Giacaglia (1967) in order to regularize a four-body problem in which three primaries of arbitrary masses revolve in circular orbits around their center of mass in the equilateral equilibrium configuration and a body of infinitesimal mass moves in their field, studies the equation (changing somewhat his notations)

$$\left|\frac{df}{dw}\right|^2 = |g(w)|^2|f - f_1||f - f_2||f - f_3|.$$

Mavraganis (1988) for the global regularization of the magnetic-binary problem solves the equation

$$\left|\frac{df}{dw}\right|^2 = r_1^3 r_2^3 . |hbox$$

For other examples in the more general case see Hagihara (1975).

References

Arenstorf, R. F. : 1963, *Astron. J.* **68**, 548.
Birkhoff, G. D. : 1915, *Rend. Circolo Mat. Palermo*, **39**, 265.
Broucke, R. : 1965, *Icarus*, **4**, 8.
Burrau, C. : 1906, *Vierteljahrsschrift Astron. Ges.* **41**, 261.
Deprit, A. and Broucke, R. : 1963, *Icarus*, **2**, 207.

Giacaglia, G. E. O. : 1967, *Astron. J.*, **72**, 674.
Hagihara, Y. : 1975, *Celestial Mechanics, Vol IV, Part 1*, Japan Society for the Promotion of Science, Tokyo.
Lemaître, G. : 1955, in A. Beer, ed(s)., *Vistas in Astronomy*, Vol **1**, Pergamon Press, Oxford, p. 207.
Levi-Civita, T. : 1904, *Acta Mathematica*, **30**, 305.
Mavraganis, A. G. : 1988, *Celestial Mechanics*, **42**, 169.
Szebehely, V. : 1967, *Theory of Orbits*, Academic Press, New York and London.
Thiele, T. N. : 1895, *Astron. Nachr.* **138**, 1.
Wintner, A. : 1930, *Math. Z.* **32**, 675.

Publ. Obs. Astron. Belgrade No. 49 (1995), 159-162

INFLUENCE OF PHOTOSPHERIC PARAMETERS ON SOLAR SPECTRAL LINE PARAMETERS

S. ERKAPIĆ and I. VINCE
Astronomical Observatory, Volgina 7, 11050 Belgrade, Yugoslavia

Abstract. Spectral line profiles for 31 solar spectral line from the Belgrade observational program have been synthesized previously. We gave a short review on the sensitivity of those spectral lines examining the behaviour of some line profile parameters (equivalent width, central residual flux, full-half width) induced by independent variations of temperature, gas pressure and electron density gradient in the atmosphere model. The results displayed as gradients of line profile parameters have shown high sensitivity of spectral lines to the temperature and a negligible sensitivity to the pressure and electron density change.

1. INTRODUCTION

A long-term observational program of 31 selected solar spectral line profiles has been carried out at Belgrade Observatory since 1987 (Vince *et al.*,1988). The so far obtained results have shown that long-term changes of spectral lines are present and related probably to solar activity (Skuljan *et al.*, 1992). In several previous papers (Erkapić and Vince, 1993a, 1993b, 1994) we examined theoretically the influence of photospheric physical parameters on the spectral line profiles from our observational program. In this paper we present the averaged results in comparative form.

2. METHOD OF CALCULATIONS

Our analysis is based on the synthetic spectral line profiles referring to integrated solar flux radiation obtained with OSLO-HARVARD model of solar atmosphere (Maltby *et al.*, 1986) under the assumption of LTE.

By independent variations of temperature, gas pressure and electron density gradient in the atmosphere model up to $\check{a} = \pm 5\%$ we calculated relative changes of different line profile parameters. Parameters were normalized to their unchanged model values. Among all parameters equivalent width, central residual flux and full-half width were of main interest. Three spectral lines were excluded from further analysis for all photospheric parameters and the CrI 529.83 line for temperature changes because the non-LTE affects them prominently.

3. RESULTS AND DISCUSSION

In Table I we give the results of our calculations as gradients of equivalent width, central residual flux and full-half width ($\delta EW_n/\delta\check{a}$, $\delta F_{cn}/\delta\check{a}$, $\delta FW_n/\delta\check{a}$) for the positive change of temperature, gas pressure and electron density gradient (T, P_g, N_e). In the case of negative change of photospheric parameters we have the opposite behaviour.

TABLE I

Gradients of equivalent width, central residual flux and full-half width of the synthesized line profiles for the change of temperature, gas pressure and electron density gradient in the OH model

	$\delta EQ_n/\delta\check{a}$ (10^{-3}/ %)			$\delta F_{cn}/\delta\check{a}$ (10^{-3}/ %)			$\delta FW_n/\delta\check{a}$ (10^{-3}/ %)		
λ (nm)	T	P_g	N_e	T	P_g	N_e	T	P_g	N_e
CaI 526.17	-22.98	-0.61	-0.93	21.46	2.71	2.34	-10.87	0.38	0.19
CaI 558.20	-22.39	-0.73	-1.10	18.91	2.63	2.31	-10.43	0.35	0.13
CaI 560.13	-22.23	-0.73	-1.12	18.62	2.64	2.33	-10.38	0.34	0.12
CrI 529.67	-31.55	-0.10	-0.62	25.51	3.18	2.86	-16.76	0.51	0.28
CrI 529.74	-30.08	-0.49	-0.44	23.82	2.36	2.05	-12.48	0.41	0.36
CrI 529.80	-31.56	-0.49	-0.40	25.78	2.02	1.72	-12.21	0.45	0.41
CrI 529.83	–	0.08	-0.63	–	3.57	3.24	–	0.55	0.24
FeI 519.79	-37.81	0.31	0.08	23.16	0.13	0.13	-5.60	0.29	0.17
FeI 519.87	-28.14	0.34	-0.79	14.54	3.89	3.68	-15.27	0.58	0.08
FeI 525.02	-38.70	-0.25	-0.39	45.03	1.78	1.74	-18.07	0.57	0.47
FeI 527.32	-29.17	1.08	-0.81	10.11	3.98	3.79	-14.72	0.85	-0.07
FeI 527.34	-24.45	-0.21	-0.94	18.53	3.33	3.18	-12.72	0.37	0.06
FeI 530.74	-32.49	-0.33	-0.63	33.64	2.00	1.96	-14.63	0.50	0.34
FeI 539.83	-20.18	-0.49	-1.16	13.93	2.46	2.40	-8.29	0.35	0.03
FeI 557.61	-26.73	0.71	-1.05	10.09	3.56	3.44	-12.85	0.70	-0.14
MnI 539.47	-101.33	2.32	2.27	51.50	-1.14	-1.14	-8.92	0.30	0.28
MnI 543.25	-120.92	3.08	2.99	43.12	-1.10	-1.08	-8.92	0.30	0.28
NaI 538.26	-25.52	-1.10	-0.61	17.37	2.41	2.08	-8.77	0.35	0.40
NaI 568.82	-24.20	-1.09	-0.61	15.25	2.85	2.51	-9.52	0.45	0.25
NiI 519.72	-43.78	1.43	0.54	14.10	-0.41	-0.19	-2.43	0.11	0.01
CI 538.03	105.31	-5.31	-10.55	-19.99	0.99	1.97	11.65	-0.63	-1.24
CrII 523.73	39.43	-1.71	-5.66	-24.00	0.13	3.48	8.68	-0.17	-1.10
CrII 530.59	55.54	-0.66	-7.07	-14.74	0.14	1.84	4.24	-0.20	-0.63
FeII 519.76	20.36	-2.64	-4.77	-7.89	5.91	4.85	13.97	0.24	-1.58
FeII 542.53	30.03	-2.02	-5.01	-23.56	2.31	4.21	10.24	0.19	-1.34
ScII 523.98	15.16	-0.11	-4.40	-9.78	0.33	3.19	4.38	0.22	-0.75
ScII 552.68	12.95	-1.38	-3.92	-9.72	3.06	4.24	7.23	0.21	-1.34
TiII 533.68	11.96	-1.17	-3.79	-9.61	2.63	4.22	6.33	0.22	-1.14

Our calculations were done for positive and negative change of photospheric gradients separately. The obtained values of normalized line profile parameters and appropriate gradients show behaviour that is not quite linear. Here we neglect that fact and Table uppercase i contains gradients averaged over positive and negative changes of

photospheric parameters. The behavior of line profile parameters remain unchanged.

Spectral lines are most sensitive to the temperature changes with equivalent width as the most sensitive parameter. The full-half width is the least sensitive parameter for almost all spectral lines. Compared to that the sensitivity of these lines to the pressure and electron density changes is negligible with central residual flux as the most sensitive parameter for almost all lines. (Gradient value $\delta A_n/\delta\check{a} = 0.001/\%$ is equal to the change of 0.1% of the line profile parameter A_n).

According to the general behavior of the line parameters with the change of temperature, we can divide our spectral lines into two groups. First group, consisted of all single-ionized atom lines and the CI 538.03 neutral atom line, have increasing EW_n and FW_n and decreasing F_{cn} with positive change of temperature gradient. The rest of neutral atom lines belong to the second group that shows the opposite behaviour. This can be explained on the basis of simplified line formation theory (Gray, 1976), according to which the gradient of equivalent width depends on excitation energy of the transition lower level for the first group of lines and on the difference of excitation and ionization energy for the second group.

The change of central residual flux hides in itself mixed behaviour of continuum and central absolute flux. Continuum flux has approximately the same gradient value over the whole wavelength ($\lambda\lambda 519 - -569$nm) interval slightly decreasing with increasing wavelength for positive temperature change. Continuum flux gradient is greater than central absolute flux gradient for the first group of lines and less for the second group of lines. Low value of $\delta F_{cn}/\delta\check{a}$ always implies that continuum and central absolute flux gradients have similar values. Great value of $\delta F_{cn}/\delta\check{a}$ implies great difference between continuum and central absolute flux gradient. In the second group of lines the main reason for decreasing intensity with increasing temperature is ionization of absorbing atoms, and in the first the increase in the hydrogen ionization.

Among all spectral lines the most sensitive are two manganese lines and the CI 538.03 line. The neutral carbon line shows high sensitivity to the temperature change because it has the highest lower level excitation energy ($E_l = 7.68eV$). Also it is formed deep in the photosphere (almost coincident with the continuum), where temperature gradient is relatively high. Two manganese lines owe their high sensitivity to the large difference of excitation and ionization energy ($E_l - E_i = 7.44eV$).

In the case of pressure and electron density changes most of the spectral lines have negligible sensitivity, but the prevailing behaviour is decreasing equivalent width with positive change of pressure and electron density. This can be explained also according to the same simplified theory of Gray, that claims that all single-ionized and neutral atom lines from the elements, that are mainly in that same stage of ionization in the solar atmosphere, decrease in intensity with positive change of pressure gradient and electron density gradient. This is mainly due to increasing opacity in continuum flux. This is valid for our single-ionized spectral lines and the CI 538.03 line. According to the same theory all neutral lines from the elements that are mainly ionized in the solar atmosphere should be insensitive to the pressure (gas and electron) change. Judging from the values of gradient of line profile parameters in Table I this is also true for most of our neutral lines. However, there are several number of exceptions.

Two manganese lines and nickel line have significant positive changes of EW_n with

increasing pressure and electron density of the magnitude similar to that of single-ionized atom lines. These three lines represent the only cases where the continuum flux gradient is less than central absolute flux gradient. The same remarks concerning relation of continuum and central absolute flux gradient with temperature change are valid here also.

Clear graphical dependence between behaviour of line profile parameters and atomic parameters can be seen only for temperature changes between the gradients of EW_n and the excitation energy of the lower level in the transition : the higher the excitation level, the larger the $\delta EW_n/\delta\check{a}$. Every other combination of line profile parameter gradient and other atomic parameters (ionization energy, effective principal quantum number, $\log g_l f_{lu}$ *etc.*) shows spreading of data and inconclusive picture. This means that all atomic parameters are working simultaneously.

References

Erkapić, S. and Vince, I. : 1993a, *Publ. Astron. Obs. Belgrade*, **47**, 80.

Erkapić, S. and Vince, I. : 1993b, *Proc. 16th Symposium on the Physics of Ionized Gases, Book of Contributed Papers*, ed. M.Milosavljević, Inst. Nucl. Sci. "Vinča" and Inst. "Braća Karić", Belgrade, Yugoslavia, 369.

Erkapić, S. and Vince, I. : 1994, *Proc. 17th Symposium on the Physics of Ionized Gases, Book of Contributed Papers*, eds. B. Marinković and Z. Petrović, Inst. Phys., Belgrade, Yugoslavia, 326.

Gray, D. : 1976, *The Observation and Analysis of Stellar Photospheres*, Wiley, New York, Sydney, Toronto.

Maltby, P., Avrett, E. H., Carlsson, M., Kjeldseth Moe, O., Kurucz, R. L., Loeser, R. : 1986, *Ap. J.* **306**, 284.

Skuljan, J., Karabin, M., Vince, I., Kubičela, A. : 1992, *Bull. Astron. Belgrade*, **145**, 1.

Vince, I., Kubičela, A., Arsenijević, J. : 1988, *Bull. Astron. Belgrade*, **139**, 25.

Publ. Obs. Astron. Belgrade No. 49 (1995), 163-166

Mg II h AND k LINES IN THE GHRS SPECTRA OF α Ori

D. JEVREMOVIĆ and I. VINCE
Astronomical observatory, Volgina 7, 11050 Belgrade, Yugoslavia
E-mail darko@aob.aob.bg.ac.yu
E-mail ivince@aob.aob.bg.ac.yu

Abstract. We dearchived the echelle spectrum of α Ori from HST archive and compared it with prediction of BLE model of chromosphere.

1. INTRODUCTION

The resonance doublet of singly ionized Mg, occurring at 2795.5 Å (k) and 2802.7Å (h) frequently displays emission cores in stars later than F spectral type. Mg II h and k lines are much better diagnostics of the physical properties in the stellar chromospheres than usually used Ca II H and K lines, because of the larger abundance and higher ionization potential of magnesium.

The noncoronal supergiant α Ori (Betelgeuse, HD 39801, M2Iab) is one of the most studied late type star. Copernicus observations of MgII h and k lines in the spectrum of the α Ori were analyzed by Bernat and Lambert (1976), and IUE observations by Basri and Linsky (1979), Dupree et al. (1984).

This paper is our first attempt of using HST data and multi-level radiative transfer code known as MULTI.

2. OBSERVATIONS AND REDUCTIONS

We dearchived the echelle spectrum taken with Goddard High Resolution Spectrograph on April 27, 1991 within GTO program No.1195. Duration of four expositions was 656 seconds in the accumulation mode with the small scientific aperture. Observations covered wavelengths between 2790.74 and 2805.72 Å in the twentieth order of ECH-B. Spectra were processed with standard procedures by STScI software except for the vacuum-to-air corrections to the wavelengths, which we applied according to :

$$\lambda_{air} = \lambda_{vac}/f(\lambda_{vac}),$$

where

$$f(\lambda) = 1.0 + 2.735182 \times 10^{-4} + 131.4182/\lambda^2 + 2.76249 \times 10^8/\lambda^4 \ .$$

We also rescaled fluxes to stellar surface using equations (2) and (3) from Jevremović and Vince (1994).

3. MODEL CHROMOSPHERE, ATOMIC DATA AND LINE FORMATION CODE

There are two published models of chromosphere of α Ori : Basri et al. (1981;BLE) and Hartmann and Avrett (1984). The first model was constructed by fitting Mg II k, CaII K and H profiles and CII $\lambda\lambda$ 1334, 1335 resonance lines fluxes assuming hydrostatic equilibrium which results plannar geometry. The second model tried to explain chromospheric extent and formation of Alfven wave driven stellar wind. In our calculations we used the first, BLE model, because our version of MULTI maintains only plannar geometry and problems with output fluxes described in Hartmann and Avrett's paper.

The model chromosphere was interpolated in the logarithm of the mass column density on to a depth grid of 80 points to ensure good convergence properties. Since the model chromospheres are essentially linear relationships between temperature and logarithm of mass column density, the interpolation procedure should not introduce any significant errors.

For the calculation of Mg II h and k lines we used 6 level + continuum model of atom. The energy levels and oscillator strengths we used were taken from Black et al. (1971) and the collisional rates from Mendoza (1981). In Table I :re presented atomic data for magnesium that are used in our calculations.

TABLE I
Atomic data for magnesium

Level	Energy (cm^{-1})	Statistical weight g
1	0.0	2
2	35669.5	2
3	35761.0	4
4	69805.4	2
5	71489.5	6
6	71490.3	4
cont.	121267.4	1

The computations were carried out using a multi-level non-LTE radiative transfer program known as MULTI (Carlson 1986, Carlson 1991). We used version 2.0 dearchived from CCP7 Computer Program Library. The line radiation intensities were calculated under the assumption of complete redistribution.

Background opacities are calculated using opacity package from LINEAR (Auer et al. 1972)

4. RESULTS

In Fig. 1. is presented the HST spectrum of α Ori. However the Mg II h and k lines are contaminated by clearly visible MnI and FeI absorption features. Fig. 2. presents results of our calculation for Mg II h and k line formation. We can conclude that the BLE model does not describe well the chromosphere of α Ori and an improvement of the BLE model is necessary.

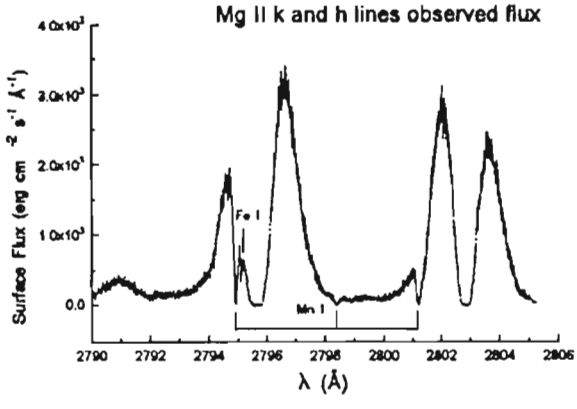

Fig. 1. The HST spectrum of α Ori

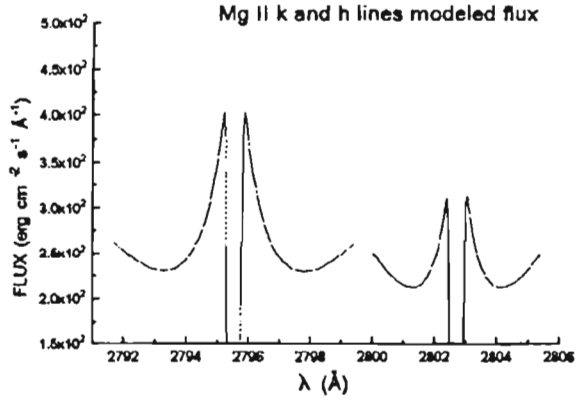

Fig. 2. Results of our calculation for Mg II h and k line formation

References

Auer, L. H., Heasley, J. N. and Milkey, R. W. : 1972, *Kitt Peak National Observatory, Contribution*, **555**.
Basri, G. S. and Linsky, J. L. : 1979, *Astrophys. J.* **234**, 1023.
Basri, G. S., Linsky, J. L., Eriksson, K. : 1981, *Astrophys. J.* **251**, 16?.
Black, J. H., Weisheit, J. C., and Laviana, E. : 1972, *Astrophys. J.*, **177**, 567.
Bernat, A. P. and Lambert, D. L. : 1976, *Astrophys. J.* **204**, 830.
Carlsson, M. : 1986, *A Computer Program for Solving Multi-Level Non-LTE Radiative Transfer Problems in Moving or Static Atmosphere*, Uppsala Astronomical Observatory Report No.33.
Carlson, M. : 1991, in *Stellar Atmospheres : Beyond Classical Models*, eds. Crivellari L., Hubeny I. and Hummer D. G., p.39.
Dupree, A., Sonneborn, G., Baliunas S. L., Guinan, E. F., Hartmann, L. and Hayes, D. P. : 1984, in *The Future Ultraviolet Astronomy based on Six Years of IUE Research*, **NASA SP-2349**, 462 **251**, 162.
Hartmann Avrett, E. G. : 1984, *Astrophys. J.*,**284**, 238.
Jevremović, D. and Vince I. : 1994, *Bul. Astron. Belgrade*, 150, 41.
Mendoza, C. : 1981, *J. Phys. B.*, **14**, 2465.

Publ. Obs. Astron. Belgrade No. 49 (1995), 167-169

FACULAE AREAS AND DANUBE RIVER FLOW. I

B. D. JOVANOVIĆ
Faculty of Agriculture, Waterarranging Institute,
Trg Dositeja Obradovića 8, 21000 Novi Sad, Yugoslavia

Abstract. The spectral decomposition theorem has been applied for searching the solar activity influence on Danube river flow at a station. According to cross-correlations a seven-year lag has been found between solar faculae areas and maximal river flow, as well as a nine-year lag for minimal river flow. Chi square test has been applied for the obtained results signification.

1. ORIGINS

Agriculture, several branches of industry and economics, as well as water resources investigations are interested in river flow fluctuations. Therefore it is of profound interest to know, to predict, the surplus or lack of water. For the time being we are still unable to influence the whole situation with our scientific tools and to change it according to our needs. So, we observe carefully the whole process, and use mathematics for predicting floods and droughts in riverbeds.

One suspects that solar activity effects many phenomena on Earth. For that reason we chose in this paper faculae areas as river flow fluctuations producers, after using previously total sunspot areas (Jovanović, 1986, 1987, 1989, 1990, 1991a, 1991b, 1993a, 1993b, 1993c, 1994a), sunspot umbrae areas (Jovanović, 1994b).

2. DATA AND DATA PROCESSING METHODS

The TOTAL FACULAE AREA on the visible solar hemisphere, corrected for sphericity, has been chosen as the solar activity parameter.

According to Jean-Claude Pecker the use of many stations together, may distort the results instead to ameliorate the eventually existing correlation between Sun activity and water flow in Danube river for example. Therefore we chose only one station and the maximal and minimal river flow series obtained by day by day observations.

The following data notations are used : time series for SOLAR ACTIVITY (yearly means) (GRFS–total areas of faculae, expressed in millionth parts of the visible solar hemisphere, published in Royal Greenwich Observatory); time series for DANUBE RIVER FLOW (yearly means) (BOQV–maximal river flow expressed in m^3/sec, BOQN–minimal river flow expressed in m^3/sec).

We had at our disposal GRFS series starting from the year 1874 until 1982 (daily observations), and river flow series since 1931 to 1990 (monthly means).

Because of the computer processing program we took the faculae areas between 1923 and 1982, and the river flow data between 1931 and 1990.

Supposing that we have to do with two stationary time series, x_t and y_t, and that we wish to assess the extent to which we can use the past x_t to predict y_t, cross-correlations are used as a criterion of evaluation. If the processes are zero-mean, we define then, by means of cross- correlations, the expected value of y_t.

Following the SPECTRAL DECOMPOSITION THEOREM, which states that the energy, or variance, of any time series can be broken down into the contribution of statistically independent oscillations of different frequencies (periods), we constructed periodograms for the series mentioned before. Each peak in the spectral periodicity function stands for a harmonic. The most outstanding one stands for the *major frequency (period)*, and the next ones for *higher harmonics*, the so-called *overtones*.

For some practical reasons we took 40 years long time series sections and looked for the highest cross-correlation values, due to solar influence, to maximal and minimal river flow.

The next step was the construction of corresponding periodograms for GRFS, BOQV and BOQN series.

The search for paired up independent oscillations with the same frequencies (periods) was the following step in our analysis.

In conclusion Fourier series residuals have been calculated. A comparison of such a frequency histogram with normal distribution function has been carried out. Finally the Chi-square test has been applied to all cases.

3. RESULTS

Let us discuss, first, the results for *maximal river flow*. The greatest cross-correlation value stands for zero year lag. Time series used were GRFS4180 and BOQV4887, so we conclude that *maximal river flow will follow, after seven-year lag, the faculae maximum*. The periodogram for GRFS shows that there are ten independent oscillations. Eight of them have their responses in eight of ten independent frequencies in the series for maximal flow, BOQV. The second overtone of the BOQV series corresponds to the major frequency of the first series. The fourth overtone of the GRFS has its pair in the eighth, the third in the fourth, the fifth in the major frequency, the sixth in the seventh, the seventh in the fifth, the ninth in the first overtone, and the eighth overtone of GRFS series in the ninth overtone of the BOQV series.

The major frequency of GRFS has the period of 12.000 years, the first overtone of 30.003 years, the second of 5.999 years, the third of 4.286 years, the fourth of 5.000 years, the fifth of 3.749 years, the sixth of 3.3 years, the seventh of 2.609 years, the eighth of 2.069 years and the ninth of 2.507 years. The oscillations are placed according to their contribution to the compounded function.

The major frequency of BOQV has the period of 3.749 years, the first overtone of 2.308 years, the second of 12.000 years, the third of 5.998 years, the fourth of 4.286 years, the fifth of 2.609 years, the sixth of 6.667 years, the seventh of 3.333 years, the eighth of 5.000 years, and the ninth overtone of 2.069 years.

The Chi-square test for BOQV's eight of ten independent frequencies gives the value of 0.998804 with one degree of freedom and a significance level of 0.3176.

Minimal river flow shows another picture of influence. According to cross-correlation tables *minimal river flow follows, after a lag of nine years, the maximal faculae area.*

According to the periodogram for BOQN series there are thirteen peaks to which correspond thirteen independent frequencies. The major one has a period of 59.988 years, the first overtone of 7.501 years, the second of 5 years, the third of 2.399 years, the fourth of 2.609 years, the fifth of 3.333 years, the sixth of 3.500 years, the seventh of 3.749 years, the eighth of 4.286 years, the ninth of 12.000 years, the tenth of 3.000 years, the eleventh of 2.069 years and the twelfth overtone of 5.999 years.

The ninth overtone of the BOQN series corresponds to the major frequency of the GRFS series, the twelfth to the second overtone, the second to the fourth, the eighth to the third, the seventh to the fifth, the fifth to the sixth, the fourth to the seventh, and the eleventh overtone of the BOQN series to the ninth overtone of the GRFS series.

Chi-square test for eight of thirteen independent frequencies of BOQN series gives the value 0.359449 with one degree of freedom and a significance level of 0.548812.

4. CONCLUSION

The spectral decomposition theorem, according to cross-correlations and periodograms, calculated for the index of solar activity known as the TOTAL FACULAE AREA on the visible solar hemisphere, corrected for sphericity, expressed in millionth parts of the visible solar hemisphere, GRFS, on one hand, and MAXIMAL, BOQV series, as well as MINIMAL DANUBE RIVER FLOW, BOQN series, expressed in m^3/sec, observed for a station, on the other, gives us the right to announce that the solar activity may influence, with the accuracy given, the maximal river flow, with a seven-year lag, and the minimal river flow after a lag of nine years.

References

Jovanović, B. D. : 1986, *Bull. Obs. Astron. Belgrade*, **136**, 73.
Jovanović, B. D. : 1987, *Bull. Appl. Math. Budapest*, **49**, No. 528-555, 39.
Jovanović, B. D. : 1989, *Bull. Appl. Math. Budapest*, **51**, No. 621, 47.
Jovanović, B. D. : 1990, *Bull. Appl. Math. Budapest*, **55**, No. 694, 1.
Jovanović, B. D. : 1991a, *Bull. Appl. Math. Budapest*, **60**, No. 772, 281.
Jovanović, B. D. : 1991b, *Bull. Appl. Math. Budapest*, **60**, No. 766, 199.
Jovanović, B. D. : 1991c, *Bull. Appl. Math. Budapest*, **64**, No. 841, 67.
Jovanović, B. D. : 1993a, *Publ. Obs. Astron. Belgrade*, **44**, 128.
Jovanović, B. D. : 1993b, *Bull. Appl. Math. Budapest*, **68**, No. 903, 47.
Jovanović, B. D. : 1993c, *Bull. Appl. Math. Budapest*, **66**, No. 870, 87.
Jovanović, B. D. : 1994a, *Bull. Appl. Math. Budapest*, **71**, No. 967, 73.
Jovanović, B. D. : 1994b, in *Uredjenje, korišćenje i zaštita voda Vojvodine*, Novi Sad, 17.
Pecker, J. C. : 1987, in *Compendium in Astronomy*, ed. D. Reidel, Dordrecht, 156.
Royal Greenwich Observatory, Daily Sunspot Areas, National Geophysical Data Center, Boulder, Colorado, USA.

Publ. Obs. Astron. Belgrade No. 49 (1995), 171-174

THE IMPORTANCE OF RADIATIVE $He^+(1s) + He(1s^2)$ PROCESSES FOR THE DB WHITE DWARF ATMOSPHERE EM-CONTINUOUS SPECTRA

A. A. MIHAJLOV[1,2], M. S. DIMITRIJEVIĆ[2], LJ. M. IGNJATOVIĆ[1] and Z. DJURIĆ[1]
[1]*Institute of Physics, P.O.Box 57, 11001 Belgrade, Yugoslavia*
[2]*Astronomical Observatory, Volgina 7, 11050 Belgrade, Yugoslavia*
E-mail EAOP021@YUBGSS21.BG.AC.yu

Abstract. The influence of the processes of radiative charge transfer and photoassociation during $He^+ + He$ collisional processes, as well as the process of the photodissociation of He_2^+ molecular ion, on the formation of continuous spectrum of the DB white dwarf atmospheres with $T_{eff} = 12000 - 20000$ K, for $\log g$ (gravity) $= 8$, is studied within the wavelength range $\lambda = 200 - 600$ nm. It is shown that the contribution of these processes relative to other relevant radiative processes is particularly important for $T_{eff} \leq 16000$ K, and increases with the decrease of T_{eff}. Moreover, it is found that the influence of the considered $He^+ + He$ radiative processes is particularly pronounced in the ultra violet range.

1. INTRODUCTION

Radiative $He^+(1s) + He(1s^2)$ processes may be of importance for continuous spectra of helium-rich star low temperature atmospheric layers (see e.g. Mihajlov and Dimitrijević 1992 and Stancil 1994). Here will be considered within DB white dwarf atmospheres, the ion-atom processes of photoassociation and photodissociation

$$He^+(1s) + He(1s^2) \Longleftrightarrow \epsilon_\lambda + He_2^+, \qquad (1a)$$

as well as the processes of the photoemission and photoabsorption charge exchange

$$He^+(1s) + He(1s^2) \Longleftrightarrow \epsilon_\lambda + \begin{cases} He^+(1s) + He(1s^2) \\ He(1s^2) + He^+(1s) \end{cases} \qquad (1b)$$

where $He_2^+ = He_2^+(1\Sigma_u^+)$, and ϵ_λ is the energy of photon with the wavelength λ. These processes will be considered here within the semiclassical approach (Mihajlov and Popović 1981; Mihajlov and Dimitrijević 1986, 1992). Our objective here is to estimate the importance of the ion-atom processes of photoassociation and photodissociation (1a) and, photoemission and photoabsorption charge exchange (1b) in comparison with the processes of emission and absorption connected with the free-free transitions of an electron in the field of atoms and atomic ions, as well as the processes

of electron - ion photorecombination and photoionization of excited atoms (*i.e.* the relevant electron - atom and electron - ion processes), in order to clarify the nature of DB white dwarf photosphere continuous spectrum for different λ and T ranges. Such results may be of significance for DB white dwarf photosphere modelling.

2. RESULTS AND DISCUSSION

All details of calculations will be given in Mihajlov *et al.* (1995). We will note here only that the present calculations are performed by using the DB white dwarf atmospheric structures of Koester, 1980.

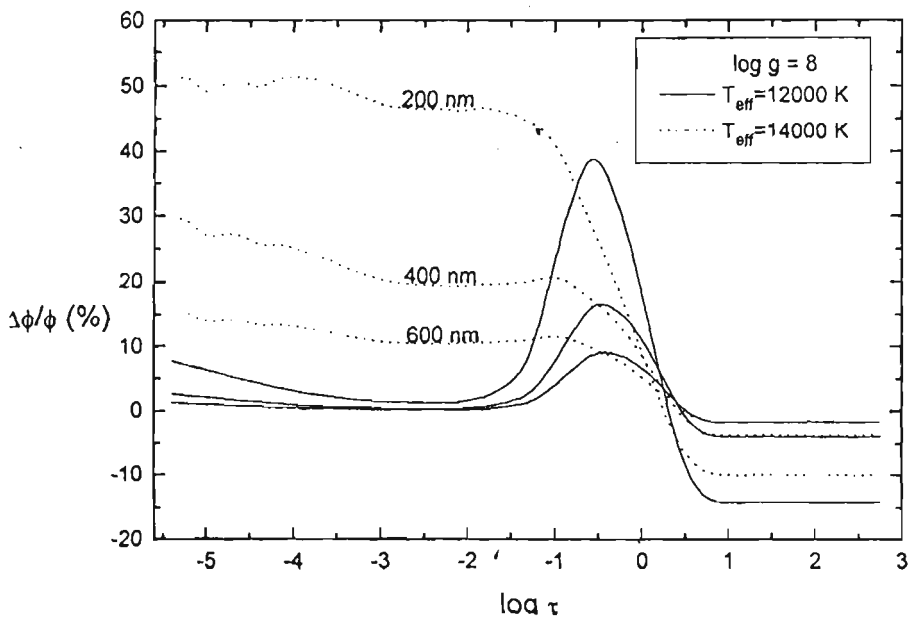

Fig. 1. Behaviour of the ratio $\Delta\Phi/\Phi$ as a function of Rosseland optical depth logarithm.

The influence of the ion - atom radiative processes (1) on the optical characteristics of the considered atmospheric layers we will illustrate here with the relative changes of the optical depth $\Delta\tau(\lambda,\tau)/\tau = [\tau'(\lambda,\tau) - \tau]/\tau$, and the emergent radiation intensity calculated for radial rays (see e.g. Mihalas 1978) $\Delta\Phi(\lambda,\tau)/\Phi(\lambda,\tau) = [\Phi'(\lambda,\tau) - \Phi(\lambda,\tau)]/\Phi(\lambda,\tau)$. Here, $\Phi'(\lambda,\tau)$ and $\Phi(\lambda,\tau)$ are emergent radiation intensities determined with and without ion-atom radiative processes (1a,b), and $\tau'(\lambda,\tau)$ is the optical depth determined with the ion-atom radiative processes (1a,b) included. In Figs. 1 and 2 the behavior of the ratios $\Delta\tau/\tau$ and $\Delta\Phi/\Phi$ as a function of τ, for $\lambda = 200$, 400 and 600 nm is demonstrated. Curves in these Figs. are for $T_{eff} = 12000$ and 14000 K, and $\log g = 8$. These curves show the quick increase of the ion-atom processes influence with the λ decrease, especially at the transition from the visible to the UV spectral range. Our calculations show as well, that the transition from

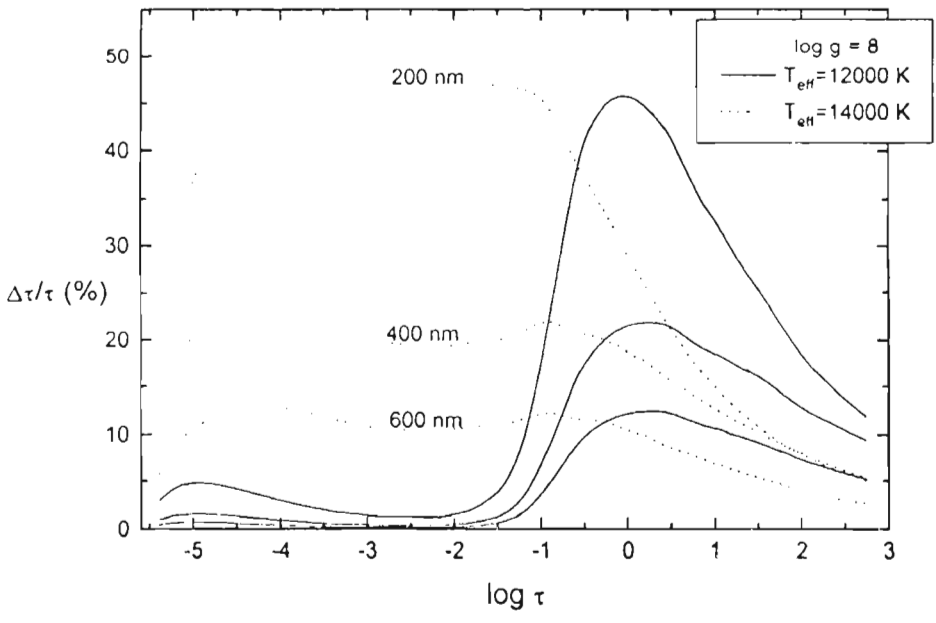

Fig. 2. Behaviour of the ratio $\Delta\tau/\tau$ as a function of Rosseland optical depth logarithm.

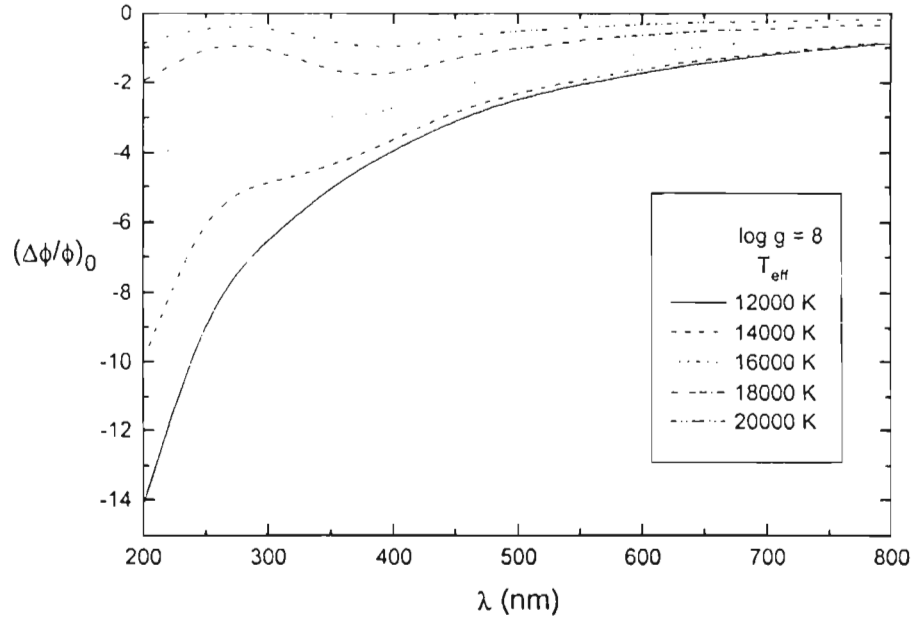

Fig. 3. Behaviour of the ratio $(\Delta\Phi/\Phi)_o = \Delta\Phi/\Phi$ for $\log\tau = 0$ as a function of λ.

$\log g = 8$ on $\log g = 7$ is not connected with considerable changes of $\Delta\tau/\tau$ and $\Delta\Phi/\Phi$. It has been found namely, that these changes are not larger than several percents in the largest part of the considered τ range (only for particular layers these changes approach to 20%).

The influence of the considered ion-atom radiative processes (1a,b) on the optical characteristics of the atmosphere as the whole might be illustrated by the quantity $\Delta\Phi/\Phi$, determined for $\log\tau = 0$, characterizing the whole outer layer with the optical depth $\tau = 1$. Namely, we found numerically that the further increase of the layer depth, does not change the $\Delta\Phi/\Phi$ value, which is shown as well in Fig. 2. The quantity $\Delta\Phi/\Phi$ for $\log\tau = 0$, denoted as $(\Delta\Phi/\Phi)_o$, is shown in Fig. 3 as a function of λ within 200 nm $\leq \lambda \leq$ 800 nm range, for $12000K \leq T_{eff} \leq 20000K$ and $\log g = 8$. One can see that the relative intensity change is negative and changes up to -14 percents. This denotes that in the contribution of the ion - atom radiative processes (1a,b) the influence of the absorption channels dominates. This change is not negligible and in order to have the real picture on the ion-atom radiative processes influence one must take into account that the final $(\Delta\Phi/\Phi)_o$ values characterize in the same time the influence of the absorption channel which decreases this value, and the emission channel which leads to its increase. In Fig. 1 is shown that changes of the optical depth, $\Delta\tau$ represent the significant disturbance of the reference τ greed for the tabular presentation of the white dwarf model and not a small perturbation. One can see in Fig. 2 as well that $\Delta\Phi$ is a strong perturbation for energetic balance considerations. Consequently, the ion-atom radiative processes (1) must be taken into account during the white dwarf atmosphere modelling and not added *a posteriori* as a correction to the result obtained by using the model when such processes have been neglected.

References

Koester, D. : 1980, *Astron. Astrophys. Suppl. Series*, **39**, 401.
Mihajlov, A. A. and Popović, M. M. : 1981, *Phys. Rev A*, **23**, 1679.
Mihajlov, A. A. and Dimitrijević, M. S. : 1986, *Astron. Astrophys.*, **155**, 319.
Mihajlov, A. A. and Dimitrijević, M. S. : 1992, *Astron. Astrophys.*, **256**, 305.
Mihajlov, A. A., Dimitrijević, M. S., Ignjatović, Lj. M., Djurić, Z. : 1995, *Astrophys. J.*, in press.
Mihalas, D. : 1978, *Stelar Atmospheres*, (Chap. 7.7), W. H. Freeman, San Francisco.
Stancil, P. C. : 1994, *Astrophys. J.*, in press.

Publ. Obs. Astron. Belgrade No. 49 (1995), 175-178

T-T PLOTS OF RADIO SPURS BETWEEN 38, 408 AND 1420 MHz

J. MILOGRADOV-TURIN
Department of Astronomy, Mathematical Faculty,
Studentski trg 16, p.b. 550, 11000 Beograd, Yugoslavia
E-mail epmfm21@yubgss21.bg.ac.yu

S. NIKOLIĆ
Petnica Science Center, p.b.40, 14000 Valjevo, Yugoslavia
E-mail enikolsi@ubbg.etf.bg.ac.yu

Abstract. The T-T plots of the North Polar Spur, the Spur in Aquarius, Taurus and Pegasus, using data at 38, 408 and 1420 MHz of the same resolution of $7^\circ.25 \times 8^\circ.25$, reduced to the case of scaled areas, are presented. The T-T graphs for all spurs have shown clear splitting of branches supporting the reality of quasihysteresis effect. It was shown that this splitting may have astronomical reasons. In an attempt to explain this effect earlier introduced 4V (four vector) model was applied.

1. INTRODUCTION

Since the first radio observations of the sky in the continuum were made several spurs have been noticed. It was found that many spurs can be joined into loops : e.g. the North Polar Spur (NPS) is part of Loop I, the Spur in Aquarius is a part of Loop II. Four major loops are generally recognized and are clearly seen in radio-continuum surveys. In addition, several further radio loop structures were proposed (Milogradov-Turin, 1970, 1972).

The plots of brightness temperature at one frequency against brightness temperature at the other frequency (T-T plots) can provide information about the spectrum of a spur (Turtle et al., 1962). Early T-T graphs were plotted for constant declinations, but later it was done at constant galactic latitudes (e.g. Berkhuijsen, 1971) as a more useful way to investigate Galactic objects. It was already shown by Berkhuijsen (1971) that the latitudinal T-T graphs of the NPS region at 240 and 820 MHz were divided into two branches : one outside the main ridge of the NPS and the other inside it. Such a fork - like structure is called also "quasihysteresis". She has found that the gap between them was real. According to the interpretation of Berkhuijsen (1971) the gap may be due to presence of a smooth extra component, which has a low spectral index and is related to an extended HII region in these lines of sight. The splitting of T-T graphs for frequencies between 10 and 408 MHz for the NPS and several other loops was found by Milogradov-Turin (1982) and shown not to be caused

by an HII region (Milogradov-Turin, 1982, 1987). She interpreted it as a presence of four components of radiation (Milogradov-Turin, 1982, 1985, 1987).

2. DATA

The data at 38 MHz were those from the 38 MHz survey of Milogradov-Turin and Smith (1973). Since the spur in Aquarius was laying in the region where comparatively high ionospheric absorption was present, correction for it was applied (Milogradov-Turin and Smith, 1973). The 408 MHz data were got from Haslam and Salter (1983), while the 1420 MHz data were received from Reich (1990), both convolved to the resolution of the 38 MHz survey of $7^\circ.25 \times 8^\circ.25$ by the authors.

3. T-T PLOTS

In this work T-T graphs were plotted along constant latitudes, every 4°, in regions of four observed spurs : NPS, the Spur in Aquarius, Taurus and Pegasus for all combinations of frequencies. An example is given on Figure 1.

On the majority of graphs the splitting was clearly found (Nikolić, 1994). In those cases when it was less clear, convincing explanations could be found (e.g. uncertain amount of ionospheric absorption, lower quality data etc.). Investigation has shown that sidelobes could not produce this feature (Nikolić, 1994).

4. DISCUSSION

As it was shown by Milogradov-Turin (1982) an inaccuracy in position of the main ridge of a spur could give a fork - like T-T graph. A study was done (Milogradov-Turin, 1982, Nikolić, 1994) showing that no clear dependence of the position of the main ridge of the NPS on frequency exists. This work has shown that the quasihysteresis is a real astronomical effect since it appears in all combinations of three used frequencies on the data corresponding to the scaled aerials measurements.

A possible explanation of the quasihysteresis effect was proposed by Milogradov-Turin (1982, 1985, 1987) by the 4V model. Its basic idea is that the radiation from a spur can be represented by a sum of four vectors. The first component is extragalactic by origin. It has a high spectral index. This component consists of the relict radiation and of the integrated emission from external galaxies (labeled as $\vec{e}$ on Figure 2). The second component, $\vec{d}$, is originating within the Galactic disk and therefore it is assumed to be constant for a given galactic latitude, within a region containing a spur. The spectral index of the disk radiation is less than the spectral index of the extragalactic component. The third component, $\vec{s}$, is related to the spur itself. It has a lower spectral index than the Galactic disc. The fourth component, $\vec{h}$, is originating in the region outside the main ridge of a spur and it has a high spectral index. It is almost isotropic in a layer next to a spur decreasing sharply towards the main ridge. Such a behaviour could be expected from a component originating in a shell of the SNR. An example how the sum of four vectors reproduces a quasihysteresis effect is given in Figure 2.

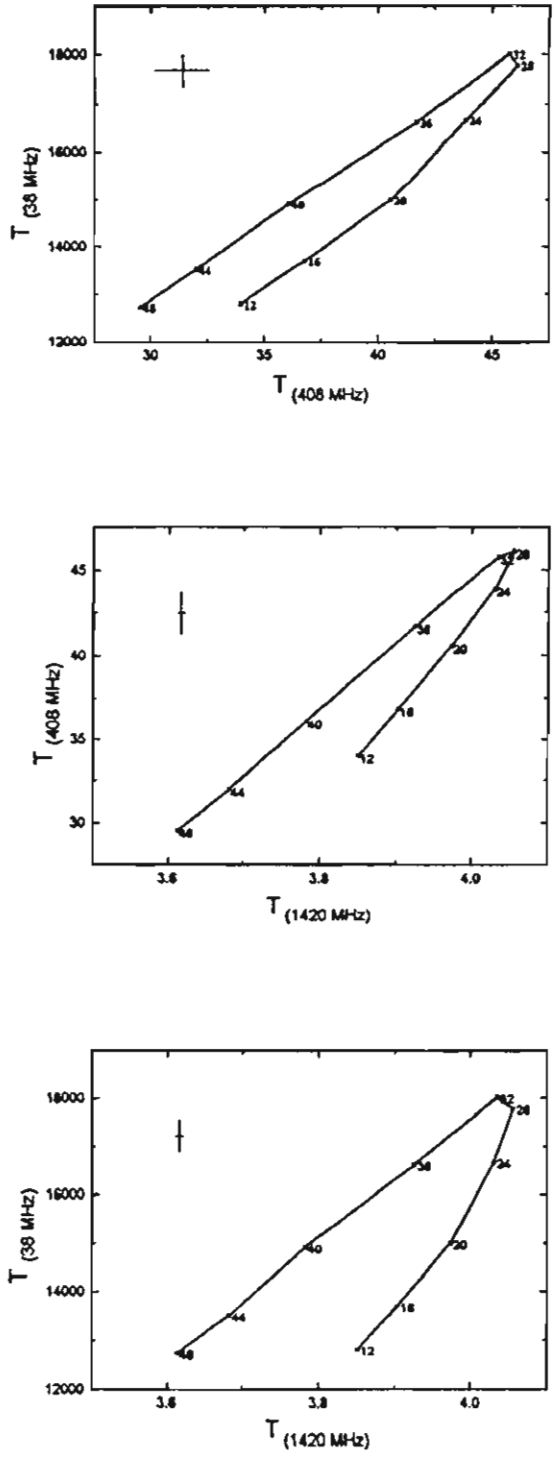

Fig. 1. T-T plots for the NPS on $b = 38°$, for all three combinations of frequencies with typical errors in the upper left corners.

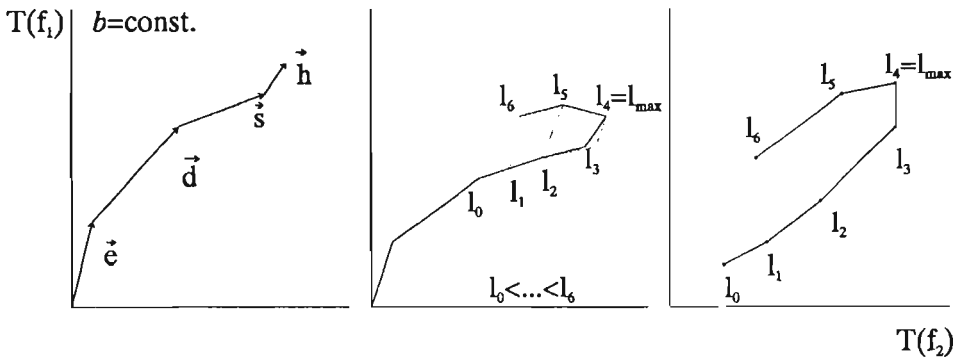

Fig.2. The construction of the T-T plots for a spur according to the 4V model

Fig. 2. The construction of the T-T plots for a spur according to the 4V model.

Existence of the quasihysteresis effect for all spurs has been interpreted by Milogradov-Turin (1982, 1985) as presence of a high spectral component outside the ridge in all spurs. This was named a "curvature rule" (Milogradov-Turin, 1985).

Acknowledgements

We are grateful to Drs. C. G. T. Haslam, C. J. Salter and W. Reich for convolving their surveys to desired resolution and Dr. P. Reich for clarifying our questions about 1420 MHz survey.

References

Berkhuijsen, E. M. : 1971, *Astron. Astrophys.* **14**, 359.
Haslam, C. G. T., Salter, C. J : 1983, private communication.
Milogradov-Turin, J. : 1970, *Publ. Dept. Astron. Univ. Beograd*, **2**, 5-9.
Milogradov-Turin, J. : 1972, M.Sc. Thesis, University of Manchester.
Milogradov-Turin, J. : 1982, Ph. D. Thesis, University of Belgrade.
Milogradov-Turin, J. : 1985, in *The Milky Way Galaxy*, IAU Symp. 106, van Woerden, H., Allen, R. J. and Burton, W. B. eds., D.Reidel Publ. Co., Dordrecht, Boston, Lancaster.
Milogradov-Turin, J. : 1987, *Publ. Ast. Inst. Czek. Acc. Sci.* **69**, 225.
Milogradov-Turin, J., Smith, F. G. : 1973, *Mon. Not. Roy. Ast. Soc.* **161**, 269.
Nikolić, S. : 1994, M.Sc. Thesis, University of Belgrade.
Reich, W. : 1990, private communication.
Turtle, A. J., Pugh, J. F., Kenderdine, S., Pauliny-Toth, I. I. K. : 1962, *Mon. Not. Roy. Ast. Soc.* **124**, 297.

Publ. Obs. Astron. Belgrade No. 49 (1995), 179-182

ON THE DECIPHERING OF COMPLEX TIME-SERIES

J. NUSPL
Konkoly Observatory, Budapest, P.O.Box 67., H-1525
E-mail nuspl@ogyalla.konkoly.hu

Abstract. The final aim during the deciphering analysis of a recorded data set of time-series observations is to extract the information in the best usable form to understand the dynamical processes working in the background and generating the observable.

In simple cases a frequency decomposition is enough for this purpose but in more complex situations we have to look for more sophisticated methods. A new possibility based on the geometrical picture of phase-space reconstruction methods will also be drafted which can give a more direct bridge between observations and the governing equations.

1. GENERAL FORM OF HARMONICALLY PERTURBED TIME-SERIES

In the first approximation a linear description gives a good fit to the behavior of dynamical systems. According to this the time dependent variations may be considered as harmonic ones and we can use the following mathematical model function

$$f(t) = \sum_i a_i * \sin(\omega_i * t + \phi_i)$$

for the observed time series.

In weakly nonlinear systems where the parameters becomes time dependent we can generally suppose their slow variation. Hence, we can use average values of them for a bit of time interval but the decomposition requires a proper resolution in the frequency domain which means observations long enough in time. However, the two requirements mentioned before can not be satisfied at the same time because increasing the continuous time interval of analysis, the using of quasi constant averages for the parameters will lose its right.

So, in the case of closely spaced frequencies we have to apply another approach if the time dependence is faster.

The time dependence of parameters may be described by a similar decomposition, i.e.

$$a_i(t) = \sum_j A_{ij} * \sin(\alpha_{ij} * t + \sigma_{ij}),$$

$$\omega_i(t) = \sum_j B_{ij} * \sin(\beta_{ij} * t + \chi_{ij}),$$

$$\phi_i(t) = \sum_j C_{ij} * \sin(\gamma_{ij} * t + \psi_{ij}).$$

Of course, the frequencies and phases in these expressions are independent from the basic ones. Inserting these terms into our mathematical model formula the full expression will be

$$f(t) = \sum_i [\sum_j ...] * \sin([\sum_k ...] * t + [\sum_l ...]).$$

This form may be transformed into a simpler one (similar to the original expression) using trivial trigonometric and analytical relations

$$f(t) = \sum_{ijkl} b_{ijkl} * \sin(\Omega_{ijkl} * t + \tau_{ijkl}).$$

The frequencies appeared in the above formula are linear combinations of the original ones

$$\Omega_{ijkl} = \nu_i * \omega_i + n_{ij} * \alpha_j + m_{ik} * \beta_k + r_{il} * \gamma_l$$

and the amplitudes and phases may also be expressed by the original values.

This means, however, that performing the usual Fourier analysis we can get a very complicated and scrambled spectral distribution of the power. Even in the simplest amplitude modulation case, the original form of the function is

$$f(t) = A * \sin(\Omega * t + \Phi) * sin(\omega * t + \phi),$$

and this may be transcribed into

$$f(t) = a_1 * sin((\omega - \Omega) * t + \phi_1) + a_2 * sin((\omega + \Omega) * t + \phi_2).$$

The original frequency disappear and we can detect power in the spectrum at two non-physical frequencies. Of course, the physical interpretation would be completely wrong if one identified these frequencies with real pulsation modes.

One has to note that phase and frequency modulations get similar splitting producing completly mixed power spectra. Nevertheless, we can see from this transformation that the information about the time dependent parameters will be decoded into the pattern of frequencies. Using long term observations we can (in principle) recognize and separate the real frequencies from the detected ones.

2. ARMA PROCESSES AND PREDICTION

We can improve the resolution in frequency using autoregressive AR (or general autoregressive-moving average ARMA) processes. The procedure is iterative and its essence may be understand easily from a geometrical visualization which is equivalent to the generally used one at identification of stochastic processes (see Box, 1971. and Hannan, 1970.).

We consider a dynamical system with several degrees of freedom but we measure only one of the observables which may be even an integrated value, e.g. the total

luminosity of a star. The observations distributed equidistantly form a well ordered time series $(m_1, m_2, ..., m_i, ...)$ but we allow gaps in this data set.

This one dimensional observation represents the full underlying dynamical behavior of the system and we can extract that information from it. The followings are based on Takens embedding theorem and its generalizations.

¿From the ordered set of the observations we can form a new set of M-dimensional vectors

$$X^t = (m_t, m_{t-\tau}, ..., m_{t-M*\tau}),$$

where τ means the time interval between two consecutive observations. We can visualize these vectors as points of an M-dimensional space. Due to the theorems mentioned these points will draw up a differentiable manifold topologically equivalent to the original phase-space attractor of the solution. (For example, in the case of a harmonic oscillator measuring the elongation and constructing a 2-dimensional embedding the reconstructed phase-space trajectory will be an ellipse.)

An autoregressive process is defined by

$$X_t = \alpha_1 * X_{t-1} + \alpha_2 * X_{t-2} + ... + \alpha_M * X_{t-M} + \beta_t.$$

The last term of this expression may also be considered as a prediction error if we consider the right hand side as a prediction formula for X_t. In this picture we can describe the AR definition as a linear transformation of the points in the M-dimensional embedding space.

This transformation will drag the points of the reconstructed phase-space trajectory starting from a given observation track. Fitting this dragging path to the reconstructed one we can determine the parameters of the best approximating AR process. During this fitting procedure we have to minimize the cumulative quadratic prediction error for all tracks and data points.

In a second step we can use these parameters to mend the gaps of observation. (Considering the harmonic oscillator the observational tracks will draw up the different segments of the ellipse according to the phase of observation. Using the similar flow of nearby segments we can draw the missing parts of the reconstructed trajectory.) In observational series mended this way can again be analyzed giving a better resolution.

In general we can determine only a local flow of the reconstructed phase-space trajectory and predict forward or backward for a limited interval.

Nonlinear systems may be chaotic whith a diffuse power spectra. In spite of this, the reconstructed phase-space trajectory will tend to fit a simple low dimensional manifold, the attractor of the realized solution (Kolláth, 1990). We can use the local prediction methods described above in this case, too, but we can not decompose it to several independent harmonic components of the variation.

3. FROM TOPOLOGY TO DYNAMICS

In this case the real information about the system is represented by the topological structure of the attractor. However, if our embedding dimension is higher then three, it is difficult or ambiguous (or impossible) task to guess its shape. Hence, we have

to use some algorithmic procedure for identification. The algebraic topology supplies these tools in a ready form for us. These methods are widely used in other parts of the physics, e.g. in solid state physics or particle physics.

The topological property of a manifold may be described by its homology group. (The topological features, e.g. twisting, connectedness or unconnectedness, etc., are transformed in this way into an algebraic structure. A good introduction into these technics is given by *Nash*, 1983). The so called 'exact sequences' procedure gives a direct way to determine the homology group of a given manifold.

There exists a one-to-one connection between the homology group of a manifold and the cohomology group of differential forms defined on the manifold. These differential forms correspond to our differential equations used in the every-day work.

Next steps of an algorithmic approach could be given as followings :

- draw the reconstructed phase-space trajectories with different imbedding dimensions
- determine the best dimension from these embeddings
- extract the empirical attractor manifold
- compute and represent the homology group of this manifold
- map it to the dual cohomology group of differential forms

In this way we can get 'directly' the governing equations from our observations.

The application of the procedure mentioned before to real and noisy astrophysical observations is in progress.

References

Box, G. E. P. and Jenkins, G. M. : 1971, "Time series analysis, forecasting and control", Holden Day.

Hannan, E. J. : 1970, "Multiple time series", Wiley.

Kolláth, Z. : 1990, *M.N.R.A.S.* **247**, 377.

Nash, C. and Sen, S, : 1983, "Topology and Geometry for Physicists", Academic Press, New York.

Publ. Obs. Astron. Belgrade No. 49 (1995), 183-186

CCD AT BELGRADE LARGE TRANSIT INSTRUMENT

S. M. PETKOVIĆ and I. PAKVOR
Astronomical Observatory, Volgina 7, 11050 Belgrade, Yugoslavia

Abstract. A project for the installation of CCD electrooptical sensors on the Large Transit Instrument (LTI) of Belgrade Observatory is given. The basic task is the realization of the hardware and software with the selection of the optimal CCD sensor and standard personal computer for the purpose of functional verification of the entire system.

1. SELECTION OF THE CCD ELECTROOPTICAL SENSOR

The first phase of the project related to the installation of the CCD electrooptical sensor on LTI ought to provide functional verification of the hardware and software. Having this fact in mind, the basic criterion for the selection of the CCD sensor is to satisfy requirements for meridian observations. The basic parameters, which the sensor has to satisfy are determined by the characteristics of the LTI (f=2578 mm,O=190 mm). The working observation area is 3 to 4 mm and the illumination at the place of CCD sensor, according to the magnitude of the observed star, is :

m = 0	5 lx
m = 8	3×10^{-3} lx
m =10	$0{,}5 \times 10^{-3}$ lx

On the other hand, the minimal number of pixels in the working area which is needed for time registration is 100. Comparing the given requirements with the characteristics of the commercial CCD sensors, one comes to the conclusion that the only problem is the noise level at the ambiental temperature above the 0°C. For example, the FT 800P sensor has the entire width of the sensor field of 5,044 mm. The effective number of the pixels horizontally is 774 and vertically 580. In the working area there are more than 300 pixels which also exceeds the required task. The sensitivity of the of FT 800P sensor for the spectral region of the light which corresponds to the light of observed stars is 30mV/lx or 30μV/mlx. This would be completely satisfactory for stars up to 10th magnitude. With certain software averaging the observations of fainter objects would be possible.

2. ELEMENTS OF THE HARDWARE OF CCD OPTICAL SENSORS

In the first phase of installing of CCD optical sensors on LTI, the use of standard components are envisaged, mostly the existing elements with only a few new most

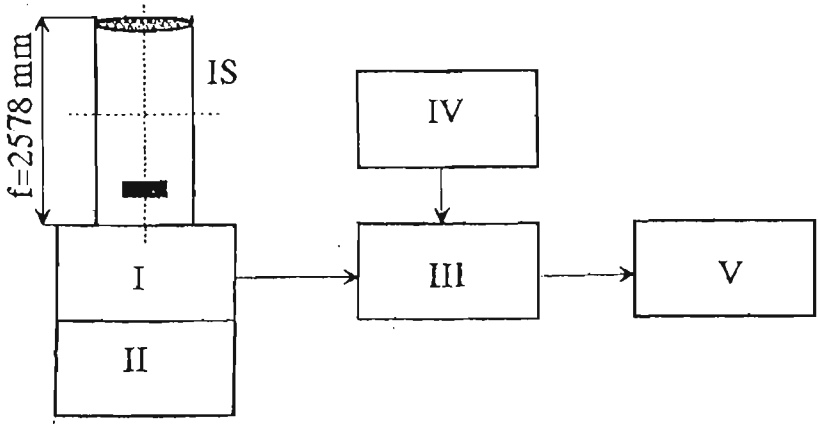

Fig. 1. IS - LTI, I - CCD camera, II - cooling, thermostat, temperature control, device against fogging, III - interface block, IV - main clock, V - personal computer and equipment.

necessary devices. The general block scheme of the proposed system is given in Fig. 1.

The CCD camera and cooling device (thermostat, temperature measuring and control of the CCD sensor, heater against fogging) are installed directly on the eye-piece end of the LTI tube and connected with the interface device. As the LTI is not provided for photometry nor spectroscopy but only for the registration of star transits, it is logical to apply binary monochromatic system of CCD camera (Fig.2).

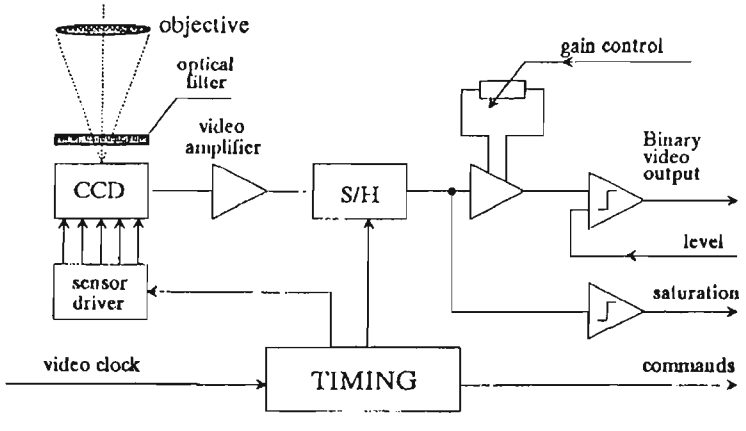

Fig. 2. The scheme of CCD camera system.

The basic commands which arrive at CCD camera are the video clock and comparison level. The video clock determines the CCD scanning regime which depends on the observation object. From the video camera the signal goes to time interface device (Fig. 3)

The basic function of time interface device is to determine the binary (BCD) time code to the serial video signal and to send such signal by serial RS-232 connection to PC input.

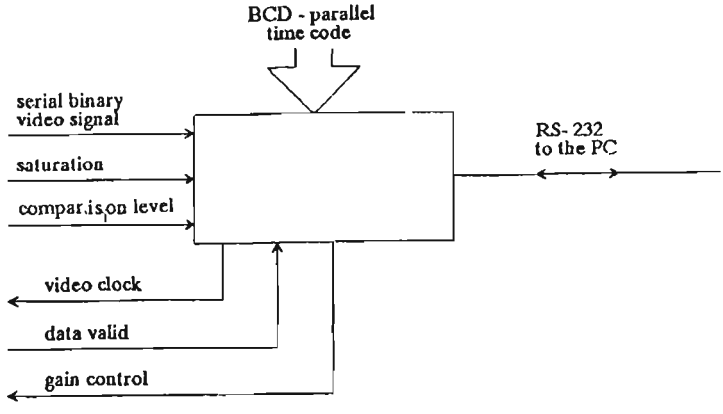

Fig. 3. The time interface device.

3. THE PRINCIPLES OF THE CONSTRUCTION OF CCD CAMERA FOR FUNCTIONING IN THE REAL TIME

The functioning in the real time during star observations with the Large Transit Instrument supposes the establishment of the correspondence between each illuminated pixel of CCD sensor and the time t(UTC) obtained from the local T/P standard. The moment of illumination of each individual pixel, the interval of integration time of the illuminated pixel, intensity of the illumination, velocity and direction of star-image motion across matrix of pixels and jitter of the star-image are the basic parameters (excluding LTI instrumental errors) for time determination of meridian passages. To define the basic conception for functioning in real time t(UTC) it is necessary firstly to analyse the basic structure of the concrete CCD sensor. Simplified structure of the sensor is shown in Fig.4.

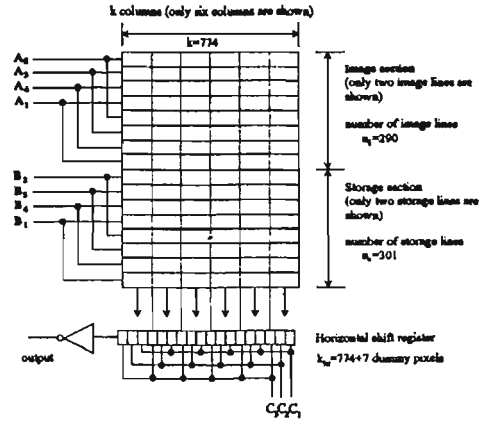

Fig. 4. FT 800P simplified diagram.

4. THE BLOCK SCHEME OF CCD CAMERA FOR LTI

For the determination of the correspondence between local time t(UTC) and the image of observed star, it is necessary to register the address of each illuminated pixel in the CCD matrix and to take into consideration all transport delays.

The principle block scheme of the data preparation for the treatment in the computer is given in Fig. 5.

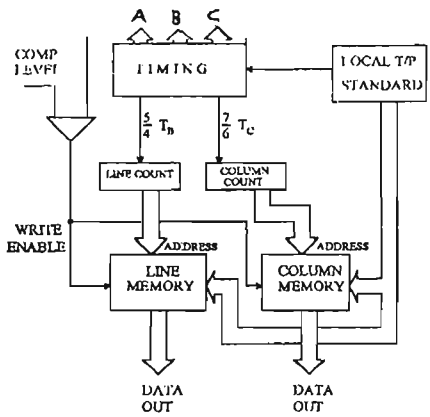

Fig. 5. FT 800P simplified diagram.

From the local T/P standard the device for the timing is incited and the parallel BCD code, which represents the code of the local time t(UTC), is carried out. This code is in correspondence with the image position in line and column memories so that the data of these memories contain definite functional dependence with t(UTC).

The timing device generates :

- four phase clock A1,...,A4
- four phase clock B1,...,B4
- three phase clock C1,...,C3
- the impulse sequences with periods of 5/4Tb and 7/6Tc which represent the clock for the line address counter and for the column address counter.

References

Davis Philip, A. G., Hayes, D. S. and Adelman, S. J., eds : 1990, CCDs in Astronomy, New Methods and Applications of CCD Technology.

Mackay, C. D. : 1986, Charge-Coupled Devices in Astronomy, Ann. Rev. Astron. Astrophys. 24 : 255-83.

Publ. Obs. Astron. Belgrade No. 49 (1995), 187-190

BELGRADE OBSERVATIONS OF SL9 IMPACT ON JUPITER

L. Č. POPOVIĆ, A. KUBIČELA, J. ARSENIJEVIĆ,
D. JEVREMOVIĆ and I. VINCE
Astronomical Observatory, Volgina 7, 11050 Belgrade, Yugoslavia
E-mail lpopovic@aob.aob.bg.ac.yu

Abstract. CCD observations of the perturbations in Jupiter's atmosphere caused by the impact of fragments of the comet SL9 on this planet are presented. The appearance and evolution of "dark spots" in Jupiter's atmosphere in the V and R spectral region were recorded.

1. INTRODUCTION

The impact of comet Shoemaker–Levy 9 1993e (SL-9) on Jupiter occurred from 16 to 22 July 1994. At Belgrade Observatory we observed perturbation in Jupiter's atmosphere during and after the impact time.

Generally, we have three possibilities to observe the consequences of SL-9 comet crash into Jupiter. Namely, direct observations (photograph) of Jupiter's disc, spectral observations of Jupiter and the photometry of the impact flashes reflected from Jupiter's satellites. Two facts were important for the selection of our observing program. First, during the impact period Jupiter was not more than about 32° above the horizon and second, we have just prepared a CCD camera for the first use at the 65 cm refractor. So, we decided to observe Jupiter's disc with CCD camera in V and R spectral regions. Here, we present a part of results of our successful observations.

2. OBSERVATIONS

The observations were carried out at the Belgrade Observatory from 17th July till 8th August covering the impact period and 17 days after it – until the visibility of Jupiter became very poor.

Santa Barbara Instrument Group model ST–6 professional CCD imaging camera was attached to the Zeiss 65/1055 cm refractor. The refractor aperture was reduced to 40 cm. Two glass filters were used : VG–14 for the visual (V) region and RG–8 for the red (R) region.

Using the spectral response data of the camera given by the manufacturer and the spectral transmission curves of the glass filters, it was estimated that the camera plus VG–14 filter yields an overall spectral response having the maximum (normalized to 100%) at 530 nm, full width (FW) at 50% from 500 nm to 560 nm and FW at 5%

from 475 nm to 590 nm – which is close to V spectral region of Johnson and Morgan (1951). However, the camera plus RG-8 combination yields a less symmetric overall spectral response with the maximum (normalized to 100%) at 730 nm, FW at 50% from 700 nm to 920 nm and FW at 5% from 680 nm to 1000 nm. The maximum itself is close to Stebbins and Whitford's R region in their six-color system (Stebbins and Whitford, 1945), but because of the very extended red wing of the camera plus RG-8 spectral response curve, we only conditionally refer to it as "R' We also estimated that the effective sensitivity of the camera-filter system in our R region is about 15 times higher than in the V one.

Some details about our observation are given in Table 1 (date of observations, the time interval, the spot of fragments, which was seen in Jupiter's atmosphere).

Table 1 Observations of Jupiter. I - Date of observations, II - the time interval of observations, III - the spots of fragments seen in Jupiter's atmosphere and IV - number of obtained images. On July 17 and 18 were taken two and tree images in R filter (in brackets).

I	II	III	IV
17. 7.	18 : 34–20 : 14	E, A, C	22 (2R)
18. 7.	18 : 30–21 : 17	G, H	65 (3R)
20. 7.	18 : 42–19 : 44	C, K, L	12
23. 7.	18 : 10–19 : 57	K, L, GR, Q1, H	36
24. 7.	18 : 27–19 : 25	H, E, A, C	4
25. 7.	18 : 36–19 : 25	UWK, L, GR	12
26. 7.	19 : 57	H E	1
29. 7.	18 : 27–19 : 39	E, C, P2, UWK	23
30. 7.	19 : 14–19 : 23	K, L, GRQ1	4
31. 7.	18 : 31–20 : 01	GRQ1 H E	31
05. 8.	18 : 55–18 : 57	H, TV, E	2
06. 7.	18 : 30–19 : 16	UWK, LG	15
08. 7.	18 : 31–18 : 58	UWK	6

During and after impact period we made 233 images of Jupiter. Some of them are presented in Figs. 1-3.

3. DISCUSSION AND CONCLUSION

By the inspection of our CCD images we can conclude :

– All observed traces of fragments in the V spectral region were darker than surrounding Jupiter's atmosphere. For the medium-size impact traces we obtained a considerably lower contrast in the R spectral region.

– Scrutinizing all obtained images we were not able to detect small impact traces like, e.g., D, N, or Q2. According to the marvelous images taken by Hubble Space Telescope (Macchetto, 1994) our estimate of the angular sizes of these impact spots were approximately $0''.6$, $0''.3$ and $0''.2$, respectively. Slightly bigger one as, for example, Q1 being about $1''.1$, was detected in our images of Jupiter. We consider this as an

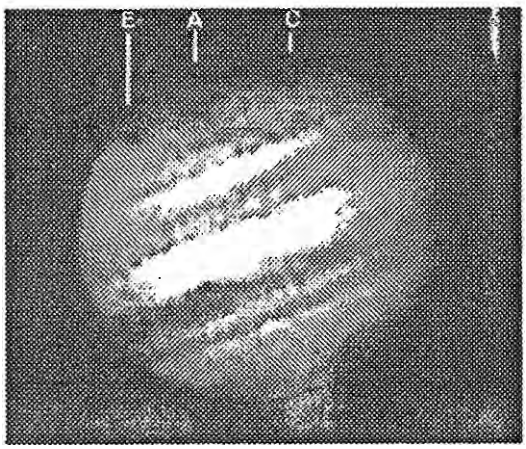

Fig. 1. Jupiter on 17. 7. 94. at 18 : 56 UT. The image shows, from west to east, the impact sites of fragments E, A and C. The darkest and most complete feature corresponds to the fragment E, which is the youngest, being old only 3.8 hours. South is up and west is to the left.

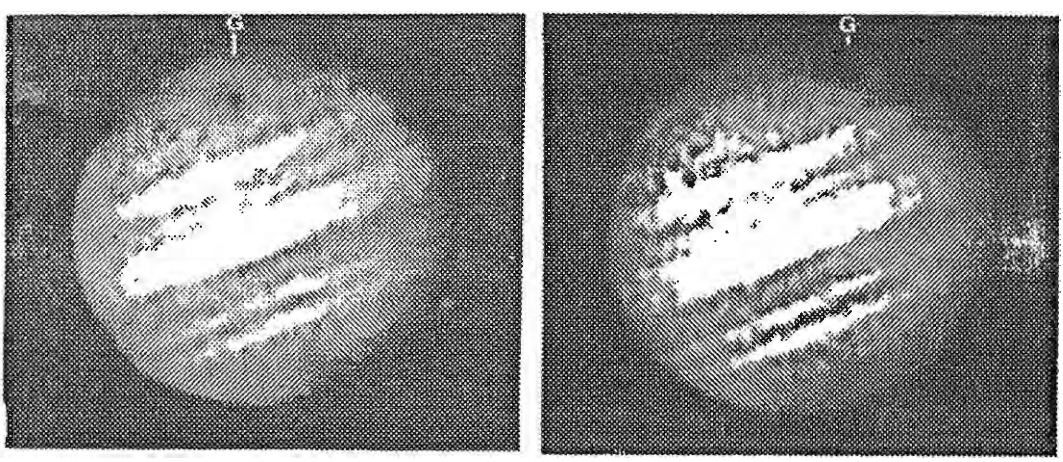

Fig. 2. Jupiter on 18. 7. 94. at 19 : 20 UT (left) and 20 : 06 (right). A huge dark elliptical spot with a dark core at its north–east is seen around the impact site of the fragment G just 11.5 hours after the impact (left). About one hour later, at 20 : 06 UT the impact structure G was close to the central meridian (right).

indication that our overall realized resolution (atmosphere + telescope + CCD + displaying facility) is somewhere around 1″. Obviously, the nominal CCD resolution of about 0.5 arc sec per pixel was not achieved because of the other contributors – most probably the Earth's atmosphere, especially considering the high zenith distance

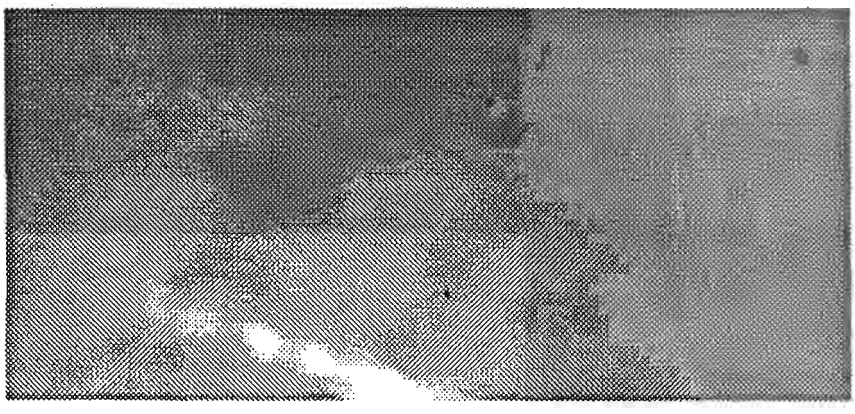

Fig. 3. Jupiter on 6. 8. 94. at 19 : 04 UT. Dark structure is seen east from the central meridian. It comprises the impact-traces U, W and K. The age of K trace is 488.3 hours. Here one can see that formation of a new dark belt, "SL-9 belt", in the atmosphere of Jupiter takes place.

of Jupiter.

– None of the large observed spots disappeared during the observation campaign. They gradually lost their individuality by extending in longitude, merging with neighboring impact traces and behaving as though they were taking part in building a "new" dark belt in Jupiter's atmosphere. This "SL-9 belt" was not yet completed till the end of our observational campaign (8. 8. 1994).

References

Johnson, H. L. and Morgan, W. W. : 1951, *Astrophys. J.* **114**, 522.
Macchetto, F. D. : 1994, *ESA Bull.* **79**, 85.
Stebinns, J. and Whitford, A. E. : 1945, *Astrophys. J.* **102**, 318.

Publ. Obs. Astron. Belgrade No. 49 (1995), 191-193

THE ROLE OF FUNDAMENTAL ASTROMETRY IN ASTRONOMICAL RESEARCH

S. SADŽAKOV
Astronomical Observatory, Volgina 7, 11050 Beograd, Yugoslavia
E-mail ssadzakov@aob.aob.bg.ac.yu

B. D. JOVANOVIĆ
Faculty of Agriculture, Waterarranging Institute,
Trg Dositeja Obradovića 8, 21000 Novi Sad, Yugoslavia

Abstract. The role of Fundamental Astrometry in astronomical researches in general is considered. One of its crucial tasks is the setting up of suitable coordinate system affording high accuracy of positiion determination of celestial bodies of the order of 10^{-8} to 10^{-10} radians.

1. INTRODUCTION

Astrometry is primarily concerned with the positions and geometric and kinematic properties of the celestial bodies, their groupings and distribution throughout the Universe. The wealth of astrometric data is turned to account in the studies of structural, kinematical and dynamical problems of the stellar systems, the solar system bodies being the object of particular attention.

One of Astrometry's foundations is the system of astronomical constants whose outstanding quality must be the highest possible accuracy coupled with its complete intrinsic concordance.

The first and the most important task of Astrometry is the setting up of suitable coordinate system, allowing the study of the solar system bodies as well as the other objects in the Universe. Such a system cannot but be embodied by, and be dependent on, celestial bodies, the Earth, the Sun, the stars and extragalactic objects inclusive. (Yatskiv, Gubanov 1980).

The requirements put on such a coordinate system are :

1. The system must be strictly and unambigueusly defined. Methods of its setting up must be simple and mutually independent.

2. The setting up of a fundamental coordinate system should not, if possibly, depend on any hypotheses whatever.

3. The accuracy inherent in a fundamental coordinate system ought to be of the order of $0''.001$ or better, i.e. $5\ 10^{-9}$ radians.

4. The fundamental coordinate system must be inertial, i. e. its only permissible motion is rectilinear uniform one.

2. INERTIAL FUNDAMENTAL COORDINATE SYSTEM

Historically, it is by steps, logically following each other, that the fundamental coordinate systems have been materialized. Their origin, by force of circumastances, had to be ascertained through intermediary of stars. The stars proper motion imposed the need to look toward the pointlike extragalactic nenulae, which are devoid, through their enormous distances, of a perceptible proper motion. However, great difficulties were met due to their poor definition on account of their faintness and indistictiveness (Yatskiv 1983).

The quasars, whose extragalactic position was discovered in 1963, appeared at once as a welcome help. Some of them were observable in both the optical and radio wave-length band.

The application of the VLBI (very long base interferometry) technique for angular position determination of these objects marks the beginning of a new era in dealing with the problem of the inertial coordinate system. Nowadays, it is considered that such a coordinate system, to be inertial, must have the directions of its axes defined by extragalactic radio sources, its origin coinciding with the barycentre of the solar system. Still, it cannot but be quasi-inertial in consequence of its origin being subjected to a slight acceleration and the directions of its axes, in principle, are not strictly steady. Due to such a state of affairs this coordinate system bears appropriate name : it is called "conditional inertial coordinate system" (Mueller 1981).

Nor is the realization of such a system in practice, in the sense of the theory of relativity, rigorous, but it proved highly convenient in the everyday actual work. Many astronomers took such a practical approach. In reductions it is necessary to take into account the small, so called relativistic, corrections.

Currently, the setting up of an inertial coordinate system is feasibly with an accuracy of 10^{-8} to 10^{-9} radians. This meets the requerements of the contemporary fundamental and applied researches in Astronomy and related sciences. Mostly used is the equatorial coordinate system, i.e. the one whose basic plane is given by equator and is materialized by star positions and their proper motions as given in the fundamental catalogues, allowing for the composite motion of the observer. By applying the astronomical constants involved, such as that of precession, as well as others, one achieves a fairly satisfactory approximation of an inertial coordinate system.

References

Yatskiv, Ya. S., Gubanov, V. S. : 1980, "Ob osnovnykh koordinatnykh sistemakh, primenjaemykh v astrometrii i geodinamike", *Geodinamika i astrometriya*, Kiev, 110–120.

Yatskiv, Ya. S. : 1983, "O sostojanii i tendeciyakh razvitiya astronomicheskikh issledovanij", *Astrometriya i astrofizika*, **49**, 3–9.

Mueller, I. I. : 1981, "Reference Coordinate Systems for Earth Dynamics : A Preview (Review)" in *Procc. of the 56-th Colloq. of the IAU*, Varsaw, 1980, Dordrecht, 1-22.

Publ. Obs. Astron. Belgrade No. 49 (1995), 195-199

INTERNATIONAL SPECIAL PROGRAMMES OF MERIDIAN OBSERVATIONS OF REFERENCE AND PROGRAMME STARS

S. SADŽAKOV, Z. CVETKOVIĆ and M. DAČIĆ
Astronomical Observatory, Volgina 7, 11050 Belgrade, Yugoslavia
E-mail ssadzakov@aob.aob.bg.ac.yu

Abstract. The new methods in astrometry have aided the development of fundamental research in astrometry. At many observatories in the world the compilations of star catalogues containing a large number of stars proposed by the IAU are in progress. The accuracy of the determined star positions and proper motions is expected to increase due to the applications of VLBI, Hipparcos satellite, as well as of the automatic meridian circles.

1. INTRODUCTION

In the recent time the spectrum of astrometric programmes has become less comprehensive. Once defined as a "science of the measuring of angles on the celestial sphere" through a "science about space and time", astrometry is nowadays most clearly defined as a science which studies geometrical and kinematical characteristics of some celestial bodies, of their groups, as well as those of the universe as a whole (Yatskiv, 1983); or astrometry is the science determining the positions, motions, sizes and geometry of celestial bodies, as well as their distances.

Astrometry is a foundation of astronomy, it yields a high-accuracy system of celestial coordinates, the distance scale in the universe and a consistent system of astronomical constants.

A large body of data obtained from astrometrical observations is used in stellar astronomy for the purpose of studying the structure, kinematics and dynamics of stars, stellar systems and galaxies and also in celestial mechanics for improving the theory of motion of the Solar-System bodies.

The astrometric research offers to related sciences for their practical needs all necessary data concerning the Earth's rotation, the positions of the Solar-System bodies, defines the reference coordinate systems used in cartography, navigation, etc. There is a close relationship between astrometry and gravimetry, astrometry deals with the spatial determination of the coordinates of celestial bodies, it studies their translatory rotational motion on the basis of observations (largely terrestrial).

The realization of the reductions of astronomical observations is impossible without using the results and methods of gravimetry and celestial mechanics in view of their close relationship through astronomical constants and astrometric observations.

In the epoch of active space exploration the practical role of astronomy becomes more important every year and the practical necessities stimulate the development of the fundamental astrometric research.

2. THE GREAT CATALOGUES REALIZED RECENTLY

At many astronomical observatories all over the world the praxis of producing stellar catalogues containing a large number of stars from various proposed and accepted lists of the international astronomical institutions has been continued.

At Brorfelde a catalogue containing 6427 stars (1969-1975) brighter than $m = 11$ was compiled by using a meridian circle with photographic circle reading. The stars originate from the lists of NPZT, FK4 Sup, high-velocity O-B stars inside 20 *pc*, fainter than in GC from associations and stars around them. The reference stars are from FK4. The mean-square error of a single measurement in right ascension is $0''.086$, i.e. $0''.104$ in declination. The average number of observations is 5. For the purpose of a better linking to the reference system an additional smoothing has been done (Helmer and Fogh Olsen, 1982).

After the circle modernization by installing a photoelectric micrometer the so-called Carlsberg Authomatic Meridina Circle (CAMC) was obtained. In the period 1981-1982 it was used for observing 1577 stars up to $m = 11$. This programme includes 425 FK4 stars being reference for it, or more precisely : 167 stars from AGK3 in the zone $+88° - +89°$, 115 stars around the north galactic pole, as well as FZT, GC stars, the reference ones in the vicinity of radio sources appearing in the earlier programmes of this instrument. The mean-square error of a single observation is $\pm 0^s.0138$ and $\pm 0''.216$ (Helmer et al., 1983).

The other catalogue obtained with CAMC is from the period 1982-1983. It contains 1071 stars as follows : 146 AGK3 stars from the zone $+88° - +89°$, 68 stars situated in the vicinity of the north galactic pole, FZT-programme stars, reference stars from the vicinity of radio sources. The FK4 reference stars are not in the general list. The determination accuracy is the same as in the first catalogue. This meridian circle was mounted at the La Palma Observatory and from May 1 to December 12, 1984, 35154 transits of 5292 stars were observed, or more precisely : 2369 AGK3R stars, 1296 SRS ones, 838 reference stars between $m = 11$ and $m = 13$ within a solid angle of $1° \times 1°$ around the radio sources from the IAU list, 227 FZT stars, 406 AGK3 stars and 139 SAO stars. The mean-square error of a single observation is $\varepsilon_\alpha \cos\delta = \pm 0''.193$ $\sec z$, $\varepsilon_\delta = \pm 0''.184$ $\sec z$. At the zenith distance $z = 30°$ the accuracy is the same as at Brorfelde, but the number of observations is higher.

At the Cerro Calan Observatory in Chile several catalogues have been compiled with various instruments. The Absolute Pulkovo Catalogue for right ascension in the southern sky, the so-called *SPu*71 has been examined for the purpose of discovering and also removing the systematic and random errors which earlier were not taken into account. For each observing night are formed the equations for the correction determination of the Bessel-reduction-formulae coefficients. The calculation of these corrections shows that they are negligible, indicating that the catalogue is free of large systematic errors. In the process of examining another version of the catalogue

has been obtained, more accurate as for the random errors. The observations with the Repsold Meridian Circle between 1963 and 1970 have yielded two catalogues. The first one contains 18 583 measurements for 2756 SRS stars, 336 BS stars and 215 reference ones from FK4 in the zone from $-20°$ to $-40°$. The system of the instrument was determined from 59 reference-stars series with 1936 measurements within the zone from $+41°$ to $-68°$. The mean-square error for the equator-point determination was $\pm 0''.33$ (Carrasco, 1978).

The other catalogue compiled by the Pulkovo astronomers is due to the classical observations using the relative method, whereas the treatment was performed by using the quasi-absolute method and the corrections were applied only for FK4 stars. Detailed examinations and analyses of the obtained results were done. The right-ascension catalogues were given in the instrumental system realized on the basis of the quasi-absolute method, whereas the declination ones were given in the FK4 system. The SRS Catalogue contains 5491 stars, out of them 828 BS stars, 356 DS stars, whereas the programme stars were taken from the zone between $-50°$ and $-80°$, i.e. from a belt of interest to the determination of coordinates of these stars. The mean-square errors for the reference stars are $\pm 0^s.015$ and $\pm 0''.39$, and for the programme stars are $\pm 0^s.018$ and $\pm 0''.41$ (Zverev et al., 1983).

With the Airy Meridian Circle of the Greenwich Observatory were performed observations between 1942 and 1954 on the basis of which their last catalogue was compiled and published. After March 30, 1954 there have been no observations with this instrument. For the observational-data treatment the absolute method was used. In addition to 255 fundamental stars the catalogue also contains 255 FZT Herstmonceux stars and 76 stars situated in the vicinity of the north celestial pole and observed in both culminations (Tucker et al., 1983).

At Herstmonceux with the Cook Meridian Circle brought over from Greenwich have been obtained the first three absolute catalogues based on 76 azimuthal and 235 hour stars from the FK4 fundamental catalogue.

The catalogue $1H_x50$ contains 18 114 stars and the observations meant for its compilation were performed between 1957 and 1961. The origins of its stars are : 835 $FK4$, 1408 $FK4Sup$, 13 803 $AGK3R$, 635 from various FZT lists, 1045 from Blau's list and 37 $FK3$ double stars not included in $FK4$.

The second catalogue $2H_x50$ was compiled between 1961 and 1969. It contains 816 other $FK4$ stars, 1352 $FK4Sup$ ones, 5866 stars from the common catalogue of line-of-sight velocities, $GCRV$ (for the purpose of improving their proper motions), 352 variable stars and stars in the vicinity of quasars, $FK3$ double stars not included in $FK4$ and a few others. The total number of stars in the catalogue is 8736 stars.

The third catalogue $3H_x50$ contains 835 other $FK4$ stars, 3539 from the catalogue $Wash$ 50 Zod, 1715 NPZT stars, 251 variable stars from $GCRV$ etc. The total number of stars is 6728 stars.

With $Washington$ 6" Meridian Circle 14 916 stars were observed between 1963 and 1971 by applying the absolute method and a catalogue known as W_{50} was obtained. It contains 1147 $FK4$ stars (out of them 203 hour, 34 azimuthal, 98 refraction and 812 others), 3681 BS bright stars (including 1409 $FK4Sup$ ones), 154 stars situated in the vicinity of radio sources, 9631 SRS Programme stars, 141 stars of the Washington

and Richmond FZT programmes, 121 carbon stars and 33 high-proper-motion ones (Hughes and Scott, 1982).

3. THE CHARACTERISTICS OF PRESENT STAR CATALOGUES

From the appearance of the first fundamental catalogue of Auvers the idea to define a coordinate system purely kinematically has not been seriously considered.

The astronomers need a fundamental system defined through the equatorial coordinates which also involves the elements describing the Earth's rotation in space (precession and nutation), as well as the equinox motion.

The positions of the true equinox and of the true equator are time functions in a determined coordinate system and they offer a dynamical definition of this coordinate system, as well as of the true-equator-coordinate-system motion.

The daylight observations of the Sun, inner planets, stars, as well as of the Moon, are very important for the equnox correction of a star catalogue. In praxis also appear other difficulties in the determination of the dynamical equinox for the right-ascension origin in star catalogues, which gives rise to a disagreement between the definition and realization of used stars, especially when this incoincidence is in correlation with the ephemeris-time.

In the precession-constant determination use has been made of dynamical and kinematical methods, together or independently. The kinematical determinations of the precession constant by using the galactic-rotation models are more accurate than purely dynamical solutions.

Such a pragmatical approach has allowed a final accuracy of the $FK5$ Catalogue, the highest possible in view of the available observational results, being of the order of $0''.15$ per century.

In order to achieve an improvement of the $FK5$ system, a system based on the dynamical definition and knowledge of the motion of one celestial body, in our case that of the Moon, is considered.

There are results of the 15-year cycle of laser observations, as well as those referring to the motion of a point near the Moon's mass centre which in its motion has an orbit of 40 cm in diameter corresponding to $0''.001$ - $0''.002$ in longitude in the dynamical coordinate system for more than ten years. There are difficulties affecting good knowledge of the lunar motion because the order of the errors is $0''.3$ due to the bad determination of the systematic deviation of the apparent-lunar-figure centre, as well as due to the movement of its mass centre.

On account of a low number of the zodiacal stars which occult the Moon, in a fundamental catalogue it is difficult to improve the parameters used in the classical determination of the celestial coordinate system on the basis of the lunar laser data.

Nowadays one utilizes VLBI with which extragalactic radio sources are observed, and used as fundamental points of a fixed coordinate system.

In this case one should know the exact equator position in the system because the observed declinations are referred to the instantaneous terrestrial rotation axis. Only relative right ascensions are obtained giving rise to a new problem of an independent equinox determination.

In addition to the declination determination of a pulsar by using VLBI the ecliptic longitude and latitude are derived from the analysis of the pulsar retardation during the Earth's orbital heliocentric motion. The method precision exceeds $0''.1$ and it does not attain the desired accuracy.

A great progress is expected by the realization of the Hipparcos Programme which comprises 100 000 stars whose positions and proper motions will be determined with an accuracy of $\pm 0''.002$ per year. The Hipparcos System will not be inertial and the coordinate system will be *a priori* defined so that its residual ro .ation is inevitable.

This system will be connected to VLBI and the Hipparcos Catalogue will materialize a geometrically constant celestial sphere accurate to $0''.002$. This accuracy will gradually decrease due to the accumulation of random errors in proper motions.

The Hipparcos System will be fixed, it will be independent of any terrestrial motion parameter and it will be used as a reference for all motions.

References

Carrassco, G. : 1978, "Final results of relative declination observations made with the Repsold meridian circle at Cerro Calan", *Modern Astrometry*, IAU Colloq. **48**, Vienna, 455–461.

Helmer, L., Fogh Olsen, H. J. : 1982, "Meridian observations made in Brorfelde (Copenhagen University Observatory) 1969-1975. Positions of 6427 stars brighter than 11.00 vis.mag.", *Astron. Astrophys. Suppl. Ser.* **49**, No 1, 13-60.

Helmer, L., Fabricius, C., Einicke, O. H., Thoburn, C. : 1983, "Meridian observations made with the Carlsberg Automatic Meridian Circle at Brorfelde (Copenhagen University Observatory) 1981-1982", *Astron. Astrophys. Suppl. Ser.* **53**, No 2, 233-245.

Hughes, J. A., Scott, D. K. : 1982, "Results of observations made with the six-inch transit circle, 1963-1971", *Publ. U.S. Naval Obs.* sec. ser. **XXIII**, pt.III, 165–481.

Tucker, R. H., Buontempo, M. E., Gibbs, P., Swifte, R. H. : 1983, "Third Greenwich catalogue of stars, Sun, planets and Moon for 1950.0", *Royal Green ıich Obs. Bull.* **187**, 1.

Yatskiv, Ya. S. : 1983, "O sostoyanii i tendentsiyakh razvitiya astrometricheskikh issledovanij", *Astrometryc i Astrofizika*, **49**, 3-9.

Zverev, M. S., Baturina, G. D., Gnevyscheva, K. G., Naumova, A. A., Plozhencev, D. D. : 1983, "O katalogakh sklonenij zvezd SRS, BS i FK4, poluchennykh pulkovskimi astronomami iz nablyudenij na meridiannom kruge observatorii Serro-Kalan (Chili) v 1963-1968 godakh", *A. Ž.* **60**, v. 5, 1022-1025.

Publ. Obs. Astron. Belgrade No. 49 (1995), 201-205

MULTIDISCIPLINARY STUDIES OF THE VARIATIONS IN THE BELGRADE MEAN LATITUDE

S. SADŽAKOV, G. DAMLJANOVIĆ and S. NINKOVIĆ
Astronomical Observatory, Volgina 7, 11050 Belgrade, Yugoslavia
E-mail ssadzakov@aob.aob.bg.ac.yu

Abstract. The topic concerns the importance of the studies of the variations in the Belgrade mean latitude and their connection with the seismical activity of the soil on which the instrument is mounted.

1. INTRODUCTION

The first determinations of the precise Belgrade longitude (λ) at the Belgrade Observatory were begun in 1938 (Brkić, 1968) by using a small transit instrument (Bamberg, $2r = 100mm$, $f = 1000mm$), whereas the precise latitude (φ) was determined for the first time in 1947 (Djurković,Ševarlić, Brkić, 1951) by using a visual zenith-telescope (Bamberg, $2r = 110mm$, $f = 1287mm$); from January 1949 till now the latter has been regularly determined by applying Talcott's method.The following values have been found

$$\lambda = -1^h 22^m 03.^s 212$$

and

$$\varphi = +44°48'13.''167 \pm 0.''008.$$

The results obtained concerning the Belgrade latitude (Grujić et al., 1989) indicate an effect of latitude variation due to the polar-motion influence, as well as to the nonpolar ones. The nonpolar influences have various sources : the instrument, the observers, the catalogue, the atmosphere, the geophysical changes of the soil etc.

An analysis of the z-term and the instrument's inclination β (Djokić, 1970, and Djokić, 1975) indicated correlation between them. Also, it revealed a tendency of the instrument's permanent drifting to the southwest, an effect explaining partially the real decreasing of the Belgrade latitude.

On the basis of the results of the geodynamical studies obtained up to now one can conclude that there are horizontal and vertical shiftings of the soil upon which Belgrade lies. In 1988 multidisciplinary studies of the variations in the Belgrade mean latitude including seismological, geodetic, astronomical, geological and geophysical examinations concerning the area of Belgrade and aimed at establishing mutual relationship in the obtained results (Sadžakov, Grujić, 1991) were initiated.

Therefore, our research concerning the variations in the Belgrade coordinates of requires examinations of the soil shifting. The results obtained by comparing the latitude variations at Belgrade and Warsaw (Jozefoslaw) based on astronomical observations (Teleki, 1969) fully confirm that such a study is justified.

The latitude stations of Belgrade and Warsaw are almost on the same meridian so that any polar influences in the differences of their latitudes (instantaneous) are negligible. Therefore, these differences are subjected to the influences of the local factors.

Since the Belgrade latitude determinations cover a significantly long time (from 1949 till now, without interruptions), it is possible to use the astronomical material, together with the available seismological data (covering 1964-1985), in order to attempt answering the question of whether the seismical processes cause variations in the latitude. Indications concerning the seismical activity can be found by studying the evidence on the earthquakes which took place in the given area. It is necessary to incorporate the foci of those earthquakes which caused microseismical effects on the Belgrade territory. In view of this fact in the present paper only the earthquakes above the magnitude threshold of $M = 3$ are included. This threshold value corresponds to the lower reliability limit of the seismic data obtained with the Belgrade seismograph.

2. STUDIES OF LATITUDE VARIATIONS

The astronomical observational material gathered between 1949 and 1985 was treated in the FK5 system.

We started from the basic formula :

$$\varphi - \varphi_0 = x * COS\lambda + y * SIN\lambda + z \tag{1}$$

$$\lambda - \lambda_0 = (1/15) * (x * SIN\lambda - y * COS\lambda) * tg\varphi \tag{2}$$

where : λ_0 (the west longitude) and φ_0 are the mean longitude and the mean latitude,φ is the observed latitude, x and y are the coordinates of the pole with respect to the mean one, and z is a term being a sum of all the nonpolar influences, such as the catalogue errors, refraction anomalies, instrument errors, shortcomings in the data treatment, various geophysical factors, etc. The mean latitude φ_0 for a given moment is that latitude value for a station from which all the nonpolar and polar periodical terms are excluded. The results of φ_0 examinations have confirmed its variable character. The secular variations may be due to the secular motion of the mean pole whereas the others are due to the local changes of the site position (Kulikov, 1962).

By eliminating the most important periodic polar motions from the latitude variations one obtains the value of the mean latitude (φ_0') by use of Orlov's formula

$$\varphi_0' = \frac{1}{20} \sum_{i=0}^{i=4} (\varphi_i + \varphi_{i+5} + \varphi_{i+6} + \varphi_{i+11}) \tag{3}$$

The results obtained in this way are presented in Figs 1 - 2. In Fig. 1 there is a rectilinear trend, whereas in Fig. 2 the trend is parabolic.

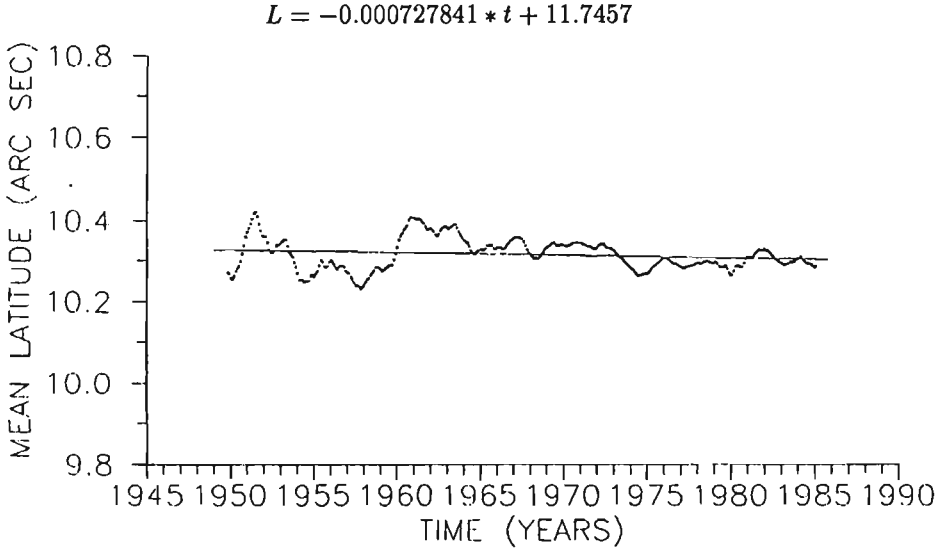

Fig. 1. The curve of variations in the mean latitude with linear trend (L).

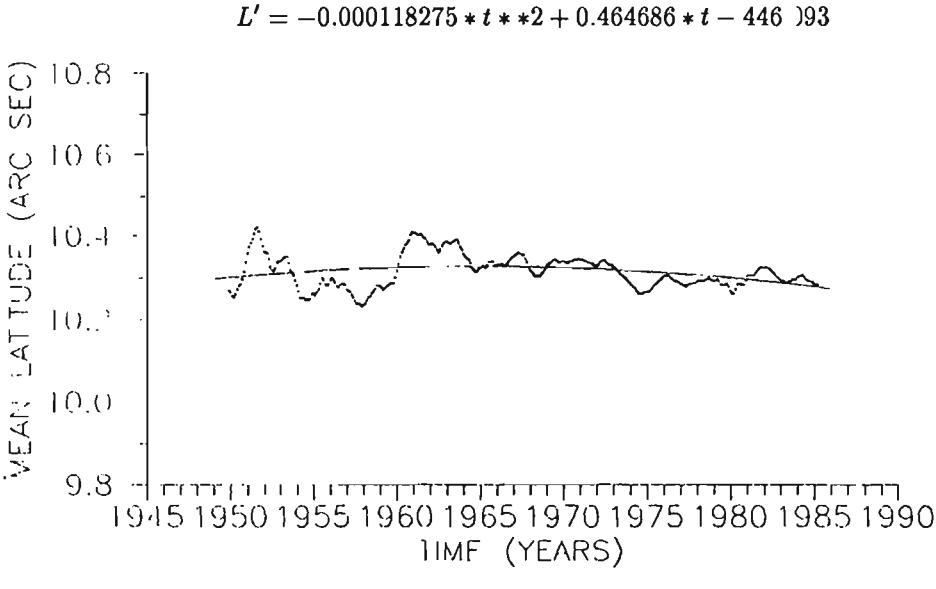

Fig. 2. Variations of the mean latitude with their parabolic approximation (L').

Some periodic low-intensity influences, remaining after the application of Orlov's formula are discovered by use of the spectral analysis. In view of their small amount they will not be taken into account in the further work.

3. ANALYSIS OF THE OBTAINED RESULTS

The first analysis of the Belgrade-Warsaw latitude differences after removing from the Belgrade material certain systematic errors (Damljanović, 1994) and the polar periodicities (by using Orlov's formula) shows that the Belgrade mean latitude has changed significantly, whereas in the case of Warsaw the corresponding value has remained almost unchanged. Looking for an explanation of such a "stormy" latitude curve for Belgrade the correlation between the great earthquakes and the mean-latitude changes was examined. A list of great earthquakes which have ocurred in the Belgrade area made does not enable us to draw any definite conclusion as yet.

It is well known that Belgrade is situated within a seismically active region and Warsaw within a seismically stable one. This circumstance enables us to judge about the earthquake influence on the Belgrade mean-latitude value (and generally on the latitude values) on the basis of a comparison between the two stations (it would be better if there were more of them and if the Warsaw material were more thoroughly examined concerning systematic errors). In the future a re-retreatment of the two materials is expected on the basis of significantly improved coordinates, proper motions and parallaxes for the stars observed at both stations which will be available as a result of the Hipparcos mission (ESA, 1989).

As a consequence a cooperation of astronomers, seismologists, geodesists, geophysicists and others concerning the present task has developed. This cooperation is realised as a scientific project after which the present article is named.

Our research is aimed at establishing the parameters of detailed seismic regionalization of the extended area of Belgrade on the basis of the data concerning the geological composition, the seismotectonic construction and the seismoenergetic capacity of the given area. This will be the base to the study and establishing of the short-term natural phenomena which precede a severe earthquake within the extended area of Belgrade.

4. CONCLUSIONS

The obtained results presented in Figs. 1-2 indicate a realistic decrease in the mean latitude of Belgrade as time function (secular trend) caused by global (e. g. movements of the continental plates) and local factors (local soil movements where the instrument is mounted and where the seismical activities are of importance). During a few last years both groups of factors have been intensively studied. For this purpose nowadays the most modern instruments and techniques giving high-accuracy data are used (like VLBI). Lokally, existing measurements are used and their re-retreatment is done by applying new accurate catalogues and other achievements of modern astronomny.

In view of what has been said above we hope that at least a partial explanation of the behaviour of the Belgrade mean latitude found here will be offered in the near future.

References

*** : 1989, *Hipparcos mission, ESA, SP-1111*, Vol.II, 252.

Brkić, Z. : 1968, "Služba tačnog vremena i promena geografske dužine, njeni radovi i izgledi za dalji razvoj", *Publ. Obs. Astron. Belgrade*, **12**, 57–61.

Djurković, P., Ševarlić, B. and Brkić, Z. : 1951, "Determination de latitude de l' Observatoire Astronomique de Belgrade, 1947 ", *Publ. Obs. Astron. Belgrade*, **4**, 88.

Djokić, M. : 1970, "Analyse de l'influence de variation d'inclinaison des axes du tube zénithal (à Belgrade) sur la valeur de la latitude ", *Bull. Astron. Belgrade*, Vol. **XXVIII**, F.1, No 123, 15–22 .

Djokić, M. : 1975, "Some characteristics of the vertical axis inclination of the zenith telescope in Belgrade", *Publ. Obs. Astron. Belgrade*, **20**, 84–89.

Damljanović, G. : 1994, "On the systematic errors of declinations and proper motions from the Belgrade zenith-telescope observations in the period 1960-198", *Bull. Astron. Belgrade*, **150**, 29–35.

Grujić, R., Djokić, M. and Jovanović, B. : 1989, "Analysis of changes in Belgrade geographic latitude over the period 1969.0–1975.0", *Bull. Astron. Belgrade*, **141**, 7–14.

Kulikov, K. A. : 1962, "Izmenajemost sirot i dolgot", *Moskow*.

Sadžakov, S. and Grujić, R. : 1991, "Multidisciplinary studies of the variations in the mean geographic latitudes of Belgrade", *Bull. Astron. Belgrade*, **143**, 77–79.

Teleki, G. : 1969, "Comparison of latitude variations obtained from observations in Belgrade and Jozefoslaw (place near Warsaw) ", *Bull. Astron. Belgrade*, **XXVII No 2**, 58–67.

CIP – Каталогизација у публикацији
Народна библиотека Србије, Београд

520/524 (082) (0.034.2)

HUNGARIAN-Yugoslav Astronomical Conference (1 ; 1995 ; Baja)
I Hungarian-Yugoslav Astronomical Conference, Baja, Hungary, 26-27. April, 1995 [Elektronski izvor] / edited by Istvan Vince, Milan S. Dimitrijevic and Lajos Balazs ; CD prepared by Milan S. Dimitrijevic and Tatjana Milovanov. - Belgrade : Astronomical Observatory, 2008 (Belgrade : Astronomical Observatory). - 1 elektronski optički disk (CD-ROM) : tekst, slika ; 12 cm

Nasl. sa naslovnog ekrana. - "Conference proceedings, paper edition in Publ. Obs. Astron. Belgrade, no 49 (1995)" - - > etiketa na disku. - Tiraž 100. - Bibliografija uz svaki rad. - Registar.

ISBN 978-86-80019-20-8
1. Vince, Istvan [уредник]
a) Астрономија - Зборници
COBISS . SR-ID 147386124